IMPROVING BIO-OIL FURANS YIELDS BY THERMO-CATALYTIC REFORMING PROCESS INVESTIGATING DIFFERENT FEEDSTOCKS AND CATALYSTS

by

JOÃO DUARTE NAVALHO SANTOS

A thesis submitted to the University of Birmingham for the degree of DOCTOR OF PHILOSOPHY

School of Chemical Engineering

University of Birmingham

November 2019

UNIVERSITY OF
BIRMINGHAM

University of Birmingham Research Archive

e-theses repository

This unpublished thesis/dissertation is copyright of the author and/or third parties. The intellectual property rights of the author or third parties in respect of this work are as defined by The Copyright Designs and Patents Act 1988 or as modified by any successor legislation.

Any use made of information contained in this thesis/dissertation must be in accordance with that legislation and must be properly acknowledged. Further distribution or reproduction in any format is prohibited without the permission of the copyright holder.

UNIVERSITY OF BIRMINGHAM

Improving Bio-oil Furans Yields via Thermo-Catalytic Reforming process investigating different Feedstocks and Catalysts

João Duarte Navalho Santos

Doctor of Philosophy, 2019

THESIS ABSTRACT

Lignocellulosic biomass is known as a second-generation biomass which means it is non-food competing. It is the most abundant renewable resource existing, and presently it is considered as a promising feedstock for the synthesis of green chemicals and biofuels for reducing transportation emissions and dependence on fossil fuels. Steel slag are by products of the steel industry, which are composed of various metal oxides promoting a catalytic effect on pyrolysis products improving their quality. It is a cheap and sustainable alternative to replace zeolites, the most common cracking catalysts.

In this research, a TCR (Thermo-Catalytic Reforming) reactor and steel slag are used to transform lignocellulosic biomass into high quality bio-oils. TCR is a combination of intermediate pyrolysis followed by a second post reforming step. Intermediate pyrolysis heats biomass to moderate temperatures between 400–500°C in the absence of oxygen, with a short vapour residence time (seconds) and moderate solid residence time (minutes). Post reforming is achieved at temperatures between 500-800°C with extended vapour and char residence times. One characteristic of the process is that the final products (bio-oil, syngas and biochar) contains a higher energy density than the original feedstock (superior than other pyrolysis technologies) having the advantage to be easily transported and stored.

Oat hulls and sugarcane bagasse were processed in the TCR working with temperatures between 400-500 ºC in the intermediate pyrolysis reactor and 500-700 ºC in the reforming unit. Steel slag were applied in the system in two different ways: 1) mixed with the biochar in the reforming unit at different mass ratios (30, 70 and 100 wt% of steel slag); 2) mixed with the feed and introduced in the intermediate pyrolysis reactor at different mass ratios (10, 20 and 30 wt% of steel slag).

The introduction of steel slag in the TCR reactor increased the H_2 yield by 80.0% and consequently the HHV by 12.3% for the syngas. The steel slag also upgraded the bio-oil by reducing the viscosity, water content and acid number by 46.6, 55.1 and 65.7% respectively. Moreover, the HHV of the same bio-oil raised 22.0%. All these improvements make the pyrolysis oil more attractive and suitable to be used as a biofuel.

In terms of furfural and furans, the best results (2.8 and 9.8%, respectively) were achieved by introducing 100 wt% of steel slag in the reformer and using sugarcane bagasse as a feedstock.

Key words: Thermo-Catalytic Reforming, Pyrolysis, Bio-oil, Sugarcane Bagasse, Oat Hulls, Steel Slag.

ACKNOWLEDGEMENTS

The author would like to thank the following:

- His academic supervisor Professor Andreas Hornung of the Fraunhofer UMSICHT Institute and co-supervisor Dr Miloud Ouadi of the Chemical Engineering Department of University of Birmingham for their support, supervision, effort and determination during the execution of this project.

- Fernando Contadini of RenewCo and Christian Furlan of Cosan for providing the sugarcane bagasse for the TCR experiments.

- Dr Nizar Ghazireh of Tarmac for providing the steel slag for the TCR trials.

- All his colleagues of the Bioenergy Group at the Chemical Engineering department for their technical support, enthusiasm, availability and moral help. Special thanks to Dr Hessam Jahangiri and Dr Lais Speranza.

- His family and friends for their unconditional presence and support in any kind of circumstance.

- The Engineering and Physical Science Research Council (EPSRC) for awarding this project.

LIST OF CONTENTS

	Page
1. INTRODUCTION	1-6
1.1 EPSRC Project Scope	3
1.2 PhD Project Aims and Objectives	4
1.3 Thesis Layout	5
2. BACKGROUND	7-47
2.1 Pyrolysis	7-23
2.1.1 Fundamentals of Slow, Intermediate and Fast Pyrolysis	9
2.1.2 Pyrolysis Products	14
2.1.3 Biomass Thermal Decomposition	20
2.2 Pyroformer Reactor and TCR Technology	23
2.3 Current State of the Art for Furfural and 2-MF Production	28
2.4 Xylose-Rich Biomass	34
2.5 Catalytic Pyrolysis	39
3. EXPERIMENTAL METHODOLOGY	48-74
3.1 Raw Materials	48
3.2 Raw Materials Characterisation	50-53
3.2.1 Proximate Analysis	50
3.2.2 Ultimate Analysis	51
3.2.3 Chemical Composition	52
3.2.4 HHV	53
3.2.5 Inductively Couple Plasma (ICP)	53
3.3 TCR Setup	53

3.4 TCR Experimental Procedure 56

3.5 Products Characterisation 67-71

3.5.1 Oil and Char Ultimate analysis 67

3.5.2 Oil and Char Ash content 67

3.5.3 HHV 68

3.5.4 Viscosity 68

3.5.5 Density 69

3.5.6 *Total Acid Number (TAN)* 69

3.5.7 Water Content 69

3.5.8 Gas Chromatography Mass Spectrometry (liquid-GC-MS) 70

3.5.9 Gas Analysis 70

3.6 Bio-oil Upgrading 71-74

3.6.1 HDO Process 71

3.6.2 Catalysts Preparation 73

3.6.3 Porosimetry 73

3.*6.4 X-Ray Diffraction (XRD)* 74

4. RESULTS AND DISCUSSION 75-177

4.1 Raw Materials Characterisation 75-79

4.1.1 Feedstock Characterisation 75

4.1.2 Steel Slag Metal Composition 78

4.2 Different Reforming Temperatures in TCR Process 79-109

4.2.1 Bio-oil Analysis 80

4.2.2 GC-MS Analysis of Bio-oil 90

4.2.3 Gas Analysis 95

4.2.4 Char Analysis 100

4.2.5 Mass Balance and Energy Yield 105

4.3 Different Reactor Temperatures in TCR Process 109-134

4.3.1 Bio-oil Analysis 110

4.3.2 GC-MS Analysis of Bio-oil 116

4.3.3 Gas Analysis 121

4.3.4 Char Analysis 126

4.3.5 Mass Balance and Energy Yield 130

4.4 Steel Slag as an In-situ Catalyst in the TCR process 134-169

4.4.1 Bio-oil Analysis 136

4.4.2 GC-MS Analysis of Bio-oil 142

4.4.3 Gas Analysis 149

4.4.4 Char Analysis 154

4.4.5 Mass Balance and Energy Yield 161

4.4.6 Textural Properties 165

4.5 HDO of TCR bio-oil 169-177

4.5.1 GC-MS Analysis of Bio-oil 170

4.5.2 Bio-oil Analysis 174

5. CONCLUSIONS AND FUTURE WORK 178

REFERENCES 185

APPENDIX A 214

APPENDIX B 215

APPENDIX C 218

LIST OF PUBLICATIONS 250

LIST OF ILLUSTRATIONS

Page

Figure 1 - Pyrolysis products applicability 8

Figure 2 - TCR char 15

Figure 3 - TCR oil 17

Figure 4 - Biomass compounds: (a) cellulose, (b) hemicellulose, and (c) lignin 20

Figure 5 - Pyrolysis primary reactions 21

Figure 6 - Pyroformer reactor 24

Figure 7 - TCR reactor (lab scale) installed at Fraunhofer UMSICHT 25

Figure 8 - Simplified reaction mechanism of acidic degradation of pentosan to furfural 29

Figure 9 - Hydrogenation and HDO of furfural to MF 31

Figure 10 - Oat hulls 36

Figure 11 - Sugarcane bagasse 37

Figure 12 - Catalytic pyrolysis reactions of biomass 40

Figure 13 - In-situ and ex-situ catalytic pyrolysis 42

Figure 14 - Steel slag (6 mm) 46

Figure 15 - Sugarcane bagasse pellets 49

Figure 16 - Oat hulls pellets 50

Figure 17 - PFD of the TCR-2 plant 54

Figure 18 - TCR-2 software (Siemens SIMATIC Win CC) 55

Figure 19 - Cleaning of the auger screw reactor 56

Figure 20 - Post reformer disassembled and empty 57

Figure 21 - Post reformer gas tube before and after cleaning 58

Figure 22 - Condensing unit being cleaned 58

Figure 23 - Post reformer connected to the auger pyrolysis reactor and condensing unit 59

Figure 24 - Washing bottle containing TCR aqueous phase from bio-oil 60

Figure 25 – Gas filtration unit (activated carbon, candle and glass wool filters) 60

Figure 26 - Feed hopper where the pelletised biomass was introduced 62

Figure 27 - TCR oil (aqueous phase on the top; organic phase on the bottom) 63

Figure 28 - Pelletisation with SS: (a) OH mixed with SS (30 wt%), (b) OH pellets, and (c) SS powder 65

Figure 29 - HDO autoclave reactor 72

Figure 30 - Filtration of HDO bio-oil 73

Figure 31 - GC-MS chromatograms of SB bio-oil and compounds detected at 450 ºC (reactor temperature) and different reforming temperatures (500, 600 and 700 °C) 92

Figure 32 - GC-MS chromatograms of OH bio-oil and compounds detected at 450 ºC (reactor temperature) and different reforming temperatures (500, 600 and 700 °C) 93

Figure 33 - Mass balance of SB and OH trials at different reforming temperatures (pyrolysis temperature = 450 ºC) 106

Figure 34 - Energy yield of SB and OH trials at different reforming temperatures (pyrolysis temperature = 450 ºC) 108

Figure 35 - GC-MS chromatograms of SB bio-oil and compounds detected at 500 ºC (reforming temperature) and different pyrolysis temperatures (400, 450 and 500 °C) 118

Figure 36 - GC-MS chromatograms of OH bio-oil and compounds detected at 500 ºC (reforming temperature) and different pyrolysis temperatures (400, 450 and 500 °C) 119

Figure 37 - Mass balance of SB and OH trials at different pyrolysis temperatures (reforming temperature = 500 ºC) 131

Figure 38 - Energy yield of SB and OH trials at different pyrolysis temperatures (reforming temperature = 500 ºC) 134

Figure 39 - GC-MS chromatograms of SB bio-oil and compounds detected at 400 and 500 ºC (pyrolysis and reforming temperature) and different SS ratios in the reformer 145

Figure 40 - GC-MS chromatograms of OH bio-oil and compounds detected at 400 and 500 ºC (pyrolysis and reforming temperature) and different SS ratios in the reformer 146

Figure 41 - GC-MS chromatograms of OH bio-oil and compounds detected at 400 and 500 ºC (pyrolysis and reforming temperature) and different SS ratios in the OH feed 147

Figure 42 - Mass balance of SB and OH trials at different SS ratios (Pyrolysis and Reforming temperatures = 400 and 500 ºC) 160

Figure 43 - Energy yield of SB and OH trials at different SS ratios (Pyrolysis and Reforming temperatures = 400 and 500 ºC) 163

Figure 44 - X-ray diffractograms of SS, SB raw, SB char, OH raw and OH char 168

Figure 45 - GC-MS chromatograms of TCR bio-oil after HDO treatment 173

LIST OF TABLES

Page

Table 1 - Conditions and product distribution of different types of pyrolysis 8

Table 2 - TCR-2 experimental parameters 66

Table 3 - Feedstock characterisation 77

Table 4 - SS metal composition 79

Table 5 - TCR run conditions with different reforming temperatures 80

Table 6 - SB and OH bio-oil characterization at different reforming temperatures (Pyrolysis temperature = 450 ºC) 81

Table 7 - Bio-oil and fuel properties from literature review at different reforming temperatures using several feedstocks and pyrolysis technologies 85

Table 8 - Compounds detected and identified by GC-MS of the SB and OH bio-oil at different reforming temperatures (pyrolysis temperature = 450 ºC) 91

Table 9 - SB and OH permanent gas composition at different reforming temperatures (Pyrolysis temperature = 450 ºC) 96

Table 10 - Pyrolysis gas composition from literature review at different reforming temperatures using several feedstocks and pyrolysis technologies 98

Table 11 - SB and OH biochar characterisation at different reforming temperatures (Pyrolysis temperature = 450 ºC) 101

Table 12 - Biochar characterization from literature review at different reforming temperatures using several feedstocks and pyrolysis technologies 103

Table 13 - TCR runs conditions with different pyrolysis temperatures 109

Table 14 - SB and OH bio-oil characterization at different pyrolysis temperatures (Reforming temperature = 500 ºC) 111

Table 15 - Bio-oil and fuels properties from literature review at different pyrolysis temperatures using several feedstocks and pyrolysis technologies 114

Table 16 - Compounds detected and identified by GC-MS of the SB and OH bio-oil at different pyrolysis temperatures (reforming temperature = 500 ºC) 117

Table 17 - SB and OH permanent gas composition at different pyrolysis temperatures (Reforming temperature = 500 ºC) 123

Table 18 - Pyrolysis gas composition from literature review at different pyrolysis temperatures using several feedstocks and pyrolysis technologies 125

Table 19 - SB and OH biochar characterisation at different pyrolysis temperatures (Reforming temperature = 500 ºC) 127

Table 20 - Biochar characterization from literature review at different pyrolysis temperatures using several feedstocks and pyrolysis technologies 129

Table 21 - TCR runs conditions applying different ratios of SS in 2 methods 135

Table 22 - SB and OH bio-oil characterization at different SS ratios (Pyrolysis and Reforming temperatures = 400 and 500 ºC) 137

Table 23 - Bio-oil and fuels properties from catalytic pyrolysis found in the literature review 141

Table 24 - Compounds detected and identified by GC-MS of the SB and OH bio-oil at different SS ratios (Pyrolysis and Reforming temperatures = 400 and 500 ºC) 144

Table 25 - SB and OH permanent gas composition at different SS ratios (Pyrolysis and Reforming temperatures = 400 and 500 ºC) 150

Table 26 - Pyrolysis gas composition from catalytic pyrolysis found in the literature review 153

Table 27 - SB and OH biochar characterisation at different SS ratios (Pyrolysis and Reforming temperatures = 400 and 500 ºC) 155

Table 28 - Biochar characterization from catalytic pyrolysis found in the literature review 158

Table 29 - Texture properties of SS, SB raw, OH raw, SB char and OH char 166

Table 30 - HDO conditions applying different temperatures and catalysts 170

Table 31 - Compounds detected and identified by GC-MS of TCR bio-oil after HDO treatment 172

Table 32 - TCR bio-oil characterization after HDO treatment 175

Table 33 - Bio-oil and fuels properties from HDO treatment found in the literature review 176

Table 34 - Mass balance calculations (1) 215

Table 35 - Mass balance calculations (2) 216

Table 36 - Energy yield calculations 217

Table 37 - SB characterisation (average, standard deviation and coefficient of variation) 218

Table 38 - OH characterisation (average, standard deviation and coefficient of variation) 218

Table 39 - SB bio-oil characterisation at different reforming temperatures (Pyrolysis temperature = 450 °C) (average, standard deviation and coefficient of variation) 219

Table 40 - OH bio-oil characterisation at different reforming temperatures (Pyrolysis temperature = 450 °C) (average, standard deviation and coefficient of variation) 220

Table 41 - SB gas compositon at different reforming temperatures (Pyrolysis temperature = 450 °C) (average, standard deviation and coefficient of variation) 221

Table 42 - OH gas compositon at different reforming temperatures (Pyrolysis temperature = 450 °C) (average, standard deviation and coefficient of variation) 222

Table 43 - SB biochar characterisation at different reforming temperatures (Pyrolysis temperature = 450 °C) (average, standard deviation and coefficient of variation) 223

Table 44 - OH biochar characterisation at different reforming temperatures (Pyrolysis temperature = 450 °C) (average, standard deviation and coefficient of variation) 224

Table 45- Mass balance of SB trials at different reforming temperatures (Pyrolysis temperature = 450 °C) (average, standard deviation and coefficient of variation) 225

Table 46 - Mass balance of OH trials at different reforming temperatures (Pyrolysis temperature = 450 °C) (average, standard deviation and coefficient of variation) 226

Table 47 - Energy yield of SB trials at different reforming temperatures (Pyrolysis temperature = 450 °C) (average, standard deviation and coefficient of variation) 227

Table 48 - Energy yield of OH trials at different reforming temperatures (Pyrolysis temperature = 450 °C) (average, standard deviation and coefficient of variation) 228

Table 49 - SB bio-oil characterisation at different pyrolysis temperatures (Reforming temperature = 500 °C) (average, standard deviation and coefficient of variation 229

Table 50 - OH bio-oil characterisation at different pyrolysis temperatures (Reforming temperature = 500 °C) (average, standard deviation and coefficient of variation) 230

Table 51 - SB gas compositon at different pyrolysis temperatures (Reforming temperature = 500 °C) (average, standard deviation and coefficient of variation) 231

Table 52 - OH gas compositon at different pyrolysis temperatures (Reforming temperature = 500 °C) (average, standard deviation and coefficient of variation) 232

Table 53 - SB biochar characterisation at different pyrolysis temperatures (Reforming temperature = 500 °C) (average, standard deviation and coefficient of variation) 233

Table 54 - OH biochar characterisation at different pyrolysis temperatures (Reforming temperature = 500 °C) (average, standard deviation and coefficient of variation) 234

Table 55 - Mass balance of SB trials at different pyrolysis temperatures (Reforming temperature = 500 °C) (average, standard deviation and coefficient of variation) 235

Table 56 - Mass balance of OH trials at different pyrolysis temperatures (Reforming temperature = 500 °C) (average, standard deviation and coefficient of variation) 236

Table 57 - Energy yield of SB trials at different pyrolysis temperatures (Reforming temperature = 500 °C) (average, standard deviation and coefficient of variation) 237

Table 58 - Energy yield of OH trials at different pyrolysis temperatures (Reforming temperature = 500 °C) (average, standard deviation and coefficient of variation) 238

Table 59 - SB bio-oil characterisation at different SS ratios (Pyrolysis and Reforming temperatures = 400 and 500 °C) (average, standard deviation and coefficient of variation) 239

Table 60 - OH bio-oil characterisation at different SS ratios (Pyrolysis and Reforming temperatures = 400 and 500 °C) (average, standard deviation and coefficient of variation) 240

Table 61 - SB gas compositon at different SS ratios (Pyrolysis and Reforming temperatures = 400 and 500 °C) (average, standard deviation and coefficient of variation) 241

Table 62 - OH gas compositon at different SS ratios (Pyrolysis and Reforming temperatures = 400 and 500 °C) (average, standard deviation and coefficient of variation) 242

Table 63 - SB biochar characterisation at different SS ratios (Pyrolysis and Reforming temperatures = 400 and 500 °C) (average, standard deviation and coefficient of variation) 243

Table 64 - OH biochar characterisation at different SS ratios (Pyrolysis and Reforming temperatures = 400 and 500 °C) (average, standard deviation and coefficient of variation) 244

Table 65 - Mass balance of SB trials at different SS ratios (Pyrolysis and Reforming temperatures = 400 and 500 °C) (average, standard deviation and coefficient of variation) 245

Table 66 - Mass balance of OH trials at different SS ratios (Pyrolysis and Reforming temperatures = 400 and 500 °C) (average, standard deviation and coefficient of variation) 246

Table 67 - Energy yield of SB trials at different SS ratios (Pyrolysis and Reforming temperatures = 400 and 500 °C) (average, standard deviation and coefficient of variation) 247

Table 68 - Energy yield of OH trials at different SS ratios (Pyrolysis and Reforming temperatures = 400 and 500 °C) (average, standard deviation and coefficient of variation) 248

Table 69 - TCR bio-oil characterization after HDO treatment (average, standard deviation and coefficient of variation) 249

LIST OF ABBREVIATIONS

2-MF	2-Methlyfuran
BET	Brunauer–Emmet–Teller
BJH	Barrett, Joyner, and Halenda
CHP	Combined heat and power
EPSRC	Engineering and Physical Science Research Council
GC-MS	Gas Chromatography Mass Spectrometry
HDO	Hydro deoxygenation
HHV	Higher heating value
HPLC	High-performance liquid chromatography
ICP	Inductively Couple Plasma
MSW	Municipal Solid Waste
OH	Oat hulls
PAHs	Polycyclic aromatic hydrocarbons
PCBs	Polychlorinated biphenyls
PFD	Process flow diagram
SB	Sugarcane bagasse
SS	Steel slag
TCR	Thermo-Catalytic Reforming
TGA	Thermo Gravimetric Analysis
TAN	Total acid number
WP	Work Packages
XRD	X-ray diffraction

1. INTRODUCTION

This chapter has the goal of exposing the main ideas for the current project, presenting the relevant information of this research work in terms of aims, fundamental concepts and vital strategies for the present and future context. The impact of biomass and biofuels as an alternative source of energy is contextualised according to the environmental and economic dynamics inside of the European reality.

Biofuels are considered one of the most efficient routes for reducing transportation emissions and dependence on fossil fuels. Among many possibilities of biofuel production and supply, fuels from biomass are very interesting because they do not contribute to extra CO_2 emissions and additionally this option reduces the amount of biogenic wastes and residues entering landfill and incinerators. Additionally, the use of agricultural waste such as oat hulls and sugarcane bagasse is advantageous for the biofuels sector because it does not compete with food production and land use to grow energy crops (Rathmann et al., 2010). Lignocellulosic biomass is the most abundant renewable resource existing and is the only source of renewable fixed carbon. Presently it is considered a promising feedstock for the production of sustainable fuels for the future (Lichtenthaler and Peters, 2004).

Sugars obtained from cellulose and hemicellulose can be converted to bioethanol via fermentation, but this process is not economic or efficient, as it is very energy intensive (Börjesson, 2009). In addition, 1st generation biomass for energy production competes with its use to grow food crops making less land available for agricultural purposes (Stefanidis et al., 2014). For that reason, furan series have started to receive increasing attention as a novel fuel candidate. Converting sugars from cellulose and

hemicellulose into furans through hydrolysis and acid-catalysed dehydration is also possible. However, the process is not profitable or efficient due to the energy intensity of the process and also because concentrated sulphuric acid is used as a catalyst, which is particularly corrosive and extremely toxic increasing the cost for equipment maintenance and requires expensive construction materials (Dias et al., 2005). In addition, the synthetic process requires the use of externally sourced hydrogen and many solvents and catalysts which further increase operational costs. For industrial scale-up, the process must take many steps to achieve the final product for mass production. All these facts can encourage furans production using the Thermo-Catalytic Reforming (TCR) process, which may be a more economically viable process and thus have started to attract more attention as an alternative process route (Huber, Iborra et al. 2006, Lange, van der Heide et al. 2012).

Furans have been used as gasoline additive blending components for many decades and indeed the properties of 2-Methylfuran (2-MF) are recognised for one of the most promising fuels to be used in engines (Roman-Leshkov et al., 2007). 2-MF boiling point (64 ºC) is lower than ethanol (78 ºC) and consequently closer to gasoline (32.8 ºC). Its lower flash point (-22 ºC) is a clear advantage to avoid the cold engine start issues normally linked to bio-ethanol. Moreover, ethanol energy density (21.3 MJ/L) is approximately 25% lower than 2-MF (28.5 MJ/L), implying lower mileage (Zhang et al., 2013). It is stable in storage and cannot become contaminated by absorbing water from the atmosphere, as is the case with ethanol. The double bonds of furans molecules indicate their higher resistance to auto-ignition and therefore to engine knocking. 2-MF is also expected to have some beneficial effect on the reduction of particulate emissions because of the presence of oxygen in the molecule (Zhao et al., 2007).

In this research, TCR process is proposed to combine intermediate pyrolysis with post catalytic reforming in the complete absence of oxygen converting lignocellulosic biomass into bio-oil, which may contain furfural, furfural alcohols, and a range of other oxygenated aromatic compounds as intermediate liquid products. The novelty of TCR technology is the utilisation of char as the catalyst for upgrading pyrolysis liquids. Furthermore, the internal hydrogen synthetized can be used for the hydro treatment upgrading step to achieve the desirable 2-MF production, without the need for externally sourced hydrogen.

1.1 EPSRC Project Scope

This project was funded by the Engineering and Physical Science Research Council (EPSRC) leading to a collaboration between the University of Birmingham (School of Biosciences, Environmental Health Sciences group, Chemical and Mechanical Engineering) and Fraunhofer UMSICHT Germany. It was an important part of the development initiatives of biomass conversion using TCR technology, with the focus on making furan fuels. The research programme consists of 3 main Work Packages (WP):

- WP1 - Modelling and experimental study of furan bio-oils as engine fuels. The products made from the TCR are complex and a reasonable yield of furans is desired, given its attractive properties. When biomass-derived furan products are used in engines as fuels, there will be some uncertainties. No one has tested furans produced via the TCR process as mixtures with other compounds for combustion engine use. This will be the first time to examine combustion characteristics and emissions of a furan bio-oil (different from the pyrolysis product) in automotive engines.

- WP2 - Production, characterisation and catalytic optimisation of furans from biomass (described in the section 1.2).
- WP3 - Study of impact on human health and the environment. The assessment of toxicological effect and impact on human health and environment by biofuels containing furans will also be the first time to answer questions in the relevant concerns from the public. It is expected that the toxicity of furans will be acceptable for use as fuels, but the answer can only become available after the research.

This project revealed the perspective of a novel pathway for novel biofuels from biomass catalytic conversion.

1.2 PhD Project Aims and Objectives

The project aim is to investigate an entire technological route for the use and production of 2-Methylfuran (2-MF) and other furans precursors to 2-MF (furfural and furfuryl alcohol) within a mixture of bio-oil produced from a TCR process, as a novel engine fuel through biomass thermal conversion.

This research is part of the WP2 of the EPSRC project and it aims to achieve the following goals:

a) To improve the understanding of concepts for production of bio-oils with 2-MF and other furans as a component within the oil starting with lignocellulosic biomass.
b) To develop practical technology methods for the efficient production of biofuels containing 2-MF and other furans.

c) To optimise the yield of 2-MF through catalytic upgrading of bio-oils.

In this research, TCR technology is used to transform lignocellulosic biomass into bio-oil. It is crucial to define the ideal biomass type and understand its thermal degradation behaviour and also the chemical compounds produced during the pyrolysis of the feedstock. This will establish the optimal parameters for experiments using the TCR process.

The bio-oils obtained will be tested to determine their fuel physical and chemical compositions. The idea is to verify if the TCR process produced sufficient yields of bio-oil containing reasonable furfural and intermediate compounds for a further upgrading step to 2-MF.

Once optimal yields of furfural and furfuryl alcohols in the TCR bio-oil are obtained, the intermediate liquid will be submitted to a consequent hydro deoxygenation (HDO) step for upgrading to 2-MF.

1.3 Thesis Layout

The thesis is organized mainly into 4 Chapters: background (literature review), experimental methodology, experimental results (with the respective discussion) and conclusions. Numerous and different points are discussed between the different chapters, which are broken down further into sub sections:

a) Background (Chapter 2) – a general literature review is performed to emphasize the main topics related to this project. This chapter looks into the three main groups of pyrolysis (slow, intermediate and fast), the features and advantages of the TCR technology, the current process to produce furans and 2-MF, the use of

biochar and steel slag (SS) as a catalyst in pyrolysis processes and the HDO treatment to convert furans in 2-MF.

b) Experimental Methodology (Chapter 3) – the practical methodology is described and explained in terms of chemical and physical characterisation of the feedstocks and TCR products (bio-oil, biochar and syngas). The TCR and HDO experimental procedures are also covered in this chapter.

c) Results and Discussion (Chapter 4) – this chapter shows all the results and practical work developed. The TCR reactor processed sugarcane bagasse (SB) and oat hulls (OH) with temperatures between 400-500 °C in a first stage (auger pyrolysis reactor) and then a maximum of 700 °C in a second stage post-reforming reactor. SS are also tested as a catalyst in two different scenarios: mixing with the feedstock and mixing with biochar inside of the post-reforming reactor. Bio-oil upgrading through HDO using Cu based catalyst is also investigated in this chapter.

d) Conclusions and Future Work (Chapter 5) – overall conclusions and recommendations.

e) References

f) Appendix

2. BACKGROUND

The present chapter starts with an overview of the fundamentals of slow, intermediate and fast pyrolysis, followed by the properties and applicability of the pyrolysis products and the thermal composition of the biomass. This chapter also identifies the features and advantages of the TCR process, the current pathways for furans and 2-MF formation and the selection of the ideal biomass according to the objectives of this work. The use of SS, biochar and other catalyst to improve the pyrolysis products are also explored. Lastly, a general description of HDO treatment to produce 2-MF from furans is discussed.

2.1 Pyrolysis

Pyrolysis is the thermal degradation of biomass and it involves a group of chemical mechanisms producing radical elements. This process is endothermic requiring a heat input and it works with lower temperatures (300-800 ºC) when compared to gasification (800-1200 ºC) (Mahmood, Brammer et al. 2013). After moisture removal, pyrolysis is the first stage of gasification and combustion technologies and it is generally characterised into three main groups: slow, intermediate, fast and flash (Collard and Blin 2014). Each applies different heating rates, temperatures and vapour/solid residence times to the feedstock, however a common parameter is that heating of the feedstock always occurs in the absence of oxygen (Wang, Dai et al. 2017). Every type of pyrolysis process produces the same products (bio-oil, biochar and syngas) which are highly variable depending on the pyrolysis technique applied. The different applications of the pyrolysis products can be found in Figure 1.

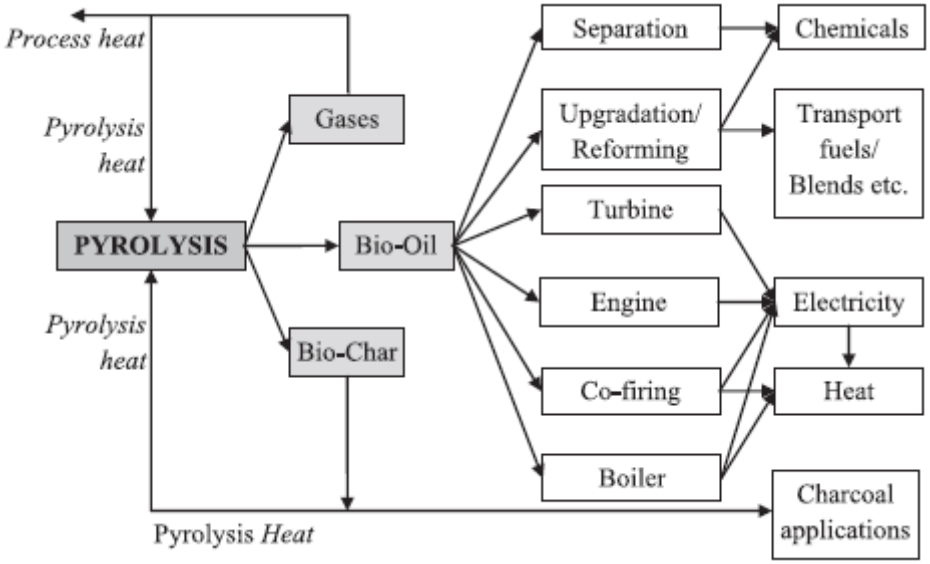


Figure 1 – Pyrolysis products applicability (Dhyani and Bhaskar 2018)

Low temperatures and extended solids residence time optimise the biochar formation, mild temperatures and moderate solids residence time favour liquids production (but with lower yields than fast and flash pyrolysis), and high temperatures with very short residence times enhance the conversion of feedstock to bio-oil (Bridgwater 2012). The three pyrolysis groups are specified in Table 1.

Table 1 - Conditions and product distribution of different types of pyrolysis (Bridgwater 2012)

Type	Conditions	Char	Bio-oil	Gas
Slow	~300 ºC, long solid residence time (hrs.-days)	35%	30%	35%
Intermediate	~400 ºC, moderate solid residence time (min)	25%	50%	25%
Fast	~500 ºC, short solid residence time (< 2s)	12%	75%	13%
Flash	~600 ºC, short solid residence time (< 1s)	7%	83%	10%

Intermediate pyrolysis also works with higher temperatures and the char yield can increase depending on the feedstock (Hornung 2013). Therefore, it is crucial to emphasize the role of the chemical nature of the feedstock in the pyrolysis products composition and distribution (Collard and Blin 2014).

2.1.1 Fundamentals of Slow, Intermediate and Fast Pyrolysis

Typically, slow pyrolysis is a batch system despite of the existence of a few works using the continuous process (Crombie and Mašek 2014, Cong, Mašek et al. 2018). It involves slow heating rates, low temperatures (normally below 300 ºC) long residence times and the main product is char (Park, Lee et al. 2014). The majority of the slow pyrolysis works are oriented for biochar formation and utilisation, however the liquids and gases produced can also be used as a fuel at the production site (Stamatov, Honnery et al. 2006). In addition, the high content of acetic acid and other acids compounds in the oil make this pyrolysis liquid suitable for pesticide applications (Hagner, Tiilikkala et al. 2018). This process can tolerate water present in the biomass, which has a direct effect on the biochar properties promoting the formation of activated carbons (Carrier, Hugo et al. 2011). For biochar production moisture content between 15 and 20% is the usual range (Park, Lee et al. 2014). The feedstock particle size can differ from wood logs to pellets and although the wood is the most common biomass for slow pyrolysis, this process can also work with rice straw, palm, bamboo, sugarcane bagasse and nut shells (Aziz and Deraman 2013, Moreira, Orsini et al. 2017).

Carbonisation is the oldest method for biomass processing and consequent char production, where the solid residue is the wanted product (Carrier, Hugo et al. 2011). It

consists in slow pyrolysis without the condensation of the vapours, which can be used to provide heat to the system (Antal and Gronli 2003).

Torrefaction is another approach to apply slow pyrolysis, operating with mild temperatures (225-300 ºC) to improve the biomass fuel properties and the respective calorific value (Prins, Ptasinski et al. 2006). During torrefaction surplus volatiles and moisture are extracted from the biomass, while the main compounds (cellulose, hemicellulose and lignin) are partially degraded originating the organic volatiles (van der Stelt, Gerhauser et al. 2011). The final material is solid called “torrefied” biomass and it is easier to be stored and transported due to the reduction of volume and weight improving the energy density per unit volume (Batidzirai, Mignot et al. 2013). Torrefied feedstock needs less power to be grinded and its hydrophobic features make this solid residue more resistant in terms of water absorption (Prins, Ptasinski et al. 2006, van der Stelt, Gerhauser et al. 2011). Torrefaction is also considered as a biomass pre-treatment for pelletisation, combustion, pyrolysis and gasification originating a syngas with lower tars content and making these thermo-chemical processes more efficient and easier to operate (Batidzirai, Mignot et al. 2013).

Intermediate pyrolysis requires mild temperatures (around 400 °C), moderate heating rates (200-300 ºC/min), efficient cooling system for the organic vapours to minimise thermal post-degradation, solid residence times in minutes with a short vapour residence time (seconds) (Neumann, Meyer et al. 2016) and produces relatively equal yields of all products (solids, liquids and gas).

Depending on the feedstock and process parameters applied, intermediate pyrolysis can yield energy vectors with improved physical and chemical properties

(Neumann, Meyer et al. 2016). This process is capable of converting large materials (chips, pellets and briquettes) and also fine particles down to dust (from shredding, grinding and chopping) with higher moisture contents when compared to other pyrolysis technologies (Hornung 2013). Intermediate pyrolysis has the ability to process a varied range of materials, such as industrial residues, sewage sludge, organic waste, algae, digestate, forest residues, grass, de-inking sludge and agricultural waste (Mahmood, Brammer et al. 2013, Ouadi, Brammer et al. 2013).

The products from the intermediate process present different properties compared to the slow and fast pyrolysis. Slow and intermediate pyrolysis are the most suitable techniques to produce biochar, however intermediate pyrolysis offers shorter solid residence times (Hornung 2013). Moreover, slow pyrolysis is a limited process mostly used for char formation and it is rarely seen to produce a reasonable bio-oil (high tars content) or to be associated with combustion to generate heat and power (Yang, Brammer et al. 2014).

The most relevant variation between fast and intermediate technologies is the solid residence times, causing a different heating rate to the biomass. It leads to a better control of the chemical reactions and a lower thermal cracking of the bio-components in the intermediate pyrolysis, resulting in less tar formation and a general optimization of the process (Dhyani and Bhaskar 2018). Pyrolysis oil from the intermediate process contains less viscosity, tars and ashes (lower contamination level) and it is easier to separate the organic phase from the aqueous phase, contrasting with fast pyrolysis (Zhang, Chang et al. 2007, Yang, Brammer et al. 2014). Another limitation of fast pyrolysis is the processing of different feedstocks, which need to have a low water content and a fine particle size when processed by a fluidised bed reactor (extra energy to mill or grind)

making the separation between vapours and char harder (Hornung, Apfelbacher et al. 2011). This requires extra filters and post cyclones to extract the dust and char present in the pyrolysis gases. Furthermore, fast pyrolysis is only well succeeded converting woody feedstocks and normally the bio-oil produced is rich in ashes, water, tars and acids (Abu El-Rub, Bramer et al. 2004, Mahmood, Brammer et al. 2013).

The benefits of mixing biochar with fresh biomass were proven via intermediate pyrolysis. The extended residence time of the solid residue has a catalytic effect in the quality of the bio-oil, increasing the calorific value, producing lighter organic compounds (mainly aromatics such as benzene, toluene and ethylbenzene and olefins) and reducing the moisture content and viscosity (Hornung, Apfelbacher et al. 2011, Ouadi, Brammer et al. 2013).

Solids, liquids and vapours from intermediate pyrolysis have interesting chemical and physical properties that can be used as energy vectors. The biochar can be used as solid fuel in gasification and combustion plants to generate heat and power (Yang, Brammer et al. 2014). It can also be an optimum soil fertilizer/conditioner (depending on feedstock), which can sequester carbon from the soil (Kebelmann, Hornung et al. 2013). The bio-oil presents a low level of oxygen, water, tars and viscosity, being a good fuel to combust in boilers, engines and other heat/power systems (Ouadi, Kay et al. 2012). After upgrading, the intermediate pyrolysis oil can be blended with gasoline and diesel and applied as a transportation fuel in conventional engines (Hossain, Ouadi et al. 2013). The gas fraction contains a low ash content and a reasonable amount of condensable organic vapours, which offer a good calorific value to be burnt in combined heat and power (CHP) systems (Kebelmann, Hornung et al. 2013).

Fast pyrolysis is a continuous process and it applies high heating rates, short vapour residence times and yields higher quantities of liquids (up to 75 wt% on a dry basis) (Yang, Brammer et al. 2014). Under these parameters the organic material degrades very fast forming char and pyrolysis gases, which are condensed generating the bio-oil and non-condensable gaseous compounds considered as a remaining product (Pattiya 2018). The aim of fast pyrolysis is to avoid extra breaking of the pyrolysis products into non-condensable elements to maximise the liquid yields (the desirable product), controlling rigorously the following process conditions (Bridgwater 2012, Dickerson and Soria 2013, Blanco and Chejne 2016):

a) Very high heating rates (up to 300 ºC/s) to raise the heat transfer on the feedstock particles.
b) Reaction temperatures around 500 ºC and vapours temperature between 400-450 ºC. These conditions maximise bio-oil yields at the expense of permanent gases and char.
c) Short solid and vapour residence times (usually less than 2 seconds) to reduce secondary reactions.
d) Fine biomass particle size (normally less than 3 mm) to guarantee quick reactions, higher thermal conductivity and heat transfer in fluidised bed reactors.
e) Feed moisture content below 10 wt% to decrease the water in the bio-oil.
f) High condensation efficiency for the organic vapours to minimise thermal post-degradation and increase the bio-oil formation and collection.
g) Quick extraction of the biochar to reduce vapour cracking.

Theoretically, fast pyrolysis is able to convert any kind of biomass. However, this process has only shown consistent and reasonable results using woody feedstocks (Pattiya 2018). The feedstock composition and the process parameters influence the type of pyrolysis chemical mechanisms in the reactor, but normally the reactions taking place are a combination of polymerisation, rearrangement, breaking and dehydration (Dickerson and Soria 2013).

Bio-oil production through fast pyrolysis has some benefits such as high thermal efficacy, atmospheric pressure conditions and the simplicity of the operation (Oasmaa, Kuoppala et al. 2003). This pyrolytic liquid can be applied as an energy vector or for production of chemical compounds (Czernik and Bridgwater 2004). The secondary products of fast pyrolysis (solid residue and gas fraction) are also considered to be valuable materials for heat and power generation (Czernik and Bridgwater 2004).

2.1.2 Pyrolysis Products

There are three main products from the biomass pyrolytic process, which are the biochar, the bio-oil and the permanent gas fraction. Their properties and yields are influenced mainly by biomass composition and pyrolysis conditions.

Biochar (Figure 2) is an aromatic polycyclic carbon and solid residue left after the pyrolysis conversion of carbonaceous biomass characterised by a high proportion of carbon, low volatility and small amounts of hydrogen and oxygen (Dhyani and Bhaskar 2018). However, TCR biochar is free of polycyclic aromatic hydrocarbons (PAHs) and polychlorinated biphenyls (PCBs) and it contains a low level of dioxins being a reliable and valid carbon source in terms of safety, health and environmental concerns. Usually, the char is extracted from the gas fraction in the cyclone step and it contains the majority

of the inorganic material existing in the original feed. The physical and chemical features of the biochar are affected by the pyrolysis parameters and feedstock composition. For example, the higher heating value (HHV) can vary from 20 to 36 MJ/kg and the carbon amount between 53 and 96 wt% (Hu and Gholizadeh 2019). Additionally, during pyrolysis, the biochar production may range from 10 to 40 wt% depending on the process conditions. In terms of physical properties, the temperature can increase the surface area between 100 and 500 m^2/g due to the formation of a microporous structure (Chen, Yang et al. 2016). Below 400 °C, there is an incomplete elimination of biomass volatiles and consequently, the alteration of the char surface area is insignificant. From 400 to 900 °C, the surface area of the biochar starts to rise gradually (Hu and Gholizadeh 2019).



Figure 2 - TCR char

Biochar has the capacity to retain water in different soils (up to 25% compared with no added biochar treatments) and to provide carbon, nitrogen and inorganics for agricultural fields improving the quality of the crops (Mollinedo, Schumacher et al.

2015). Moreover, it is extremely stable when introduced in the soil environment and it can perform carbon sequestration for hundreds of years (Laird 2008). For those reasons, biochar is considered to be an optimum fertiliser and soil amendment, being utilised for hundreds of years as an eco-friendly solution to improve and remediate the quality of the soils (Hood-Nowotny, Watzinger et al. 2018). Energy production is also one of the ways to valorise the biochar from pyrolysis. It can be a solid fuel for combustion, gasification and boilers, fulfil the heating necessities for pyrolysis, and for syngas/hydrogen production through thermal cracking treatment or steam reforming (Huber, Iborra et al. 2006, Goyal, Seal et al. 2008). Some works explored the biochar microscopic surface area for the elimination of contaminants in gas and water, by the adsorption of metal ions from water and the removal of SO_2 or NO_x present in the gas (Ahmad, Rajapaksha et al. 2014, Mohan, Sarswat et al. 2014). Another application of the char is the catalytic conversion, which is related to its surface properties and inorganic composition (Mullen, Boateng et al. 2010).

Bio-oil (Figure 3) is a dark brown organic liquid produced from the pyrolytic conversion of biomass and it is the most interesting energy vector in the pyrolysis process (Hu and Gholizadeh 2019). This oil is formed through a quick condensation of the organic vapours and it results of the depolymerisation and thermal breaking of hemicellulose, lining and cellulose (Lede, Diebold et al. 1997). It is composed of water, nitrogen and hundreds of chemical species such as esters, alkenes, aldehydes, ethers, ketones, acids, furans, alcohols, sugars, phenols and other oxygenated compounds making this pyrolysis product reactive and thermodynamically unstable (Milne, Agblevor et al. 1997, Isahak, Hisham et al. 2012). For that reason, it is necessary to upgrade the bio-oil for fuel engine

applications. Viscosity is also a relevant requirement for the pyrolysis oil, impacting the pumping and fuel spraying performances of the engine. According to some studies, the viscosity of the oil should be no more than 20 mm^2/s at 40 ºC (Garcìa-Pérez, Chaala et al. 2006).



Figure 3 - TCR oil

The bio-oil properties are influenced by some processing conditions such as solids residence time, heating rate, temperature, kind of biomass and particle size of the feed. Some pyrolysis secondary reactions produce water, which is present in the bio-oil composition creating two separate fractions (organic phase and aqueous phase). The aqueous phase is a mixture of water solvable compounds (mostly phenol, acid acetic and hydroxyl acetone) and due to its limited chemical properties (such as heating value) cannot be applied as a fuel vector (Zhang, Yan et al. 2005). A catalytic treatment via reforming which promotes water-gas shift reactions helps to valorise the aqueous phase

producing green hydrogen (Li, Xu et al. 2009). The organic fraction can be exploited as a fuel (directly or upgraded to improve the oil quality) or for the production of chemical compounds. Generation of heat and power through gas turbines/engines, furnaces, combustors and boilers are some of the applications for the organic phase of the bio-oil without catalytic conversion which has shown success (Gust 1997, Chiaramonti, Bonini et al. 2003). For transportation purposes, the pyrolysis oil can be treated via the upgrading process (such as HDO, emulsification, hydrocracking and catalytic esterification) and mixed with gasoline and diesel to be used in engines (Goyal, Seal et al. 2008). Valuable chemicals can also be extracted in the organic phase to be applied in flavouring additives, pharmaceutical compounds, preservatives, fertilising material and resin components (Czernik and Bridgwater 2004, Balat 2011).

The gas produced in pyrolysis is the consequence of the degradation and cracking of complex compounds from the original biomass. It is mainly composed of carbon monoxide (CO), hydrogen (H_2), carbon dioxide (CO_2), methane (CH_4) and other light hydrocarbons such as ethane, propane and propene (Park, Yoo et al. 2012). If the condensation process is not efficient, the pyrolytic gas can contain some volatiles such as xylenes, benzene, acetaldehyde, pentane and toluene (Pattiya 2018).

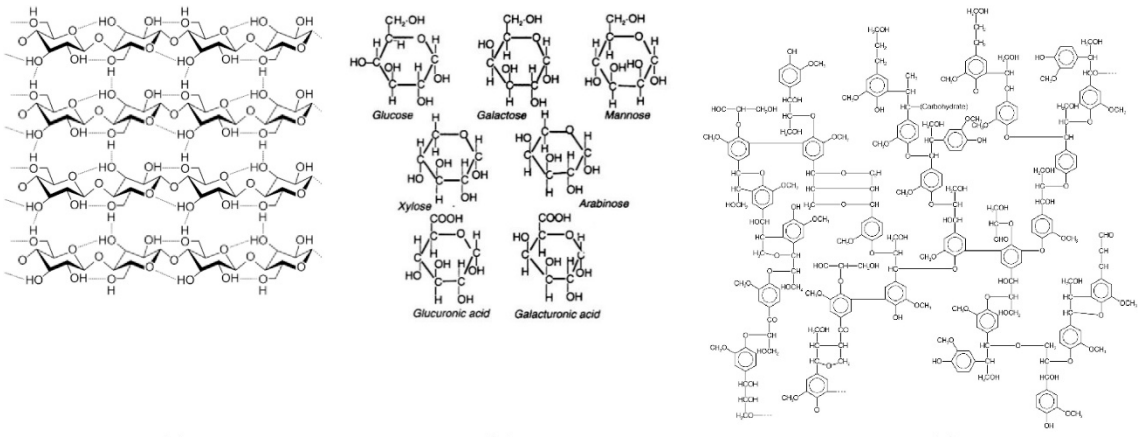
Park et al. (2012) worked with pyrolysis at 520 ºC processing wild reed and they produced a syngas with 56.1% of CO_2, 28.6% of CO and a HHV of 10.9 MJ/kg. The composition of the pyrolysis gas is influenced by the reactor parameters, the chemical structure and the particle size of the feedstock. Cellulose and hemicellulose decomposition enhances the production of CO and CO_2 due to the thermal cracking of carbonyl and carboxyl groups (Uddin, Daud et al. 2014). The reforming of aromatics and

methoxy groups present in the lignin produces a gas rich in CH_4 and H_2 (Yang, Yan et al. 2007). Light hydrocarbons result in the degradation of methylene and ethylene bonds (Guoxin, Hao et al. 2009). The water content in biomass is another factor affecting the syngas yield. More moisture means less gas produced, which is attributed to the higher removal of water-soluble compounds present in the pyrolysis gas (Dasappa, Paul et al. 2004). The particle size of the feed also influences the composition and yield of the gaseous product. Bigger particle size inhibits the cracking reactions of hydrocarbons and volatiles, producing less CO, H_2 and subsequently more CO_2 and light hydrocarbons (Hasan, Wang et al. 2017). Additionally, larger particles have a negative impact on the heating rate of biomass, decreasing the gas yield for higher biochar production (Hu and Gholizadeh 2019). In terms of temperature, when there is an increment, the thermal cracking, devolatilisation and degradation of biomass are stimulated. Concurrently, secondary reactions such as dehydrogenation, decarboxylation, deoxygenation and decarbonylation favour the production of volatiles (He, Xiao et al. 2010). As a consequence, the pyrolysis vapour is richer in H_2 and CO but it contains less CO_2 and hydrocarbon gases.

The combustible gases of the pyrolytic gas (H_2, CO, CH_4 and other hydrocarbon gases) can be combusted as a fuel in industrial facilities generating heat and power (Goyal, Seal et al. 2008). If the syngas contains a high level of H_2, it can be used for fuel cell applications. However, high H_2 yields are not normally obtained via fast or slow pyrolysis unlike with TCR technology.

2.1.3 Biomass Thermal Decomposition

Pyrolysis thermal mechanisms for the conversion of biomass can be designated in a simultaneous combination of fragmentation, isomerisation, condensation, dehydration, rearrangement, aromatisation, cracking, polymerisation and char formation (Vamvuka 2011, Dickerson and Soria 2013). The components of biomass (cellulose, hemicellulose, lignin, water, inorganics and extractives) and the reactor parameters have a strong influence in the pyrolysis reactions. Figure 4 shows the chemical composition of cellulose, hemicellulose and lignin.



(a) (b) (c)

Figure 4 - Biomass Compounds: (a) cellulose, (b) hemicellulose, and (c) lignin (Dhyani and Bhaskar 2018)

The pyrolysis reactions can be classified as primary (Figure 5) and secondary. Depolymerisation, fragmentation and charring (char formation) are part of the primary reactions (Collard and Blin 2014). Depolymerisation is the prevailing mechanism of pyrolysis and it implies the breaking of the monomer's bonds, producing volatiles and gases (Garcìa-Pérez, Chaala et al. 2006, Mullen, Boateng et al. 2010). Fragmentation is responsible for the formation of incondensable vapours and short chain compounds due

to the disintegration of the linkage between the polymer and monomers (Morf, Hasler et al. 2002). Charring reactions cause the condensation of benzene rings during the pyrolytic process stimulating the production of char (Van de Velden, Baeyens et al. 2010). The components obtained during primary reactions are not chemically stable and for that reason they suffer recombination and cracking reactions (secondary reactions). During recombination reactions heavier elements are produced or incorporated onto biochar surface, while lighter elements are formed by the cracking of primary compounds (Zhang, Hu et al. 2018). Additionally, the biochar formed can also promote secondary reactions. Morf et al. (2002) showed that the secondary reactions are the dominant reactions, affecting the properties and the quality of the pyrolysis products.

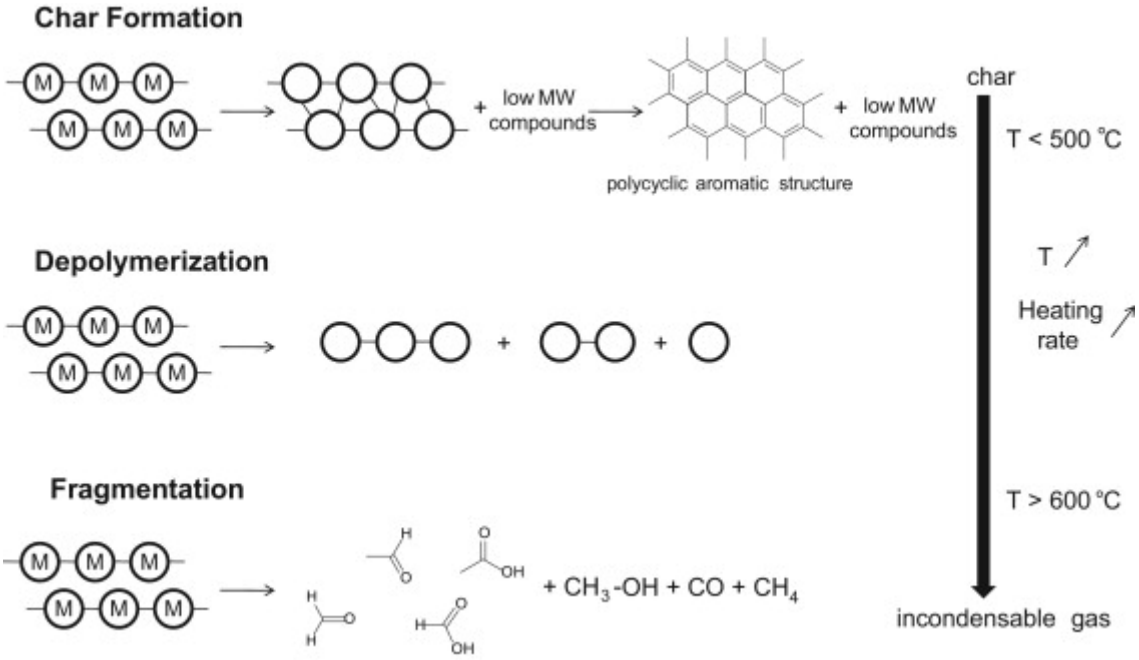


Figure 5 - Pyrolysis Primary Reactions (Collard and Blin 2014)

Under 500 ºC the main reactions occurring in pyrolysis are mostly decarbonylation, depolymerisation, dehydration and decarboxylation (Shen, Wang et al.

2009). The biomass structure is not significantly changed until 200 ºC, however between 200 and 500 ºC the pyrolysis compounds suffer dehydration and some aliphatic elements are converted (400-500 ºC) (Garcìa-Pérez, Chaala et al. 2006). The main reason is the production of C_2 hydrocarbons and CH_4, attributed to the rupture of the alkyl components in the C-H bonds (Hu and Gholizadeh 2019). Above 300 ºC, the carbonyl and carboxyl elements are formed due to the carbohydrates present in the biomass (Stefanidis, Kalogiannis et al. 2014). Between 250 and 500 ºC the decomposition of hemicellulose (220-350 ºC) and cellulose (315-400 ºC) occurs, where the depolymerisation activity is quite intense and so achieving the best bio-oil yield from 400 to 500 ºC (Yang, Yan et al. 2007). When the temperature is higher than 500 ºC, the main reactions taking place are fragmentation, dehydrogenation and aromatisation (Blanco and Chejne 2016). Above 550 ºC more gas is formed due to the fragmentation process and close to 600 ºC, there are more aromatic rings in the biochar demonstrating the existence of aromatisation reactions (Yang, Yan et al. 2007). Lignin is the most stable compound, but the hardest biomass component to be degraded. Its chemical decomposition occurs from 160 to 900 ºC, however the most relevant weight loss is between 350 and 600 ºC (Williams and Besler 1996).

Lignin contributes to a larger formation of biochar, while a higher percentage of cellulose and hemicellulose in the biomass produces more bio-oil (Akhtar and Saidina Amin 2012). Biomass rich in lignin has a negative impact on bio-oil quality causing high viscosity, low stability, high average molecular weight and worse combustion performance (Fahmi, Bridgwater et al. 2008). On the other hand, a higher proportion of cellulose and hemicellulose benefits the pyrolysis oil properties making it more suitable as a fuel due to the presence of glucose, xylose, mannose, galactose and arabinose in their

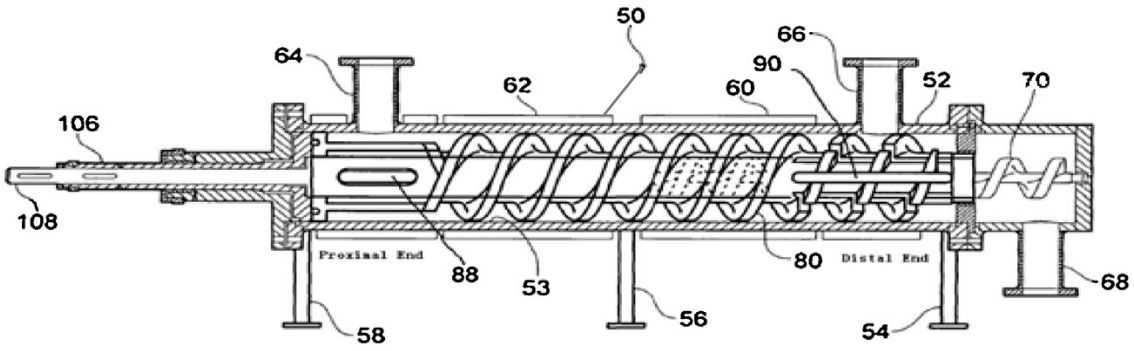
composition. The biomass extractives are the non-structural elements (sugars, fatty acids, proteins, phenolics, resin oils and sterols) that can be removed with solvents such as hexane, ethanol, benzene, toluene and water (Roy, Pakdel et al. 1990). Wood extractives lead to a loss of bio-oil formation and levoglucosan production, and its extraction can cause a reduction of 64% and 34% in oxygen and hydrogen present in the biochar, respectively (Kallioinen, Vaari et al. 2003). Inorganic compounds are converted to ash and they promote biomass degradation, charring, water reactions, non-condensable vapours production and a decrease of bio-oil yields (Scott, Paterson et al. 2001). Ash composition and content can influence the chemical properties and the distribution of the pyrolytic products. Sodium and potassium are the most active components. Low amounts of these elements can stimulate biochar formation (Fahmi, Bridgwater et al. 2008). Alkali metals can also affect the thermal degradation reactions of pyrolysis, creating macro-polymer substances through the disintegration of monomers (ring breaking) (Scott, Paterson et al. 2001).

2.2 Pyroformer Reactor and TCR Technology

The Pyroformer (Figure 6) intermediate pyrolysis reactor (patented by Hornung and Apfelbacher at Aston University) was one of the first intermediate pyrolysis reactors to be built after the Haloclean rotary kiln (cycled-spheres reactor). The Pyroformer is essentially an auger screw reactor inclosing a carbon steel compartment (horizontal position) including two co-axial rotating screws (Hornung 2013). This reactor operates at a pressure of up to 1 MPa, its heating system is external through heating bands, and the design is appropriate to process high ash content biomass and to maximise the contact time between organic vapours and pyrolysis biochar (Ouadi, Brammer et al. 2013).

Throughout the process, the internal screw transports a mix of fresh feedstock and recycled char fraction along the reactor, which is heated at standard pyrolysis temperatures (Santos, Ouadi et al. 2019). The external screw gives a quantity of the char fraction back for recycle, increasing the heat transfer of the feedstock (Yang, Brammer et al. 2014). Additionally, the biochar layer in the reactor protects the feed from extremely high temperatures and low heating rates thus avoiding fast pyrolysis reactions (Hornung 2013). During this stage biomass is transformed into char, vapours and volatile gases. The remaining biochar (that is not recycled in the reactor) exits to the solid drop out pipe of the Pyroformer and the pyrolysis gas phase moves through the gas outlet pipe (Ouadi, Brammer et al. 2013).

The effect of char recycling is the novelty of this reactor type, creating an additional catalytic effect in the process. This leads to a better quality pyrolysis oil when compared to commercial bio-oils from fast pyrolysis due to oil formation with lower molecular weight, less water content and less heavy tar formation, as well as increased yields of fuel gases (H_2 and CO) generating a considerably higher heating value (Yang, Brammer et al. 2013).



106 External Screw Shaft, 108 Internal Screw Shaft, 64 Feed Inlet Pipe, 62,60,52,50 Electrical Heating Bands, 58,56,54 Supports, 88 External Screw Slot, 90 External Screw Slot, 80 External Screw, 70 Internal Screw, 68 Solid Drop Out Pipe, 66 Gas Outlet Pipe

Figure 6 - Pyroformer reactor (Hornung and Apfelbacher, Patent GB 246 0156, 2009)

TCR technology is a combination of intermediate pyrolysis (development from Pyroformer reactor) and post catalytic treatment (Reforming). It was developed and implemented by Fraunhofer UMSICHT and it belongs to a bio-battery model used to provide energy from renewable materials (Neumann, Meyer et al. 2016). A picture of the unit is shown in Figure 7.



Figure 7 - TCR reactor (lab scale) installed at Fraunhofer UMSICHT

This process contains two essential steps: 1) intermediate pyrolysis when the thermal heating of biomass occurs in the complete absence of oxygen at mild temperatures, and 2) reforming stage when catalytic cracking of vapours occurs at elevated temperatures to promote the formation of synthesis gas and organic vapours which when quenched yield bio-oils with superior physical and chemical properties (Santos, Ouadi et al. 2019).

The intermediate pyrolysis stage in the TCR technology occurs in an auger reactor (update version of the Pyroformer) with temperatures from 400 to 500 ºC and solid residence times between 5 and 10 minutes (Hornung 2014). Intermediate pyrolysis products are transported to the auger reactor downstream, where the first reforming treatment is performed between the biochar and condensable vapours, causing a catalytic effect in all products and a consequent improvement of their chemical properties (Neumann, Binder et al. 2015).

TCR process also includes a reforming step, where the intermediate pyrolysis gases and solid phase are conveyed to the post reformer operating in a temperature range between 500 and 700 ºC. Within the reformer, organic vapours are catalytically reformed into higher yields of synthesis gas at temperatures ≈700 °C. The gas exiting the reactor is partially condensed generating three different products: an organic oil phase (6-11 wt%), an aqueous phase (21-26 wt%) and gas fraction (27-44 wt%). The main compounds of gas phase are hydrogen (maximum of 55 vol%), carbon dioxide (maximum of 35 vol%), carbon monoxide (maximum of 25 vol%), methane and a portion of hydrocarbons (Neumann, Binder et al. 2015). During the reforming step different types of chemical reactions occur in the post reformer, mainly (Neumann, Meyer et al. 2016):

$C + H_2O \leftrightarrow H_2 + CO$ (Water gas reaction) (1)

$CO + H_2O \leftrightarrow CO_2 + H_2$ (Water gas shift reaction) (2)

$CH_4 + H_2O \leftrightarrow CO + 3H_2$ (Steam reforming reaction) (3)

$C + 2H_2 \leftrightarrow CH_4$ (Hydrogasification reaction) (4)

$CO_2 + C \leftrightarrow 2CO$ (Boudouard reaction) (5)

$C + ½O_2 \leftrightarrow CO$ (Partial oxidation reaction) (6)

At lab scale, TCR is heated by electricity using heating blankets. During the experiment the solid fraction (char) remains in the post reformer and is only extracted intermittently throughout the process. To guarantee an efficient separation between the organic liquid component and the gas fraction the TCR has a cooling system working with temperatures from -3 to +10 ºC to cool down the vapours from the post reformer. Before being routed to an exhaust system, the gas phase goes directly to a gas analyser and calorimeter to quantify its composition and HHV (Neumann, Jager et al. 2016). To avoid the contamination of the gas analyser from aerosols and other impurities, the plant is installed with active carbon bag filter and also with a gas wash bottle containing biodiesel (Neumann, Meyer et al. 2016).

In addition to agricultural, organic and industrial wastes with a high water and ash contents (low ash melting points as well), the TCR process is also able to convert plastic residues from and co-form rejects (Ouadi, Greenhalf et al. 2018). The residues treated normally contain a HHV superior to 8 MJ/kg and a moisture content below 20% which improves the thermal efficiency of the technology as less energy is required to evaporate any extra water in the biomass (Neumann, Jager et al. 2016). Technically, TCR can convert feedstocks with a moisture content up to 30% which is beneficial in terms of energy consumption as the drying step can be avoided.

TCR products can be used in diverse applications from different areas. The gas fraction can generate heat and power through CHP, bio-oil can be blended with diesel and gasoline to be used in engines, and char can be applied in combustion or gasification processes and as fertiliser or soil conditioner (Kirby, Hornung et al. 2017).

TCR is a safe technology operating without the utilisation of externally sourced solvents, catalysts or any chemical product, and it works at atmospheric pressure (Ahmad,

Jager et al. 2018). Its flexibility in terms of plant control provides a large variety of value-added products such as an improved quality bio-oil which is easy to store and transport, a stable and energy dense biochar with similar features to anthracitic coal and a syngas rich in H_2 (Neumann, Meyer et al. 2016, Ouadi, Jaeger et al. 2017). Another advantage of this process is the efficient design which can convert most of the energy introduced from the original biomass (Ahmad, Jager et al. 2018).

2.3 Current State of the Art for Furfural and 2-MF Production

Furfural is a key oxygenated compound having C=C and C=O bonds. The high stability furfural is attributed to the C=C bonds composed of one 5 member ring and 6 electrons (Danon, Marcotullio et al. 2014). Furfural can be produced from renewable biomass and agricultural wastes rich in xylose (sugarcane bagasse, oat hulls, and corncobs) and it can be used for the production of a large variety of important non-petroleum-derived chemicals (such as furfuryl alcohol and 2-MF), competing with crude oil (Zeitsch 2000). This compound can also be used in many industrial processes such as oil refining, plastics and the pharmaceutical and agrochemical industries where it is transformed into perfume intermediates, chemical solvents, medicine compounds and pesticides (Panagiotopoulou and Vlachos 2014).

The furfural is obtained through the following steps: production of pentoses such as xylose, submitting the hemicellulose material to hydrolysis and the final conversion into furfural by acid-catalysed dehydration of pentoses (Figure 8) (Dias, Pillinger et al. 2005).

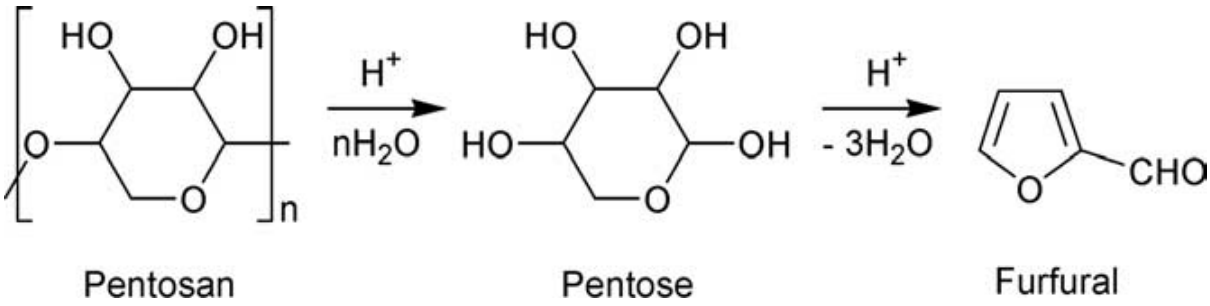


Figure 8 - Simplified reaction mechanism of acidic degradation of pentosan to furfural (Dias, Pillinger et al. 2005)

Presently, furfural production is an energy-intensive process due to long side reactions which causes a decrease of furfural yield because of extensive residence times, and the necessity for substantial waste disposal. The need for high pressure steam to heat the reaction is also a drawback in this process (Dias, Pillinger et al. 2005). Concentrated sulphuric acid, which is particularly corrosive and extremely toxic, is used as a catalyst which brings serious issues compared to homogeneous catalytic processes such as problematic separation and recycling of the mineral acid and product contamination (Weingarten, Cho et al. 2010). For these reasons, enhancements to the chemical technology behind the furfural production is necessary in order to improve the sustainability of furan-based chemical industries.

Microwave irradiation has been suggested as an alternate method to improve the dehydration process for furfural production as it offers a fast and efficient heating promoting better reaction rates and avoiding the formation of certain by-products and so results in higher furfural yields (de la Hoz, Diaz-Ortiz et al. 2005, Qi, Watanabe et al. 2008). Heterogeneous catalytic conversion using solid catalysts has taken a relevant role in converting pentose to furfural due to its high selectivity and high reaction. Moreover,

it can be recycled easily offering more environmentally attractive properties for practical operations (Yan, Wu et al. 2014).

Humins, a solid carbonaceous species, are the undesired co-product obtained during the production of furfural from xylose. This is responsible for the low furfural yields (between 45% and 50%) using an industrial batch process (Montane, Salvado et al. 2002). In the last few years, some works have shown different ways to achieve better furfural yields by inhibiting the humins production. One technique is to apply organic solvents (ethyl acetate and methyl isobutyl ketone) to absorb the furfural from the aqueous fraction (Vlachos and Caratzoulas 2010). Supercritical CO_2 has also been used to extract furfural (Sako, Sugeta et al. 1995).

However, due to furfural's affinity to polymerize in storage it is not a suitable option for a fuel candidate (Xiong, Wan et al. 2016). The option of transforming furfural to 2-MF is mentioned in several current works due to its high energy density and high octane number making 2-MF a promising biofuel (Huber, Iborra et al. 2006, Lange, van der Heide et al. 2012).

To produce 2-MF first it is necessary to convert furfural to furfuryl alcohol (2-furanmethanol) through hydrogenation and then apply HDO in the intermediate furfuryl alcohol to get the desired product 2-MF as it is shown in Figure 9 (Ordomsky, Schouten et al. 2013, Dong, Zhu et al. 2015).

Conventional route for 2-MF production is the use of energy fossils and requires catalytic oxidation. Developing a new way to produce 2-MF from biomass-derived chemicals is extremely desirable, not only from the perspective of the green sustainable chemistry but also to mitigate the fossil energy crisis by using a large amount of biomass

resources available efficiently (Dong, Zhu et al. 2015). All these reasons can boost furfural production through the TCR process, followed by a HDO treatment, to achieve the desirable formation of 2-MF. Compared to hydrocarbons, 2-MF has a better combustion efficiency (caused by its oxygen atom) and higher octane number (Yan, Wu et al. 2014). Therefore, 2-MF has been blended with gasoline to be used as fuel for vehicles (Srivastava, Jadeja et al. 2016).

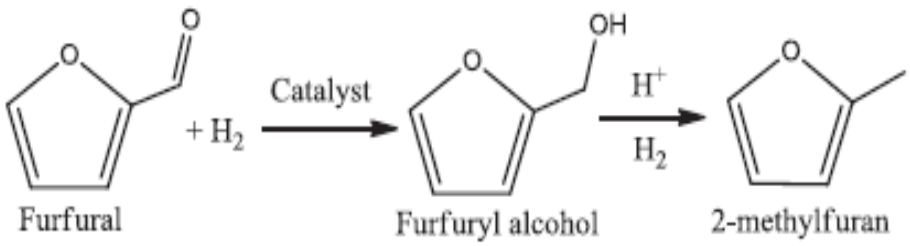


Figure 9 - Hydrogenation and HDO of furfural to MF (Yan, Wu et al. 2014).

HDO works in the presence of a catalyst under H_2 pressure and it is classified to be the most efficient method to upgrade pyrolysis bio-oil (De, Saha et al. 2015). This process converts aldehydes, oxygenated and unsaturated elements into hydrocarbons, due to its selectively to cleave the C-O/C=O bonds (carbonyl group) of the oxygenates compounds and at the same time preserving the C-C/C=C bonds (Ren, Yu et al. 2013, Xiong, Wan et al. 2016). This step is quite relevant to improve the oil properties for fuel applications, removing aromatics from the bio-oil and subsequently to increase the affinity between the temperature and viscosity (Isahak, Hisham et al. 2012, Xiu and Shahbazi 2012).

HDO can be divided into two different classes: high and atmospheric pressure. The first one applies high H_2 pressure to hydrogenate aromatic rings reducing the oxygen

content present in acids, phenols, esters and aldehydes (Cheng, Wei et al. 2017). There are several reactions that take place during this method according to the chemical composition of the bio-oil, including dehydration, hydrogenation, hydrocracking, decarboxylation and hydrogenolysis (Pourzolfaghar, Abnisa et al. 2018). Atmospheric H_2 pressure has similar conditions compared to high pressure, however, it differs in the type of catalyst, operating conditions (mainly pressure) and in the role of H_2 on the upgrading reaction (Yang, Shi et al. 2019). The scientific community has used HDO atmospheric pressure in industrial scales for lignin compounds to minimise the operation cost (Pourzolfaghar, Abnisa et al. 2018).

One of the main difficulties of HDO is to have low consumption of H_2 with an efficient deoxygenation process (Cheng, Wei et al. 2017). In terms of H_2 consumption, HDO can be defined in two categories: in situ H_2 source and ex situ H_2 source. In situ H_2 source uses the same autoclave for H_2 production and to treat the pyrolysis oil, avoiding issues with H_2 storage and transportation (Yang, Shi et al. 2019). On the other hand, ex situ H_2 source requires industrial H_2 from water electrolysis or fossil fuels as a H_2 donor, making this process less desired (Muradov 2017). This method also needs high H_2 pressures (up to 30 MPa) to solubilise H_2 in the liquid fraction to decrease the oxygen amount of the pyrolysis oil (Duan and Savage 2011). It has also been reported the use of external H_2 during the hydrogenation of furfural to 2-MF adding various noble metal and bimetallic catalysts (Dong, Zhu et al. 2015). This situation can lead to a number of obstacles connected to hydrogen utilization, such as the cost to compress, storage and transport (especially in isolated locations), the design of the reactor, issues related to solubility and dilution of the hydrogen, which increase the cost and complexity of the process (Gandarias, Requies et al. 2012, Panagiotopoulou and Vlachos 2014). A different

way to provide hydrogen to convert furfural to 2-MF may be the catalytic transfer hydrogenation, where the H_2 molecule is replaced for the hydrogen donor. In this process, alcohols are a good option as hydrogen donors because they are not corrosive and they may be obtained from ethanol or butanol using biomass as substrate (Chia and Dumesic 2011, Jae, Zheng et al. 2013).

The biggest challenge of having a competent and reasonable HDO is the selection of the catalyst which should be efficient, economic and environmentally friendly. The catalyst stability may be an issue to convert furfural to 2-MF due to the high temperatures which increases the energy cost and the coke production as well (Yan, Wu et al. 2014). The deactivation catalysts during the 2-MF production through furfural hydrogenation is the main issue of the process because of the production of undesired co-products (furan, tetrahydrofuran and C-4 compounds) (Zheng, Zhu et al. 2008). Additionally, this method of conversion is quite exothermic (142 kJ/mol) causing difficulties in terms of temperature control (Yang, Zheng et al. 2004).

Chromium-based catalysts were described as efficient for 2-MF production, however, their toxicity makes them less attractive (Xiong, Wan et al. 2016). Molybdenum carbide has a high selectivity to convert furfural to 2-MF but it presents very acidic features stimulating the polymerisation of furfural and creating an unstable environment for HDO process (Nakagawa, Tamura et al. 2013). Although precious metals such as ruthenium and palladium showed a good furfural conversion yield they are extremely expensive, easily deactivated, hard to regenerate and not economically viable (Panagiotopoulou and Vlachos 2014). Mesoporous silica catalysts contain large surface areas and they can convert 82% of furfural, nevertheless the process is extremely slow

(more than 25h) and it leads to the formation and deposit of carbon in the catalyst substrate, which leads to a catalyst deactivation and consequent reduction of HDO reactions between the surface and the product upgraded (Yan, Wu et al. 2014).

Cu-based catalysts have been mentioned as the most promising option to convert furfural to 2-MF (Sitthisa and Resasco 2011, Dong, Zhu et al. 2015). Recently, the combination between Cu and Zn or Cu and Mn as a catalyst showed strong stability and efficiency in 2-MF production by HDO. The good interaction among these two groups of metals brings the production of mixed oxide phases and consequently a breakage of the C-O bond (Zheng, Zhu et al. 2008, Srivastava, Jadeja et al. 2016). Moreover, the combination between manganese/zinc Cu-based catalysts and Al_2O_3 and SiO_2 supports increases the selectivity and activity of the HDO process (Zheng, Zhu et al. 2008). Both catalytic supports are cheap, practical to be used in industry, and they promote the interaction and dispersion of copper improving the catalytic performance (Dong, Zhu et al. 2015).

2.4 Xylose-Rich Biomass

Lignocellulosic agricultural waste is considered one of the most available and cheap green resources for the bioenergy area and biofuels production (Chareonlimkun, Champreda et al. 2010). Current methods to exploit biomass, like extraction of pure cellulose or combustion to generate electricity, are harmful to the environment and not lucrative for the industry (Boussarsar, Roge et al. 2009). In this regard, thermochemical processes are becoming popular in converting biomass into valuable products, constituting a different approach for lignocellulosic residues application in terms of sustainability and profitability (Dhyani and Bhaskar 2018).

Lignocellulosic materials are generally composed of cellulose (40-60%), hemicellulose (20-40%) and lignin (10-25%). Hemicellulose biomass is getting more appreciation because of its high xylan content. This xylan content is mainly formed by xylose which is a very interesting chemical in the biofuels industry (Boussarsar, Roge et al. 2009). According to the previous section furfural can be obtained using lignocellulosic feedstocks containing a high level of xylose. Furfural has an annual production of 250 000 tons and the present method to extract this chemical compound from xylose sources is the acid-catalysed dehydration (Lichtenthaler and Peters 2004). Oat hulls and sugarcane bagasse have been recognised as one of the most promising xylose-rich biomass for furfural production (Yan, Wu et al. 2014).

Currently, oat is one of the most produced cereals in the world and its hulls (residue from oat milling process) have a unique potential as renewable source of biomass due to its global and annual availability. OH can be a promising feedstock to produce liquid and gaseous fuels and heat through thermochemical processes (pyrolysis, gasification, combustion) (Qazanfarzadeh and Kadivar 2016).

The composition of OH (Figure 10) is mainly cellulose (35-45%), hemicellulose (32-35%) and lignin (17-20%) and the hull represents between 20 and 35% of the entire grain weight (Skiba, Budaeva et al. 2017). One of its advantages is the low ash content (between 4.5 and 5.2%) and the homogenous morphologic and particle size that does not need to be milled when treated (Skiba, Budaeva et al. 2017). Due to the high amount of hemicellulose, oat hulls are a good source of furfural and xylose (sugar pentose) (Lawford, Rousseau et al. 2001). However, some kinetic parameters of oat hulls need to be understood to develop this process (Qazanfarzadeh and Kadivar 2016).

Nowadays, OH is essentially used for combustion to generate energy due to its calorific value of 16 MJ/kg or for the production of high-value cellulose components (Valdebenito, Pereira et al. 2017). This agricultural residue also presents a reasonable nutritive value and is used in the animal and human food industry (Qazanfarzadeh and Kadivar 2016). In addition, there are some studies on the application of OH for ethanol production via chemical hydrolysis (Skiba, Budaeva et al. 2017). It is relevant to highlight the value of this waste in terms of local and annual availability and to explore its potential in the biofuels production market (Valdebenito, Pereira et al. 2017).



Figure 10 - Oat hulls

Sugarcane is the biggest farming harvest on earth and the main residue formed (bagasse) results from the milling of the sugarcane to extract its juice for ethanol or sugar production (Varma and Mondal 2017). SB (Figure 11) is a raw material available worldwide generated in 115 countries (such as USA, India, Australia, Brazil etc.) and its production is larger and more efficient in tropical and sub-tropical climates (Chauhan,

Varun et al. 2011). Brazil and India are the main SB producers in the world and this industry represents a relevant role for the energy needs in developing countries (Jain, Wei et al. 2016). Normally, 1000 kg of fresh sugarcane can generate 280 kg of dry bagasse, 110 kg of sugar and 45 kg of molasses (Varma and Mondal 2017). For ethanol production, cane straw and bagasse residues represent around 35% of the total sugarcane weight (Rocha, Nascimento et al. 2015).



Figure 11 - Sugarcane bagasse

SB components are dispersed in a lamella structure and their composition is around 40-50% of cellulose, 20-30% of hemicellulose, 20-25% of lignin and 1.5-3% of ash (Varma and Mondal 2017). Presently, more than 500 sugarcane species are cultivated in Brazil and 20 new species have been created every single year (Rocha, Nascimento et al. 2015). However, the chemical composition of the different SB species do not diverge significantly from the main compounds (Rocha, Nascimento et al. 2015). The SB cellulose contains amorphous and crystalline components which need to be submitted to physical and thermochemical treatments to have access to the polysaccharides elements

(Jain, Wei et al. 2016). Milling is a good example of a physical process to raise the particle surface area of the SB. Thermochemical treatments such as acid reagents, ammonia, steam explosion and alkaline hydroxide have been described to convert SB crystalline components into polysaccharide elements (Chandel, Antunes et al. 2013, Maryana, Oktaviani et al. 2014, Ramos, da Silva et al. 2015). The results of these thermochemical processes on the chemical structure of the SB can be analysed via enzyme digestion, electron miscopy and x-ray diffraction (Jain, Wei et al. 2016).

Currently, SB (after juice extraction) is getting more popular for ecological and economic reasons owing to its high availability, low cost and applicability in different industrial areas such as biofuels, paper pulp and biochemicals (Jain, Wei et al. 2016, Al Arni 2018). SB is mainly used for the generation of heat and power through combustion in boilers located in sugar mills for onsite consumption (Rocha, Nascimento et al. 2015). Nevertheless, this scenario is not energy efficient (only 26%), causes waste management issues at the plant and the ashes produced during the process are responsible for health hazards (Varma and Mondal 2017). As an alternative, due to its high calorific value, SB can be used for biofuel production via thermochemical technologies making this residue a valuable raw material for pyrolysis processes (Varma and Mondal 2017). In addition, SB is also utilised in more than forty applications such as animal feed, treatment of cancer (important and strong antioxidants from the acids compounds of lignin), boards and the production of sugar, pulp, furfural, paper and ethanol (Rocha, Nascimento et al. 2015, Jain, Wei et al. 2016).

2.5 Catalytic Pyrolysis

Catalytic pyrolysis is another option to remove the oxygen and upgrade the properties of the pyrolysis products, particularly for the bio-oil which cannot be used directly as a fuel engine. Biomass composition contains alkali metals which can stimulate some catalytic reactions, therefore a bio-oil upgrading step should be always reflected according to the final application (Kan, Strezov et al. 2016). Sodium and potassium are the main elements responsible for the cracking of vapours decreasing the bio-oil quality and quantity, and, according to their concentration the reactions can be more intense than char cracking (Wang, Dai et al. 2017).

Catalytic pyrolysis reactions are extremely complex, thus the selection of the reactor parameters and an efficient, cheap and stable catalyst are vital to make the process beneficial and productive (Hu and Gholizadeh 2019). High heat transfer and a decent biomass/catalyst proportion are crucial to guarantee the efficient contact between the organic vapours and the catalyst surface avoiding thermal degradation. The proper catalyst should promote the following reactions (Figure 12): hydrogenation, oligomerisation, decarbonylation, dehydration, cracking, decarboxylation and deoxygenation (Tan, Zhang et al. 2013).

The catalysts tested by pyrolysis are mostly solid acids (silica-alumina, zeolites, silicates and fluid catalytic cracking catalyst), metal oxides (copper, zirconia, ceria and zinc) and inorganics (sulphates, chlorides and phosphates) (French and Czernik 2010, Lappas, Kalogiannis et al. 2016). They can be classified in two categories (zeolite and non-zeolite) and their nature, chemical composition and structure have a direct effect to improve the pyrolysis products properties and yields (Dhyani and Bhaskar 2018). Zeolites are the most popular in catalytic pyrolysis due to their prolonged activity and stability for

bio-oil production. Non-zeolite catalysts have been used as well; mainly minerals, noble metals and metal oxides (Hu and Gholizadeh 2019). However, analysing, understanding and comparing the global performance of the zeolite and non-zeolite catalysts for the purpose of improving and selecting the most efficient ones in the pyrolysis conversion of biomass is required.

In the last few years catalytic pyrolysis has been tested via two main routes, in-situ and ex-situ (Figure 13). The former is an integrated pyrolysis system and implies the introduction of the catalyst inside of the pyrolysis reactor (Wang, Johnston et al. 2014). The latter (ex-situ) includes a downstream process where the organic vapours are upgraded in the presence of a catalyst (Dhyani and Bhaskar 2018).

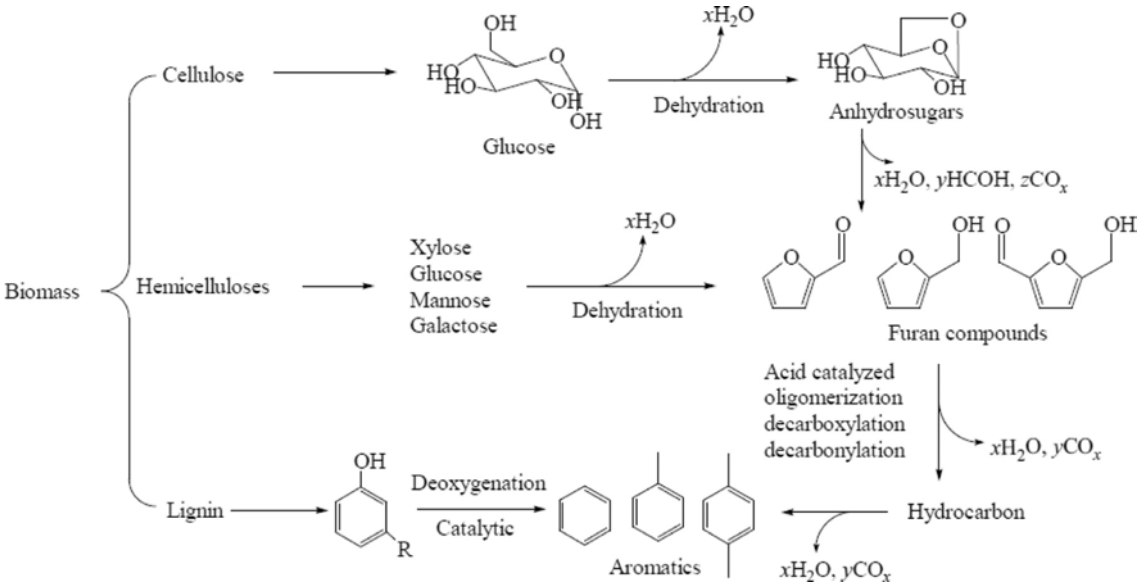


Figure 12 - Catalytic pyrolysis reactions of biomass (Tan, Zhang et al. 2013)

During the in-situ process the catalyst is introduced into the reactor to favour thermal cracking reactions and the conversion of heavy components present in the bio-oil to lighter ones (Foster, Jae et al. 2012). However, a higher cracking rate requires more

catalyst and a consequence is the extra production of coke (French and Czernik 2010). In-situ pyrolysis decreases the biochar produced and maximises the formation of aromatics and light compounds in the bio-oil (Yildiz, Pronk et al. 2013). This integrated catalytic system is limited and less flexible owing to the use of a single reactor operating at the same parameters for the pyrolytic and catalytic reactions (Lappas, Kalogiannis et al. 2016). The main challenge is to find a robust, active and stable catalyst which is easy to regenerate, and can resist the reactor's mechanical environment and improve the quality of the bio-oil by reducing its oxygen and coke content (Wang, Johnston et al. 2014).

Ex-situ catalytic pyrolysis, like HDO, is also used to upgrade and improve the properties of the bio-oil. Compared to the in-situ process, ex-situ technology is more efficient in removing oxygen from the pyrolysis oil due to the lower homogeneity of the catalyst applied increasing the selectivity of the process (Nguyen, Zabeti et al. 2013). Additionally, the ex-situ process has a higher selectivity and flexibility to produce more specific compounds and, as the catalyst is placed in an external reactor the final products can be easily removed (Yildiz, Pronk et al. 2013). The main inconveniences of this route are the rapid deactivation of the catalyst and the high cost of the technology, particularly for industrial units (Gholizadeh, Gunawan et al. 2016).

TCR technology is able to minimise some negative aspects of the current in-situ and ex-situ catalytic routes such as coke formation, limitation/flexibility of the process, selection of a proper catalyst and the economic viability for larger plants. The biomass conversion occurs in the intermediate pyrolysis reactor and then the condensable vapours produced undergo the catalytic treatment in a different reactor (called the reforming unit). This makes it easy to set different experimental conditions according to the product

desired and a process easy to operate. In addition, the catalyst used is the biochar generated in the previous step (auger intermediate pyrolysis reactor) which is constantly produced throughout the process thus avoiding the concern of selecting an adequate catalyst that is easy to regenerate. Biochar formed via TCR can be considered as an inexpensive sacrificial catalyst. It has excellent chemical and morphologic characteristics, such as surface area, making this carbonised solid catalytically active in converting organic vapours to high-quality pyrolysis liquids (Jager, Conti et al. 2016, Ahmad, Jager et al. 2018).

It has been proven that upgrading treatment of the volatiles before their condensation is presently the most efficient way to minimise the amount of water and oxygen in the pyrolysis liquid which leads to a higher calorific value bio-oil composed of low molecular weight elements (Dhyani and Bhaskar 2018).

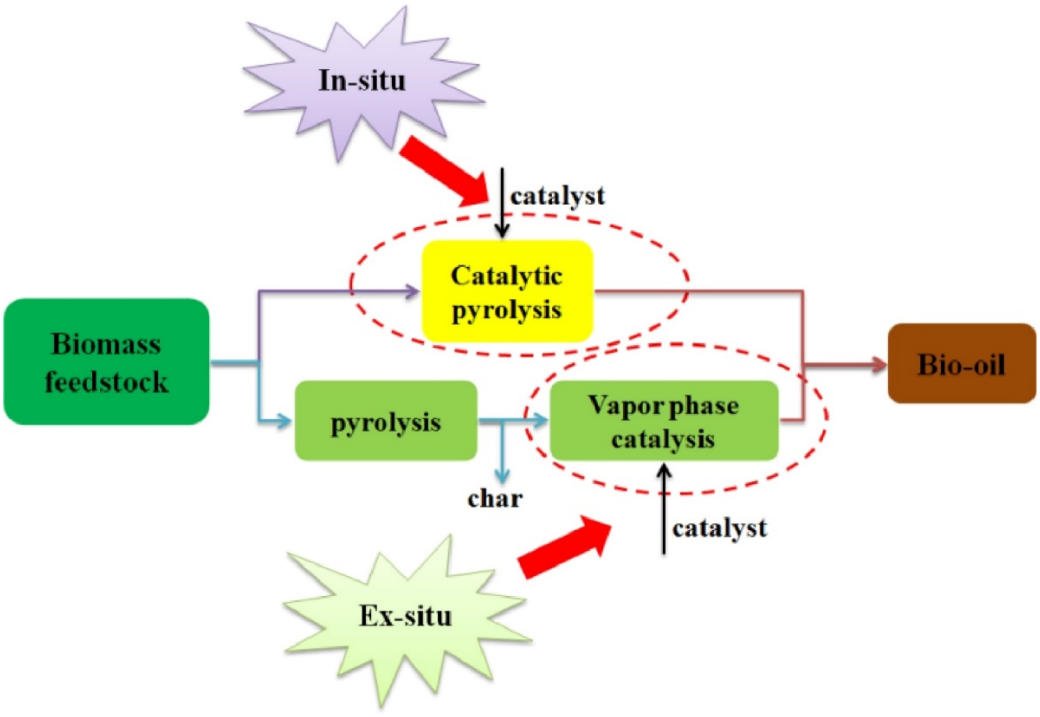


Figure 13 – In-situ and ex-situ catalytic pyrolysis (Wang, Dai et al. 2017)

Zeolite catalysts are the most popular for upgrading bio-oil through catalytic pyrolysis, and these include HZSM-5, Beta zeolite, SAPO-34, Y zeolite, ZSM-5 and Mordenite (Hu and Gholizadeh 2019). Their production cost is generally low and its application generates more aromatics and coke (Carlson, Jae et al. 2010). The zeolite size pore affects the formation of aromatics and coke and larger pores are related to higher yields of coke (Jae, Tompsett et al. 2011). Another relevant factor is the acidity of the zeolite, where lower acidity levels produce more coke and fewer aromatics (Nguyen, Zabeti et al. 2013).

HZSM-5 and ZSM-5 zeolite catalysts are the most tested in catalytic pyrolysis. ZSM-5 has less selectivity, acidity and thermochemical stability, making the HZMS-5 more attractive for aromatics production and to promote catalytic reactions in the biomass such as aromatisation, decarbonylation, cracking, isomerisation, decarboxylation, cyclisation, oligomerisation, deoxygenation and alkylation (Duman, Pala et al. 2013, Hu and Gholizadeh 2019).

HZMS-5 was tested in a pyrolysis fixed bed reactor converting microalgae and the bio-oil produced presented a lower oxygen content (19.6 wt%) and a higher calorific value (32.6 MJ/kg) compared to no catalytic treatment at the same conditions (Pan, Hu et al. 2010). Zang et al. (2009) and Stephanidis et al. (2011) used the same zeolite to pyrolyse corncobs and beech wood respectively, and the bio-oil in both studies showed a higher calorific value and aromatics content and a decrement of oxygenated compounds compared to the runs without HZMS-5 (Zhang, Xiao et al. 2009, Stephanidis, Nitsos et al. 2011).

Some works have experimented ZSM-5 catalyst in a pyrolysis fixed bed reactor using glucose, rice husks, maple wood and furans as feedstock (Williams and Nugranad 2000, Jae, Tompsett et al. 2011). The general results were a substantial reduction in the yield and oxygen content of the bio-oil. The chemical structure of ZSM-5 was also altered by adding some metals such as Mo, Ni, Zn, Ga, Co, Pd and Pt. This modification influenced the alkylation and cyclisation reactions increasing the zeolite acidity and the aromatics yields, especially using the Ga metal (Li, Li et al. 2014, Engtrakul, Mukarakate et al. 2016).

Zeolite catalysts favour the production of coke which is deposited on the catalyst surface filling the respective pores. Consequently, the catalyst is deactivated reducing its durability and the coke formed also absorbs the bio-oil organics resulting in lower quality and quantity increasing the cost of the process (Hu and Gholizadeh 2019).

Mesoporous catalysts, including Al-SBA-15, MCM-41 and Al-MCM-41, are also an option for catalytic pyrolysis of biomass. The last works developed in a circulating fluid bed reactor demonstrated the effect of mesoporous catalysts in the pyrolysis oil composition increasing the phenolics content and reducing the concentration of acids (carboxylic acid) and carbonyls (Iliopoulou, Antonakou et al. 2007). Moreover, an increment of the silica/alumina ratio in this kind of catalyst led to an increase of the organics and aromatics in the bio-oil but a lower liquids production (Adam, Antonakou et al. 2006). The use of mesoporous catalysts shows a clear indication of upgrading treatment, however, the deoxygenation process is incomplete (Iliopoulou, Antonakou et al. 2007).

Some works investigated the application of mineral catalysts such as MgO, dolomite, SiO_2, CaO, limestone and K_2O through pyrolysis of cellulose, pine sawdust,

lignin and poplar wood using a fixed bed reactor at 500 ºC (French and Czernik 2010, Zhang, Hu et al. 2018). CaO and MgO (basic oxides) inhibited the production of tar and phenolics in the bio-oil whilst coke and gaseous products presented higher levels (Zhang, Hu et al. 2018). On the other hand, the use of acid oxides indicated more tar formation. In another research, Na_2CO_3 catalyst produced a very unstable bio-oil but the application of Pt on its surface enhanced the quality and the stability of the same pyrolysis oil (Nguyen, Zabeti et al. 2013).

Transition metals have also been experimented as a catalyst in pyrolysis. Zn, Fe and Cu maximised the generation of aliphatic carbons and aromatics converting oxygenated compounds (Karnjanakom, Bayu et al. 2016). Other metals such as Zr and Ti, increased the formation of ketones in the pyrolysis-oil (Mante, Rodriguez et al. 2015). The introduction of nickel catalysts in a pyrolysis reactor at 400 ºC raised the bio-oil yields and reduced the oxygen content of the oil from 20 to 10 wt% (Dilcio Rocha, Luengo et al. 1999).

The current catalysts used in the pyrolysis process are not the most appropriate to significantly improve the properties of the bio-oil, therefore, the creation of alternatives which are more solid, effective, economic and stable is required. Recently, iron components have proven their ability to optimise the hydrogenation of carbonyl compounds to produce furans and to reduce the acidity of the bio-oil (Lee, Kim et al. 2014, Yang, Li et al. 2017). In addition, the same iron components were tested at pyrolysis conditions for 8 h and no catalyst deactivation was detected, making this metal a promising candidate for upgrading the pyrolytic products (Moud, Kantarelis et al. 2018).

The present thesis investigated the utilisation of steel slag as a catalyst in the TCR experiments. Due to its high iron composition (~25%), SS (Figure 14) can promote decarboxylation and dehydration reactions converting polysaccharides into furans and CO_2 (Yang, Li et al. 2017). Moreover, SS has a high content of Ca (~30%) and Mg (5%) which help to produce more hydrocarbons in the bio-oil (Nokkosmäki, Kuoppala et al. 2000). A few studies tested the application of blast furnace slag (via thermogravimetric and continuous fixed bed pyrolysis) and SS (via thermogravimetric pyrolysis) for bio-oil production (Luo and Feng 2016, Luo and Feng 2017, Sun, Seetharaman et al. 2018, Yao, Yu et al. 2018). However, no references to the use of SS as a catalyst in a thermo-catalytic reactor to favour the conversion of biomass in a furanic bio-oil was found in the literature.



Figure 14 - Steel slag (6 mm)

Blast furnace slag and SS are the two main by-products from the steel/iron industry. The iron is produced in a blast furnace having the blast furnace slag as a by-

product while the SS is a waste from the steel making process using an electric arc furnace or a basic oxygen furnace (Sun, Seetharaman et al. 2018). It is important to highlight that SS and blast furnace slag have different applications and chemical/physical properties, especially in the iron content where the SS contains a significantly higher concentration compared to the blast furnace slag (Luo and Feng 2017).

Approximately one million tonnes of SS are produced per year in the UK and this steel industry waste is mostly composed of calcium silicates and ferrites mixed with fused oxides or iron, magnesium, aluminium and manganese (Yao, Yu et al. 2018). SS is a non-porous, strong and dense material having a high resistance to crushing.

In recent years, SS has been used as aggregate for construction (unbound and bound sub-bases, cappings, fills such as earthworks and backfill to structures), as asphalt surfacing (giving a high resistance to abrasion and polishing under heavy traffic) and as a soil conditioner for agriculture (Luo and Feng 2016, Sun, Seetharaman et al. 2018).

3. EXPERIMENTAL METHODOLOGY

This chapter describes the experimental methodology applied in this work and it also provides information about the methods and equipment used in product characterisation and practical trials. The first section details the kinds of feedstocks used and how they were treated, pelletised and characterised before the experimental tests. The second section explains how the TCR experiments were performed, specifying the procedure and the type of equipment utilised. The third section describes the methodology behind the analyses of the TCR products formed and the catalytic characterisation description of the SS and biochar. The final section is dedicated in explaining the HDO process, including its procedure and parameters. All the characterisation tests were made in duplicate and average values are reported.

3.1 Raw Materials

Sugarcane bagasse used in the TCR experiments was supplied from Cosan Biomassa S/A (Brazil). 100 kg of SB was received and its moisture content was approximately 6 wt%. The Malt Miller Ltd (UK) provided 120 kg of oat hulls with a moisture content around 14wt%. Steel Slag was supplied from Tarmac CHR Company (UK) in two different sizes: 1 mm (dust) and 6 mm (Figure 14, 2.5 Catalytic Pyrolysis section). The 6 mm SS was used in the TCR post-reformer as a solid catalyst, whereas the dust was mixed with OH through pelletisation to promote a catalytic effect in the auger intermediate pyrolysis reactor (both scenarios will be detailed and described further in this chapter).

As both feedstocks (SB and OH) received contained a moisture content <15 wt.%, no drying was required before pelletisation and thermal conversion. Pelletisation was necessary and performed using a KKP 300 F (22 kWe) motorised pelletiser with a total capacity of 300 kg/h throughput (Pellets formed were 6 mm diameter by 23 mm length). The SB and OH pellets are shown in **Figures 15 and 16**, respectively.



Figure 15 - Sugarcane bagasse pellets

Due to the SB physical properties and pelletiser mechanical limitations, it was not possible to blend this feedstock with SS dust via pelletisation to produce a homogeneous pellet containing in situ catalyst. The pellets produced were fragile and easily breakable even with the introduction of water and polymers as a binder. On the other hand, the pelletisation between OH and SS dust was successful creating solid and stable pellets.

Prior to pelletising, the feedstocks were analysed in order to determine the proximate, ultimate, chemical compositions and higher heating value (HHV), while SS was characterised in terms of metal composition.



Figure 16 - Oat hulls pellets

3.2 Raw Materials Characterisation

The feedstocks (SB and OH) were analysed for proximate and ultimate analysis, chemical composition and HHV. SS were characterised in terms of metal composition.

3.2.1 Proximate Analysis

Proximate analysis characterisation (reported in wt%) was used in SB and OH biomass to calculate the moisture, ash, volatiles and fixed carbon contents on a dry basis.

Total moisture content was determined by drying the sample at 105 ± 3°C in a muffle furnace (CARBOLITE CWF1300) with an inert atmosphere for 3 h. The percentage of moisture was calculated based on the amount of mass lost (according to ASTM E1756-08).

The ash content was calculated using the same muffle furnace at 575 ± 25 °C for 5 h. The ash percentage was determined by weighing the amount of sample left in the muffle furnace after the heating process was completed (according to ASTM E1755-01).

Volatiles and fixed carbon were determined by Thermo Gravimetric Analysis (TGA) technique (NETZSCH TG 209 F1 IRIS) on dry basis. Approximately 15 mg of dried feedstock was put in a crucible and heated to 900 ± 10 °C (heating rate of 10 °C/min) in a nitrogen atmosphere (flow rate of 60 ml/min) and hold time for 15 min (according to BS EN 15148:2009). The fixed carbon was measured based on the amount of sample left in the crucible, while the volatiles represent the percentage of mass lost during the heating.

3.2.2 Ultimate Analysis

SB and OH dried samples were sent to an external accredited laboratory (Medac Ltd) to quantify the elemental content (C, H, N and S) of both feedstocks. The C, H, N analysis (with oxygen determined by difference) was carried out according to ASTM E777 and ASTM E778, and reported in wt%. The sulphur content was measured according to ASTM E775. The original analytical method (using the Thermo FlashEA® 1112 Elemental Analyzer) was performed by complete oxidation of the solid (flash combustion), transforming all organic and inorganic compounds in combustion elements. The combustion gases produced passed through a chromatographic column using helium as the inert gas, and then the thermal conductivity detector (TCD) calculated the percentage of each element (C, H, N and S) providing an output signal to the system.

3.2.3 Chemical Composition

Cellulose, hemicellulose, lignin, xylose and extractives contents of SB and OH were calculated by Celignis Analytical. The final balance was ash calculated by difference.

Biomass extractive-free samples were characterized for cellulose, hemicellulose, xylose and lignin content according to ASTM E1758-01. Solid samples were hydrolysed using 72% (w/w) acid sulfuric in a thermostatic bath at 30 ºC for 1 h. The hydrolysed acid was diluted to 4% (w/w) by mixing distilled water and autoclaved at 120 ºC for 1h. Consequently, the acid solution was cooled and filtered.

Soluble lignin obtained from the filter was measured using Ultraviolet-visible spectroscopy (absorbance at 280 nm).

The liquid filtered contains monomeric elements from the hydrolysis of polymeric carbohydrates which were analysed through high-performance liquid chromatography (HPLC) to quantify the content of cellulose, hemicellulose and xylose. A Shimadzu device carrying a RID-6A refraction index detector and an Aminex HPX 87H (300 mm × 7.8 mm, BIO-RAD) column was utilized during this process. The mobile phase was acid sulfuric (0.005 mol/L) at 40 ºC.

For the determination of the extractive content, a DIONEX Accelerated Solvent Extraction (ASE-200) was used operating at 100 ºC and 1500 psi. The extractive solvent selected was the ethanol (95%) and the minimum of sample required was 30 g of sample. The weight of extractives was calculated as the mass loss in the sample due to the extraction in the ASE-200.

3.2.4 HHV

Higher and lower heating values differ by in the inclusion of the evaporation latent heat. HHV accounts the energy required to evaporate the water, while for the lower heating value the same energy is not assumed as heat. The HHV (MJ/kg) of SB and OH was determined on dry basis using the unified correlation for fuels developed by (Channiwala and Parikh, 2002) where C (wt%) is carbon weight fraction, H (wt%) of hydrogen, S (wt%) of sulphur, O (wt%) of oxygen, N (wt%) of nitrogen and A (wt%) of ash:

$$HHV\ (MJ/kg) = 0.3491\ (C) + 1.1783\ (H) + 0.1005\ (S) - 0.1034\ (O) - 0.0151\ (N) - 0.0211\ (A) \quad (7)$$

3.2.5 Inductively Couple Plasma (ICP)

The sample of SS was digested using a combination of HNO_3 and HCl. The acid solution was made up to volume using deionised water resulting in a concentration of 5 g/L. Then, the solution (5 was analysed using a Varian 720ES ICP-OES to calculate the SS metal composition.

3.3 TCR Setup

The TCR-2 bench scale reactor was constructed, installed and commissioned at the laboratory of Fraunhofer UMSICHT Institute, Germany with a capacity to process up to 2 kg/h of biomass. The entire plant works in the absence of oxygen using nitrogen supply (1) and the temperature is measured through several K type thermocouples

installed along the unit. The process flow diagram (PFD) of the experimental setup is shown in Figure 17.

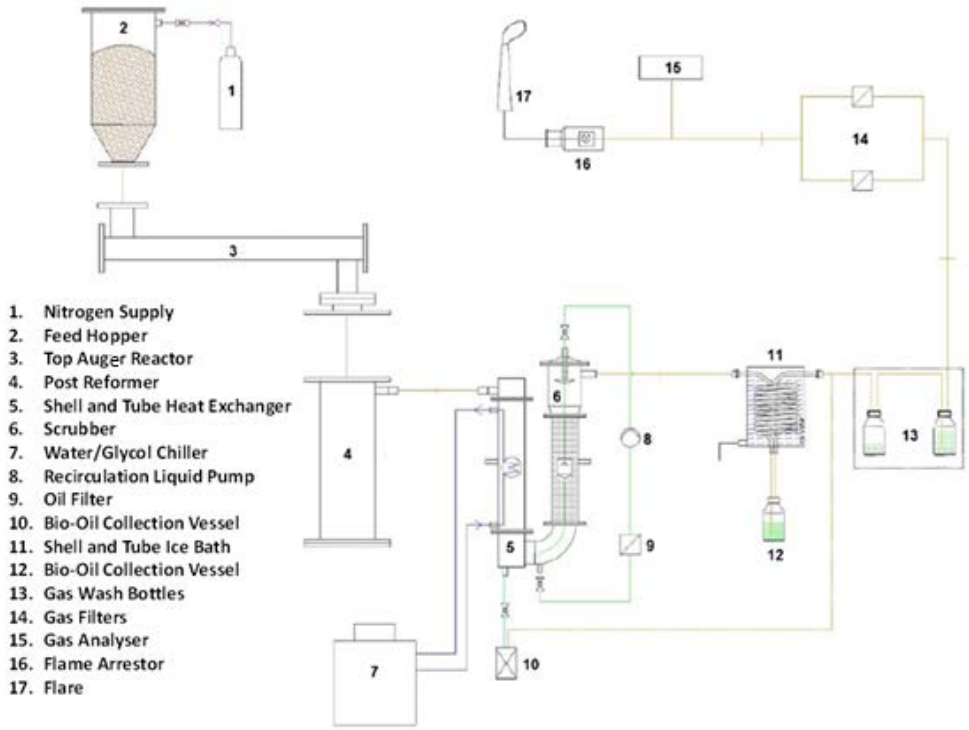


Figure 17 – PFD of the TCR-2 plant

In the condensing unit, condensable vapours from the post reformer are quenched by means of a shell (5) and tube condenser designated scrubber (6) within a u-tube condenser using a mixture of water and glycol from a chiller (7) to maintain the temperature at -5 ºC. Attached to the condensing unit, there is a vessel (10) to collect the bio-oil from the organic vapours condensed before. Condensable vapours exiting the condenser are further quenched by means of an ice bath cooler (11) using a vessel containing the bio-oil aqueous phase (12) from the previous TCR runs. The aqueous phase has the function of acting as a solvent and it helps to collect the residual liquid and also to clean the vapours produced.

a b

The remaining vapours (non-condensable gases) are directed into the filtration unit composed of two wash bottles and a filter for aerosol and other contaminants capture. The first bottle is filled with activated carbon (13a), the second is a candle filter (13b) and lastly, a glass wool filter (14). Then the permanent gases are directed to an online gas analyser/calorimeter (15) for detection and gas totalisation before flaring (16 and 17).

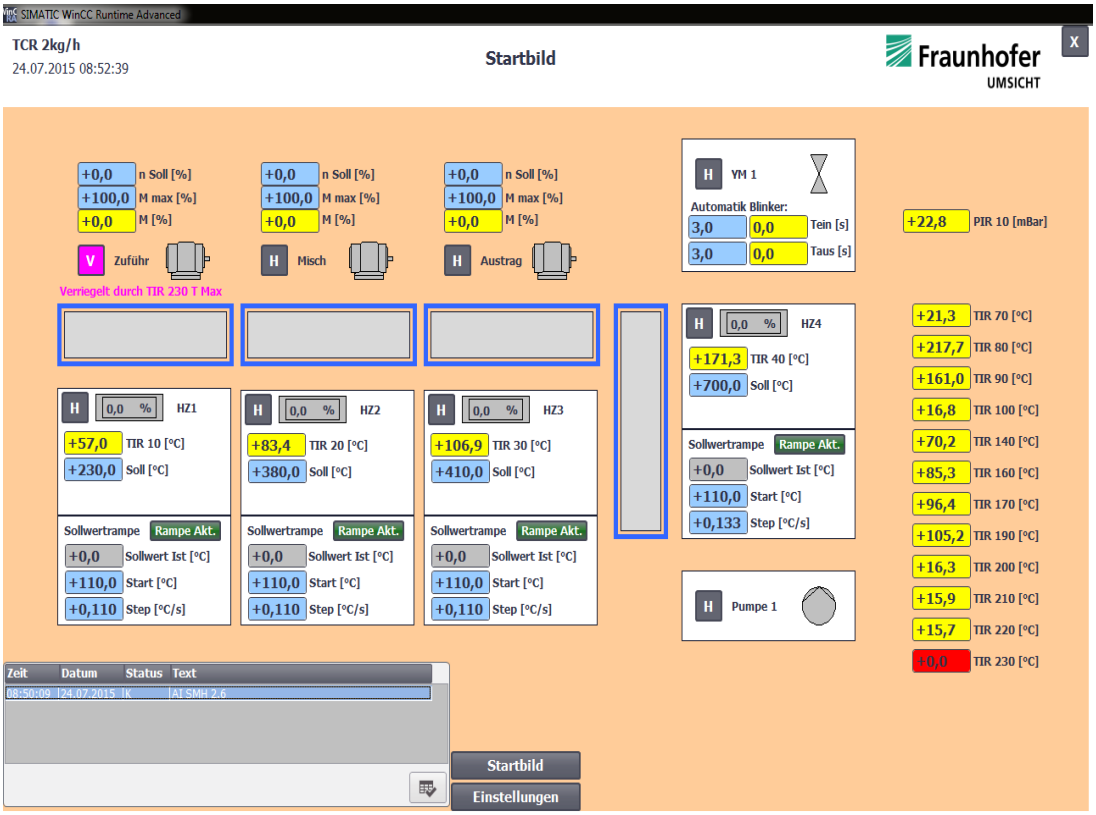


Figure 18 – TCR-2 software (Siemens SIMATIC Win CC)

In addition, the TCR-2 reactor is totally insulated and equipped with the necessary devices and fittings. The process control is performed using a Siemens SIMATIC Win CC software (Figure 18) where the parameters of the unit can be changed offering a wide range of options in terms of TCR products composition and distribution.

3.4 TCR Experimental Procedure

Before every TCR-2 experiment, the reactor was firstly disassembled and cleaned. From the auger pyrolysis reactor (including both screws) remaining feedstock not converted from previous runs were removed (Figure 19). The post reformer was emptied extracting the biochar produced (Figure 20).

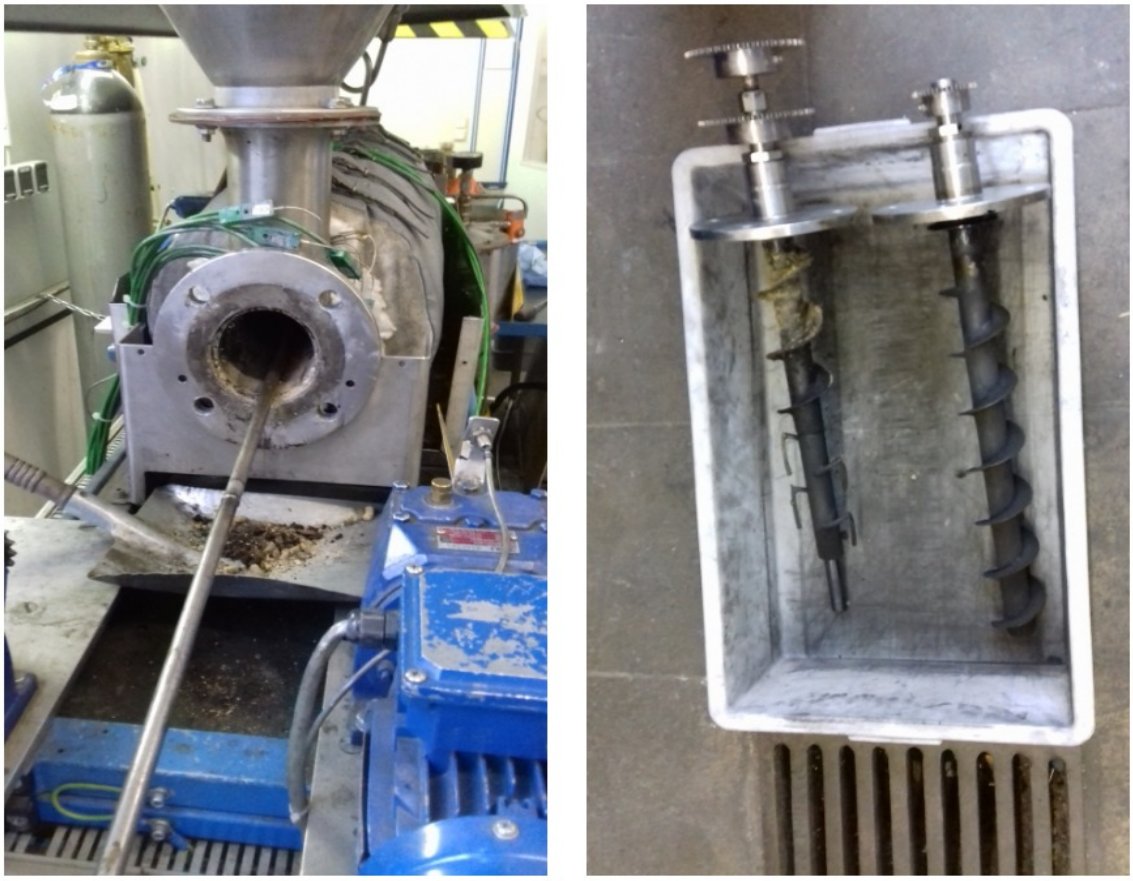


Figure 19 - Cleaning of the auger screw reactor

Moreover, the dust and fine particles from the biochar and SS present in the gas tube of the reforming unit were removed to prevent blockages in the following trials (Figure 21). Lastly, the condensing unit was cleaned as it can be observed in Figure 22 to avoid the contamination between different bio-oils produced in different experiments

with different operating conditions. All the material obtained from the cleaning was weighed and included in the mass balance.



Figure 20 - Post reformer disassembled and empty.

After the cleaning process, the post reformer was filled with 500 g of biochar or SS or a mixture in different ratios between both. Fresh biochar from the previous SB and OH runs was used, according to the type of feedstock processed and reactor parameters applied. The biochar had the role of promoting a catalytic effect in the condensable vapours and also in avoiding the entry of fine particles and dust in the outlet of the post reformer. Subsequently, the outlet of the auger pyrolysis reactor was attached to the inlet of the post reformer as shown in Figure 23.

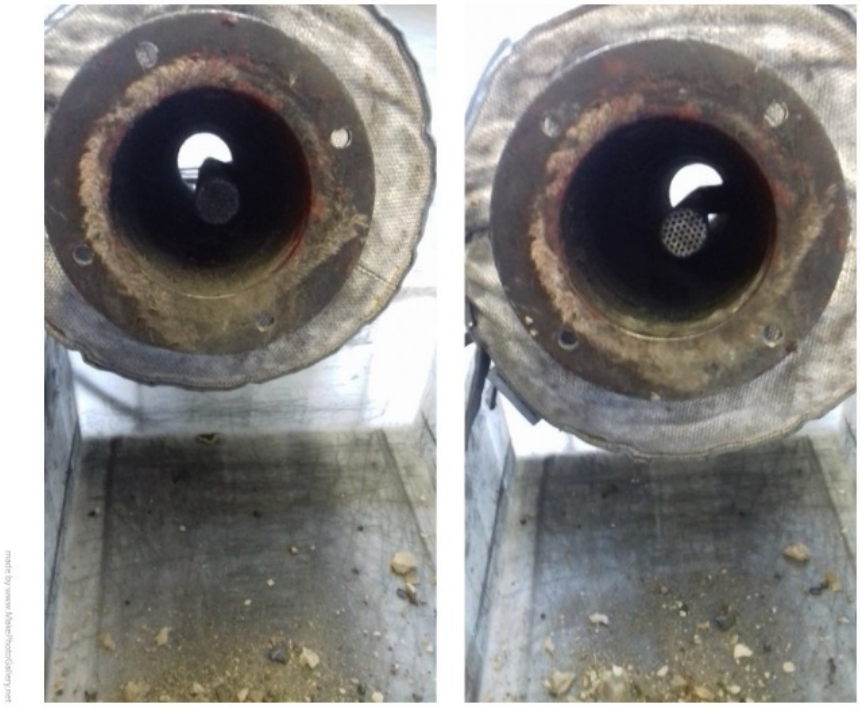


Figure 21 - Post reformer gas tube before and after cleaning



Figure 22 - Condensing unit being cleaned



Figure 23 - Post reformer connected to the auger pyrolysis reactor and condensing unit

The washing bottle connected to the ice bath after the condensing unit was filled with 650 mL of aqueous phase produced in the previous trials (Figure 24). Figures 23 and 24 also shows the bio-oil collection vessel attached to the condensing unit. In the filtration unit, activated carbon, candle and glass wool filters were weighed, replaced and connected to the plant (Figure 25). Then, the entire TCR-2 plant was closed and flushed with N_2 at 80 mbar in order to perform a leakage test certifying the unit was tight and properly assembled. The N_2 pressure was subsequently reduced to 40 mbar to remove the

oxygen from the system. When the gas analyser indicated an oxygen content below 0.5% the N_2 flow was stopped.



Figure 24 - Washing bottle containing TCR aqueous phase from bio-oil



Figure 25 – Gas filtration unit (activated carbon, candle and glass wool filters)

Before the experiment, the auger screw reactor was gradually heated for 80 minutes to 200 °C in the first area (to evaporate light volatile compounds) and between 400 and 500 ºC in the second and third area (for intermediate pyrolysis reactions) before the introduction of feedstock. In the post reformer stage, the temperatures were set between 500 and 700 ºC. During the heating process, the rotating screws were also turned on and the speeds of the inner and outer screws were 4 rpm and 1.25 rpm (revolutions per minute) respectively. The calibration of the screws was studied and established according to the right time required for an efficient conversion of the feedstock through pyrolysis.

Once the TCR had reached steady state temperature the first screw in the auger reactor was stopped and the sealed hopper (Figure 26) was opened to feed the plant with 3.5 kg of pelletised biomass (SB or OH). Consequently, the feed hopper was closed and the unit was flushed with N_2 again to decrease the oxygen below to 0.5%. When the N_2 flow was stopped, the first screw in the auger reactor was turned on initiating the introduction of biomass into the TCR-2 at a rate of up to 1.4 kg/h. The solid residence time was estimated to be between 5 and 10 min. Due to the process design of the auger screw reactor, the carbonised biomass produced promoted an internal catalytic effect improving the quality of the TCR-2 products. The biochar and permanent gases formed were transported by the screws to the reforming unit. The biochar residence time entering in the post reformer was totally regulated through the screws speed of the auger reactor.

The post reformer had the double function of collecting the char produced from the previous step and of converting the permanent gases into a syngas rich in H_2, due to the catalytic effect caused by the reactions between the biochar and the pyrolysis vapours. During the reforming process, the condensable organic vapours were also catalytic upgraded enhancing their chemical and physical fuel properties. The biochar rich in

carbon and with low hydrogen and oxygen contents remained in the post reformer until the end of the experiment.



Figure 26 - Feed hopper where the pelletised biomass was introduced

Subsequently, upgraded organic vapours were quenched at -5 ºC in the condensing unit to guarantee a complete separation between the pyrolysis liquid and the gas fraction. The bio-oil formed was collected and stored every thirty minutes in an external vessel. Then, the remaining non-condensable vapours passed through the filtration unit for aerosols, fine particles and other contaminants removal. The cleaned gas was directly measured and analysed via an online gas analyser/calorimeter.

TCR-2 experiments took around 3 h to be completed and 20 minutes to stabilise. The plant was operated in a semi-continuous mode with a pressure of approximately 70 mbar controlled by a pressure indicator and the TCR software . The unit temperature and the gas flow meter were registered every 15 minutes, while the density, HHV and composition of the gas were saved automatically. When no gas production was observed, the experiment was considered concluded and consequently, the heaters and auger reactor screws were switched off.



Figure 27 - TCR oil (aqueous phase on the top; organic phase on the bottom)

The unit cooled down overnight and in the next day, the reactor was disassembled and cleaned again. For the mass balance, all the liquids collection vessels, filters and wash

bottles were weighed. Additionally, the biochar from the post reformer was collected, separated (by physical methods), weighed and sent for analysis. The organic and aqueous phases of the bio-oil were separated using a separating funnel (see Figure 27). After 24 h, the organic and aqueous phases were stored separately, measured and sent for characterisation. The permanent gas data (density, HHV and chemical composition) was uploaded from the online gas analyser/calorimeter and further analysed. To guarantee the reproducibility of the results all trials were performed in duplicate.

TCR-2 experiments were divided into three main groups:

1) The first group (Set I) was carried out at the same intermediate pyrolysis temperature (450 ºC) in the auger screw reactor and three different reforming temperatures (500, 600 and 700 ºC) in the post reformer using OH and SB as a feedstock in different runs. These parameters were applied to understand which reforming temperature was able to favour a higher production of furfural and 2-furanmethanol in the OH and SB bio-oil. The post reformer was initially filled with biochar only.
2) The second group (Set II) was performed with the same reforming temperature (500 ºC in this case) varying the intermediate pyrolysis temperatures (400 and 500 ºC) converting OH and SB separately. The new variables implemented had the objective to realise which pyrolysis temperature caused higher yields of furfural and 2-furanmethanol in the OH and SB bio-oil. The post reformer was initially charged with biochar only.
3) In the first part of the third group (Set IIIa), SS (6 mm) was mixed with OH and SB biochar (in different trials) in the post reformer at different proportions (30,

70 and 100 wt% of SS in the reforming unit). In the second part of the third group (Set IIIb), SS (powder) was pelletised only with OH at different ratios (10, 20 and 30 wt% of SS in the feed composition) and introduced in the auger screw reactor (it was not possible to pelletise SS with SB). The difference between OH pellets and OH pellets mixed with SS can be seen in Figure 28. These experiments helped to comprehend the catalytic effect of the SS (with 2 different methods) on the upgradation of the pyrolysis products. The intermediate pyrolysis temperature (400 ºC in this case) and the reforming temperature (500 ºC) were always kept the same for all experiments with SS.

The experimental parameters for the different assays can be observed in Table 2.

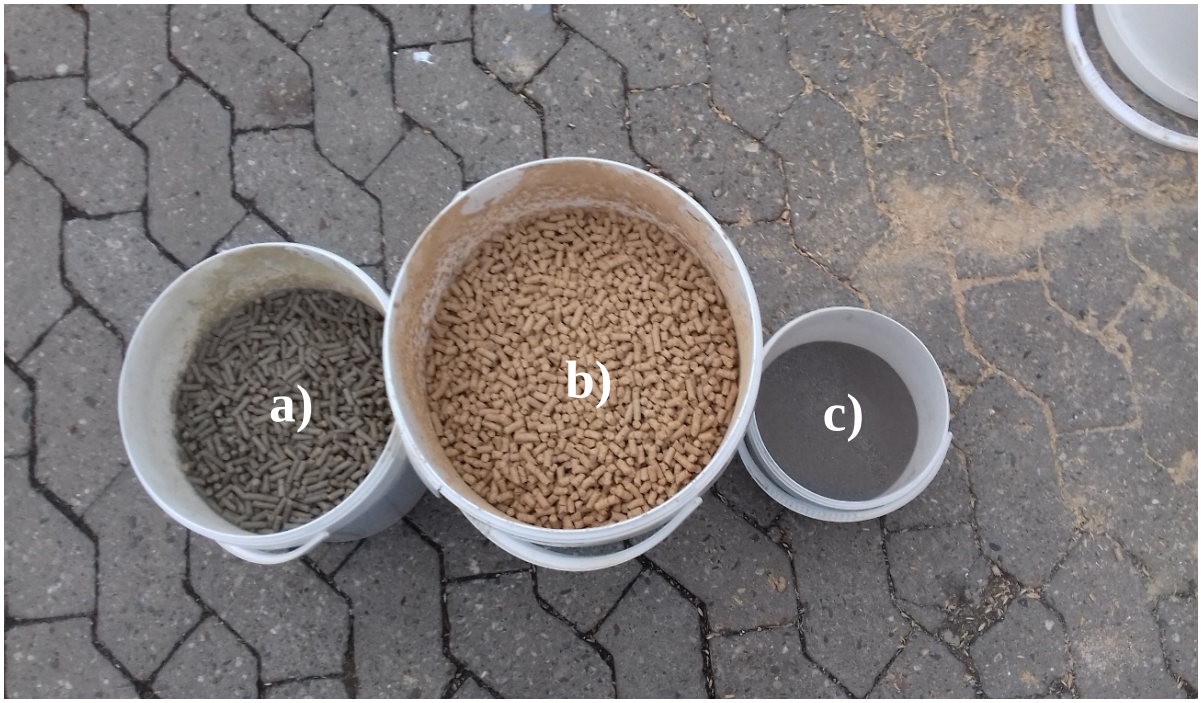


Figure 28 - Pelletisation with SS: (a) OH mixed with SS (30 wt%), (b) OH pellets, and (c) SS powder

Table 2 - TCR-2 experimental parameters

Assay	Feedstock	Pyrolysis Temp. (ºC)	Reforming Temp. (ºC)	SS Application	SS (wt%)	Char (wt%)
			SET I			
1	OH	450	500	-	-	100
2	OH	450	600	-	-	100
3	OH	450	700	-	-	100
4	SB	450	500	-	-	100
5	SB	450	600	-	-	100
6	SB	450	700	-	-	100
			SET II			
7	OH	400	500	-	-	100
8	OH	500	500	-	-	100
9	SB	400	500	-	-	100
10	SB	500	500	-	-	100
			SET IIIa			
11	OH	400	500	Reformer	30	70
12	OH	400	500	Reformer	70	30
13	OH	400	500	Reformer	100	-
14	SB	400	500	Reformer	30	70
15	SB	400	500	Reformer	70	30
16	SB	400	500	Reformer	100	-
			SET IIIb			
17	OH	400	500	Feed (Reactor)	10	100
18	OH	400	500	Feed (Reactor)	20	100
19	OH	400	500	Feed (Reactor)	30	100

3.5 Products Characterisation

After the experiments, the biochar, bio-oil and permanent gases were analysed to determine their chemical and physical properties. It is important to know the chemical composition of the bio-oil for fuel applications in engines in terms of efficiency and performance. Bio-oil samples were analysed to calculate the elemental composition, ash content, HHV, viscosity, density, total acid number (TAN), water content and chemical compounds. The fuel properties of the bio-oil (viscosity, density, TAN and water content) were characterised by Monition Ltd.

3.5.1 Oil and Char Ultimate analysis

The elemental composition of solid and liquid fuels are relevant to determine the carbon, hydrogen and oxygen contents which are directly associated to the HHV. A higher oxygen amount in the bio-oil leads to a lower calorific value and increases the instability of the oil accelerating the polymerisation reactions. High nitrogen and sulphur contents are related to NO_x and SO_x emissions when the pyrolysis oil is combusted. Moreover, these two compounds (N and S) can cause engine wear and corrosion due to its strong acidity level. C, H, N and S content of the OH/SB oil and char were calculated applying the same method as section 3.2.2. Furthermore, the oxygen was determined by difference ($100 - \sum$ (CHNS + ash)).

3.5.2 Oil and Char Ash content

Ash is composed of several alkali metals (potassium, calcium and sodium) responsible for some engine performance issues such as deposition, corrosion, blocking and erosion of the fuel pump, injectors and fuel line.

Oil ash percentage was obtained following ASTM D482 standard. A muffle furnace at 775 °C was used to combust the carbonaceous compound obtained from carbon residue. Subsequently, the ash produced after the combustion was quantified to calculate the respective fraction of the initial bio-oil. The quantification of ash in the char was determined at 575ºC as described in section 3.2.1 according to ASTM E1755-01.

3.5.3 HHV

Channiwala et al. (2002) fuels equation (7) was used to calculate the HHV of the OH/SB oil and char.

3.5.4 Viscosity

Viscosity characteristics depend on the pyrolysis conditions and the kind of biomass processed being one of the most relevant bio-oil properties for fuel applications in engines. A bio-oil with a reasonable viscosity content is beneficial for the prevention of internal leakages located in the fuel pump and line, increasing the brake power. However, a bio-oil containing high viscosity limits the fuel flow and favours engine blockages. The presence of alcohols and a small amount of water decreases the pyrolysis oil viscosity improving its stability, combustion and atomization.

The viscosity of all bio-oil samples was determined with a Cannon–Fenske Routine glass capillary viscometer (ASTM D445). Throughout the analysis, the viscometer setting was at 40ºC allowing passage of a specific pyrolysis oil quantity over the capillary. The viscosity final result is the multiplication of the oil travelling time (registered before) and the viscometer constant.

3.5.5 Density

Density is a significant feature for the determination of the pyrolysis oil consumption rate. A bio-oil rich in high molecular weight components presents higher values of density.

The bio-oil density was measured at 22 °C using a glass hydrometer between 0.8 and 1.0 g/cm^3 (ASTMD1298).

3.5.6 *Total Acid Number (TAN)*

ASTM D664 was the reference to calculate the oils acid number, using a Mettler Toledo V20 Compact titrator (potentiometric titration technique). The solvents toluene and isopropanol (50/50) served to dissolve the bio-oil. Thereafter a solution of KOH (0.1 N) was the reagent selected to titrate potentiometrically the bio-oil using a combination electrode.

3.5.7 Water Content

The water present in the bio-oil (formed due to the water reactions during pyrolysis) is linked to the moisture content of the biomass. A bio-oil with a high water content gives phase separation issues and contains a lower ignition temperature, HHV and a poor immiscibility with gasoline/diesel fuels. This leads to an increment of viscosity and polymerization of the bio-oil affecting the atomisation and the engine combustion performance.

Mettler Toledo V30 Compact Volumetric Karl Fischer titration was used to determine the water percentage of the OH/SB oils (ASTM E203). The value obtained of the total sample was revised to weight percent.

3.5.8 Gas Chromatography Mass Spectrometry (liquid-GC-MS)

GC-MS was performed to detect the most abundant chemical compounds present in the OH/SB pyrolysis oil.

Bio-oil samples were diluted in ethanol (1:10 ratio) and analyzed with a gas chromatograph coupled with a mass spectrometer Shimadzu GCMS-QP2020. Chromatograph was equipped with a 30 m nonpolar 0.25-mm inner diameter (i.d.), 0.25-µm film thickness DB-5ms (column name) and 1.5 m middle polar 0.15-mm i.d., 0.15-µm film thickness VF17ms (column name) column set from Agilent. Helium with 5.0 purity was used as carrier gas in all experiments. The injection volume was set to 1µL. The measurements were performed at a constant linear velocity (40 cm/min) of carrier gas. The temperature of the GC oven was programmed from 40 °C (3 min hold) to 320 °C (3 min hold) at 10 °C/min. The temperatures of the injector, MS-interface and MS was set to 250, 280 and 200 °C respectively. The quadrupole MS detector was operated at a scan speed of 5000 Hz using a mass range of 35-500 m/z. Solvent cut time was 3 min.

3.5.9 Gas Analysis

The permanent gases produced were frequently analysed and measured using a Gas analyzer MGA 12, Dr Födisch Umweltmesstechnik according to EN 15267-3 standard test procedure. The gas analyser methodology was established on an infrared photometer (CO, CO_2, CH_4), an electrochemical cell (O_2) and a TCD (H_2). The percentage not detected was presumed to be hydrocarbons which the levels were above of the analyser limits. The Union Instruments CWD2005 process gas analyser was used to

calculate the HHV of the gas fraction. The calibration of the gas analysers were performed prior to the experiments.

3.6 Bio-oil Upgrading

The pyrolysis oil properties produced via TCR-2 indicate that the fuel would need to either be blended with conventional fuels or further upgraded before being applied as an engine fuel. This is due to its high oxygen and water content, viscosity and acid number. In addition, one of the goals of this project was to convert furfural, 2-furanmethanol and other furans in 2-MF. This bio-oil conversion and the consequential improvement of its properties were only possible implementing SS in the TCR reactor and upgrading the pyrolysis liquid via HDO. HDO process, catalysts preparation and the catalytic characterisation of the OH/SB biochar and SS are described in the following sections.

3.6.1 HDO Process

TCR bio-oil was hydrodeoxygenated in the Fraunhofer UMSICHT Institute and all the experiments were performed in an autoclave reactor (Parr 4575, 500 mL) demonstrated in Figure 29. The reactor was equipped with an electric blanket furnace and a stirrer. Cu-Zn/Al_2O_3 and Cu-Mn/SiO_2 (powder) were the catalysts selected for the HDO and all typical procedures were implemented for the HDO process.

For each test, 30 g of bio-oil and 3 g of catalyst (10 wt% of the oil) were introduced in the autoclave. The reactor was closed, connected to the HDO plant and purged with nitrogen for 10 minutes to remove the oxygen. Consequently, the N_2 flow was closed and the system was flushed with H_2 during 10 minutes to remove the resident nitrogen. Then,

the reactor was filled with H_2 till 90 bar of pressure and the stirrer was set at 400 rpm. The autoclave temperature was raised to 280 or 380 ºC (depending on the experiment) and maintained constant for 7 h. Additionally, the stirring (400 rpm) and the H_2 pressure (90 bar) were also kept constants. After cooling (using an electrical fan), the upgraded bio-oil and the catalysts from the HDO autoclave were separated through filtration using a separator funnel (Figure 30).



Figure 29 - HDO autoclave reactor

During the HDO treatment, TCR-2 bio-oil with higher furfural and 2-furanmethanol yields was used. Two different temperatures were applied (280 and 380 ºC) with two different catalysts (Cu-Zn/Al_2O_3 and Cu-Mn/SiO_2) performing a total of four HDO experiments. The HDO operation conditions and the selection of catalysts were based on the works developed by Yang and Zheng (Yang et al., 2004, Zheng et al., 2008).



Figure 30 - Filtration of HDO bio-oil

3.6.2 Catalysts Preparation

Cu-Zn/Al_2O_3 (atomic ratio: Cu/Zn/Al = 54.5/27.3/18.2) and Cu-Mn/SiO_2 (molar ratio: Cu/Mn/Si = 1/1.12/1.13) catalysts were prepared by Riogenic Lab (USA). The technique applied was the impregnation of metal and nitrate salts as precursors with the respective supports in oxide form (Al_2O_3 and SiO_2). The thermal calcination/reduction was performed in a hydrogen atmosphere at 450 ºC for 4 hours at 40 Mpa.

3.6.3 Porosimetry

The surface area of the OH/SB (raw material and biochar) and SS was determined using a Micromeritics Baflex Surface Characterisation device. Before the analysis, 0.5 g of the sample was heated at 200 ºC during 2h to remove contaminants. Nitrogen was the

gas selected for the porosimetry experiments and its absorption on the material surface created a monolayer which was used to calculate the specific surface area. Whereas the nitrogen capillary condensation allows the measurement of the pore volume/size and size distribution. The 3Flex Version 4.05 software was used to process the data and the Brunauer–Emmet–Teller (BET), which is an extended version of the Langmuir model, was used to calculate the surface areas

3.*6.4 X-Ray Diffraction (XRD)*

XRD is one of the experimental analytical methodologies applied to identify the crystalline phase of a material. This technique provides information about the structure, composition, and physical properties of materials.

The crystalline phases of the SS, and OH/SB (raw material and biochar) were analyzed by a Bruker D2 Diffractometer applying a Co $K_{\alpha 1}$ and $K_{\alpha 2}$ radiation (λ = 1.788965 Å and 1.792850 Å) in θ/θ reflection mode. The diffracted Co K_{β} radiation (λ = 1.620790 Å) was removed by a Ni filter placed in front of the detector. The X-ray source was a sealed tube with a cobalt anode and it was used a LYNXEYE position sensitive detector. There was a 1.0 mm exit slit between X-ray source and sample. The 3 mm knife edge was used all the analyses.

4. RESULTS AND DISCUSSION

The goal of this chapter is to show, compare and discuss all the experimental results obtained. This chapter starts with the raw materials characterisation results and then investigates the data from TCR-2 experiments in three different sections: a) changing the reforming temperature of the post reformer; b) varying the pyrolysis temperature of the auger screw reactor and; c) mixing SS in different ratios with the feed in the pyrolysis reactor and with the biochar in the reforming unit. Subsequently, the HDO results of the bio-oil are presented and discussed. The chapter concludes with a general discussion of the experimental findings, identifying the optimal process route and the limitations of the practical work performed.

All the experiments carried out in this project had the objective of improving the scientific limitations found and described in Chapter 2. For that reason, the effect of the TCR technology using different biomass and SS as a catalyst to optimise the properties of the bio-oil for fuel engines application was investigated.

4.1 Raw Materials Characterisation

Both feedstocks (SB and OH) were analysed through ultimate/proximate analysis, lignocellulosic composition and HHV. SS was characterised in terms of metal composition.

4.1.1 Feedstock Characterisation

The ultimate/proximate analysis, HHV and lignocellulosic composition of the SB and OH pellets used in the TCR experiments are shown in Table 3. In general SB and OH

pellets have a similar elemental composition and HHV. The HHV of SB is slightly higher compared to the OH due to its lower moisture and oxygen content and higher carbon content. However, the high calorific value of these lignocellulosic residues makes them valuable for biofuels production through thermochemical technologies (Varma and Mondal, 2017). Results from the ash content show a low level for both feedstocks which is an advantage for bio-oil production via intermediate pyrolysis (Abu El-Rub et al., 2004). In terms of lignocellulosic composition, the high hemicellulose level of the biomasses investigated indicates a good source of furfural and xylose components. It is detailed in Table 3 that the percentages of xylose in the SB and OH composition are 32.4 (39.4*82.3) and 26.5% (35.3*75.2), respectively.

The SB characterisation values of the current work do not present a close correlation when compared to the literature (Al Arni, 2018, Boussarsar et al., 2009, Rocha et al., 2015, Varma and Mondal, 2017). There are more than 500 sugarcane species and their chemical composition can be slightly different (Rocha, Nascimento et al. 2015).Only the ash (3.1 wt%), water (5.4 wt%) content and the elemental composition (44.9 wt% of carbon, 5.9 wt% of hydrogen and 45.8 wt% of oxygen) found in Varma and Mondal (2017) study is similar to Table 3. Al Arni (2018) investigated bagasse with moisture, ash content and HHV of 8.5, 5.9 wt% and 18.2 MJ/kg, respectively. The hemicellulose and lignin percentage presented by Rocha et al. (2015) and Boussarsar et al. (2009) were 27.8 and 21.6 wt% for the first work and 26.2 and 20.4 wt% for the second one. The same articles published lower xylose contents in the SB composition (24.0 and 24.1 wt%, respectively).

OH characterisation values obtained are representative compared to the literature results found (Abedi and Dalai, 2017, Valdebenito et al., 2017, Zhang et al., 2013). Abedi

and Dalai (2017) reported for the same type of biomass 41.8, 6.4, 44.7 wt% and 16.8 MJ/kg for C, H, O and HHV, respectively.

Table 3 - Feedstock characterisation

	SB	**OH**
Ultimate analysis (dry basis)		
C (wt%)	43.7	40.6
H (wt%)	5.1	6.0
N (wt%)	0.10	1.1
S (wt%)	0.61	<0.1
O (wt%) (difference)	46.5	49.9
Proximate analysis (dry basis)		
Moisture (wt%)	6.0	14.8
Ash (wt%)	4.0	2.4
Fixed Carbon (wt%)	17.2	26.4
Volatiles (wt%)	72.8	56.4
HHV (MJ/kg)	16.4	16.0
Lignocellulosic composition		
Cellulose (wt%)	43.6	39.6
Hemicellulose (xylose) (wt%)	39.4 (82.3)	35.3 (75.2)
Lignin (wt%)	10.8	10.3
Extractives (wt%)	2.2	12.4

However, the same study showed a lower level of moisture (8.5 wt.%) and a higher amount of ash (5.8 wt.%), which is a disadvantage for char production and their respective properties (Mayer et al., 2012). The work developed by Valdebenito et al. (2017) showed oat hulls composed of 38.7 wt% of cellulose, 34.4 wt% of hemicellulose (26.2 wt% of xylose) and 11.1 wt% of lignin. Zhang et al. (2013) calculated the elemental composition (C, H and O) and HHV for OH obtaining 43.5, 4.7, 45.9 wt% and 16.1 MJ/kg, respectively.

4.1.2 Steel Slag Metal Composition

SS metal composition is shown in Table 4 and the main elements found were calcium, iron and magnesium. ICP technique could not identify all the compounds of SS such as metal oxides. Calcium is the major metal in SS and its presence in the pyrolysis feed promotes the formation of char and ash in its composition (Mayer et al., 2012). Moreover, calcium and manganese stimulate the production of hydrocarbons in the pyrolysis oil (Nokkosmäki et al., 2000). The high iron composition of SS can favour decarboxylation and dehydration reactions converting polysaccharides into furans and CO_2 and decreasing the acid level of the pyrolysis liquids (Lee et al., 2014, Yang et al., 2017).

The metal composition of SS can vary according to the industrial process and operational conditions (Matthaiou et al., 2019). Sun et al. (2018) worked with SS containing similar amounts of Ca (35.7%), Fe (24.9%) and Mg (5.1%) but higher Si (24.0%) content. From the Matthaiou´s et al. (2019) study, SS presented a similar Fe percentage (23.8%) although the Ca (12.1%), Mg (0.83%) and Si (6.7%) contents were considerably different.

Table 4 - SS metal composition

Element (dry basis)		**Element** (dry basis)	
Ca (%)	30.6	Sr (ppm)	169.5
Fe (%)	24.1	Pb (ppm)	147.5
Mg (%)	4.9	Sn (ppm)	30.5
Mn (%)	1.9	Zr (ppm)	22.0
Si (%)	1.9	Sb (ppm)	17.5
Al (%)	1.3	Cu (ppm)	14.0
P (%)	0.59	Zn (ppm)	14.0
Ti (%)	0.59	Bi (ppm)	11.5
V (%)	0.50	Ce (ppm)	5.5
Na (%)	0.42	Lu (ppm)	4.0
K (%)	0.20	Mo (ppm)	4.0
Cr (%)	0.18	Li (ppm)	3.0
B (ppm)	219.0	Y (ppm)	3.0
Ba (ppm)	205.0	Ni (ppm)	2.5
Ga (ppm)	177.0	Er (ppm)	2.0

4.2 Different Reforming Temperatures in TCR Process

In the first set of tests, TCR trials were performed changing only the reforming temperature. The other experimental conditions were kept constant as demonstrated in Table 5.

Table 5 - TCR runs conditions with different reforming temperatures

Experimental Conditions	Set 1 (Trial 1 to Trial 6)
Intermediate Pyrolysis Temperature	450 ºC
Reforming Temperature	500, 600 and 700 ºC
Feedstock	SB and OH
Feed Consumption	3.5 kg (Pellets)
Feed Rate	1.4 kg/h
Solid Residence Time	Minutes
Gas Residence Time	Seconds
Biochar (Reformer)	500 g
SS (TCR)	-

4.2.1 Bio-oil Analysis

The properties of the bio-oil organic phase from SB and OH runs, after separation from the aqueous phase, are shown in Table 6. For both feedstocks, the results show an increase in carbon content and HHV when the post reformer reaches higher temperatures. Consequently, it is observed a lower oxygen level when higher reforming temperatures are applied. A low oxygen content leads to a better calorific value and reduces the instability of the oil deaccelerating the polymerisation reactions and the ageing effect of the bio-oil (Ouadi et al., 2018).

Comparing the HHV value of the bio-oil for all experiments with the original feedstock (16.4 and 16.0 MJ/kg for SB and OH, respectively), the potential of the TCR technology in valorising the energy density of biofuels per unit volume is recognised.

Additionally, TCR runs decreased the oxygen present in the pyrolysis oil from the initial feedstock favouring the properties and the stability for fuel applications (Yang et al., 2013).

Table 6 - SB and OH bio-oil characterization at different reforming temperatures (Pyrolysis temperature = 450 ºC)

	SB			**OH**		
Reforming Temperature (°C)	**500**	**600**	**700**	**500**	**600**	**700**
Ultimate analysis						
C (wt%)	71.3	74.6	77.2	72.2	77.4	78.8
H (wt%)	7.1	7.4	8.0	8.2	7.5	7.2
N (wt%)	0.69	0.56	0.54	1.9	2.7	2.5
S (wt%)	0.10	0.10	0.18	0.68	0.76	0.77
O (wt%) (diff.)	20.8	17.4	14.1	17.0	11.7	10.7
Fuel Properties						
HHV (MJ/kg)	31.1	33.0	34.9	33.2	34.6	35.0
Ash (wt%)	<0.001	<0.001	<0.001	<0.001	<0.001	<0.001
Water (wt%)	4.7	2.2	1.9	4.8	3.9	2.3
TAN (mg KOH/g)	27.7	17.3	15.6	30.5	21.4	17.7
Viscosity (mm^2/s)	24.9	13.7	12.1	36.5	35.4	17.8
Density (kg/m^3)	1062	1060	1059	1074	1082	1072

The HHV of bio-oil increased from 31.1 to 35.0 MJ/kg. OH experiments displayed better results due to the higher carbon content and lower oxygen level present in the pyrolysis oil.

Low nitrogen and sulphur contents shown in Table 6 are associated with low NO_x and SO_x emissions when the pyrolysis oil is combusted. Moreover, small portions of these two compounds can minimize engine wear and corrosion due to its strong acidity level (Hossain et al., 2013).

The ash content was <0.001% for all the experiments. It is crucial to have a bio-oil with a low ash composition due to the problems related to engine performance such as blocking, corrosion, deposition and erosion of the fuel line, injectors and fuel pump (Huber et al., 2006).

Concerning water content, lower reforming temperatures showed higher percentages which give lower ignition and combustion temperatures in the cylinders and subsequently lower NO_x emissions (Ouadi et al., 2013). Another feature of a bio-oil with a modest moisture level is the reduction in polymerisation which improves the atomisation and the engine combustion performance (Ikura et al., 2003). However, when the pyrolysis oil contains less water the energy density is higher. Under this fact, it is easier to mix the bio-oil with petrol fuels due to a better miscibility and there are less issues separating the organic phase from the aqueous one (Chiaramonti et al., 2003). If the phase separation is not efficient, the water present in the bio-oil might lead to metal electrochemical reactions further up and there is the possibility of microorganisms growing and decreasing the stability of the oil (Schleicher et al., 2009). The water is

formed due to the moisture of the biomass and also during the dehydration reactions which occur in the thermal degradation of the feedstock (He et al., 2009). All SB trials at different reforming temperatures contain less moisture when compared to OH. This may be caused due to the lower water content present in the raw SB as observed in Table 3.

The TAN of SB and OH oil decreased with higher reforming temperatures. Thus, there are less organic acid compounds and a reduction of wear and corrosion in engine components. The existence of phenolics and other unidentified elements in the oils plus the water content may justify the high acid number of the pyrolysis oil at lower reforming temperatures found in this work (Santos et al., 2019). This can be minimised by mixing the bio-oil with biodiesel or other alkaline fuels. Results from Table 6 show a lower acidity of the SB bio-oil which is attributed to the lower water content present in its composition when compared to the OH oil.

The present study points to higher viscosity with lower reforming temperatures. At higher reforming temperatures the organic vapours have a more efficient cracking producing lighter chemical compounds causing a lower viscosity level. For that reason, the best results were achieved at 700 ºC (12.1 and 17.8 mm^2/s for SB and OH bio-oil, respectively). According to some studies, the viscosity of the oil should be no more than 20 mm^2/s at 40 ºC (Garcìa-Pérez et al., 2006). A low viscosity level would be beneficial to the flow characteristics and consequently results in more complete pumping and combustion creating a better engine power performance (Santos et al., 2019). A bio-oil with a reasonable viscosity content is beneficial for the prevention of internal leakages located in the fuel pump and line, increasing the brake power and the lubricity. On the other hand, a bio-oil containing high viscosity limits the fuel flow and favours engine blockages causing incomplete combustion and engine power loss (Zhang et al., 2013).

Density is a significant characteristic for the determination of the consumption rate of the pyrolysis oil and it is associated with the engine performance in terms of fuel injection time and fuel spray penetration in the cylinder (Yamane et al., 2001). Higher reforming temperatures lead to the production of compounds with a lower molecular weight, and so, decreases the density of the bio-oil. The only exception found in this trials was in the conversion of OH at 600 ºC. Oil with lower density led to better combustion and more stable engine operation.

Table 7 shows the properties of several bio-oils from different feedstocks and pyrolysis technologies according to the literature review.

The present work at 500 ºC (reforming temperature) obtained significantly better results in terms of HHV, ash and water content compared to fast pyrolysis process using the same biomass (SB) and similar pyrolysis temperatures (around 450 ºC), increasing the quality for fuel applications. Pattiya and Suttibak (2017) and Islam et al. (2010) produced SB fast pyrolysis oil (at 430 and 475 ºC, respectively) containing more 49.5 and 88.0% of oxygen., more 393.6 and 357.4% of water and less of 14.2 and 24.4% of calorific value, respectively. The oxygen and water contents of the bio-oil from fast pyrolysis are usually between 30-50% and 10-20%, respectively (Bridgwater, 2012).

Table 7 - Bio-oil and fuels properties from literature review at different reforming temperatures using several feedstocks and pyrolysis technologies

Pyrolysis Type	Temperature (ºC)		Biomass / Fuel	C (wt%)	H (wt%)	N (wt%)	S (wt%)	O (wt%)	HHV (MJ/kg)	Ash (wt%)	Water (wt%)	TAN (mg KOH/g)	Viscosity (mm^2/s)	Density (kg/m^3)	Ref.
	Reactor	Reformer													
Fast	430	-	SB	59.9	7.7	0.90	-	31.1	26.7	0.41	11.7	-	23.2	1100	1
Fast	475	-	SB	52.6	7.4	0.75	0.07	39.1	23.5	0.06	11.6	-	21.5	1150	2
Intermediate	450	-	Barley straw	62.7	8.1	1.4	-	25.8	28.9	0.20	5.8	30.9	30.5	1150	3
TCR	400	500	SB	53.7	9.7	1.1	0.30	35.2	24.3	<0.10	25.6	11.1	-	-	4
TCR	400	600	SB	71.4	5.4	1.3	0.10	21.8	28.8	<0.10	7.2	12.3	-	-	4
TCR	400	700	SB	-	-	-	-	-	33.9	<0.10	2.6	16.1	-	-	4
TCR	450	500	Digestate	78.0	8.3	5.2	1.2	7.0	36.3	0.20	2.0	8.8	-	-	5
TCR	450	750	Digestate	79.6	7.0	5.2	1.1	7.0	37.4	0.10	2.0	5.1	40.0	-	5
TCR	450	600	Wheat Husk	56.3	7.8	4.8	1.4	29.7	26.0	<0.001	1.0	29.9	145.2	-	6
TCR	450	700	MSW	83.7	7.5	1.8	0.20	6.7	38.2	<0.05	3.2	2.9	6.5	-	7
TCR	450	700	Co-form rejects	87.6	8.1	0.27	0.05	3.8	39.3	0.10	0.10	0.78	1.7	-	8
TCR	450	700	SB	77.2	8.0	0.54	0.18	14.1	34.9	<0.001	1.9	15.6	12.1	1059	9
-	-	-	Biodiesel	78.9	12.6	<0.10	0.74	8.4	37-40	<0.10	0.37	0.49	1.9-6.0	880	10
-	-	-	Diesel	84-87	13-16	<0.10	<0.10	1.0	42-45	<0.01	0.05	0.03	1.9-5.5	820-850	11

1 - (Pattiya and Suttibak, 2017); 2 - (Islam et al., 2010); 3 - (Yang et al., 2014); 4 - (Ahmad et al., 2018); 5 - (Neumann et al., 2016); 6 - (Santos et al., 2019); 7 - (Ouadi et al., 2017); 8 - (Ouadi et al., 2018); 9 - Present work; 10 - EN 14214; 11 - EN 590.

The most relevant variation between fast and intermediate technologies is the solid residence times, causing a different heat transfer to the biomass. It leads to better control of the chemical reactions and a lower thermal cracking of the bio-components in the intermediate pyrolysis, resulting in less tar formation and general optimization of the process (Dhyani and Bhaskar, 2018). Pyrolysis oil from the intermediate process contains less water, tars and ashes (lower contamination level) and it is easier to separate the organic phase from the aqueous phase, contrasting with fast pyrolysis (Yang et al., 2014, Zhang et al., 2007).

The benefits of mixing biochar with fresh biomass were proven via intermediate pyrolysis. The effect of char recycling is the novelty of this reactor type creating an additional catalytic effect in the process. This leads to a better quality pyrolysis oil when compared to commercial bio-oils from fast pyrolysis due to oil formation with lower molecular weight (mainly aromatics such as benzene, toluene and ethylbenzene and olefins) increasing the calorific value of the bio-oil (Hornung et al., 2011, Ouadi et al., 2013).

Yang et al. (2014) worked with the Pyroformer reactor converting barley straw under intermediate pyrolysis conditions and operating with similar temperature as this section (450 ºC). The HHV presented were lower (28.9 MJ/kg) in comparison to the current set of tests which can be explained as being due to the catalytic activity occurring inside the post-reformer reactor. In addition, TCR runs could produce better bio-oil in terms of fuel properties (mainly at higher reforming temperatures) except for the viscosity.

It has been demonstrated that the utilisation of biochar as a catalyst in the reforming unit upgraded the organic vapours into high-quality pyrolysis liquids. This carbonised solid presents a good surface and other chemical and structural properties which promotes a catalytic treatment in the volatiles before their condensation, reducing the content of water and oxygen and increasing subsequently the HHV of the pyrolysis liquid (Dhyani and Bhaskar, 2018, Jager et al., 2016).

Ahmad et al. (2018) and Neumann et al. (2016) reported the same trend when they increased only the reforming temperature through TCR technology. With the increment of temperature both works show an improvement of the bio-oil properties such as less water and oxygen, more carbon content and better HHV. The experimental conditions (biomass and reforming temperature) of the present study were identical to Ahmad et al. (2018), except in the temperature of the intermediate pyrolysis reactor. Ahmad et al. (2018) produced a bio-oil with lower carbon and HHV and higher water and oxygen contents, which might be explained due to lower pyrolysis temperature (400 ºC) and SB feedstock with a different chemical composition. On the other hand, Neumann et al. (2016) obtained better results analysing the lowest reforming temperature (500 ºC) between both works. SB and OH biomasses contain more oxygen and less carbon and hydrogen (Table 3) when compared to digestate (38.5, 51.8 and 6.3 wt%, respectively), affecting the properties and the quality of the pyrolysis liquid.

Under the same conditions as Miloud's et al. (2017) and Miloud's et al. (2018) works, where MSW and co-form rejects were processed via TCR at 700 ºC reforming temperature, the bio-oil revealed better fuel properties in relation to HHV, moisture, TAN and viscosity. Once again, the justification was found in the chemical composition of

MSW and co-form rejects feedstocks presenting a higher calorific value (18.3 and 20.4 MJ/kg, respectively) and lower oxygen content (31.4 and 30.2 wt%, respectively). Co-form rejects contain a high polypropylene content which is converted directly into hydrocarbons.

In the work developed by Santos et al. (2019), the TCR oil from wheat husk at 600 ºC indicated a worse quality when compared to SB and OH trials at the same temperature. The different chemical composition found in the wheat husk might be the reason for the differences. Despite the slight differences between the results of the present work and the values found in the literature review for the reasons mentioned previously, the SB and OH bio-oil are in agreement with the standards of the TCR technology.

In comparison to biodiesel, the heating value of bio-oil from SB and OH on average at 700 ºC was very close to the measured heating value of this fuel (37.0 MJ/kg). The TCR oil was found to be satisfactory, however this is not the case when compared to diesel (42 MJ/kg). The difference between pyrolysis liquid and diesel is related to the higher oxygen content of biomass-derived fuels, due to the presence of certain compounds such as carboxyl hydroxyl, aldehyde, ether and carbolic groups (Liu et al., 2014). The oxygen content of OH was slightly higher with 8.4 wt% for biodiesel, but almost 10 times higher than the diesel (1.0 wt%). Therefore, SB/OH bio-oil and biodiesel present lower combustion power due to the higher oxygen amount in their chemical composition (McDonnell et al., 1999).

Tables 6 and 7 also display a parallel carbon value between the SB/OH oil (77.2 and 78.8 wt%) and biodiesel (79.9 wt%), but diesel contains around 6.6-8.8% more carbon. Hydrogen contents in the biodiesel and diesel (12.6 and 13.0 wt%) were

approximately 62% higher than OH experiment at 700 ºC (8.0 wt%). The small amount of nitrogen and sulphur in the SB oil, biodiesel and diesel might produce a combustion gas with low NO_x and SO_x emissions.

The analysis of the fuel properties between the pyrolysis liquid and biodiesel/diesel are essential to evaluate the potential as an engine fuel. The ash content was <0.001% for all the experiments. This value is acceptable in comparison with diesel (0.01%) and biodiesel (0.10%) for engine applications and furnaces.

SB and OH trials contain more water than biodiesel (0.37 wt%) and diesel (0.05 wt%) attributed to the higher amount of oxygen in the bio-oil. Consequently, the HHV of the pyrolysis liquid is less attractive as an energy vector.

The acid number found in this work is relatively high compared to biodiesel (0.49 mg KOH/g) and diesel (0.03 mg KOH/g). This may be caused by the water content of the SB/OH oils and a chemical composition rich in phenolics. In general, a high acid number is not suitable for engine applications as it causes corrosion and damage to fuel system components (Ouadi et al., 2018).

Results from the viscosity show a SB oil at 700 ºC (12.1 mm^2/s) with more than the double of the value of the biodiesel (6.0 mm^2/s) and diesel (5.5 mm^2/s). A reasonable viscosity is positive to lubricate the engine system reducing mechanical wear, however is harmful to the flow characteristics provoking engine power loss and inefficient combustion (Hossain et al., 2013).

In terms of density, SB/OH bio-oil has higher values when compared to biodiesel (880 kg/m^3) and diesel (850 kg/m^3). The existence of more oxygenated compounds in the pyrolysis oil causes a liquid more dense due to the presence of higher weight molecules.

When a bigger mass of dense liquids are injected in the system, the heating process of the oils is not so efficient affecting the performance of the engine (Yamane et al., 2001).

In conclusion, TCR oil from SB and OH indicated some positive aspects to be applied as fuel for engines when compared to other pyrolysis technologies as fast pyrolysis. It demonstrated sufficient quality to be burned in CHP engines, boilers, combustors or similar applications.

However, some of the physical and chemical properties may affect the performance and the lifetime of the engine contrasting with the utilisation of the biodiesel and diesel. Therefore, to be used as a transportation fuel or blended with fossil fuels, it is necessary to submit this bio-oil to a HDO upgrading treatment.

Moreover, the pyrolysis liquid is highly miscible with diesel and biodiesel which can improve the characteristics of the fuel alleviating some negative aspects during the operation of the engine (Yang et al., 2013).

4.2.2 GC-MS Analysis of Bio-oil

The organic fraction of SB and OH bio-oils were analysed through GC-MS and the results are demonstrated in Table 8. The concentration (%) given in Table 8 provides information about an estimated mass fraction of each organic compound. Figures 31 and 32 show the chromatograms of the bio-oils at different reforming temperatures, where the 16 most important and abundant peaks were identified (each spectrum contains around 250 peaks related to different chemical compounds). The main peaks identified in this study for the SB bio-oils were also found in Ahmad et al. (2018) work, which also converted SB at the same reforming temperatures (500, 600 and 700 ºC) via TCR technology.

Table 8 - Compounds detected and identified by GC-MS of the SB and OH bio-oil at different reforming temperatures (pyrolysis temperature = 450 ºC)

	Uncertainty = 2.3 - 2.7%		SB			OH		
	Reforming Temperature (ºC)		**500**	**600**	**700**	**500**	**600**	**700**
#	**Group**	**Chemical Compound**	**Conc. (%)**			**Conc. (%)**		
1	Aromatic	Benzene	1.6	2.2	3.9	0.93	3.2	3.2
2	Aromatic	Toluene	2.9	3.99	4.9	3.2	6.1	4.6
3	Furan	Furfural	2.4	1.2	-	0.93	0.19	-
4	Furan	2-Furanmethanol	0.39	0.16	-	1.2	0.29	0.13
5	Aromatic	Benzene, 1,3-dimethyl-	1.0	0.9	0.9	0.71	1.3	0.93
6	Aromatic	1,3,5,7-Cyclooctatetraene	1.5	2.3	4.4	1.2	3.3	3.5
7	Phenol	Phenol	6.1	7.6	7.7	5.7	6.6	5.1
8	Phenol	Phenol, 2-methyl-	3.3	4.4	6.6	3.0	5.2	4.7
9	Phenol	Phenol, 3-methyl-	5.6	6.9	4.4	4.7	5.3	3.4
10	Phenol	Phenol, 2,4-dimethyl-	1.3	1.3	0.52	1.1	1.1	0.44
11	Phenol	Phenol, 4-ethyl-	7.8	6.4	1.9	6.2	3.8	2.5
12	Aromatic	Naphthalene	2.1	3.2	14.3	1.4	4.8	7.1
13	Furan	Benzofuran, 2,3-dihydro-	5.0	5.1	2.9	2.2	2.8	1.6
14	Aromatic	Naphthalene, 1-methyl-	0.88	1.3	2.5	1.1	1.4	1.5
15	Aromatic	Acenaphthylene	0.34	0.60	2.6	0.51	1.1	1.8
16	Aromatic	Phenanthrene	0.31	0.16	2.0	0.37	0.45	1.3
-	Total Furans	-	9.9	9.5	8.4	5.8	8.6	5.6

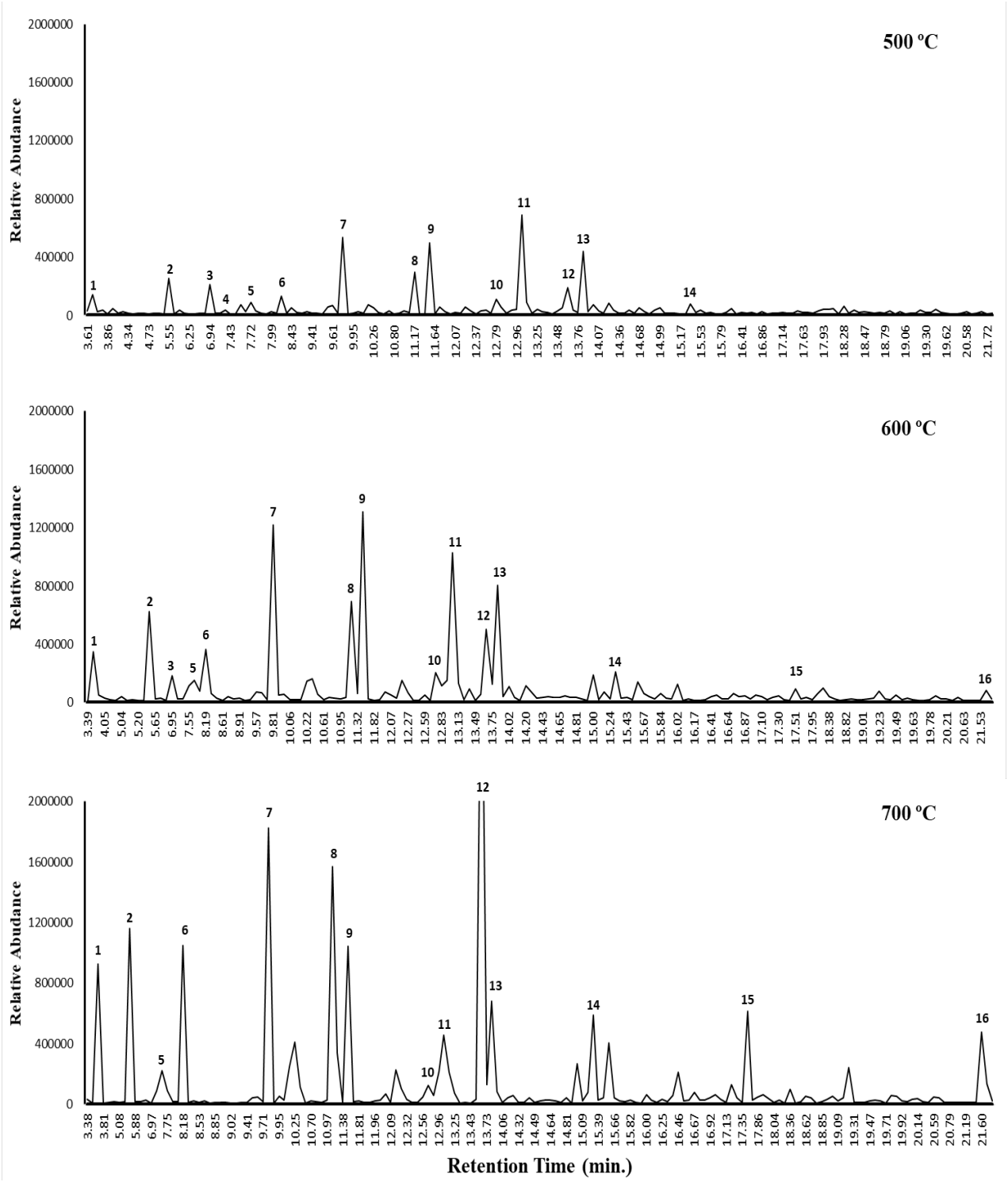


Figure 31 - GC-MS chromatograms of SB bio-oil and compounds detected at 450 ºC (reactor temperature) and different reforming temperatures (500, 600 and 700 °C)

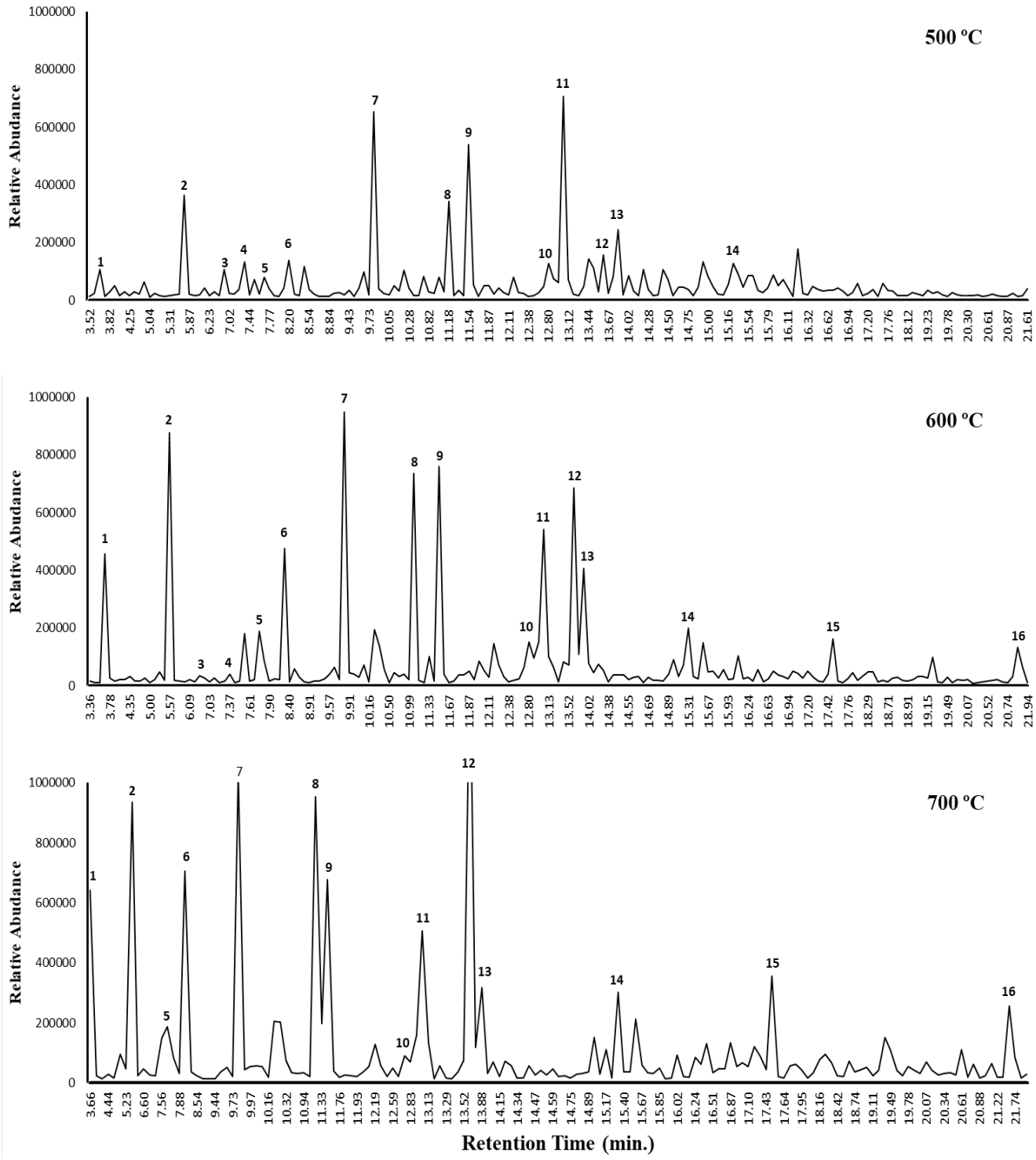


Figure 32 - GC-MS chromatograms of OH bio-oil and compounds detected at 450 ºC (reactor temperature) and different reforming temperatures (500, 600 and 700 °C)

Generally, the pyrolysis oils are a mix of complex chemical compounds containing carbons chains between C5 and C15 (Balat, 2011). It can be analysed that the SB and OH bio-oils are mostly composed of aromatics and oxygenated organic compounds such as phenols and furans. Aromatics and phenols are collectively the biggest fractions of the pyrolysis liquids and furans are the less abundant compound. Phenols are derived from lignin while furans from hemicellulose and its presence in TCR liquids proves that both compounds were thermally degraded during the pyrolysis conversion (Yin et al., 2013). Phenols and furans are all flammable organics, however, phenols are also one of the reasons for high acidity of the oils (Yang et al., 2014). This can explain the high acid number found in Table 6 for SB and OH bio-oils. Inversely, aromatic hydrocarbons may guarantee good combustibility of the oil for application as energy fuels which can improve blending capabilities with fossil fuels (Ouadi et al., 2017). It is observed through the peaks that the chemical composition of both bio-oils at the same temperature is quite similar regarding the chemical group. This is consistent with the similarities between the chemical composition of SB and OH biomasses (Table 3) and respective bio-oils (Table 6).

Lower reforming temperatures are the most efficient to produce furans (including furfural and 2-furanmethanol). The highest yields for these chemical compounds were achieved by converting SB at 500 ºC (9.9% of furans). Converting cellulose at low temperatures reduces the polymerisation reactions, raising the number of free radicals and subsequently promoting the formation of aldehyde, carboxyl and carbonyl compounds (Shafizadeh and Lai, 1972). This extra proton addition can favour the production furfural and 2-furamenthanol at low heating temperatures (Roman-Leshkov et al., 2007). SB oil

contains more furans due to its higher amount of hemicellulose and xylose when compared to OH feedstock (Table 3).

Higher temperatures in the post reformer generate less furfural and 2-furanmenthanol, however, an increment of phenols and aromatics was observed. Lignin degradation contrasts cellulose and hemicellulose, favouring the formation of phenols when higher temperatures are applied. Additionally, the presence of biochar in the reformer might help to break the lignin structure stimulating the production of phenols. Between 500 and 600 °C, the increase of aromatics (such as benzene, toluene and naphthalene) could improve the fuel properties and the HHV of the SB and OH oils (Table 6) resulting in better engine performance.

When the reforming temperature was set at 700 ºC, a significant reduction of furans in the bio-oil was observed. Interestingly, the same trend occurred in the phenols yields when compared to the pyrolysis oils produced at lower reforming temperatures. One of the explanations can be the occurrence of secondary reactions such as deoxygenation which converted phenols to aromatics (Ahmad et al., 2018). Moreover, the increase of aromatics in the bio-oil at 700 ºC is evident in Table 8.

It is visible that the variation of reforming temperature has a substantial effect on the properties of the pyrolysis liquid changing its chemical composition and quality.

4.2.3 Gas Analysis

The biomass decomposition and the following catalytic treatment in the reforming unit are responsible for the production of permanent gases (Yang et al., 2014). The gases detected from gas fraction (Table 9) were H_2, CH_4, CO, CO_2 and C_XH_Y. H_2O is not present in Table 9 because most of the water was condensed in the cooling system to produce

pyrolysis oil. There is no oxidation-reduction reaction during this process due to the total absence of oxygen.

Table 9 - SB and OH permanent gas composition at different reforming temperatures (Pyrolysis temperature = 450 ºC)

	SB			OH		
Reforming Temperature (°C)	**500**	**600**	**700**	**500**	**600**	**700**
Component						
H_2 (vol%)	25.7	30.4	30.9	15.8	30.1	31.6
CH_4 (vol%)	13.5	9.6	10.2	7.0	5.8	6.9
CO (vol%)	20.2	18.5	23.6	25.5	21.2	25.2
CO_2 (vol%)	28.8	25.6	21.8	25.6	20.9	18.5
C_XH_Y (vol%)	2.3	2.0	1.4	2.7	2.4	1.5
Non-detectable compounds (vol%)	9.5	13.9	12.1	23.4	19.7	16.5
HHV (MJ/kg)	15.9	17.0	18.4	15.3	18.0	18.8
Density (kg/m^3)	0.89	0.78	0.73	1.2	1.0	0.96

At the lowest reforming temperature (500 ºC) CO_2 is the main component for both feedstocks. CO_2 production is associated to the decomposition of hemicellulose and cellulose due to the thermal cracking of carbonyl and carboxyl groups (Uddin et al., 2014). These reactions occur mainly at lower temperatures which are in agreement with the reduction of CO_2 volume when the reformer reaches higher temperatures. It is observed in Table 9 a higher CO_2 amount in the SB gas for all reforming temperatures which can be associated to the higher cellulose and hemicellulose content found in the

SB compared to OH (Table 3). The higher presence of CO_2 rather than H_2 in the syngas is the main reason for a lower HHV at 500 ºC.

The pyrolysis gas was composed mostly of H_2 and CO at higher reforming temperatures, except in the SB experiment at 600 ºC. When there is a rise of temperature, the degradation, devolatilisation and thermal cracking of feedstock are promoted. Simultaneously, secondary reactions such as decarboxylation, dehydrogenation, decarbonylation and deoxygenation stimulate the production of H_2 and CO (He et al., 2010). It is notable how the increase of H_2 in the syngas causes a superior HHV. Accordingly, the OH pyrolysis gas at 700 ºC is the one containing higher H_2 yield (31.6 vol%) and consequently the better caloric value (18.8 MJ/kg).

Methane production is caused by the degradation of lignin (Yang et al., 2007). The higher CH_4 percentage observed in SB runs can be linked to the bigger amount of lignin found in this biomass compared to OH feedstock.

The non-detectable gas fraction can be the presence of hydrocarbons as propane and ethylene which could not be read by the gas analyser. Light hydrocarbons and short-chain compounds result in the fragmentation and disintegration of the linkage between the polymer and monomers (Morf et al., 2002). This may be a cause of the reduction in C_XH_Y components and density when the reforming temperature is increased.

Table 10 displays the gas composition of different permanent gases from diverse biomasses and pyrolysis technologies found in the literature review.

Table 10 - Pyrolysis gas composition from literature review at different reforming temperatures using several feedstocks and pyrolysis technologies

Pyrolsysis Type	Temperature (ºC) Reactor	Reformer	Biomass	H_2 (vol%)	CH_4 (vol%)	CO (vol%)	CO_2 (vol%)	C_xH_y (vol%)	HHV (MJ/kg)	Density (kg/m^3)	Ref.
Intermediate	450	-	De-inking sludge	1.9	6.3	25.5	66.3	-	6.2	-	1
Intermediate	450	-	Digestate	7.0	5.0	43.0	40.0	-	9.7	-	2
TCR	400	500	SB	12.1	19.5	32.8	32.9	-	13.8	1.3	3
TCR	400	600	SB	20.2	12.1	29.8	27.9	-	15.3	1.2	3
TCR	400	700	SB	28.7	13.1	21.3	25.1	-	16.2	1.1	3
TCR	450	500	Digestate	21.0	5.0	14.0	40.0	-	13.1	-	2
TCR	450	750	Digestate	37.0	3.0	12.0	28.0	-	14.4	-	2
TCR	450	600	Wheat husk	19.4	12.3	26.4	26.9	3.6	20.6	1.2	4
TCR	450	700	MSW	36.0	14.0	12.0	21.0	6.0	17.2	-	5
TCR	450	700	Co-form rejects	13.0	13.0	12.3	3.1	5.0	11.0	-	6
TCR	450	700	SB	30.9	10.2	23.6	21.8	1.4	18.4	0.73	7

1 - (Ouadi et al., 2013); 2 - (Neumann et al., 2016); 3 - (Ahmad et al., 2018); 4 - (Santos et al., 2019); 5 - (Ouadi et al., 2017); 6 - (Ouadi et al., 2018); 7 - Present work.

Ouadi et al. (2013) and Neumann et al. (2016) used the intermediate pyrolysis reactor to process de-inking sludge and digestate at 450 ºC. The existence of the reforming unit in the present study affected drastically the H_2 yield and consequently the HHV. Comparing the lowest HHV of this section of runs shows the significant difference between 15.3 MJ/kg (OH at 500 ºC) and 6.2 and 9.7 MJ/kg for Ouadi et al. (2013) and Neumann et al. (2016) respectively. In the reforming stage, the biochar works as a catalyst and favours the deoxygenation reactions resulting in the formation of H_2 and improving the calorific value (Henkel et al., 2016). Moreover, when the organic vapours are in contact with the biochar at high temperatures different types of chemical reactions occur (water gas shift reaction, steam reforming reaction and hydrogasification reaction) increasing the yields of fuel gases such as H_2 and CH_4 (Neumann et al., 2016, Yang et al., 2013).

In the present work, the increment of the reforming temperature increased the H_2 volume but reduced the amount of CO_2 and the density of the syngas. The same trend was observed in the works of Ahmad et al. (2018) and Neumann et al. (2016) using the same technology to convert SB and digestate, respectively. The HHV of the present study for the three SB experiments (15.9, 17.0 and 18.4 MJ/kg) is superior to Ahmad et al. (2018) (13.8, 15.2 and 16.2 MJ/kg) for the same reforming temperatures (500, 600 and 700 °C, respectively) and feedstock. A possible reason is the lower pyrolysis temperature (400 °C) used by Ahmad et al. (2018). SB biomass also presented a slightly different chemical composition in terms of hydrogen and water content affecting the H_2 yield and automatically the HHV.

Santos et al. (2019) using wheat husk produced a TCR syngas at 600 °C and the same reactor temperature (450 °C) with better calorific value (20.6 MJ/kg) than the SB

and OH trials (17.0 and 18.0 MJ/kg, respectively). Despite of lower H_2 yield, the gas generated by Santos et al. (2019) presented higher CH_4, CO and C_xH_y volume which might have increased the HHV. In addition, the selection of feedstock has a very important role in the properties of the syngas.

On the other hand, Miloud et al. (2017) and Miloud et al. (2018) presented lower HHV producing pyrolysis gas via TCR at 700 °C with MSW (17.2 MJ/kg) and co-form rejects (11.0 MJ/kg), respectively. In this case, SB and OH demonstrated to have better potential in the production of syngas with higher energy density.

The pyrolytic gas produced in this section at high reforming temperatures contains a reasonable amount of combustible gases (H_2, CO, CH_4 and other hydrocarbon gases) and HHV to be used as an energy vector. One of the applications could be the generation of heat and power trough CHP units or burnt as a fuel onsite to meet the energy demands of the industrial plant.

4.2.4 Char Analysis

The elemental composition of the biochar, ash and its energy content is represented in Table 11. Biochar is composed of fixed carbon and ash. Fixed carbon is the solid left after the extraction of volatiles, ash and moisture and is the combustible substance of biochar contributing for the increment of the calorific value. However, the presence of ash has the opposite effect decreasing the char HHV (Laird, 2008). The SB and OH biochar contain more ash than the initial feedstock (4.0 and 2.4 wt%, respectively) since non-volatile inorganics always remain inside of the solid particle (Zhou et al., 2017).

Table 11 - SB and OH biochar characterisation at different reforming temperatures

(Pyrolysis temperature = 450 ºC)

	SB			OH		
Reforming Temperature (°C)	**500**	**600**	**700**	**500**	**600**	**700**
Ultimate analysis						
C (wt%)	70.3	77.0	78.2	79.3	81.0	78.6
H (wt%)	1.6	1.5	1.3	2.0	1.9	1.8
N (wt%)	0.39	0.34	0.43	1.1	1.0	1.0
S (wt%)	<0.10	<0.10	<0.10	<0.10	<0.10	<0.10
O (wt%) (diff.)	11.6	2.1	1.1	5.7	5.1	5.3
Ash (wt%)	16.1	19.0	18.8	11.8	10.8	13.2
HHV (MJ/kg)	24.9	28.0	28.4	29.2	29.7	28.7

Results from Table 11, show an increment of the carbon content and HHV when the reforming temperature is increased except in the OH trial at 700 °C. At higher temperatures, the aromatisation reactions are favoured increasing the aromatic rings and subsequently the C-C bonds in the char (Yang et al., 2007). This means more fixed carbon in the biochar (McKendry, 2002). It is not a coincidence that the experiment with better HHV (OH at 600 °C) is the one containing more carbon and less ash. This is even more obvious when comparing higher and lower calorific values in the biochars according to their carbon content.

The fixed carbon and ash contents calculated for OH (26.4 and 2.4 wt%, respectively) and SB (17.2 and 4.0 wt%, respectively) feedstocks are also a reflection of the results presented in Table 11. OH biochar has a better HHV for all reforming

temperatures due to the higher fixed carbon and lower ash content found in the original biomass.

Table 12 shows the composition of several biochars from different feedstocks and pyrolysis technologies according to the literature review.

SB biochars from this study presented a better energy density when compared to Mesa-Perez et al. (2013) and Doumer et al. (2015) works, which applied fast and slow pyrolysis in the conversion of the same biomass (SB). The extended residence time of the biochar in the reforming unit might cause a secondary cracking reaction producing coke and consequently a TCR char with more carbon and less water.

However, Yang et al. (2014) produced biochar with higher calorific value than the results from Table 11. In his work, wood was converted trough intermediate pyrolysis using the Pyroformer reactor at 450 °C. The different feedstock used (wood) contributed to generate biochar with a reasonable carbon amount (75.6 wt%), higher hydrogen content (3.4 wt%) and lower ash amount (10.6 wt%) when compared to the SB and OH experiments.

Ahmad et al. (2018) and Neumann et al. (2016) processed SB and digestate using the same technology (TCR) and heating the biomass with different reforming temperatures. Surprisingly, the HHV of the biochar decreased when they submit the feedstocks at higher reforming temperatures which is the opposite effect occurred in the present tests. However, above 600 ºC there are more aromatization reactions increasing the aromatic rings and consequently the carbon content of the biochar (Yang, Yan et al. 2007). Therefore, the HHV of biochar should be higher and not lower when the reforming temperature is increased.

Table 12 - Biochar characterization from literature review at different reforming temperatures using several feedstocks and pyrolysis technologies

Pyrolysis Type	Temperature (ºC)		Biomass	C (wt%)	H (wt%)	N (wt%)	S (wt%)	O (wt%)	Ash (wt%)	HHV (MJ/kg)	Ref.
	Reactor	Reformer									
Fast	470	-	SB	41.3	2.9	0.40	0.10	21.5	33.8	14.2	1
Slow	350	-	SB	65.0	4.2	0.55	-	24.8	5.5	24.3	2
Intermediate	450	-	Wood	75.6	3.4	0.22	-	10.2	10.6	30.1	3
TCR	400	500	SB	67.9	1.6	0.52	0.51	-	30.5	24.0	4
TCR	400	600	SB	65.8	0.87	0.48	0.04	-	32.6	23.1	4
TCR	400	700	SB	64.5	0.70	0.54	0.03	-	32.2	21.2	4
TCR	450	500	Digestate	83.7	4.7	2.7	0.50	8.4	38.4	18.9	5
TCR	450	750	Digestate	92.2	5.0	2.1	0.70	0.0	41.6	17.3	5
TCR	450	600	Wheat husk	76.5	2.2	3.3	0.10	6.1	11.8	28.4	6
TCR	450	700	MSW	47.3	0.8	1.0	0.30	5.7	44.9	17.0	7
TCR	450	700	Co-form rejects	83.9	1.7	0.49	0.06	1.9	11.9	30.8	8
TCR	450	700	OH	78.6	1.8	1.0	<0.10	5.3	13.2	28.7	9

1 - (Mesa-Pérez et al., 2013); 2 - (Doumer et al., 2015); 3 - (Yang et al., 2014); 4 - (Ahmad et al., 2018); 5 - (Neumann et al., 2016); 6 - (Santos et al., 2019); 7 - (Ouadi et al., 2017); 8 - (Ouadi et al., 2018); 9 - Present work.

Santos et al. (2019) processing wheat husk at 600 °C in TCR obtained a very close HHV (28.4 MJ/kg) compared to SB trial (28.0 MJ/kg) which can be correlated with similar carbon contents found in both biochars (76.5 and 77.0 wt%). OH experiment at the same reforming temperature presented a better caloric value than the previous work (29.7 to 28.4 MJ/kg) due to its lower ash content (10.8 to 11.8 wt%) and higher carbon value (81.0 to 76.5 wt%).

The same results were observed by Miloud et al. (2017) and Miloud et al (2018) studies converting MSW and co-form rejects at 700 °C via TCR. For the first work, the high ash content and low carbon value (44.9 and 47.3 wt%, respectively) reflected in a lower HHV biochar (17.0 MJ/kg) when related to SB and OH runs (28.4 and 28.7 MJ/kg, respectively). In the second work, co-forms rejects biochar presented higher carbon content (83.9 wt%) and lower ash amount (11.9 wt%) obtaining a better energy density (30.8 MJ/kg) than SB and OH runs at 700 °C.

Comparatively to classic sub-bituminous coal with a carbon content of 73.9% and a HHV of 29.05 MJ/kg (Kabe et al., 2004), this set of experiments got a very similar HHV excluding the SB char produced at 500 °C.

The char energy content is influenced by the reforming temperature used in the TCR and its valuable HHV can be useful for combustion in furnaces, gasifiers and boilers to generate heat and power (Santos, Ouadi et al. 2019). The same char has other promising applications, such as soil amendment, carbon sequestration and fertiliser (Kirby, Hornung et al. 2017). Another application of the char is the catalytic conversion, which is related to its surface properties and inorganic composition (Mullen et al., 2010).

4.2.5 Mass Balance and Energy Yield

Figures 33 and 34 indicate the mass balance and the energy yield for the SB and OH products obtained during the TCR experiments. The equations for the calculation of the mass balance and energy yield can be found in the Appendix B.

Lower reforming temperatures enhance the formation of bio-oil and char minimizing the percentage of gas. The decomposition of hemicellulose and cellulose occurs at lower temperatures (220-350 ºC and 315-400 ºC, respectively) promoting depolymerisation and devolatilization of volatiles resulting in better yields for bio-oil production (Yang et al., 2007). In some cases, lower temperatures are not sufficient for complete pyrolysis resulting in a higher biochar yield than bio-oil (Greenhalf et al., 2013). Low temperatures also help for the non-oxidation of the carbonaceous substance and causes the condensation of benzene rings through charring reactions stimulating the formation of biochar (Van de Velden et al., 2010). Moreover, it was found that low pyrolysis temperatures are beneficial for cross-linking reactions causing higher levels of biochar production (Greenhalf et al., 2012).

The best pyrolysis oil and char yields were obtained at 500 ºC for both feedstocks. OH run presented the biggest value for bio-oil production with 7.6 wt%, while SB trial was the most productive one in terms of char formation (26.6 wt%). SB experiments obtained better biochar yields when compared to OH in all reforming temperatures, due to the higher amount of lignin and ash present in the SB biomass (see Table 3).

The rise in the reforming temperature reduced the amount of condensate (bio-oil and aqueous phase) and biochar, however it increased the formation of gas resulting in the decomposition of the biochar at higher temperatures in the post reformer. When the temperature is higher than 500 ºC, the main reactions taking place are dehydrogenation,

cracking, aromatisation and volatilization (Blanco and Chejne, 2016). Gas production is mostly dependent on cracking and volatilization reactions, specifically above 575 ºC where complex volatile compounds are reduced to lighter molecules such as CH_4, CO_2 and CO (Henkel et al., 2016). In addition, char acts as a catalyst at higher temperatures and enhances the deoxygenation reaction resulting in the formation of CO, CO_2 and H_2O (Henkel et al., 2016). Secondary degradation reactions also occur at higher temperatures decreasing the liquid amount in order to maximise the gas yield.

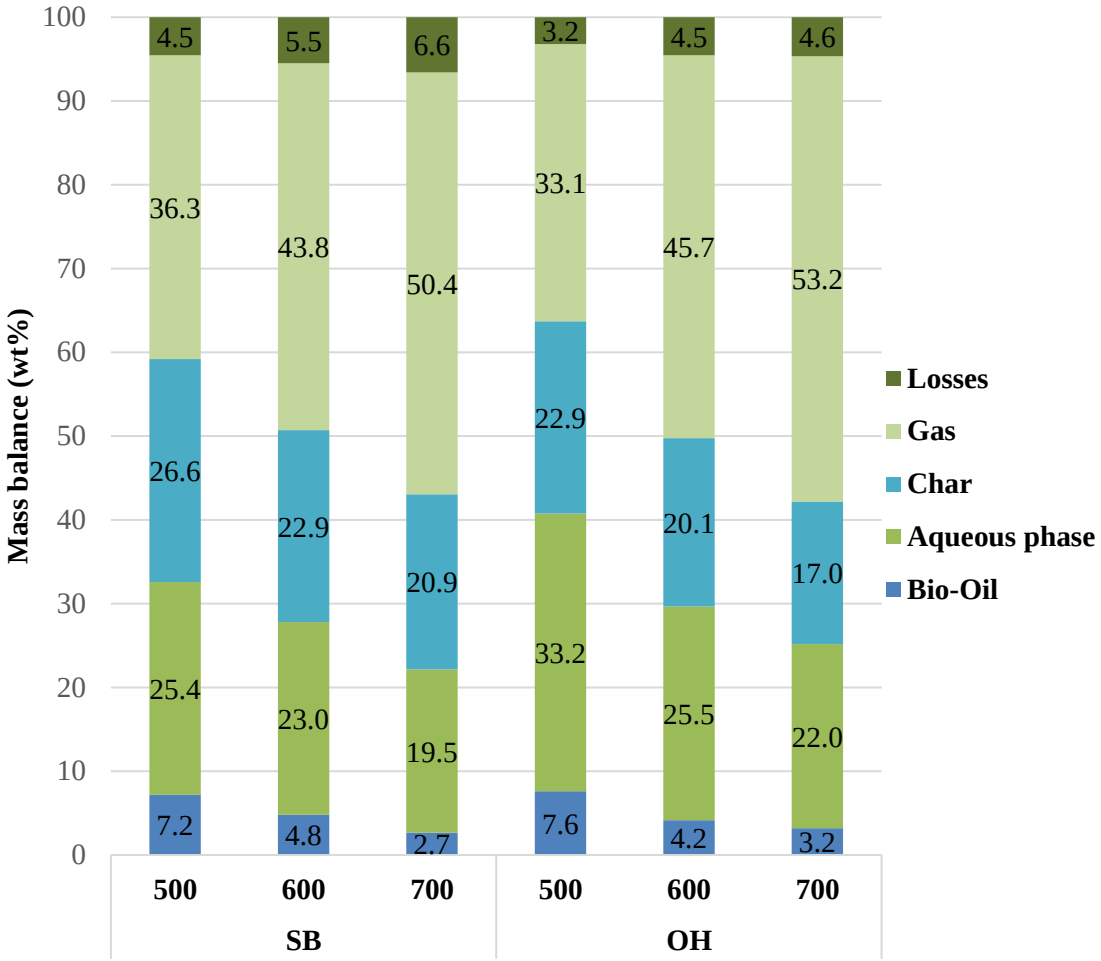


Figure 33 - Mass balance of SB and OH trials at different reforming temperatures (pyrolysis temperature = 450 ºC)

The highest gas yields were found in the conversion of SB and OH at 700 ºC where the results obtained were 50.4 and 53.2 wt%, respectively.

A good mass balance was obtained for all TCR experiments performed in this section. The biomass conversion into products was higher than 93 wt% and only 3.2 wt% was not converted in the best scenario case (OH at 500 ºC). These results show the potential of the TCR process as an efficient technology for conversion of biomass into valuable products. The losses can be justified by errors during the weight measurements, the bio-oil left in the condensing unit after each run which is tricky to determine during cleaning (Figure 22) and escaping gases not detected by the gas totalizer. For both biomasses, it was noticed an increment of mass losses when the reforming temperature was raised. Higher reforming temperatures produce more syngas and small particles (not efficiently detected by the gas totalizer due to the technology limitations) increasing the amount of escaping gases not measured through the gas totalizer.

The biggest energy fraction for the lowest reforming temperature was the biochar with 40.4% for SB and 41.7% for OH. At 500 °C, the energy yield of bio-oil and biochar from OH run were higher compared to SB trial. This may be explained due to the higher calorific value of the OH bio-oil and biochar observed in Tables 6 and 11.

With reforming temperatures at 600 and 700 °C, the main energy vector was the pyrolysis gas for both feedstocks. The energy yields of the permanent gases at 600 and 700 °C were indicated as 45.4 and 56.5% for SB and 51.1 and 65.3% for OH, respectively. OH runs at 600 and 700 °C presented better results which can be attributed to the higher amount of syngas produced and better HHV of the gas fraction (Table 9).

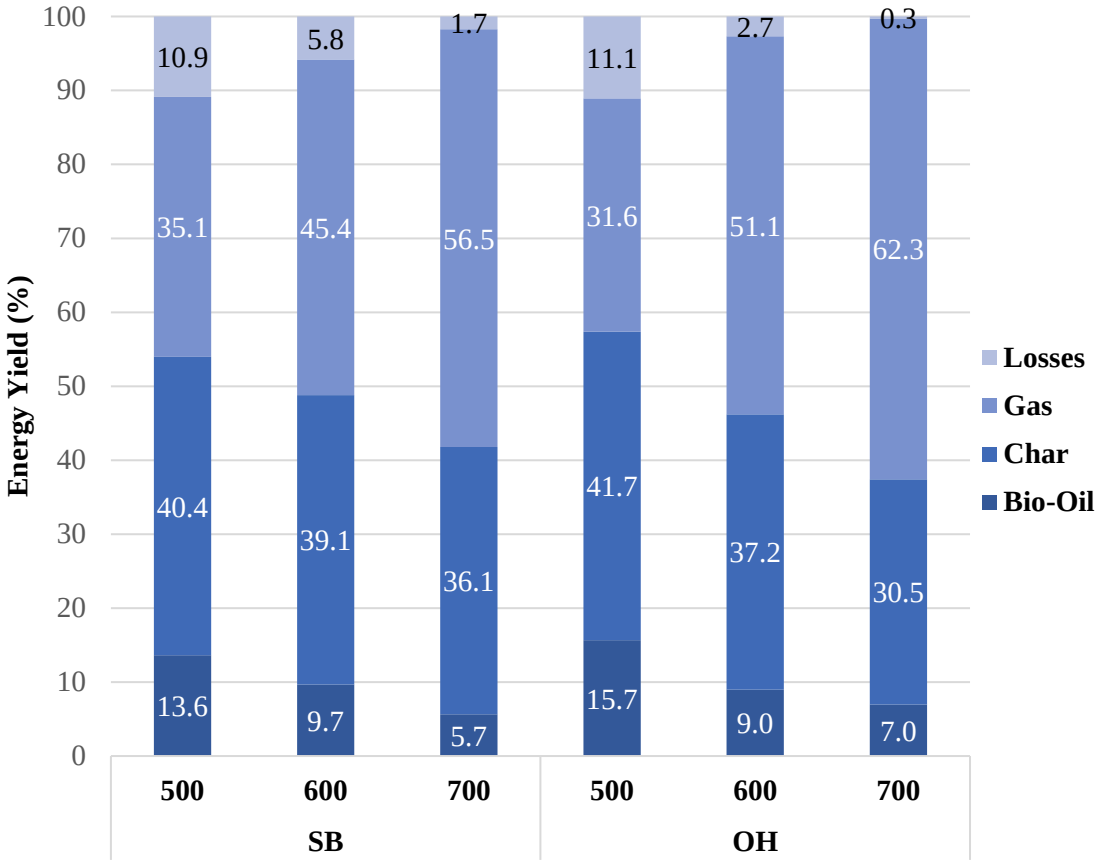


Figure 34 - Energy yield of SB and OH trials at different reforming temperatures (pyrolysis temperature = 450 ºC)

In the energy yield, the experiments at 500 °C in the post reformer were less efficient with 10.9 and 11.1% of losses for SB and OH, respectively. Applying higher reforming temperatures (600 and 700 °C) the energy losses were 5.8 and 1.7% for SB and 2.7 and 0.3% for OH, respectively. It is evident a raise in energy losses when the reforming temperature is decreased. The higher amount of bio-oil produced at lower reforming temperatures can be the key to this trend. As we have more bio-oil in the system, more bio-oil is not extracted and remains in the condensing unit for the reasons explained before. Additionally, during the separation of the organic and aqueous phase of the pyrolysis liquid some organic oil is left in the aqueous phase to avoid the

contamination of the bio-oil submitted for characterisation. Adding these technical issues, it is unavoidable to waste some energy content from the organic phase of the bio-oil affecting the energy yield of the process.

Heating SB and OH at 700 °C converted 98.3 and 99.7% of the total energy from the feedstocks into the chemical energy of the products, demonstrating the energy efficiency of the TCR technology. Nevertheless, the system energy losses can be reduced with better and efficient isolation and also by increasing the scale of the reactor.

4.3 Different Reactor Temperatures in TCR Process

In the second set, the experiments were executed shifting only the pyrolysis temperature in the reactor. The other experimental parameters were kept consistent with the first set of trials as it is showed in Table 13.

Table 13 - TCR runs conditions with different reactor temperatures

Experimental Conditions	**Set 2 (Trial 7 to Trial 10); Trials 1 and 4**
Intermediate Pyrolysis Temperature	400, 450 and 500 ºC
Reforming Temperature	500 ºC
Feedstock	SB and OH
Feed Consumption	3.5 kg (Pellets)
Feed Rate	1.4 kg/h
Solid Residence Time	Minutes
Gas Residence Time	Seconds
Biochar (Reformer)	500 g
SS (TCR)	-

The temperature selected in the reforming unit was 500 ºC according to the higher furfural and 2-furanmenthanol yields present in the pyrolysis oil from the previous runs (Table 8). Therefore, trials 1 and 4 from the first set of tests were also included in this section.

4.3.1 Bio-oil Analysis

Table 14 shows the chemical composition and fuel properties of the SB and OH bio-oils applying different pyrolysis temperatures in the reactor.

An increment of the pyrolysis temperature led to a bio-oil with less oxygen and more carbon for both biomasses. As a consequence, TCR bio-oil contains a better HHV with higher pyrolysis temperatures. This trend was also observed when the reforming temperature was increased (Table 6), emphasising the fact that the energy density of the TCR oil can be improved by raising the pyrolysis and reforming temperatures. From the results of Tables 6 and 14, it is reasonable to conclude that the reforming temperature might stimulate more depolymerisation and thermal breaking reactions of hemicellulose and cellulose resulting in a bio-oil with less oxygen, more carbon and a higher calorific value (Lede, Diebold et al. 1997).

Varying the pyrolysis temperature resulted in a bio-oil HHV between 29.1 and 33.5 MJ/kg which was lower than the range observed in the previous section (from 31.1 to 35.0 MJ/kg). Once again, OH experiments produced a pyrolysis oil with better energy density attributed to the higher carbon and lower oxygen content.

The levels of nitrogen and sulphur are acceptable if the purpose of the SB and OH bio-oils is to be burned as this reduces the damage and corrosion to the engine due to its

acidity level (Hossain et al., 2013). Additionally, low NO_x and SO_x emissions are preferable for environmental reasons.

Table 14 - SB and OH bio-oil characterization at different pyrolysis temperatures (Reforming temperature = 500 ºC)

	SB			**OH**		
Pyrolysis Temperature (°C)	**400**	**450**	**500**	**400**	**450**	**500**
Ultimate analysis						
C (wt%)	63.4	71.3	72.2	70.7	72.2	72.8
H (wt%)	8.3	7.1	8.6	8.6	8.2	8.3
N (wt%)	0.41	0.69	0.76	1.8	1.9	1.8
S (wt%)	0.39	0.10	0.29	1.3	0.68	0.68
O (wt%) (diff.)	27.5	20.8	18.2	17.6	17.0	16.4
Fuel Properties						
HHV (MJ/kg)	29.1	31.1	33.4	33.1	33.2	33.5
Ash (wt%)	<0.001	<0.001	<0.001	<0.001	<0.001	<0.001
Water (wt%)	9.9	4.7	4.2	7.8	4.8	4.4
TAN (mg KOH/g)	32.2	27.7	25.8	33.5	30.5	24.2
Viscosity (mm^2/s)	47.8	24.9	23.7	38.1	36.5	35.3
Density (kg/m^3)	1077	1062	1061	1078	1074	1072

The ash content revealed was extremely low (<0.001%) which is positive for engine applications as this minimises corrosion, blocking and deposition of sediments during its operation (Huber et al., 2006). Based on the ash content of all SB and OH oils (including the previous section) it is evident that TCR technology has the capability to produce a bio-oil containing very low residues of ash which is attractive as a fuel.

Higher pyrolysis temperatures decreased the amount of moisture which improves the HHV and the properties of the oil in terms of engine performance (Ouadi et al., 2013). The rise in the pyrolysis temperature also helps in the promotion of dehydration reactions reducing the percentage of water. However, this kind of reaction seems to be more efficient when the reforming temperature is increased which can be justified due to the lower water content present in the bio-oils reformed at 600 and 700 ºC (Table 6).

SB and OH oils present lower acidity when submitted to higher pyrolysis temperatures which was the same effect observed with higher reforming temperatures. Over again, the previous section showed better results in the reduction of the acid number of the pyrolysis liquid. The values are still high for engines, however it is important to highlight the role of the pyrolysis temperature in producing a bio-oil with lower acidity.

In terms of viscosity, higher pyrolysis temperatures were more effective in cracking the organic vapours, and so, forming lighter weight molecules and reducing the viscosity of the bio-oil. This is an advantage to improve the fuel flow of the engine causing better combustion, despite of the results are considered high for engine applications (Zhang et al., 2013). The conversion of SB at 500 ºC (pyrolysis temperature) obtained the lowest viscosity value (23.7 mm^2/s) in this set of experiments. The difference is significant when compared to the lowest TAN in Table 6 for the same kind of feedstock (12.1 mm^2/s at 700 ºC as reforming temperature).

Higher pyrolysis temperatures were able to produce lighter chemical compounds which reduced the density of the pyrolysis liquid. Lower density in a liquid fuel influences the injection time and the consumption rate which improves the engine performance (Yamane et al., 2001).

In summary, the increase of reforming temperatures showed better results than the increment of temperature in the pyrolysis reactor. The utilisation of biochar in the reformer at higher temperatures may have helped to upgrade the organic vapours improving the HHV and the fuel properties of the bio-oil. It is well known that there is a catalytic effect caused by the biochar in the TCR process, especially at higher temperatures.

The properties of several bio-oils from different biomasses and pyrolysis technologies from the literature review are summarised in Table 15.

Varma and Mondal (2017) and Treedet et al. (2017) converted SB through fast pyrolysis at 500 ºC using a semi-batch and fluidized bed reactors respectively. In both cases the HHV of the bio-oil (27.7 and 18.4 MJ/kg) was lower compared to the SB runs of the present work. Treedet et al. (2017) also produced a SB pyrolysis oil with a higher percentage of water (38.9 wt%) and more density (1259 kg/m^3) than this set of experiments. As explained previously, the different features between fast and intermediate pyrolysis were reflected in the quality of the bio-oil which are relevant to evaluate its value as an engine fuel. Additionally, the mix of biochar and fresh biomass present in the pyrolysis reactor of the TCR helped to improve the properties of the pyrolysis liquid showing the advantage of using this kind of technology.

Table 15 - Bio-oil and fuels properties from literature review at different pyrolysis temperatures using several feedstocks and pyrolysis technologies

Pyrolysis Type	Temperature (ºC)		Biomass / Fuel	C (wt%)	H (wt%)	N (wt%)	S (wt%)	O (wt%)	HHV (MJ/kg)	Ash (wt%)	Water (wt%)	TAN (mg KOH/g)	Viscosity (mm^2/s)	Density (kg/m^3)	Ref.
	Reactor	Reformer													
Fast	500	-	SB	65.7	6.9	0.69	0.03	26.7	27.7	-	-	-	-	-	1
Fast	500	-	SB	45.2	7.5	0.36	-	46.9	18.4	-	38.9	-	-	1259	2
Intermediate	500	-	SB	62.6	12.3	0.69	-	24.4	31.5	-	-	-	-	-	3
Intermediate	600	-	SB	57.1	11.1	0.62	-	31.2	29.8	-	-	-	-	-	3
Intermediate	700	-	SB	59.4	9.6	0.64	-	30.3	28.5	-	-	-	-	-	3
Intermediate	500	-	Oat Straw	15.3	11.2	0.91	1.8	70.8	27.1	-	17.1	-	-	-	4
Intermediate	450	-	Brewers grains	47.6	9.9	3.4	1.3	30.7	20.4	-	-	49.2	222	1020	5
TCR	400	500	SB	53.7	9.7	1.1	0.3	35.2	24.3	<0.10	25.6	11.1	-	-	6
TCR	450	500	Digestate	78.0	8.3	5.2	1.2	7.0	36.3	0.20	2.0	8.8	-	-	7
TCR	500	500	SB	72.2	8.6	0.76	0.29	18.2	33.4	<0.001	4.2	25.8	23.7	1061	8
-	-	-	Biodiesel	78.9	12.6	<0.10	0.74	8.4	37-40	<0.10	0.37	0.49	1.9-6.0	880	9
-	-	-	Diesel	84-87	13-16	<0.10	<0.10	1.0	42-45	<0.01	0.05	0.03	1.9-5.5	820-850	10

1 - (Varma and Mondal, 2017); 2 - (Treedet et al., 2017) ; 3 - (Henkel et al., 2016); 4 - (Aqsha et al., 2017) ; 5 - (Mahmood et al., 2013); 6 - (Ahmad et al., 2018); 7 - (Neumann et al., 2016); 8 - Present work; 9- EN 14214; 10 - EN 590.

Results from table 14 show an improvement of the bio-oil HHV when increased the pyrolysis temperature. Surprisingly, Henkel et al. (2016) had precisely the opposite trend processing SB in an intermediate pyrolysis batch reactor. However, this study changed the pyrolysis temperatures from 500 to 700 ºC and not between 400 and 500 ºC which might be the main cause for the decrease of the calorific value of the bio-oil. It is well known that the depolymerisation reactions in the cellulose and hemicellulose compounds are more active between 400-500 ºC, influencing the characteristics of the pyrolysis oil (Yang, Yan et al. 2007).

Aqsha et al. (2017) and Mahmood et al. (2013) worked with oat straw and brewers grains via intermediate pyrolysis obtaining a bio-oil with lower energy density (27.1 and 20.4 MJ/kg, respectively) when compared to the values of Table 14. For the first study the water content (17.1 wt%) was approximately four times more than the SB and OH trials at the same pyrolysis temperature (500 ºC). In the second work the acid number (49.2 mg KOH/g) and the viscosity (222 mm^2/s) were radically higher compared to SB and OH experiments at 450 ºC.

It is notorious the potential of the reforming unit in upgrading the organic vapours when they are in contact with the surface of the TCR char. As a result, the bio-oil produced contains better fuel properties and higher calorific value when compared to other intermediate pyrolysis reactors without a reformer.

The SB oil at 400 ºC of the present work revealed better results than Ahmad et al. (2018) with the same biomass and experimental conditions. The difference between both studies can be explained by the existence of many species of SB which might have diverse chemical compositions. Ahmad et al. (2018) produced a bio-oil with higher oxygen

content (35.2 wt%) and water (25.6 wt%), and lower carbon value (53.7 wt%) and HHV (24.3 MJ/kg).

On the contrary, Neumann et al. (2016) indicated a TCR bio-oil from digestate with higher carbon content (78.0 wt%) and calorific value (36.3 MJ/kg), and lower oxygen (7.0 wt%), water (2.0 wt%) and acid number (8.8 mg KOH/g) when compared to SB and OH runs at the same pyrolysis and reforming temperatures (450 and 500 ºC, respectively). The chemical composition of the digestate can be the key to achieve better results which has a higher carbon and hydrogen content (51.8 and 6.3 wt%) and lower oxygen value (38.5 wt%) than SB and OH feedstocks (Table 3).

The experiments with the lowest reforming temperature (500 ºC) presented results significantly distant from the values of diesel and biodiesel. From Table 15, it is evident the discrepancy in terms of carbon, hydrogen and oxygen content, HHV, water, TAN, viscosity and density.

In comparison to the results from the previous section at higher reforming temperatures, this bio-oil does not have the same potential in terms of fuel properties. However, it remains as a valid option for the production of the heat and power via CHP units, combustors or other similar technologies.

4.3.2 GC-MS Analysis of Bio-oil

Table 16 demonstrates the GC-MS results from the SB and OH bio-oil (organic fraction) at different pyrolysis temperatures. Additionally, the 14 most relevant and frequent peaks were identified as shown in Figures 35 and 36.

Table 16 - Compounds detected and identified by GC-MS of the SB and OH bio-oil at different pyrolysis temperatures (reforming temperature = 500 ºC)

	Uncertainty = 2.3 - 2.7%		**SB**			**OH**		
	Pyrolysis Temperature (ºC)		**400**	**450**	**500**	**400**	**450**	**500**
#	**Group**	**Chemical Compound**	**Conc. (%)**			**Conc. (%)**		
1	Aromatic	Benzene	0.54	1.6	1.9	1.6	0.93	2.3
2	Aromatic	Toluene	1.4	2.9	3.6	4.1	3.2	5.4
3	Furan	Furfural	2.5	2.4	1.9	1.2	0.93	0.19
4	Furan	2-Furanmethanol	0.47	0.39	0.39	1.3	1.2	0.53
5	Aromatic	Ethylbenzene	0.48	0.84	0.72	2.0	0.64	2.1
6	Aromatic	Benzene, 1,3-dimethyl-	0.68	1.0	1.3	0.83	0.71	1.0
7	Aromatic	1,3,5,7-Cyclooctatetraene	0.72	1.5	2.1	3.3	1.2	4.0
8	Phenol	Phenol	6.1	6.1	8.4	6.0	5.7	6.1
9	Phenol	Phenol, 2-methyl-	2.6	3.3	4.7	3.4	3.0	3.8
10	Phenol	Phenol, 3-methyl-	5.6	5.6	8.1	4.7	4.7	6.0
11	Phenol	Phenol, 2,4-dimethyl-	1.2	1.3	1.4	0.72	1.1	1.2
12	Phenol	Phenol, 4-ethyl-	13.5	7.8	8.0	4.7	6.2	4.2
13	Aromatic	Naphthalene	0.98	2.1	3.1	4.1	1.4	2.1
14	Furan	Benzofuran, 2,3-dihydro-	4.0	5.0	6.9	2.1	2.2	2.1
-	Total Furans	-	9.8	9.9	12.9	6.6	5.8	4.8

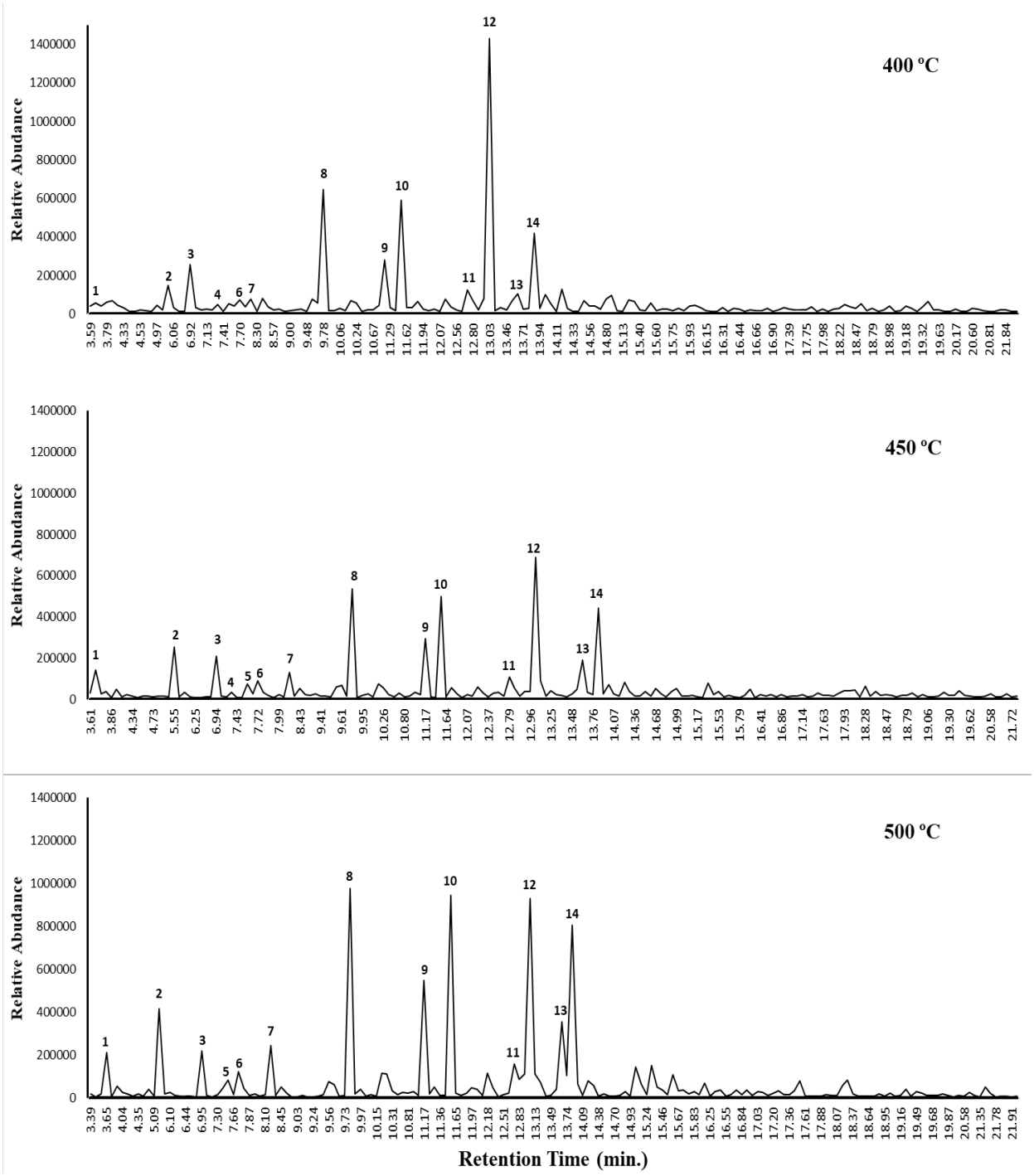


Figure 35 - GC-MS chromatograms of SB bio-oil and compounds detected at 500 ºC (reforming temperature) and different pyrolysis temperatures (400, 450 and 500 °C)

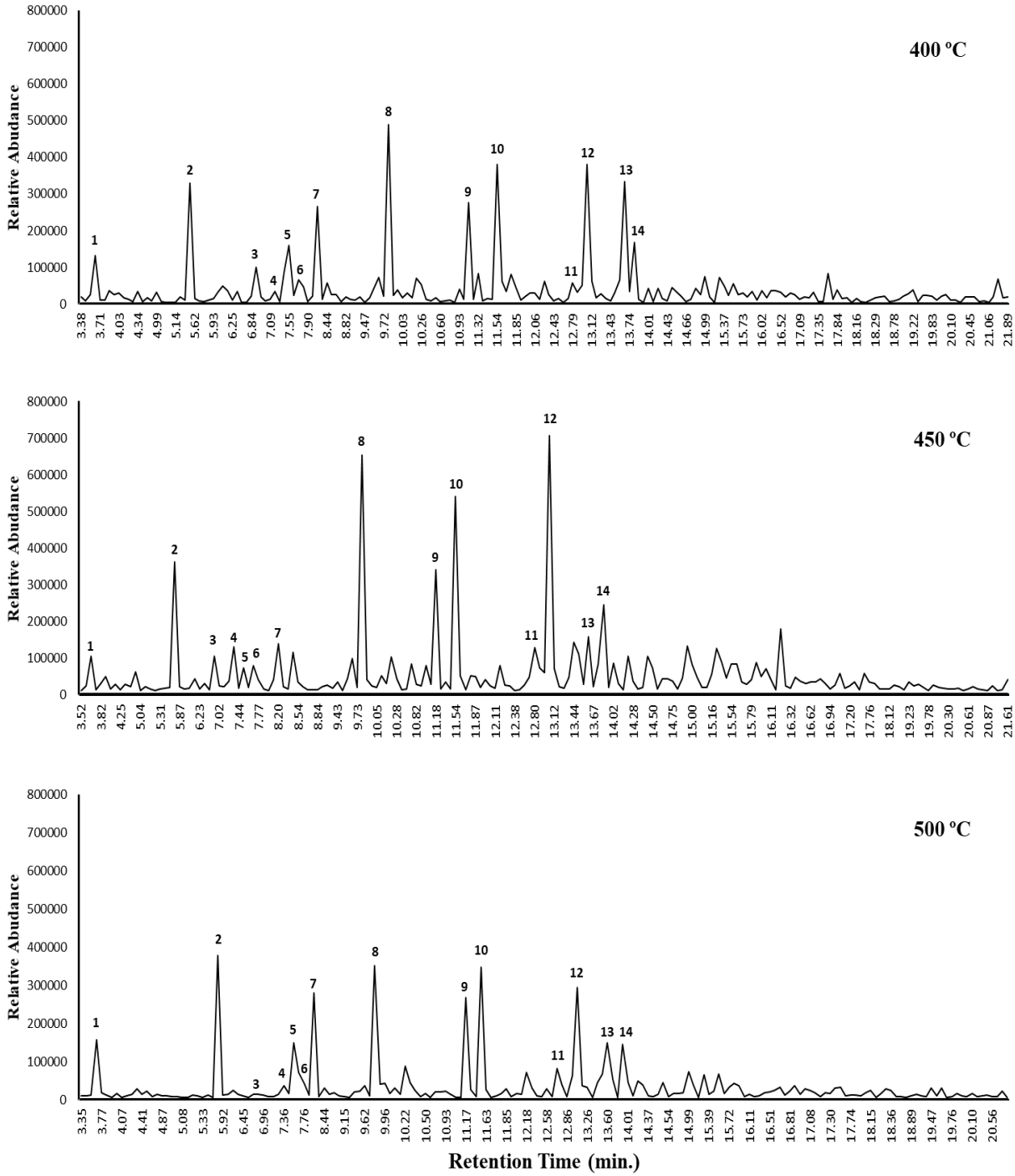


Figure 36 - GC-MS chromatograms of OH bio-oil and compounds detected at 500 ºC (reforming temperature) and different pyrolysis temperatures (400, 450 and 500 °C)

Phenols, aromatics and furans are the most common chemical compounds present in the SB and OH oils. For both feedstocks phenols represent the main group in the bio-oil which is responsible for the high acidity found in Table 14 (Yang et al., 2014). In fact, the bio-oil of the present experiments contains a higher acid number compared to the trials of the previous section (Table 8) due to the larger amounts of phenols found in the pyrolysis liquid. Inversely, the amount of aromatics present in Table 16 is lower when compared to the first set of runs (different reforming temperatures) decreasing the calorific value of the oil and its combustibility as a fuel (Ouadi et al., 2017).

Applying lower pyrolysis temperatures favour the formation of furfural and 2-furanmethanol. The pyrolysis of cellulose at lower temperatures helps in the production of free radicals (carbonyl, aldehyde and carboxyl compounds) which brings extra protons to increase the yields of furfural and 2-furanmenthanol (Roman-Leshkov et al., 2007, Shafizadeh and Lai, 1972). The percentage of furans is higher in the SB bio-oil attributed to the richer hemicellulose and xylose composition in the biomass (Table 3). The same results were observed in the runs with different reforming temperatures (Table 8)

When the pyrolysis temperature was increased the yields of aromatics were higher improving the HHV and the fuel properties of the bio-oil, as shown in Table 14. Higher pyrolysis temperatures have a significant effect on the stimulation of deoxygenation reactions increasing the level of aromatics present in the pyrolysis liquid (Vecino Mantilla et al., 2014). The same increment was observed for furans but only in the SB experiments.

Less furfural and 2-furanmethanol were produced at the highest pyrolysis temperature (500 ºC) which might be explained by the degradation of these molecules at higher heating temperatures. On the other hand, the formation of phenols was maximised

at 500 ºC. Lignin decomposition becomes easier at higher pyrolysis temperatures favouring the formation of phenols.

Ahmad et al. (2018) processed SB in the TCR reactor at the same pyrolysis and reforming temperatures (400 and 500ºC, respectively) obtaining similar results in terms of furfural (3.5%) and furans (10.9%). However, the same study also explored the conversion of SB into bio-oil when keeping the same experimental conditions but without biochar in the reforming unit. Surprisingly the percentage of furfural almost quadrupled (13.6%) and the yields of furans more than doubled (22.4%). Vecino Mantilla et al. (2014) used SB in a fixed bed intermediate pyrolysis reactor at 460ºC presenting yields of furfural and furans of 32.3 and 40.1%, respectively. Additionally, Aqsha et al. (2017) worked with the same type of reactor than the previous reference but processing oat straw (similar to oat hull) at 500 ºC. The bio-oil contained 10.6% of furfural, 5.4% of 2-furanmethanol and 19.9% of furans.

In the present study, the highest values of furfural, 2-furanmethanol and furans were 2.5, 1.3 and 12.9% respectively which are significantly lower compared to the previous literature results mentioned in the last paragraph. The biochar present in the reforming unit, which breaks down this kind of chemical compounds into different molecules, might be the cause of the low furans yields observed in Table 8 and 16.

4.3.3 Gas Analysis

The gas composition (H_2, CH_4, CO, CO_2 and C_XH_Y) of the SB and OH experiments at different pyrolysis temperatures are shown in Table 17. The non-detectable volume in the syngas might be the existence of hydrocarbons like ethylene and propane not detected by the gas analyser.

Applying 400 and 450 ºC as pyrolysis temperature, CO_2 was the main gas in SB and OH syngas. Lower pyrolysis temperatures stimulate the degradation of hemicellulose and cellulose which is linked to the cracking of carboxyl and carbonyl compounds increasing the formation of CO_2 (Uddin et al., 2014). For that reason, the TCR trials at 400 ºC revealed the highest CO_2 percentages between Table 17 and the previous section (Table 9). SB gas contains more CO_2 than OH gas due to the higher amount of cellulose and hemicellulose observed in receptive biomass (Table 3).

When the pyrolysis temperature is raised the volume of CO_2 decreases for the reasons mentioned previously related to the decomposition of cellulose and hemicellulose. Methane yields were also reduced with the increment of pyrolysis temperature which is not expected. In theory, CH_4 production is caused by the degradation of lignin promoted at higher pyrolysis temperatures (Yang et al., 2007). The higher methane volume found in SB runs might be associated to the presence of more lignin in SB biomass which was also demonstrated in the first set of trials (different reforming temperatures).

The gas analysis revealed CO to be the biggest compound present in both pyrolysis gases at 500 ºC. The explanation might be the stimulation of decarbonylation and decarboxylation reactions increasing the amount of CO (He et al., 2010).

SB at 450 ºC and OH at 500 ºC generated the syngas with better calorific values (15.9 and 17.3 MJ/kg) due to higher H_2 volume (25.7 and 23.1 vol%). These results are lower than the values of SB trial at 700 ºC as reforming temperature (previous experiments). The H_2 volume was 31.6 vol% and the HHV was 18.8 MJ/kg. Higher temperatures in the reforming unit in the presence of biochar can promote steam

reforming and water gas shift reactions increasing the production of hydrogen and the energy density of the syngas (Neumann et al., 2016, Yang et al., 2013).

Table 17 - SB and OH permanent gas composition at different pyrolysis temperatures (Reforming temperature = 500 ºC)

	SB			OH		
Pyrolysis Temperature (°C)	**400**	**450**	**500**	**400**	**450**	**500**
Component						
H_2 (vol%)	21.5	25.7	19.9	16.5	15.8	23.1
CH_4 (vol%)	15.6	13.5	10.9	11.6	7.0	6.4
CO (vol%)	21.2	20.2	32.6	26.5	25.5	29.5
CO_2 (vol%)	30.5	28.8	23.6	30.1	25.6	21.2
C_XH_Y (vol%)	2.5	2.3	2.7	3.0	2.7	3.4
Non-detectable compounds (vol%)	8.7	9.5	10.3	12.3	23.4	16.4
HHV (MJ/kg)	13.8	15.9	13.4	16.2	15.3	17.3
Density (kg/m^3)	0.90	0.89	0.98	0.91	1.2	0.85

Table 18 summarises the gas composition of different permanent gases from diverse feedstocks and pyrolysis technologies searched in the literature review.

Al Arni (2018) used a batch reactor to process SB at 500 ºC trough two pyrolysis regimes (fast and slow). For both types of pyrolysis (fast and slow) the H_2 volumes (8.7 and 9.6 vol%, respectively) were approximately less than half of the SB run with the same pyrolysis temperature (500 ºC). The same tendency was observed with Aqsha et al. (2017)

study converting oat straw at 500 ºC by a fixed bed intermediate pyrolysis reactor. In this work the amount of hydrogen produced was only 0.86 vol%. An extremely low value compared to the OH trials which use an identical kind of biomass. The reforming unit containing biochar as a catalyst could favour deoxygenation reactions resulting in the production of H_2 and improving the HHV of the pyrolysis gas (Henkel et al., 2016).

Ahmad et al. (2018) obtained a syngas with the same HHV (13.8 MJ/kg) than the present work with equal experimental conditions (TCR working with SB at 400 and 500 °C as pyrolysis and reforming temperatures). Despite Table 17 showing a higher H_2 yield (21.5 to 12.1 vol%), the higher percentage of CH_4 (19.5 to 15.6 vol%) and CO (32.8 to 21.2 vol%) found in Ahmad et al. (2018) work might justify the same calorific value between both studies. The different gas composition among both works may come from the use of diverse SB species with different chemical natures.

On the other hand, Neumann et al. (2016) converting digestate at 450 and 500 °C (pyrolysis and reforming temperature) presented a TCR syngas with lower energy density (13.1 MJ/kg) when compared to the SB (15.9 MJ/kg) and OH (15.3 MJ/kg) runs (same operating parameters). SB and OH feedstocks revealed more potential in the production of a pyrolysis gas with higher calorific value.

It is a fact that the pyrolytic gas from this set of experiments contains less hydrogen volume and HHV than the trials performed when changing the temperature of the reformer. The contact between the biochar and the organic vapours at higher reforming temperatures helps to produce a syngas richer in H_2 and consequently with better energy density. However, the quantity of combustible gases and the HHV of these experiments are sufficient to be utilised as a fuel for the production of heat and power via CHP engines.

Table 18 - Pyrolysis gas composition from literature review at different pyrolysis temperatures using several feedstocks and pyrolysis technologies

Pyrolsysis Type	Temperature (ºC)		Biomass	H_2 (vol%)	CH_4 (vol%)	CO (vol%)	CO_2 (vol%)	C_xH_y (vol%)	HHV (MJ/kg)	Density (kg/m^3)	Ref.
	Reactor	Reformer									
Fast	500	-	SB	8.7	21.5	13.9	52.3	3.6	-	-	1
Slow	500	-	SB	9.6	17.6	60.1	11.7	1.0	-	-	1
Intermediate	500	-	Oat Straw	0.86	1.22	28.8	68.1	-	-	-	2
TCR	400	500	SB	12.1	19.5	32.8	32.9	-	13.8	1.3	3
TCR	450	500	Digestate	21.0	5.0	14.0	40.0	-	13.1	-	4
TCR	500	500	OH	23.1	6.4	29.5	21.2	3.4	17.3	0.85	5

1 - (Al Arni, 2018); 2 - (Aqsha et al., 2017); 3 - (Ahmad et al., 2018): 4 - (Neumann et al., 2016); 5 - Present work.

4.3.4 Char Analysis

Table 19 indicates the ultimate analysis of the biochar, ash content and its HHV. Biochar is mainly composed of fixed carbon and ash as mentioned before.

SB biochar suffered a fluctuation in terms of carbon and energy content when the pyrolysis temperature was increased. For OH runs the biochar presented similar chemical composition and calorific value between different pyrolysis temperatures. Relating to the first set of experiments, it is observed that there is no significant impact on the properties of the biochar and its HHV when the reforming or pyrolysis temperatures are changed. The biochar from SB produced at 450 and 500 °C (pyrolysis and reforming temperatures) was the only one out of this context having a substantially lower carbon value and energy content compared to the rest of the trials.

From Table 19, SB biochar at 400 °C contains the highest calorific value (29.7 MJ/kg) attributed to the highest carbon content (79.6 wt%). Inversely, SB biochar at 450 °C is the less energetic (24.9 MJ/kg) having the lowest carbon value (70.3 wt%). Fixed carbon is the combustible compound of the pyrolysis char raising the HHV (McKendry, 2002).

Generally, for the same pyrolysis temperatures OH char presented less ash and more carbon than the SB char leading to a better HHV. This is a result of the chemical composition of both biomasses where the OH contains more fixed carbon and less ash compared to SB (Table 3). The existence of ash reduces the energy content of the biochar (Laird, 2008).

Based on the literature review Table 20 summarises the properties of different biochars from diverse feedstocks and pyrolysis technologies.

Table 19 - SB and OH biochar characterisation at different pyrolysis temperatures (Reforming temperature = 500 ºC)

	SB			OH		
Pyrolysis Temperature (°C)	**400**	**450**	**500**	**400**	**450**	**500**
Ultimate analysis						
C (wt%)	79.6	70.3	77.1	78.2	79.3	79.0
H (wt%)	2.2	1.6	1.5	2.7	2.0	2.3
N (wt%)	0.44	0.39	0.47	1.4	1.1	1.3
S (wt%)	<0.10	<0.10	<0.10	<0.10	<0.10	<0.10
O (wt%) (diff.)	2.7	11.6	2.6	2.2	5.7	1.2
Ash (wt%)	15.0	16.1	18.2	15.5	11.8	16.1
HHV (MJ/kg)	29.7	24.9	28.1	29.3	29.2	29.3

The present work produced a SB biochar (500 °C) with a HHV between Varma and Mondal (2017) and Lee et al. (2013) studies. The first author used fast pyrolysis to process SB at 500 °C obtaining a char with lower carbon content (66.9 wt%) and subsequently lower energy density (24.3 MJ/kg). However, the second author converted SB via slow pyrolysis at 500 °C producing biochar with a higher carbon value (85.6 wt%) and HHV (32.8 MJ/kg). Slow pyrolysis involves slower heating rates and longer residence times which promotes aromatisation reactions increasing the C-C bonds and the percentage of fixed carbon in the biochar (Williams and Besler, 1996).

Henkel et al. (2013) processed SB via intermediate pyrolysis (batch reactor) and the same fluctuation of the SB HHV from Table 19 was observed when the pyrolysis temperature was increased. In the same study the biochar at 500 °C demonstrated lower carbon content (71.9 wt%) and calorific value (24.3 MJ/kg) compared to the SB run for the present work at the same pyrolysis temperature. The reforming unit of the TCR enables a longer residence time of the char causing cracking reactions resulting in a final biochar richer in fixed carbon.

The same effect occurred with Aqsha et al. (2017) and Ouadi et al. (2013) works, where oat straw and de-inking sludge were processed through intermediate pyrolysis at 500 and 450 °C (respectively). For the first study the carbon content and HHV were 66.4 wt% and 23.9 MJ/kg. While for the second study the carbon value was 20.0 wt% and the HHV was 4.9 MJ/kg. Once more, the extended time of the biochar in the reformer contributed to better results in the present work.

In relation to TCR results from the literature review, Ahmad et al. (2018) produced a SB char at 400 and 500 °C (pyrolysis and reforming temperature) with higher ash content (30.5 wt%) and lower carbon value (67.9 wt%) and energy density (24.0 MJ/kg). The variance between these results and Table 19 (for the same parameters) might be due to the different chemical composition of the SB applied. Neumann et al. (2016) used digestate in the TCR at 450 and 500 °C (pyrolysis and reforming temperature) obtaining biochar with higher carbon content (83.7 wt%) but a lower calorific value (18.9 MJ/kg). This might be caused for the large presence of ash (38.4 wt%) in the digestate biochar decreasing the HHV. Additionally, digestate feedstock contains considerably high ash content (17.9 wt%) compared to SB and OH biomasses (4.0 and 2.4 wt%, respectively).

Table 20 - Biochar characterization from literature review at different pyrolysis temperatures using several feedstocks and pyrolysis technologies

Pyrolysis Type	Temperature (ºC)		Biomass	C (wt%)	H (wt%)	N (wt%)	S (wt%)	O (wt%)	Ash (wt%)	HHV (MJ/kg)	Ref.
	Reactor	Reformer									
Fast	500	-	SB	66.9	3.8	0.96	0.01	28.2	16.3	24.3	1
Slow	500	-	SB	85.6	2.8	1.1	-	1.9	8.6	32.8	2
Intermediate	500	-	SB	71.9	2.9	1.3	-	23.8	-	24.3	3
Intermediate	600	-	SB	80.3	2.3	0.79	-	16.6	-	27.4	3
Intermediate	700	-	SB	80.8	1.4	0.72	-	17.1	-	26.3	3
Intermediate	500	-	Oat Straw	66.4	2.3	1.3	0.49	20.3	11.2	23.9	4
Intermediate	450	-	De-inking sludge	20.0	2.2	0.38	<0.10	23.9	53.5	4.9	5
TCR	400	500	SB	67.9	1.6	0.52	0.51	-	30.5	24.0	6
TCR	450	500	Digestate	83.7	4.7	2.7	0.50	8.4	38.4	18.9	7
TCR	400	500	SB	79.6	2.2	0.44	<0.10	2.7	15.0	29.7	8

1 - (Varma and Mondal, 2017); 2 - (Lee et al., 2013); 3 - (Henkel et al., 2016); 4 - (Aqsha et al., 2017); 5 - (Ouadi et al., 2013); 6 - (Ahmad et al., 2018); 7 - (Neumann et al., 2016); 8 - Present work.

All the biochars from this section contain similar carbon value and energy content when likened to the classic sub-bituminous coal (73.9% and 29.05 MJ/kg, respectively). The only exception is the SB char produced at 450 °C.

As mentioned before, the properties of the biochar did not suffer significant modifications between the experimental conditions applied in this section and the last one. Therefore, the biochar from this set of experiments (different pyrolysis temperatures) is also energetically interesting to produce heat and power through boilers, gasifiers and furnaces. Moreover, it can also be utilised as a fertiliser, activated carbon and for catalytic upgrading.

4.3.5 Mass Balance and Energy Yield

The mass balance and the energy yield for the SB and OH experiments are demonstrated in Figures 37 and 38.

When the pyrolysis temperatures were lower the production of pyrolysis liquid (bio-oil and aqueous phase) and biochar increased. The formation of pyrolysis oil comes from the breakdown of cellulose and hemicellulose at lower temperatures through devolatilization and depolymerisation reactions (Yang et al., 2007). Biochar production is also favoured at low pyrolysis temperatures where charring and cross-linking reactions occur with more intensity (Greenhalf et al., 2012, Van de Velden et al., 2010).

The lowest pyrolysis temperature (400 °C) resulted in the biggest yields of SB and OH bio-oil and biochar. For the pyrolysis liquid, OH at 400 °C obtained 9.3 wt%. While for the char, SB at 400 °C was the most productive with 27.2 wt%. These values are higher than the best results from the previous section (different reforming temperatures) showing the importance of low pyrolysis temperatures if the aim is to raise the amount of

bio-oil and biochar. Table 3 shows a higher ash and lining percentages in the SB biomass which is responsible for larger biochar yields when compared to OH runs for all pyrolysis temperatures (Williams and Besler, 1996).

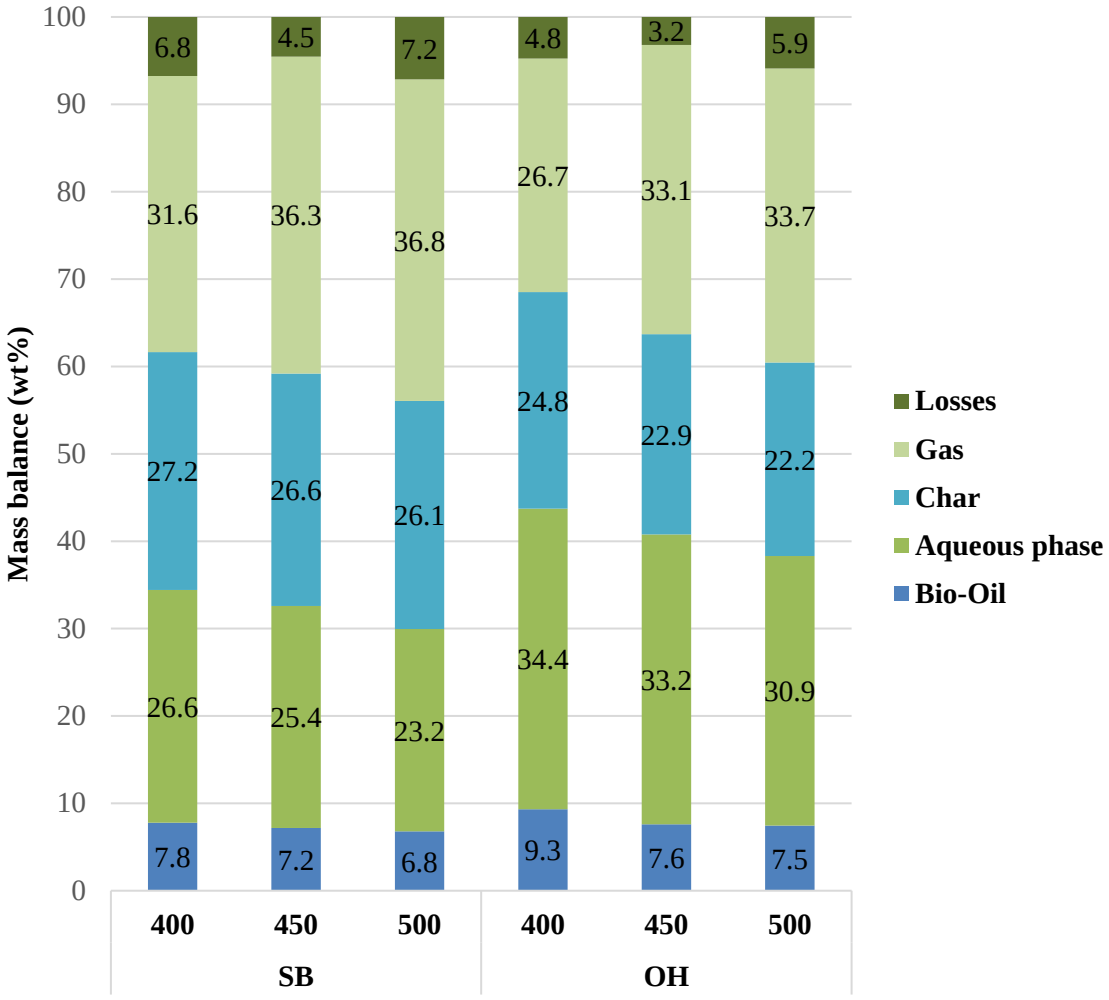


Figure 37 - Mass balance of SB and OH trials at different pyrolysis temperatures (reforming temperature = 500 ºC)

Higher pyrolysis temperatures decreased the percentage of bio-oil and char. At the same time, the gas fraction was maximised due to the degradation of biochar into lighter compounds when submitted to higher temperatures in the pyrolysis reactor. The

increment of temperature also promoted other decomposition reactions resulting in less bio-oil and more syngas (Henkel et al., 2016).

The run at 500 ºC (pyrolysis temperature) converting SB was the highest one in terms of gas production (36.8 wt%). However, the trials from the previous section using higher reforming temperatures showed better results for the same product. Above 500 ºC, the formation of syngas is stimulated trough volatilization, cracking, dehydrogenation and aromatisation reactions (Blanco and Chejne, 2016). The gas yields observed in Figure 37 are higher for SB than OH experiments due to the higher water content present in OH feedstock (Table 3). More moisture means less gas produced, which is attributed to the higher removal of water-soluble compounds present in the pyrolysis gas (Dasappa et al., 2004).

For the mass balance, the increment of pyrolysis temperature had the same effect than the increment of reforming temperature (more syngas and less bio-oil and char). However, changing the reforming temperature can cause bigger variations in the distribution of products compared to this set of trials where the difference is smaller. It is evident that the increase from 500 to 700 ºC in the reforming unit results in other chemical reactions creating a deeper modification in the quantity and distribution of the TCR products

Once again, the TCR technology presented a high efficiency in terms of balance. The conversion of biomass into valuable products was between 92.8 and 96.8 wt% and in the best experiment only 3.2 wt% was lost. As mentioned before, the losses might be explained due to errors measuring weights (feedstock, bio-oil and biochar), gases not detected by the gas analyser and the bio-oil not determined in the cleaning of the cooling system.

Biochar was the biggest energy fraction in all experiments. The best results were achieved with the lowest reforming temperatures for both biomasses, where SB and OH at 400 °C obtained 49.4 and 45.3%, respectively. Despite the present runs producing more syngas than char, the calorific value of biochar (24.9-29.7 MJ/kg) is significantly higher compared to the pyrolysis gas (13.4-17.3 MJ/kg) which can justify the results from Figure 38.

The biochar energy yields of this section are higher than the previous experiments at different reforming temperatures (Figure 34). This may be caused by the higher energy density and char production found in Table 19 and Figure 37 when compared to Table 11 and Figure 33 from the previous set of trials. However, for pyrolysis gas the situation is reversed and it can be attributed to the reasons explained previously in terms of mass balance and HHV of the syngas between both sections.

From the results in Figure 38, it is observed that the OH energy yields for bio-oil are higher than SB for any single pyrolysis temperature. This can be explained by the better energy value and higher oil production found in OH runs (Table 14 and Figure 37).

The energy losses were from 7.7 to 11.4%, where the OH trial at 500 °C was the most efficient one converting 92.3% of the energy from the feedstock into TCR products. In general, SB experiments presented more energy losses than OH which can be associated to bigger mass losses demonstrated in Figure 37.

Comparing these results with the previous section (Figure 34), it is possible to observe higher energy losses when the TCR reactor works at lower pyrolysis and reforming temperatures. In these conditions, there is more production of bio-oil which means more pyrolysis liquid not extracted from the condensing unit during the cleaning

(Figure 22). For that reason, some bio-oil energy is lost and not considered for the energy yields affecting the efficiency of the process.

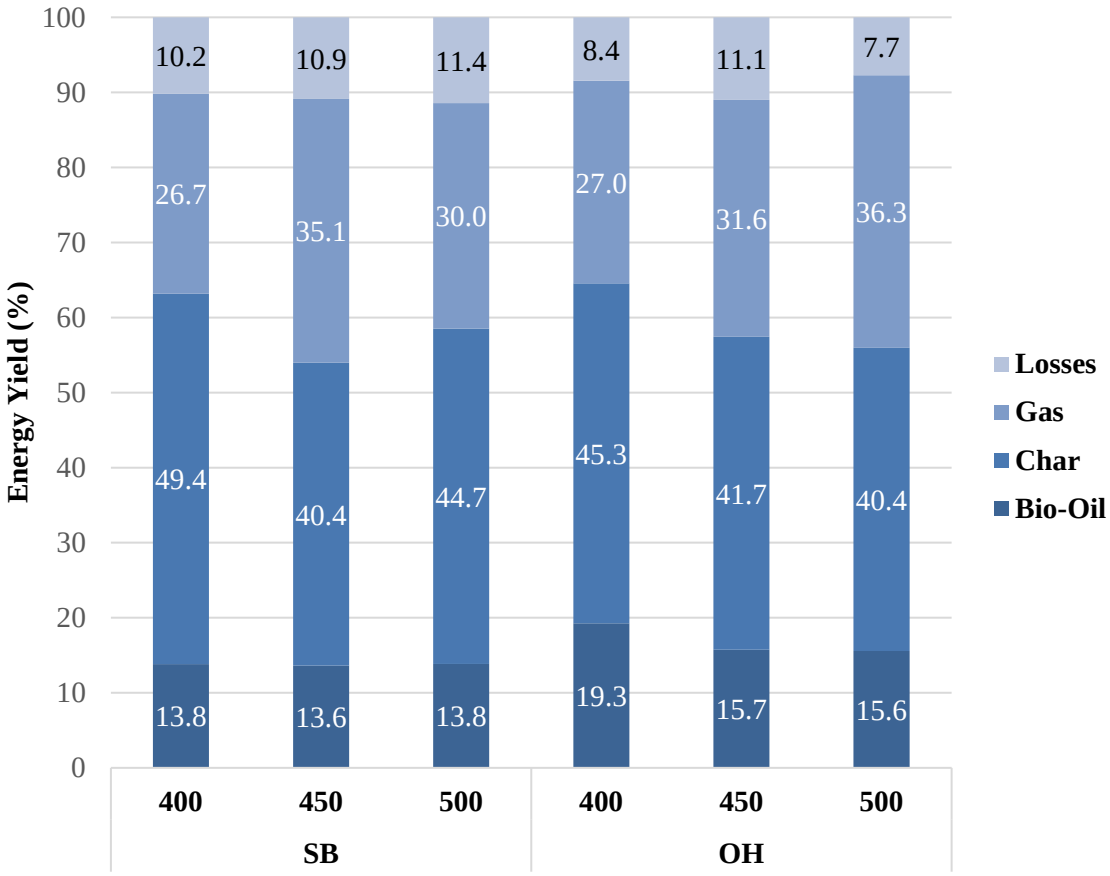


Figure 38 - Energy yield of SB and OH trials at different pyrolysis temperatures (reforming temperature = 500 ºC)

4.4 Steel Slag as an In-situ Catalyst in the TCR process

In the third set of experiments SS was used as an in-situ catalyst in the TCR process in two different methods: 1) mixed with the biochar (no pelletisation) in the reforming unit at three different ratios (30, 70 and 100 wt% of SS); 2) pelletising with OH biomass in three different proportions (10, 20 and 30 wt% of SS) and introducing the mixture in the auger pyrolysis reactor. It was not possible to pelletise SS with SB

feedstock due to the physical characteristics of the raw material and the specifications of the pelletiser. The other experimental conditions were kept constant as it is observed in Table 21.

Table 21 - TCR runs conditions applying different ratios of SS in 2 methods

Experimental Conditions	**Set 3a and 3b (Trial 11 to Trial 19)**
Intermediate Pyrolysis Temperature	400 ºC
Reforming Temperature	500 ºC
Feedstock	OH and SB
Feed Consumption	3.5 kg (Pellets)
Feed Rate	1.4 kg/h
Solid Residence Time	Minutes
Gas Residence Time	Seconds
Biochar (Reformer - 1st method)	70, 30 and 0 wt%
SS (Reformer - 1st method)	30, 70 and 100 wt%
Biochar (Reformer - 2nd method)	100 wt% (500 g)
SS pellets (Feed, Auger Reactor - 2nd method)	10, 20 and 30 wt%

The temperatures set in the auger pyrolysis reactor and reforming unit were 400 and 500 ºC respectively. This selection was according to the higher furfural and 2-furanmethanol yields present in the pyrolysis oil from the previous runs (Tables 8 and 16).

4.4.1 Bio-oil Analysis

The properties of the bio-oil from SB and OH runs mixed with different ratios of SS are summarised in Table 22.

In both bio-oils there was an increment of carbon content and energy density and a reduction of oxygen concentration when the ratio of SS in the reformer was increased. SB and OH bio-oil showed better HHV when 100 wt% of SS was introduced into the reforming unit compared to the trials with the same experimental conditions from the previous section (Table 14). An increase of 18.1 and 5.1% in carbon value, a rise of 22.0 and 5.7% in energy density and a decrease of 50.9 and 20.4% in oxygen content was noticed for SB and OH runs with 100 wt% of SS.

The same effect was observed in the introduction of SS with OH (less oxygen and higher carbon percentage and calorific value). The best results were also achieved with the highest SS proportion (30 wt%) present in the OH seed. Compared to the experiment with the same pyrolysis and reforming temperatures (Table 14) these results revealed a reduction of 24.4% of oxygen and an increment of 4.0 and 6.9% for carbon and HHV, respectively. In the OH trials, the implementation of SS in the reformer and in the feed presented similar results and improvements concerning the ultimate analysis and the HHV of the bio-oil.

SS may promote the decomposition and depolymerisation reactions of cellulose and hemicellulose producing a more stable bio-oil with lower oxygen and higher carbon and calorific value (Lede et al., 1997).

Table 22 - SB and OH bio-oil characterization at different SS ratios (Pyrolysis and Reforming temperatures = 400 and 500 ºC)

	SB (SS in the reformer)				OH (SS in the reformer)				OH (SS in the feed)		
Steel Slag (wt%)	**0**	**30**	**70**	**100**	**0**	**30**	**70**	**100**	**10**	**20**	**30**
Ultimate analysis											
C (wt%)	63.4	68.2	71.7	74.9	70.7	64.2	69.8	74.4	65.9	67.9	73.5
H (wt%)	8.3	7.2	8.3	9.0	8.6	7.9	8.8	8.9	9.6	9.3	9.4
N (wt%)	0.41	1.9	1.4	1.1	1.8	2.8	1.7	1.9	1.8	2.0	2.5
S (wt%)	0.39	1.7	1.2	1.6	1.3	1.3	1.0	0.91	0.95	1.0	1.3
O (wt%) (diff.)	27.5	21.0	17.5	13.5	17.6	23.8	18.7	13.9	21.8	19.8	13.3
Fuel Properties											
HHV (MJ/kg)	29.1	30.2	33.0	35.5	33.1	29.3	32.9	35.1	32.1	32.6	35.4
Ash (wt%)	<0.001	<0.001	<0.001	<0.001	<0.001	<0.001	<0.001	<0.001	<0.001	<0.001	<0.001
Water (wt%)	9.9	8.4	6.5	5.7	7.8	6.7	6.2	5.4	6.6	5.1	3.5
TAN (mg KOH/g)	32.2	29.1	22.6	16.7	33.5	29.2	27.4	14.3	21.1	17.3	11.5
Viscosity (mm^2/s)	47.8	45.8	30.9	25.5	38.1	35.7	32.3	30.8	28.2	26.9	21.0
Density (kg/m^3)	1077	1073	1067	1060	1078	1069	1055	1051	1040	1038	1026

Interestingly, the use of SS in the TCR process (reformer and feed) could create a pyrolysis liquid with better HHV compared to the experiments with higher reforming temperatures (600 and 700 °C) from Table 6 and higher pyrolysis temperatures (450 and 500 °C) from Table 14. To conclude, it was possible to obtain better results (higher carbon content and calorific value and less oxygen, water, viscosity, density and acid number) and save energy simultaneously reducing the reforming temperature by 200 °C and the pyrolysis temperature by 100 °C.

SB and OH pyrolysis liquids were upgraded with the implementation of SS in the reforming unit. Compared to the TCR runs with same parameters (400 and 500 °C for pyrolysis and reforming temperatures) all the fuel properties were improved when applying the three SS ratios (30, 70 and 100 wt%). Once again, the best results were achieved using 100 wt% of SS in the reformer. The water content of SB and OH oils were decreased by 42.4 and 30.8% while the acid number was reduced by 48.1 and 57.3% respectively. For the viscosity of the SB and OH experiments a decrease of 46.6 and 19.2%. was observed. The bio-oil density was reduced by 1.6 and 2.5% for SB and OH trials.

When the TCR reactor converted OH pelletised with SS an improvement in all fuel properties when applying 10, 20 and 30 wt% of SS was also verified. The biggest fraction of SS in the feedstock (30 wt%) revealed the best results compared to the values from Table 14. The water, acid number, viscosity and density of the OH pyrolysis liquid were decreased by 55.1, 65.7, 44.9 and 4.8% respectively.

The utilisation of SS in the TCR technology proved to be advantageous to improve the bio-oil fuel properties in several points:

a) Optimising dehydration reactions reducing the oxygen and moisture of the oil and subsequently raising the HHV.

b) The high percentage of iron (24.1%) could stimulate the hydrogenation of carbonyl group decreasing the acid number of the bio-oil (Lee et al., 2014, Yang et al., 2017). For that reason, the presence of acid elements is lower and so reduces the wear and corrosion in engine devices.

c) SS might promote cracking reactions producing a pyrolysis liquid richer in light chemical compounds resulting in lower viscosity and density. Thus, the bio-oil becomes better for combustion applications improving engine performance and stability.

Mixing SS with OH demonstrated to be more efficient in upgrading the bio-oil than introducing SS in the reformer. The presence of SS in the feedstock might have a double catalytic effect in the pyrolysis reactor and reforming unit further improving the fuel properties of the pyrolysis liquid. On the other hand, the introduction of SS into the reformer only upgrades the organic vapours in this stage of the experiment and not since the beginning as mentioned before.

The OH experiment with 30 wt% of SS in the feed showed better results in terms of fuel properties (water, TAN, viscosity and density) than the OH runs at higher pyrolysis temperatures (450 and 500 °C) from Table 14. Regarding the OH trials at higher reforming temperatures (600 and 700 °C in Table 6), the same run obtained inferior water content than 600 °C (3.9 wt%), lower acid number compared to 600 and 700 °C (21.4 and 17.7 mg KOH/g), lower viscosity than 600 °C (35.4 mm^2/s) and inferior density when compared to 600 and 700 °C (1082 and 1072 kg/m^3). Once again, the important role of SS in producing a bio-oil with better quality at lower pyrolysis and reforming temperatures spending less energy was demonstrated.

In Table 23 it is indicated according to the literature review the properties of several bio-oils from different feedstocks and catalytic pyrolysis technologies using diverse catalysts. The studies analysed contain similar pyrolysis and reforming temperatures than the present experiments with SS. However, the catalysts applied were from different chemical groups: zeolites (ZSM-5 and HZY); minerals (dolomite and silica); mesoporous (Mo_2C/Al_2O_3 and γ-Al_2O_3) and transition metals (nickel).

All the experiments with SS obtained lower oxygen and higher energy density compared to the studies from Table 23. The only exception was Mante's et al. (2018) research which produced a pyrolysis oil with 35.5 MJ/kg using γ-Al_2O_3 as a catalyst. However, the conversion of SB using 100 wt% of SS in the reformer obtained the same HHV (Table 22) at lower pyrolysis temperatures (400 °C).

The same trend was observed for the water content. All runs from Table 22 showed lower values than the literature review excluding Mahmood's et al. (2013) and Mante's et al. (2018) works with 6.2 and 4.9 wt%. Nevertheless, the use of 30 wt% of SS in OH could generate a bio-oil with less water content (3.5 wt%) than the previous studies.

In terms of acid number, the difference between SS trials and other catalytic pyrolysis research are noteworthy. The best result from Table 23 is 50.3 mg KOH/g, while these set of experiments could reach 11.5 mg KOH/g.

Mante et al. (2018) presented a lower value (4.1 mm^2/s) for viscosity when compared to SS runs. A pyrolysis liquid with reasonable viscosity was revealed to be positive for the prevention of internal leakages located in the fuel pump and line, increasing the brake power and lubricity.

Table 23 - Bio-oil and fuels properties from catalytic pyrolysis found in the literature review

Pyrolysis Type	Temperature (ºC)		Biomass / Fuel	Catalyst	C	H	O	HHV	Water	TAN (mg	Viscosity	Density	Ref.
	Reactor	Reformer			(wt%)	(wt%)	(wt%)	(MJ/kg)	(wt%)	KOH/g)	(mm^2/s)	(kg/m^3)	
In-situ Catalytic	450	-	SB	ZSM-5	53.8	7.4	38.5	23.5	10.7	68.8	-	1140	1
In-situ Catalytic	500	-	SB	ZSM-5	60.1	7.9	31.7	27.0	10.6	67.7	-	1140	1
In-situ Catalytic	450	-	SB	Silica	33.4	9.4	56.9	16.8	20.0	84.2	-	1110	1
In-situ Catalytic	500	-	SB	Silica	52.8	8.2	38.6	24.1	15.0	75.2	-	1170	1
In-situ Catalytic	500	-	SB	Mo_2C/Al_2O_3	48.1	7.1	43.8	21.3	-	-	19.7	-	2
In-situ Catalytic	500	-	Oat Straw	HZY Zeolite	15.8	11.2	70.8	27.1	15.5	-	-	-	3
Ex-situ Catalytic	450	500	Brewers grain	Nickel	58.4	9.3	26.7	28.7	6.2	50.3	-	-	4
In-situ Catalytic	540	-	Brown salwood	Dolomite	66.7	8.9	24.1	24.3	-	62.0	49.0	1030	5
In-situ Catalytic	500	-	Pine	γ-Al_2O_3	78.3	8.1	13.6	35.5	4.9	-	4.1	1018	6
TCR	400	500	OH	Steel Slag	73.5	9.4	13.3	35.4	3.5	11.5	21.0	1026	7
-	-	-	Biodiesel	-	78.9	12.6	8.4	37-40	0.37	0.49	1.9-6.0	880	8
-	-	-	Diesel	-	84-87	13-16	1.0	42-45	0.05	0.03	1.9-5.5	820-850	9

1 - (Mendes et al., 2016); 2 - (Patel et al., 2013); 3 - (Aqsha et al., 2017); 4 - (Mahmood et al., 2013); 5 - (Charusiri and Numcharoenpinij, 2017); 6 - (Mante et al., 2018); 7 - Present work; 8 - EN 14214; 9 - EN 590.

Apart from Charusiri's and Numcharoenpinij's (2017) and Mante's et al. (2018) works, the density of SS bio-oil was inferior than the literature review. Additionally, the lowest density value from SS trials (1026 kg/mm^3) is between the results of the previous authors (1030 and 1018 kg/mm^3, respectively).

SS showed to be a promising option for improving the properties of the bio-oil, reforming and cracking the pyrolysis vapours more efficiently than the catalysts from Table 23. The current catalysts used in the pyrolysis reactors are not the most suitable to significantly upgrade the properties of the pyrolysis liquid. SS is a solid and effective sacrificial catalyst which is a waste from the steel industry making it a very economical solution.

Unfortunately, the quality and the properties of the bio-oil from SS runs is still inferior when compared to biodiesel and diesel. However, in this case they only need minimal upgrading due to the catalytic properties of SS. It is relevant to emphasize that SS results came from the lowest pyrolysis and reforming temperatures (400 and 500 °C, respectively). It would be very interesting to see some results of using SS at higher pyrolysis and reforming temperatures in the TCR.

4.4.2 GC-MS Analysis of Bio-oil

The organic fraction of SB and OH bio-oils using different SS fractions were analysed via GC-MS. The results are shown in Table 24. Figures 39, 40 and 41 display the chromatograms of the bio-oils where the 15 most important and abundant peaks were identified. Phenols and aromatics are the main compounds of the SB and OH pyrolysis

oil. Furans are also in the top three but with lower concentrations than phenols and aromatics.

The use of SS at different proportions in the reforming unit and in the OH biomass did not vary the concentration of phenols in the pyrolysis liquid. SS does not have the same effect as higher pyrolysis and reforming temperatures to decompose lignin in phenolic compounds. Table 24 shows a SB oil with higher phenols yields attributed to the higher lignin content present in this kind of biomass (Table 3). A larger phenols percentage from the application of SS in the reformer rather than the feedstock can be observed in the OH runs. SS in the reforming unit might stimulate more cracking reactions to produce phenols from lignin.

The percentage of phenols in the present experiments was inferior to the same runs without SS from Table 16. This is also reflected in the lower acid number present in SS bio-oil shown in Table 22. In line with this reasoning is the fact the experiments mixing SS with OH presented the lowest phenols concentration and consequently the bio-oil with less acidity. SS is composed of magnesium (4.9%) which inhibits the production of phenolics in the bio-oil (Zhang et al., 2018).

Generally, the quantity of aromatics in this section was higher than the trials at the same temperatures without the application of SS. As a consequence, the SS runs indicated better energy density (Table 22). Transition metals as iron (24.1% in SS) help to maximise the production of aromatics converting oxygenated compounds (Karnjanakom et al., 2016).

Table 24 - Compounds detected and identified by GC-MS of the SB and OH bio-oil at different SS ratios (Pyrolysis and Reforming temperatures = 400 and 500 ºC)

		Uncertainty = 2.3 - 2.7%	**SB (SS in the reformer)**			**OH (SS in the reformer)**			**OH (SS in the feed)**		
	Steel Slag (wt%)		**30**	**70**	**100**	**30**	**70**	**100**	**10**	**20**	**30**
#	**Group**	**Chemical Compound**	**Conc. (%)**			**Conc. (%)**			**Conc. (%)**		
1	Aromatic	Benzene	1.9	2.2	0.28	3.6	1.2	0.92	1.1	0.92	0.90
2	Aromatic	Toluene	4.7	3.6	1.0	6.3	3.3	3.6	3.4	2.8	2.7
3	Furan	Furfural	0.19	1.3	2.8	0.12	1.2	1.7	1.0	0.75	0.58
4	Furan	2-Furanmethanol	0.30	0.19	0.68	0.25	1.1	1.3	0.82	0.47	0.33
5	Aromatic	Ethylbenzene	1.3	0.79	0.51	1.9	2.1	1.6	1.1	0.75	0.73
6	Aromatic	Benzene, 1,3-dimethyl-	1.7	0.39	0.34	1.3	0.81	0.89	1.7	0.82	0.97
7	Aromatic	1,3,5,7-Cyclooctatetraene	1.7	1.8	0.85	3.6	2.8	2.0	1.3	0.85	0.83
8	Phenol	Phenol	6.2	6.4	4.3	5.5	5.6	6.0	4.4	3.8	3.7
9	Phenol	Phenol, 2-methyl-	3.8	3.6	1.7	4.1	2.5	2.8	3.0	2.6	2.5
10	Phenol	Phenol, 3-methyl-	6.0	5.9	3.8	4.9	4.7	4.7	4.4	4.3	4.3
11	Phenol	Phenol, 2,6-dimethyl-	1.1	1.0	0.57	0.86	0.59	0.72	0.74	0.72	0.85
12	Phenol	Phenol, 2,4-dimethyl-	1.5	1.4	0.90	1.1	1.0	1.2	0.97	0.93	1.3
13	Phenol	Phenol, 4-ethyl-	6.5	7.0	9.7	3.9	7.0	6.0	5.3	5.0	4.5
14	Aromatic	Naphthalene	1.5	2.6	0.92	2.2	0.81	0.70	0.66	0.82	0.89
15	Furan	Benzofuran, 2,3-dihydro-	1.2	4.1	4.4	2.2	2.3	1.8	1.4	1.9	1.2
-	Total Furans	-	3.0	7.4	9.8	5.0	6.1	6.6	4.4	4.7	2.8

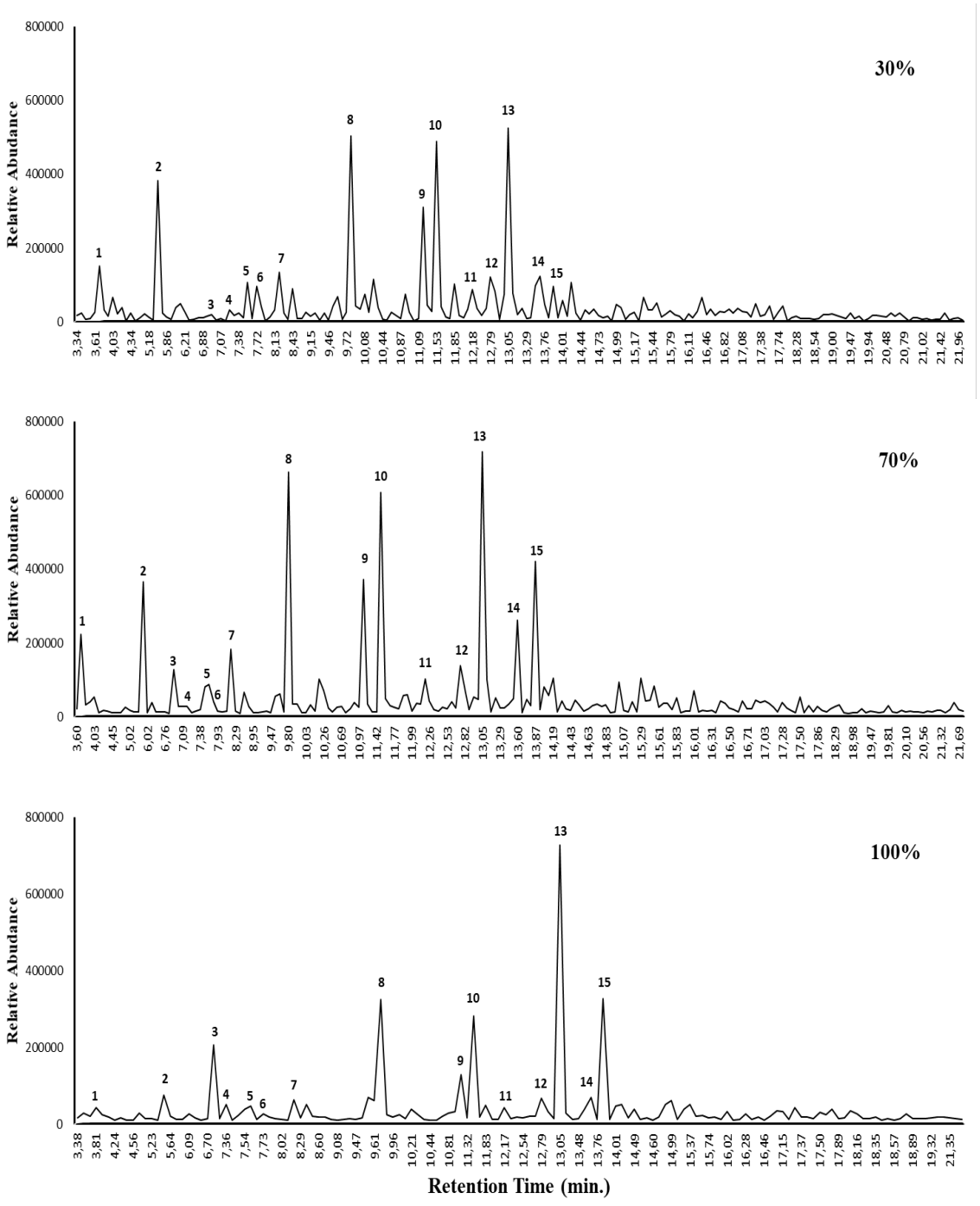


Figure 39 - GC-MS chromatograms of SB bio-oil and compounds detected at 400 and 500 ºC (pyrolysis and reforming temperature) and different SS ratios in the reformer

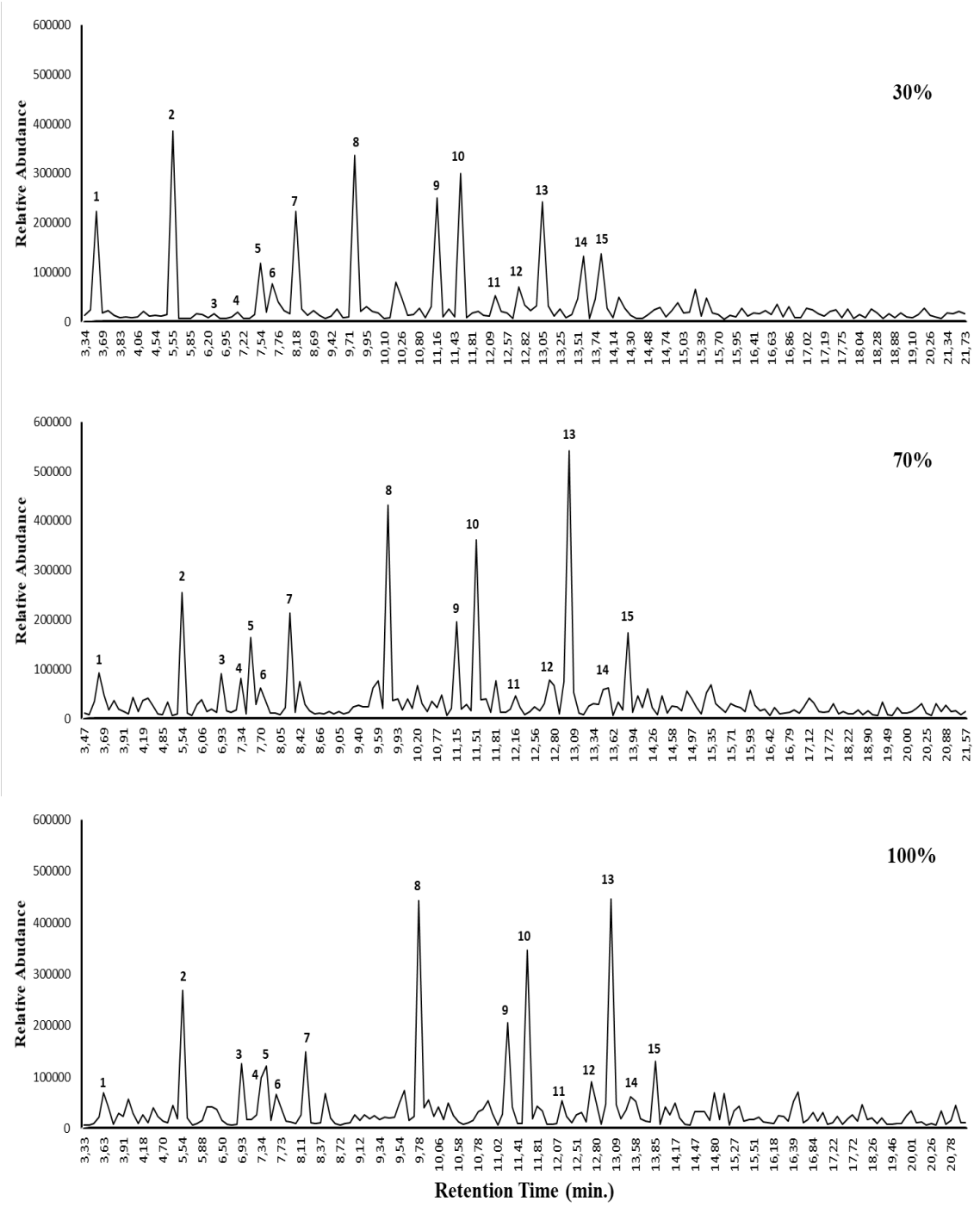


Figure 40 - GC-MS chromatograms of OH bio-oil and compounds detected at 400 and 500 ºC (pyrolysis and reforming temperature) and different SS ratios in the reformer

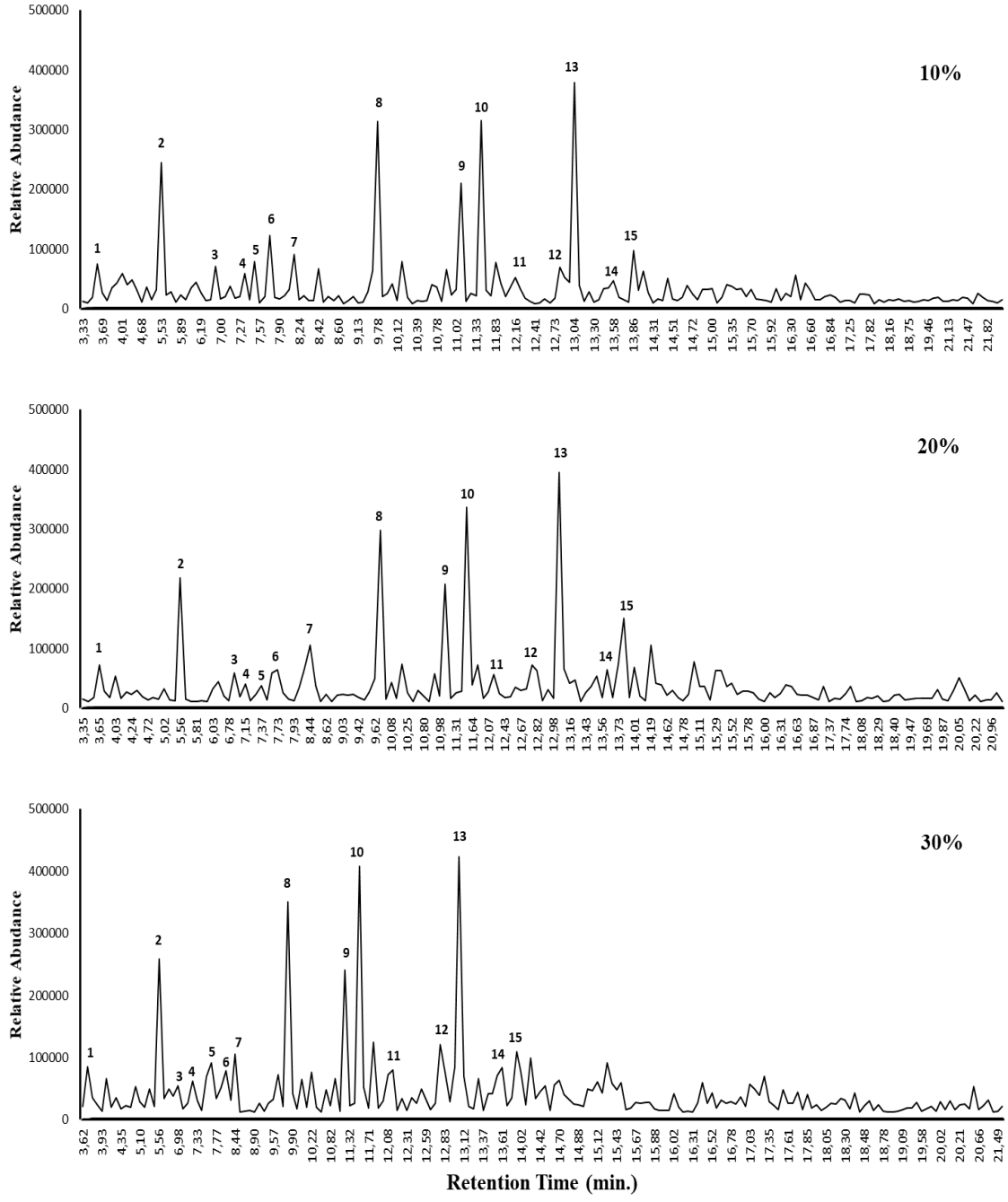


Figure 41 - GC-MS chromatograms of OH bio-oil and compounds detected at 400 and 500 ºC (pyrolysis and reforming temperature) and different SS ratios in the OH feed

For furans, only the SB and OH oils using the highest SS percentage (100%) in the reforming unit obtained superior furfural and 2-furanmethanol values when compared to the previous set of experiments under the same conditions (no SS). Due to its high iron composition SS can promote decarboxylation, hydrogenation and dehydration reactions converting polysaccharides into furans (Lee et al., 2014, Yang et al., 2017). However, when SS was mixed with the biochar (30/70 or 70/30 ratios) the conversion of carbonyl compounds in furans was not as efficient. It seems the use of biochar and SS at the same time in the reformer might minimise the catalytic effect of both materials to produce furans. The higher furans yields obtained during the experiments using 100% SS or 100% biochar supports this argument.

The conversion of SS mixed with OH produced a bio-oil with fewer furans than the OH oil using SS in the reforming unit. Additionally, when the SS fraction was increased in the feed a decrease in the yields of furfural, 2-furanmethanol and furans was noticed. The opposite effect occurred when increasing SS ratio in the reforming unit, where the percentage of these chemical compounds were raised. For that reason, the use of SS in the reformer demonstrated to be a better option to maximise the quantity of furans in the pyrolysis liquid.

In terms of furfural and furans, the best results (2.8 and 9.8%, respectively) were achieved by introducing 100 wt% of SS in the reformer and using SB as a feedstock. Despite the low values, this work with SS as a catalyst could produce a bio-oil with higher yields than some studies from the literature review (Charusiri and Numcharoenpinij, 2017, Maisano et al., 2017, Mante et al., 2018, Teixeira Cardoso et al., 2019). Teixeira Cardoso et al. (2019) and Charusiri and Numcharoenpinij (2017) processed SB and brown salwood via catalytic pyrolysis at 450 and 540 °C using ZSM-5 and dolomite as a catalyst,

respectively. In the first work the furans percentage in the pyrolysis liquid was 1.9% whereas in the second one it was 3.7%. Maisano et al. (2017) obtained a sea plant bio-oil with 1.1 and 3.1% of furfural and furans applying HZSM-5 as a catalyst via catalytic pyrolysis at 500 °C. Mante et al. (2018) used γ-Al_2O_3 through catalytic pyrolysis at 500 °C to convert pine in a bio-oil containing 0.34 and 0.36% of furfural and furans.

4.4.3 Gas Analysis

The gases detected from pyrolysis gas were H_2, CH_4, CO, CO_2 and C_XH_Y at different SS percentages in the reforming unit and mixed with OH (Table 25). Some elements like propane, ethylene and other hydrocarbons could not be detected through the gas analyser creating the non-detectable fraction showed in Table 25.

The analysis of the values of the gas composition showed different results and trends according to the use of SS in the reformer or biomass. The volumes of H_2 and CH_4 in both feedstocks decreased when the SS ratio was raised in the reforming unit. However, the increment in the proportion of SS in the OH feed resulted in an increase in the yields of H_2 and CH_4. The interaction between SS and OH in the pyrolysis and reforming reactor might promote hydrogenation, hydrogasification and water gas-shift reactions resulting in higher percentages of hydrogen and methane. SB runs presented higher methane concentrations than OH experiments due to the higher amount of lignin in the SB biomass. The degradation of lignin is responsible for the production of CH_4.

Table 25 - SB and OH permanent gas composition at different SS ratios (Pyrolysis and Reforming temperatures = 400 and 500 ºC)

	SB (SS in the reformer)				**OH (SS in the reformer)**				**OH (SS in the feed)**		
Steel Slag (wt%)	**0**	**30**	**70**	**100**	**0**	**30**	**70**	**100**	**10**	**20**	**30**
Component											
H_2 (vol%)	21.5	20.4	19.5	18.9	16.5	15.7	15.4	14.5	23.2	24.4	29.7
CH_4 (vol%)	15.6	15.1	14.7	13.1	11.6	10.7	10.1	8.8	7.3	8.4	8.7
CO (vol%)	21.2	24.9	25.8	28.6	26.5	28.9	29.2	31.5	22.6	21.5	17.4
CO_2 (vol%)	30.5	30.4	29.2	28.3	30.1	29.6	29.3	27.0	35.8	34.2	32.2
C_XH_Y (vol%)	2.5	2.0	2.1	2.8	3.0	3.7	3.1	3.0	2.7	2.7	2.5
Non-detectable compounds (vol%)	8.7	7.2	8.7	8.3	12.3	11.4	12.9	15.2	8.4	8.8	9.5
HHV (MJ/kg)	13.8	13.6	13.5	13.3	16.2	13.7	13.3	12.8	17.4	17.7	18.2
Density (kg/m^3)	0.90	0.91	0.92	0.95	0.91	0.92	0.99	1.0	0.91	0.91	0.89

The trials with higher SS quantities in the reformer maximised the CO production for SB and OH syngas while the increment of SS fraction in the OH feed reduced the volume of the same gas. For this case, SS in the reforming unit could stimulate decarbonylation, decarboxylation and deoxygenation reactions increasing the amount of CO in the pyrolysis gas.

Carbon dioxide was the only component having the same effect (lower CO_2 concentration) when the percentage of SS was increased in the reformer and in the OH biomass. The production of CO_2 is related to the breaking of cellulose and hemicellulose by the thermal cracking of carbonyl and carboxyl compounds. SS did not contribute to intensify these kinds of reactions. Nevertheless, CO_2 yields were higher for SB runs compared to OH experiments when the SS was introduced in the reformer. This may be explained by the higher cellulose and hemicellulose content found in the SB feedstock (Table 3).

The best values of this set of experiments were achieved with the utilisation of SS in the OH. It is evident how the rise of SS in the feed could upgrade the TCR gas by favouring the chemical reactions mentioned before and raising the hydrogen yields and subsequently the HHV. The advantage of using SS in the biomass is the possibility of having a double catalytic effect. First in the pyrolysis auger reactor and then in the reforming unit. The same result was observed in the production of bio-oil where SS mixed in the feed could further improve the fuel properties of the liquid compared to the introduction of SS into the reformer.

SS pelletised with OH at 30 wt% revealed the highest H_2 and calorific value with 29.7 vol% and 18.2 MJ/kg respectively. Compared to the trial with the same parameters and no catalyst (Table 17) the SS created an increment of 80.0 and 12.3% for hydrogen

volume and HHV. The same experiment can show better results than the OH runs at higher pyrolysis and reforming temperatures. OH syngas at 450 and 500 °C (pyrolysis temperatures) presented a H_2 percentage of 15.8 and 23.1 vol% and a HHV of 15.3 and 17.3 MJ/kg respectively. In Table 9 OH at 600 °C (reforming temperature) obtained a syngas calorific value of 18.0 MJ/kg. SS proved its potential as a catalyst to improve the pyrolysis gas properties. Moreover, SS is a promising option to save energy by avoiding higher pyrolysis and reforming temperatures during the TCR experiments.

Table 26 shows the gas composition of different permanent gases from diverse biomasses, catalytic pyrolysis technologies and catalysts found in the literature review. The operating conditions are similar to this set of trials except in the selection of the catalyst. The use of mesoporous (Mo_2C/Al_2O_3 and Al-MCM-41), zeolites (HZY, MCM-22 and HZSM-5) and transition metals (nickel) is observed in Table 26.

All the SS experiments produced a pyrolytic gas richer in hydrogen when compared to the literature review. In fact, the difference is significant where Mahmood et al. (2013) was the work with higher H_2 value from Table 26 with 10.0 vol%. In his study, brewers grain was converted at 450 °C in a pyroformer reactor and the gases produced were upgraded in an external vessel at 500 °C using nickel as a catalyst. The same author obtained a similar methane percentage (9.0 vol%) than the runs with SS in the OH but lower than the experiments using SS in the reformer. SS generated a syngas composed of higher volumes of combustible gases resulting in a HHV more attractive for fuel applications.

Table 26 - Pyrolysis gas composition from catalytic pyrolysis found in the literature review

Pyrolsysis Type	Temperature (ºC)		Biomass	Catalyst	H_2	CH_4	CO	CO_2	C_xH_y	Ref.
	Reactor	Reformer			(vol%)	(vol%)	(vol%)	(vol%)	(vol%)	
In-situ Catalytic	500	-	SB	Mo_2C/Al_2O_3	0.69	3.7	36.3	33.4	25.8	1
In-situ Catalytic	500	-	Oat Straw	HZY	1.30	1.5	30.6	65.5	-	2
Ex-situ Catalytic	450	500	Brewers grain	Nickel	10.0	9.0	17.0	53.0	-	3
In-situ Catalytic	450	-	Rice husk	MCM-22	2.0	2.9	25.7	38.1	-	4
In-situ Catalytic	500	-	Wood	HZSM-5	0.29	0.45	6.5	14.4	0.70	5
In-situ Catalytic	500	-	Wood	Al-MCM-41	0.66	1.3	2.7	10.5	3.0	5
TCR	400	500	OH	Steel Slag	29.7	8.7	17.4	32.2	2.5	6

1 - (Patel et al., 2013); 2 - (Aqsha et al., 2017); 3 - (Mahmood et al., 2013); 4 - (Naqvi et al., 2015); 5 - (Ratnasari et al., 2018); 6 - Present work.

Concerning the CO concentration, Patel et al. (2013), Aqsha et al. (2017) and Naqvi et al. (2015) produced gas with 36.3, 30.6 and 25.7 vol% which is higher compared to the CO average of Table 25 (SS trials). The first two authors processed SB and oat straw at 500 °C via fluidized and fixed bed pyrolysis reactors using Mo_2C/Al_2O_3 and HZY catalysts respectively. The last researcher converted rice husk in a fixed bed reactor (450 °C) applying MCM-22 to upgrade the syngas.

Ratnasari et al. (2018) was the only work obtaining a pyrolysis gas with lower CO_2 volume than the average of SS runs. In their study wood was used as a feedstock in a fixed bed pyrolysis reactor working at 500 °C with two different catalysts (HZSM-5 and Al-MCM-41). For the first catalyst (HZSM-5) the CO_2 percentage was 14.4 vol%, whereas for the second (Al-MCM-41) was 10.5 vol%.

The syngas obtained from the experiment with the highest SS proportion in the OH (30 wt%) contains an interesting yield of hydrogen resulting in a reasonable heating value to be used as a fuel to produce heat and power. The properties of the gas might be improved applying higher pyrolysis and reforming temperatures than 400 and 500 °C, influencing the catalytic effect of SS.

4.4.4 Char Analysis

The ultimate analysis, ash and calorific value of biochar from SS runs are presented in Table 27. The pyrolysis char is mainly composed of fixed carbon and ash. Fixed carbon is the combustible element of the biochar and its presence helps to raise the heating value. On the other hand, ash is not beneficial in terms of energy decreasing the HHV of the char.

Table 27 - SB and OH biochar characterisation at different SS ratios (Pyrolysis and Reforming temperatures = 400 and 500 ºC)

	SB (SS in the reformer)			**OH (SS in the reformer)**			**OH (SS in the feed)**		
Steel Slag (wt%)	**30**	**70**	**100**	**30**	**70**	**100**	**10**	**20**	**30**
Ultimate analysis									
C (wt%)	75.3	74.6	73.9	79.3	75.3	75.2	56.9	47.6	43.1
H (wt%)	1.8	1.9	2.2	1.9	2.5	2.6	1.7	1.6	1.3
N (wt%)	1.0	0.52	0.54	1.2	1.6	1.3	0.87	0.70	0.52
S (wt%)	<0.10	<0.10	<0.10	<0.10	<0.10	<0.10	<0.10	<0.10	<0.10
O (wt%) (diff.)	5.1	6.5	8.2	5.6	3.2	6.2	1.8	1.8	2.6
Ash (wt%)	16.7	16.3	15.1	12.0	17.3	14.6	38.7	48.1	52.4
HHV (MJ/kg)	27.5	27.3	27.2	29.1	28.5	28.4	20.8	17.3	15.2

When the percentage of SS was increased in the TCR experiments the carbon content and the HHV decreased. This scenario occurred in both methods: during the introduction of SS in the reformer and the trials using SS mixed with OH. The aromatisation reactions were not favoured with the implementation of SS. As a consequence, the presence of aromatic rings was reduced thereby decreasing the C-C bonds and consequently the fixed carbon in the biochar. Additionally, the HHV of all biochars from SS trials were lower compared to the experiments without SS (Table 19) but with the same pyrolysis and reforming temperatures (400 and 500 °C). Zhang et al, (2018) mentioned that the utilisation of compounds rich in Ca and Mg in pyrolysis might decrease the quantity of aromatic rings in the char. The chemical composition of SS which contains 30.6% of calcium and 4.9% of magnesium can be observed in Table 4.

In this section the biochar with better energy density (29.3 MJ/kg) was formed when converting OH and using the lowest percentage of SS in the reforming unit (30 wt%). The carbon and ash contents of this experiment were also the highest and lowest of Table 27, with 79.8 and 12.0 wt% (respectively). As described before, biochar with high carbon and low ash content contains a better calorific value.

For the same SS fraction in the reformer OH biochars presented more carbon than SB chars resulting in higher energy value. Table 3 indicates the chemical composition of both biomasses where OH contains more fixed carbon and less ash contributing to a pyrolysis char more reasonable in terms of energy.

Concerning the OH experiments, a significant difference between the results from the application of SS in the feed and the OH experiments free of SS in the biomass (with and without SS in the reformer) is observed. For the first case (SS in the feed), the concentration of carbon in the biochar is much lower and the amount of ash is

considerably higher. As a result, the HHV of these trials decreased dramatically when compared to the OH runs free of SS in the feedstock. When pellets with OH and SS are pyrolysed the biochar produced also contains the inorganic material from the SS. This led to a reduction of the carbon value and an increment in the ash content of the biochar resulting in a lower HHV. To justify this argument, it can be observed in Table 27 a decrease of carbon and an increase of ash when SS ratio in the OH is increased.

Table 28 indicates the composition of several biochars from different feedstocks and catalytic pyrolysis technologies using diverse catalysts according to the literature review. The various works investigated presented similar pyrolysis temperatures compared to this section operating with SS. The catalysts used are part of different chemical groups, such as zeolites (HZY, HZSM-5, Ni/HZSM-5 and NiCe/HZSM-5), transition metals (CeO_2, Ni/CeO_2 and Ni/Al_2O_3) and minerals (dolomite and CaO).

The runs with SS in the reformer presented higher energy density than all the results found in Table 28. One of the explanations is the superior carbon percentage of experiments of the present work. In addition, the ash content was also lower than the values found in the literature review. The pyrolysis temperatures of the studies analyzed were slightly higher (500 and 550 °C). However, the reforming temperature of this section was also 500 °C despite of the pyrolysis temperature being lower (400 °C). The TCR technology permits the stimulation of cracking reactions resulting in a pyrolysis char with more carbon, less ash and better HHV.

Table 28 - Biochar characterization from catalytic pyrolysis found in the literature review

Pyrolysis Type	Temperature (ºC)		Biomass	Catalyst	C (wt%)	H (wt%)	N (wt%)	S (wt%)	O (wt%)	Ash (wt%)	HHV (MJ/kg)	Ref.
	Reactor	Reformer										
In-situ Catalytic	500	-	Oat straw	HZY	62.4	2.6	1.0	0.59	1.8	31.6	21.4	1
In-situ Catalytic	500	-	Sea plant	CeO_2	66.2	2.3	1.8	0.58	29.2	-	23.3	2
In-situ Catalytic	500	-	Sea plant	Ni/CeO_2	62.7	2.6	1.3	0.62	32.8	-	22.7	2
In-situ Catalytic	500	-	Sea plant	HZSM-5	64.0	2.6	2.0	0.62	30.8	-	23.3	2
In-situ Catalytic	500	-	Sea plant	Ni/HZSM-5	62.7	2.6	1.3	0.62	32.8	-	22.7	2
In-situ Catalytic	500	-	Sea plant	NiCe/HZSM-5	64.0	2.6	2.0	0.62	30.8	-	23.3	2
In-situ Catalytic	500	-	Sea plant	Ni/Al_2O_3	64.5	3.2	1.9	0.48	29.9	-	24.2	2
In-situ Catalytic	500	-	Sea plant	Dolomite	63.6	2.5	1.7	0.25	31.9	-	23.0	2
In-situ Catalytic	550	-	Fruit bunch	CaO	-	-	-	-	-	19.9	25.4	3
TCR	400	500	OH	Steel Slag	79.3	1.9	1.2	<0.10	5.6	12.0	29.1	4

1 - (Aqsha et al., 2017); 2 - (Maisano et al., 2017); 3 - (Thangalazhy-Gopakumar et al., 2018); 4 - Present work.

The conversion of SS with OH produced biochar with lower carbon value, higher ash content and worse HHV related to the results from Table 28. The reason for this occurrence was already explained before (biochar obtained contains high amounts of inorganic material from SS). Nevertheless, the experiments from the literature review did not mix the catalysts with the biomasses in the shape of pellets as was done in this set of tests.

Maisano et al. (2017) tested several catalysts in the conversion of sea plant using a fixed bed reactor at 500 °C. The application of different catalysts did not significantly affect the properties of the pyrolysis char. The carbon content was between 62.7 and 66.2 wt% and the HHV was between 22.7 and 24.2 MJ/kg. The same trend was also noticed among the several SB and OH runs applying SS in the reformer at different ratios. The chemical composition and the HHV of the SB and OH biochar did not suffer relevant modifications when the percentage of SS was increased in the reforming unit. For the SB experiments the carbon content of the char varied from 73.9 to 75.3 wt% while the HHV fluctuated between 27.2 and 27.5 MJ/kg. The OH tests presented a variation from 75.2 to 79.3 wt% in terms of carbon value and between 28.4 and 29.1 MJ/kg for the energy density.

The biochar produced using SS in the reformer demonstrated to have enough properties to generate heat and power through combustion in boilers, furnaces or gasifiers (ash content < 20 wt%; HHV > 24 MJ/kg) (Mullen et al., 2010). Additionally, the same char can also be utilised as fertiliser, activated carbon or soil amendment.

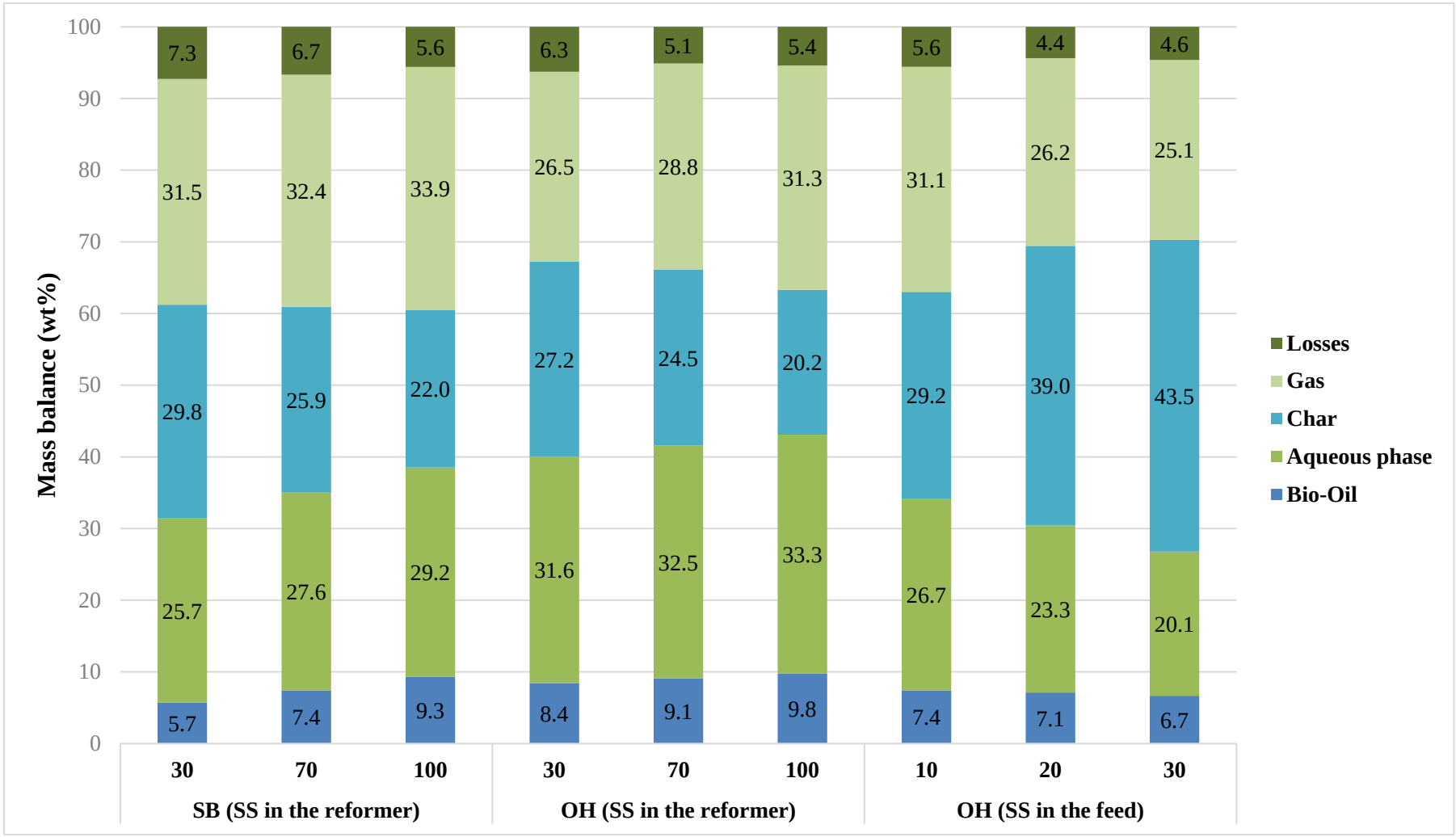


Figure 42 - Mass balance of SB and OH trials at different SS ratios (Pyrolysis and Reforming temperatures = 400 and 500 ºC)

4.4.5 Mass Balance and Energy Yield

Figures 42 and 43 show the mass balance and the energy yield of the SB and OH products at different SS ratios obtained during the TCR experiments.

The increment of SS in the reformer raised the yields of bio-oil and syngas in both feedstocks (OH and SB). Inversely, the production of SB and OH biochars decreased when the ratio of SS in the reforming unit was increased. Zhang et al. (2018) affirmed that calcium and magnesium compounds favour the formation of gas but inhibit the production of char. Additionally, Luo and Feng (2017) showed that iron can maximise the yields of bio-oil in the pyrolysis process. The three main elements of SS are Ca (30.6%), Fe (24.1%) and Mg (4.9%), and their effects during pyrolysis are in agreement with the values of Figure 42. In conclusion, SS can help to decompose cellulose and hemicellulose promoting depolymerisation and devolatilization reactions causing a higher production of bio-oil (Yang et al., 2007). At the same time SS might stimulate dehydrogenation, cracking, aromatisation and volatilization of heavier molecules optimising the formation of syngas (Henkel et al., 2016).

The mix of SS in OH biomass had the opposite effect to the previous paragraph (SS in the reformer). A decrease of the TCR bio-oil and syngas yields and an increase in the production of pyrolysis char is observed. When the percentage of SS is higher in the feedstock there is less organic matter to be converted during pyrolysis resulting in less bio-oil and syngas. The inorganic compounds from SS remain in the biochar when the pellets (OH mixed with SS) are pyrolyzed, explaining why higher fractions of SS in OH generate more pyrolysis char.

Figure 42 shows higher yields of biochar and syngas for SB runs covering all SS ratios in the reformer (30, 70 and 100 wt%). OH feedstock contains less lignin and more

moisture than SB (Table 3) yielding a mass balance with lower char and permanent gases. The presence of lignin promotes biochar production, whereas higher water content inhibits the formation of gas (Dasappa et al., 2004, Williams and Besler, 1996).

The best results for bio-oil and syngas were achieved when applying 100 wt% of SS in the reforming unit. The highest value of bio-oil was 9.8 wt% converting OH. The highest yield of syngas with 33.9 wt% was obtained when converting SB. The SB and OH experiments using 100 wt% of SS in the reformer presented higher bio-oil and syngas percentages compared to the trials at the same pyrolysis and reforming temperatures (400 and 500 °C) and without a catalyst. Once more the catalytic effect of SS attributed to its chemical composition caused superior yields of pyrolysis oil and permanent gases.

Overall, the mass losses of this set of experiments with SS were between 4.4 and 7.7 wt%. In the best scenario 95.6 wt% of the feedstock was converted into valuable products. These values are similar when compared to the previous sections where the pyrolysis and reforming temperatures of the TCR were changed. TCR technology demonstrated a high potential in terms of mass balance presenting very low losses which can be further minimised by improving the collection of the products and the accuracy of the weight measurements.

The pyrolysis char represented the biggest energy vector for all trials with SS. For the runs with SS in the reformer the main cause was the high calorific value of the biochar between 27.2-27.5 MJ/kg for SB and 28.4-29.1 MJ/kg for OH. In the same tests more syngas was produced but the HHV's were only between 13.3-13.6 MJ/kg (SB) and 12.8-13.7 MJ/kg (OH). Applying the lowest SS fraction in the reformer (30 wt%) resulted in the highest biochar energy yields with 50.0% for SB and 49.3% for OH experiments.

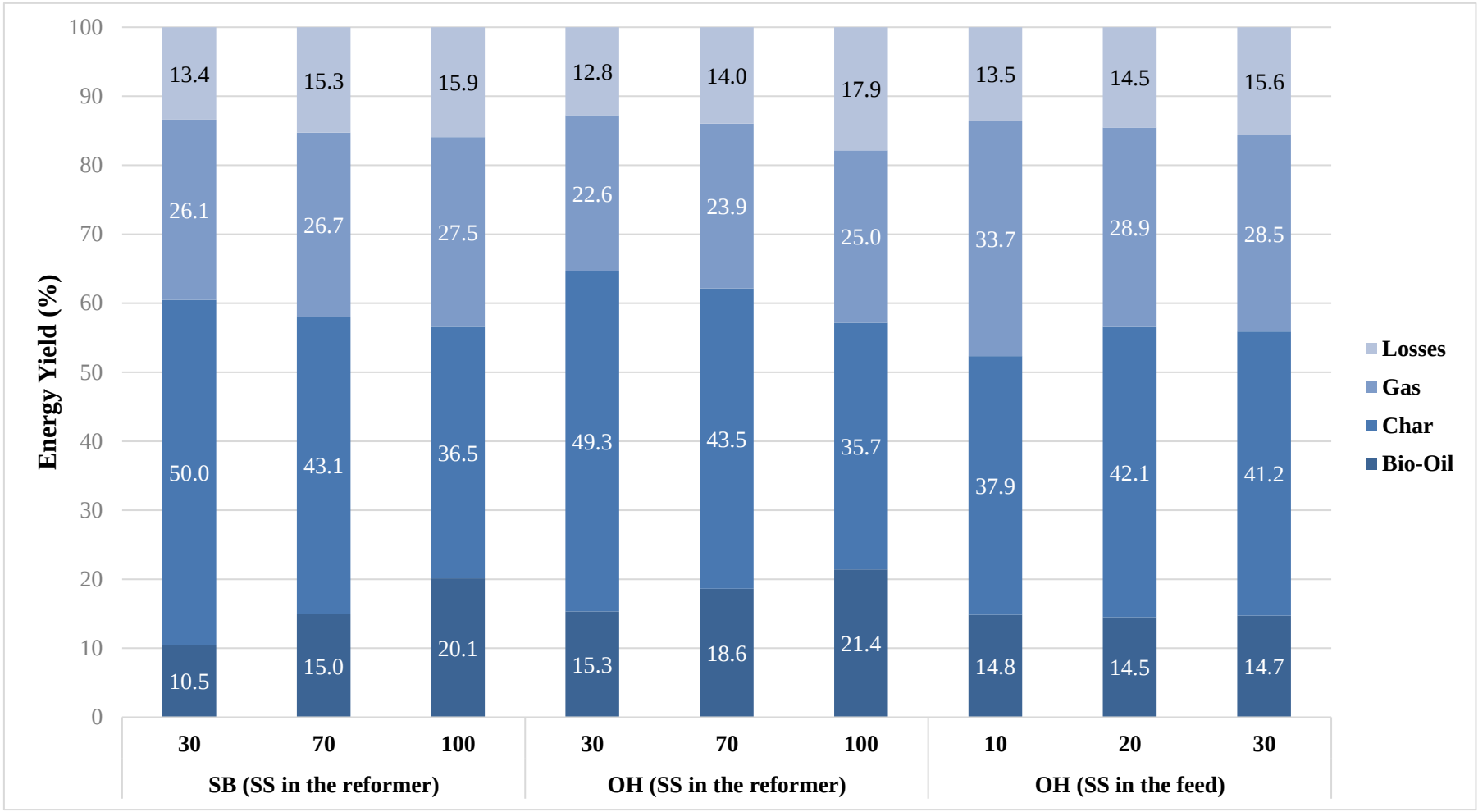


Figure 43 - Energy yield of SB and OH trials at different SS ratios (Pyrolysis and Reforming temperatures = 400 and 500 ºC)

Concerning the bio-oil, the best results were achieved using the highest ratio of SS in the reforming unit. (100 wt%). SB oil obtained 20.1% of the total energy and OH presented a value of 21.4%. The OH runs revealed better results than SB trials due to the higher volumes of bio-oil produced (Figure 42). In this situation the energy density of SB and OH bio-oil (Table 22) was quite similar not affecting the energy yields of Figure 43.

The experiments mixing SS with OH produced the pyrolysis gas with the highest energy yield from Figure 43. Despite these kinds of runs generating less gas than the experiments with SS in the reformer (Figure 42) there is a significant contrast between the respective HHV. The caloric values of SB and OH syngas using SS in the reformer were between 13.3-13.6 MJ/kg and between 12.8-13.7 MJ/kg respectively. However, the HHV of the gas fraction applying SS in the OH was between 17.4 and 18.2 MJ/kg attributed to higher hydrogen volume found in these trials.

It is clear that there was an increase in energy losses when the ratio of SS was raised. This effect occurred when implementing the catalyst in both methods and the losses were higher than the previous set of runs (different pyrolysis and reforming temperatures). For the first method (SS in the reformer) there was the increment of bio-oil and syngas yields according to the increase of SS proportion which never happened before. More oil produced leads to a higher waste of liquid in two different ways: 1) the amount of pyrolysis liquid remaining in the condensing unit is higher due to the difficulties in cleaning completely this sector of the TCR (Figure 22); 2) when bio-oil is separated through gravity some organic fraction is left in the aqueous phase to avoid the contamination of the bio-oil submitted to characterisation. More syngas produced means more escaping gases not detected by the gas totalizer. Considering these two observations

the energy wasted increases affecting the energy efficiency of the process as demonstrated in Figure 43.

The experiment with 30 wt% of SS in the reformer using OH was the most efficient of this section converting 87.2% of the energy from the feedstock into TCR products. The energy losses were between 12.8 and 17.9%, however, it may be possible to minimise them with better and more efficient isolation and scaling up the reactor.

4.4.6 Textural Properties

Biochars and SS upgraded the TCR bio-oil and syngas due to the catalytic properties of these materials. The influence of porosity, surface area and structure of these materials is studied by N_2 porosimetry and XRD characterisations.

The BET surface area, Barrett, Joyner, and Halenda (BJH) pore volume and average pore diameter of OH/SB (raw material and biochar) and SS are shown in Table 29. These parameters are relevant to determine the porosity of the materials evaluating their properties and quality for catalytic applications.

Figure 44 summarises the XRD of SS, SB raw, SB char, OH raw and OH char. XRD analysis is applied to identify the phase of a crystalline material providing information about the dimensions of the unit cell.

The SB and OH biochar utilised in these tests were formed at 400 °C (auger reactor) and 500 °C (post reformer), which are the same paraments performed in all SS trials in TCR. The objective is to create a fair comparison between the results obtained using biochar or SS at the same conditions.

The textural properties of SS raw, SB raw, OH raw, SB char and OH char is shown in Table 29. The comparison between the raw materials and the respective chars for both

biomasses indicated a reduction of the surface area and pore volume but an increase of the pore size. Zheng et al. (2008) reported that bigger particle diameter leads to lower surface area. The coke produced in pyrolysis through cracking is deposited and agglomerated in the pores and channels of the biochar decreasing the respective surface area (Srivastava et al., 2016, Wei et al., 2016).

Table 29 - Texture properties of SS, SB raw, SB char, OH raw and OH char

Samples	**S_{BET}[a] (m^2/g)**	**V_{Total}[b] (ml/g)**	**V_{micro}[c] (ml/g)**	**D_{pore}[d] (nm)**
SS	14.0	0.017	0.006	4.6
SB Raw	109.3	0.085	0.004	4.0
SB Char	73.7	0.055	0.003	5.3
OH Raw	80.4	0.054	0.032	4.0
OH Char	2.6	0.049	0.027	4.5

[a] Determined by BET method, [b] total pore volume at P/Po = 0.89, [c] t-plot method, [d] BJH method.

Lee et al. (2013) reported that the surface area of miscanthus, wood and SB biochars are less than 100 m^2/g when pyrolysed at 500 °C. The values presented in Table 29 for biochar are in agreement with the previous study. Additionally, the pore size of SB and OH biochars were 5.3 and 4.5 nm, respectively, which are considered small in terms of porosity (Abu El-Rub et al., 2004). This results in coke deposition in the pores keeping the surface area below than 100 m^2/g (Park et al., 2014).

The introduction of SS improved the bio-oil and syngas properties more in comparison with SB and OH biochars. It was observed a bio-oil with higher calorific value and lower water, acid number, viscosity and density. The same effect occurred with the syngas where SS runs revealed better H_2 yield and HHV. The physicochemical properties and the surface area of SS might promote deoxygenation, depolymerization, dehydration, hydrogenation, cracking and aromatization reactions improving its performance as a catalyst (Tan et al., 2013). The surface area of SB char was higher than SS which might be explained due to the increment of the pores of the biochar caused by pyrolysis resulting in a higher surface area (Wang et al., 2018). Carrier et al. (2011) reported an identical result using the same biomass (SB) where the pyrolysis process removed more volatile matter from SB char and this increased the volume of the pore and subsequently the surface area.

Regarding the XRD patterns (Figure 44), the peak detected at around 22° for SB and OH raw material is related to the crystalline area of cellulose existing in the feedstock (Paschoal et al., 2015, Yang et al., 2007). When the pyrolysis occurs producing the biochar, the cellulose is decomposed losing its crystalline nature (Weinstetn and Broido, 1970). For that reason, SB and OH chars do not have the same peak at 22°. Moreover, the disappearance of this peak means a higher aromaticity in pyrolysis char showing the decrement of the cellulose matter (Wang et al., 2018). The biomass is also made of hemicellulose and lignin, but their structures are amorphous and for that reason they are not reflected at XRD graphs.

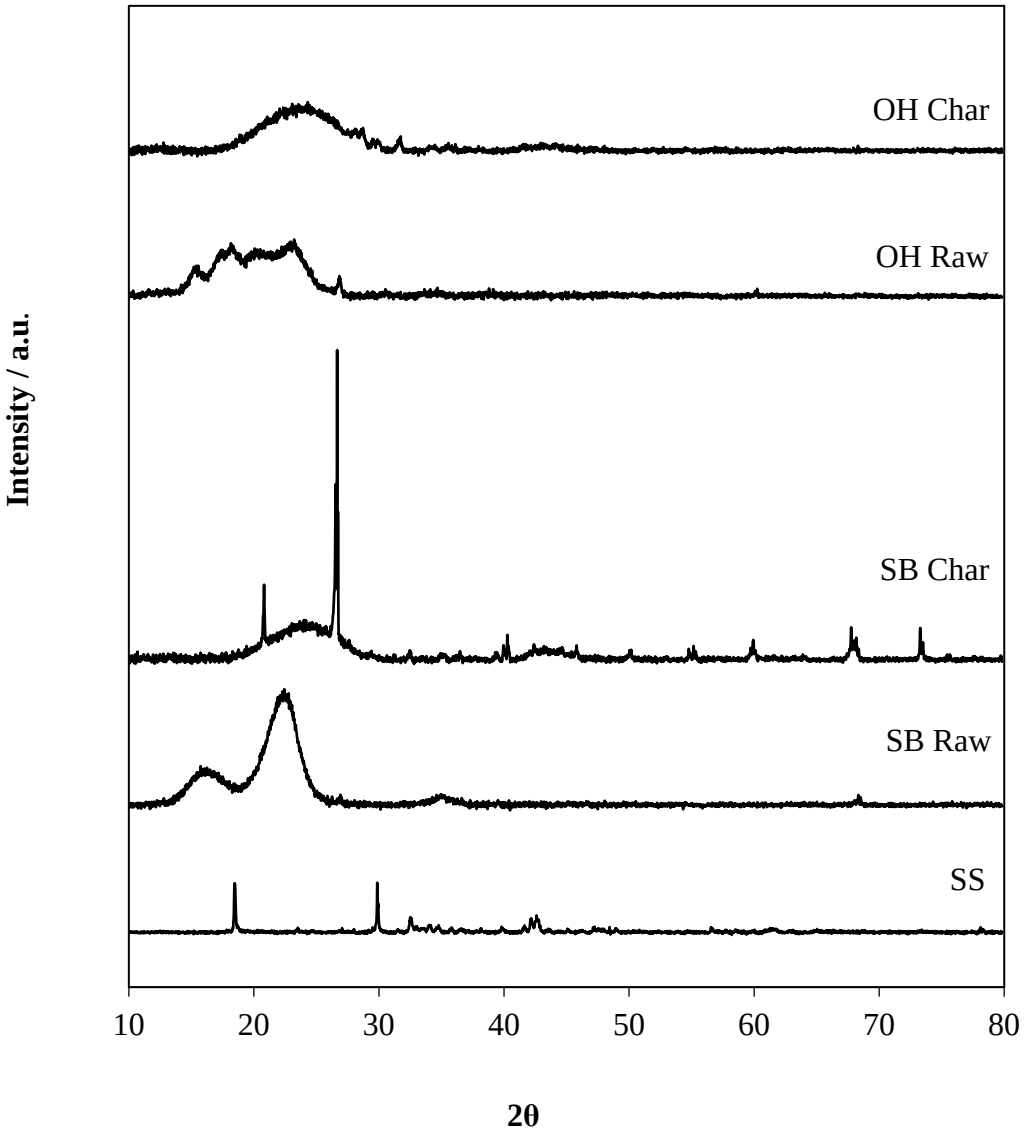


Figure 44 - X-ray diffractograms of SS, SB raw, SB char, OH raw and OH char

Relating SB and OH peaks (raw material and biochar), it is noticed from SB diffractograms more intense and wider peaks justified by the higher surface area (Table 29) and the size of the crystallites (Srivastava et al., 2016, Yang et al., 2004). The OH char presented a loss of crystalline structure when compared to SB char. In addition, the

existence of an amorphous area which might be caused by the deposit of coke over the surface of the OH char is observed (Maisano et al., 2017).

Similar X-ray diffractograms to SB raw and SB char were indicated in Varma and Mondal (2017) research, while Paschoal et al. (2015) presented an identical XRD pattern to OH raw material of Figure 44. SB char from Varma and Mondal (2017) study also indicated an intense and sharp peak at 27° which was associated to graphite. It was not found in the literature review any X-ray pattern related to OH biochar.

The XRD sample of SS displays four sharp peaks representing the big crystallite size and the relevant level of crystallinity of metal elements (Matthaiou et al., 2019). The first two peaks can be associated to $Ca(OH)_2$ at 18° and $Ca_2Fe_2O_5$ at 29°, and the peaks at 32 and 43° are representative of $Ca_3Mg(SiO_4)_2$ and $CaMg(CO_3)_2$ (Yildirim and Prezzi, 2015). In Figure 44 the presence of overlapped peaks which complicates the identification of the metals can be noted.

SS is mainly composed of calcium, iron and manganese (Table 4) which are part of the chemical composition of the peaks identified in the XRD graph. The interaction of Ca, Fe and Mg creates several active spots increasing the catalytic reactivity during pyrolysis (Baidya and Cattolica, 2015, Huang et al., 2012). As a result, the upgrading of the organic vapours is higher leading to better quality pyrolysis products as demonstrated in this section with the implementation of SS in the TCR process.

4.5 HDO of TCR bio-oil

During the HDO treatment, the TCR-2 bio-oil with the highest furfural yield from all experimental sections was submitted to four upgrading tests applying different parameters and catalysts (Table 30). The trial processing SB at 400 and 500 °C (pyrolysis

and reforming temperature, respectively) and using 100 wt% of SS in the reformer was the one selected according to the previous requirements. The HDO parameters and the selection of catalysts were based on the studies elaborated by Yang et al. (2014) and Zheng et al. (2008).

Table 30 - HDO conditions applying different temperatures and catalysts

Experimental Conditions	**HDO trial**
Catalysts (powder)	Cu-Zn/Al_2O_3 and Cu-Mn/SiO_2
Temperatures	280 and 380 ºC
Time	7 h
H_2 pressure	90 bar
Stirrer	400 rpm

4.5.1 GC-MS Analysis of Bio-oil

Table 31 displays the GC-MS results from the TCR oil after HDO upgrading (organic fraction) at different catalysts (Cu-based) and autoclave temperatures. In addition, the 24 most relevant and frequent peaks were analysed as shown in Figure 45.

At lower HDO temperatures the main compounds present in the bio-oil were aromatics and phenols. However, when the autoclave temperature was raised to 380 °C the pyrolysis oil was mainly composed of phenols and hydrocarbons (alkanes). With the increment of temperature the percentage of aromatics and phenols decreased, whereas the yields of alkanes increased. This effect occurred for both catalysts (CuZn-Al_2O_3 and CuMn-SiO_2), showing the impact of temperature on the HDO process in converting oxygenated and unsaturated elements into hydrocarbons (De, Saha et al. 2015). This can

be observed in Figure 45 where the chromatograms at higher temperatures (380 °C) presented peaks (between 20 and 24) related to hydrocarbons which cannot be identified in the GC-MS graphs at lower temperatures (280 °C). The GC-MS results from the previous sections (Tables 8, 16 and 24) did not indicate the presence of hydrocarbons in the bio-oil.

In terms of furans, the values varied between 0.24 and 1.5% and the presence of furfural or 2-furanmethanol was not detected in any HDO test. This may be attributed to the low quantities of these chemical compounds in the TCR bio-oil before upgrading or it may be a result of the HDO process which promotes dehydration, hydrogenation, hydrocracking, decarboxylation and hydrogenolysis reactions which may convert furans in other chemical elements (Pourzolfaghar, Abnisa et al. 2018).

Cheng et al. (2017) upgraded pine sawdust oil via HDO at 300 °C applying four different catalysts. The percentage of hydrocarbons were 15.6, 15.8, 16.6 and 25.3 for Co/SiO_2, Fe/SiO_2, $Fe\text{-}Co/SiO_2$ and Co/HZSM-5, respectively. Only the zeolite Co/HZSM-5 yielded a higher hydrocarbon result when compared to the bio-oil converted with $CuMn\text{-}SiO_2$ at 380 °C (18.6%), which had the highest yield of hydrocarbons within this study. Transition metals such as Cu and Mn might stimulate the production of hydrocarbons by converting aldehydes, phenols, esters and acids (Karnjanakom, Bayu et al. 2016). Additionally, the interaction between copper/manganese and silica supports (SiO_2) increases the selectivity and activity of the HDO process (Zheng, Zhu et al. 2008)

Table 31 - Compounds detected and identified by GC-MS of TCR bio-oil after HDO treatment

		Uncertainty = 2.3 - 2.7%	**$CuZn-Al_2O_3$**		**$CuMn-SiO_2$**	
		Temperature (ºC)	**280**	**380**	**280**	**380**
#	**Group**	**Chemical Compound**	**Conc. (%)**		**Conc. (%)**	
1	Aromatic	Benzene	2.3	0.39	2.3	0.35
2	Aromatic	Toluene	3.8	2.2	3.9	2.3
3	Alkane	Octane	-	0.65	-	0.72
-	-	Furfural	-	-	-	-
-	-	2-Furanmethanol	-	-	-	-
4	Aromatic	Ethylbenzene	1.5	2.8	1.6	2.4
5	Alkane	Nonane	-	0.63	-	0.91
6	Phenol	Phenol	6.9	3.2	7.0	3.2
7	Alkane	Indane	1.3	0.72	1.3	0.60
8	Phenol	Phenol, 2-methyl-	2.6	2.1	3.0	2.4
9	Phenol	Phenol, 3-methyl-	5.8	3.6	7.1	3.1
10	Alkane	Undecane	-	0.65	-	1.2
11	Phenol	Phenol, 2,4-dimethyl-	1.7	1.5	1.4	1.4
12	Phenol	Phenol, 4-ethyl-	8.8	4.6	8.9	3.2
13	Aromatic	Naphthalene	3.3	-	3.5	-
14	Alkane	Dodecane	-	1.4	-	1.6
15	Aromatic	Benzene, 1-ethyl-4-methoxy-	0.88	1.6	1.1	1.8
16	Alkane	Tridecane	-	0.66	-	1.3
17	Phenol	3-Methyl-4-isopropylphenol	-	1.7	-	1.7
18	Aromatic	Naphthalene, 1-methyl-	1.9	-	1.7	-
19	Aromatic	Naphthalene, 2-methyl-	1.0	-	0.81	-
20	Alkane	Tetradecane	-	1.2	0.36	1.4
21	Alkane	Pentadecane	0.29	1.3	0.15	2.2
22	Alkane	Hexadecane	-	2.6	-	2.7
23	Alkane	Heptadecane	-	1.3	-	3.2
24	Alkane	Octadecane	-	3.2	-	2.8

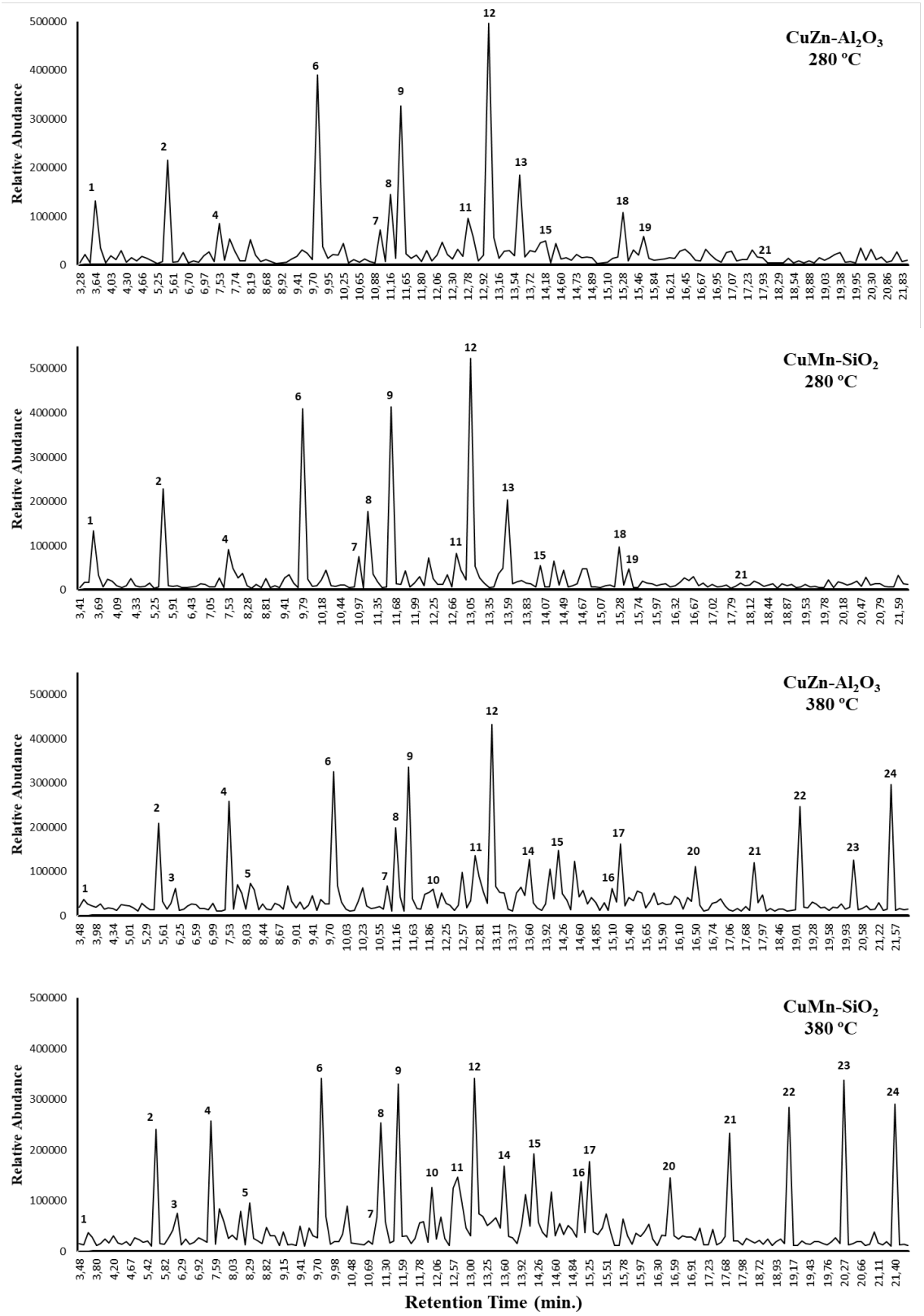


Figure 45 - GC-MS chromatograms of TCR bio-oil after HDO treatment

4.5.2 Bio-oil Analysis

Tables 32 and 33 show the chemical composition and fuel properties of TCR oil after HDO process and other bio-oils subject to the same upgrade treatment found in the literature review. The bio-oil selected was the one converted at 380 °C using CuMn-SiO_2 as a catalyst due to its higher hydrocarbon composition compared to the other HDO oils produced in this work.

The pyrolysis liquid presented in Table 32 obtained better results than all previous bio-oils (Tables 6, 14 and 22) with respect to the chemical composition and fuel properties. The carbon, hydrogen contents and calorific value were higher while the oxygen, water, TAN, viscosity and density were lower. Compared to the same bio-oil without upgrading, an increment of 11.3 and 16.6% for the carbon value and HHV respectively was observed. The oxygen, water, acid number, viscosity and density were reduced by 77.8, 70.2, 92.8, 75.3 and 5.8% respectively.

Cheng et al. (2017) and Yang et al. (2019) upgraded pine sawdust and rice stalk bio-oils via HDO at 300 and 370 °C using a H_2 pressure of 45 and 105 bar, respectively. Cheng et al. (2017) utilised Co/SiO_2, Fe/SiO_2, Fe-Co/SiO_2 and Co/HZSM-5 as a catalyst, while Yang et al. (2019) applied ZV-Al (zero-valent aluminium). Both studies obtained a bio-oil with more oxygen and less carbon, hydrogen and energy density than the present work. The water and acid number were also higher than the present work. In terms of viscosity, the values found in the literature review were significantly lower. However, a reasonable viscosity is positive for the prevention of internal leakages located in the fuel pump and line increasing the brake power and the lubricity. The different catalysts applied might be the key to explain the different results. The combination of Cu and Mn metals in SiO_2 supports improves the performance and selectivity of the catalysts increasing the

efficiency of the HDO treatment (Zheng et al., 2008). Moreover, the different temperatures and H_2 pressures utilised may also affect the results.

Table 32 - TCR bio-oil characterization after HDO treatment

Catalyst	$CuMn\text{-}SiO_2$
Temperature (°C)	380
Ultimate analysis	
C (wt%)	83.4
H (wt%)	10.7
N (wt%)	2.2
S (wt%)	0.87
O (wt%) (diff.)	3.0
Fuel Properties	
HHV (MJ/kg)	41.4
Ash (wt%)	<0.001
Water (wt%)	1.7
TAN (mg KOH/g)	1.2
Viscosity (mm^2/s)	6.3
Density (kg/m^3)	999

Table 33 - Bio-oil and fuels properties from HDO treatment found in the literature review

Pyrolysis Oil / Fuel	Autoclave Temperature (°C)	Catalyst	H_2 pressure (bar)	C (wt%)	H (wt%)	O (wt%)	HHV (MJ/kg)	Water (wt%)	TAN (mg KOH/g)	Viscosity (mm^2/s)	Ref.
Pine sawdust	300	Co/SiO_2	45	57.9	6.5	34.6	28.5	5.3	70.5	0.60	1
Pine sawdust	300	Fe/SiO_2	45	61.0	6.3	31.8	29.2	8.0	67.8	1.5	1
Pine sawdust	300	$Fe\text{-}Co/SiO_2$	45	62.4	6.6	30.2	29.1	4.9	84.2	0.25	1
Pine sawdust	300	Co/HZSM-5	45	62.4	6.6	30.2	29.8	3.6	107.4	0.18	1
Rice stalk	370	ZV-Al	105	80.4	8.7	7.0	38.5	3.0	11.5	-	2
SB	380	$CuMn\text{-}SiO_2$	90	83.4	10.7	3.0	41.4	1.7	1.2	6.3	3
Biodiesel	-	-	-	78.9	12.6	8.4	37-40	0.37	0.49	1.9-6.0	4
Diesel	-	-	-	84-87	13-16	1.0	42-45	0.05	0.03	1.9-5.5	5

1 - (Cheng et al., 2017); 2 - (Yang et al., 2019); 3 - Present work; 4 - EN 14214; 5 - EN 590.

After HDO treatment, the properties of TCR bio-oil indicated more attractive values than the biodiesel. In fact, the results obtained were very close to diesel showing the potential of this pyrolysis oil as fuel to be applied in engines. HDO process was crucial to cleave the C-O/C=O bonds (carbonyl group) of the oxygenates compounds and at the same time preserving the C-C/C=C bonds for the production of hydrocarbons (Ren et al., 2013, Xiong et al., 2016). This step was quite relevant to improve the oil properties for fuel applications, removing aromatics from the bio-oil and subsequently increasing the affinity between the temperature and viscosity (Isahak et al., 2012, Xiu and Shahbazi, 2012).

5. CONCLUSIONS AND FUTURE WORK

The objective of this chapter is to review and summarise the general conclusions and to discuss the experimental results obtained in terms of benefits, implications and limitations. In addition, recommendations for future work are also described in this section.

In this research TCR technology was proposed to convert lignocellulosic biomass into a better quality bio-oil containing furans with a special focus of the precursors to 2-MF (furfural and 2-furanmethanol). Overall, the main goals of this work were accomplished by the following points:

a) The ideal lignocellulosic biomass was identified and selected according to its chemical composition in terms of hemicellulose and xylose percentages. Subsequently, it was characterised to understand its thermal degradation effect and also the chemical elements produced during the pyrolysis.
b) The TCR process was tested by changing the pyrolysis and reforming temperatures to establish the optimal parameters to produce the bio-oil closest to the requirements mentioned before.
c) SS was used as a catalyst in the TCR to improve the quality of the bio-oil and the yields of furans present in the pyrolysis liquid.
d) TCR bio-oil was upgraded through HDO using Cu based catalysts. It was the final step to optimise the properties of the oil as an engine fuel.
e) All TCR products (bio-oil, syngas and biochar) were submitted to chemical and physical analysis to understand how their properties were modified with the application of different temperatures, feedstocks and SS ratios.

SB and OH biomasses demonstrated to have a good calorific value making these residues valuable for biofuel production through thermochemical technologies. The ash content was low for both feedstocks which is an advantage for bio-oil production via intermediate pyrolysis. The moisture found in SB and OH was enough for pelletisation respecting the standards of the TCR technology to optimise the quality and the properties of the products. For that reason, drying was not requested which allowed the saving of energy. In terms of lignocellulosic composition, the level of hemicellulose indicated a reasonable source of furfural and xylose components.

The increment of reforming temperature had a substantial effect on the properties of the TCR products changing its chemical composition, quality and quantity. For the bio-oil, the amount of carbon produced increased while the oxygen decreased thus improving the calorific value. The fuel properties of the pyrolysis liquid were improved with the reduction of the water, acid number, viscosity and density. Furfural and 2-furanmethanol production (2.4 and 1.2%, respectively) were favoured at the lowest reforming temperature (500 °C). Higher reforming temperatures resulted in higher hydrogen yields and better HHV. The biochar also improved its quality in terms of carbon, oxygen and energy density when the reforming temperature was increased. The only exception was the trial using OH at 700 °C. In terms of products distribution, lower reforming temperatures stimulated the formation of bio-oil and biochar while syngas production was more intense at higher reforming temperatures.

Increasing the pyrolysis temperature also reduced the oxygen value of the bio-oil and raised its carbon content and HHV. The water, TAN, viscosity and density were also improved (lower readings) with the increment of the pyrolysis temperature. Applying the

lowest pyrolysis temperature (400 °C) indicated the highest percentages of furfural and 2-furanmethanol in the pyrolysis liquid (2.5 and 1.3%, respectively). Concerning the syngas and the biochar, the results fluctuated and a trend was not found with the increment of the pyrolysis temperature. For the mass balance, the increase of pyrolysis temperature had the same effect than the rise in reforming temperature (more syngas and less bio-oil and char). Relating the TCR bio-oil and syngas, the increase of reforming temperatures showed better results than the increase of temperature in the pyrolysis reactor. The utilisation of biochar in the reformer at higher temperatures may have helped to upgrade the organic vapours improving the HHV and the fuel properties of the bio-oil and syngas. It is evident that the increase from 500 to 700 ºC in the reforming unit led to other chemical reactions, resulting in more variability in the quality, quantity and distribution of the TCR products.

The introduction of SS in the TCR experiments increased the carbon value and energy density of the bio-oil by 18.1% and 22.0%, respectively. Additionally, the oxygen, water, TAN, viscosity and density were reduced by 50.9, 55.1, 65.7, 46.6 and 4.8% respectively. The use of SS in the reformer demonstrated to be a better option to maximise the quantity of furans in the pyrolysis liquid, having better furfural and 2-furanmethanol yields than the runs at the same conditions but without a catalyst. Regarding the pyrolysis gas, SS created an increment of 80.0 and 12.3% for hydrogen volume and HHV respectively. It was possible to produce more bio-oil and syngas with the introduction of SS in the reformer. Generally, the best results were achieved using the highest SS proportions (100 wt% in the reformer and 30 wt% in the feedstock). However, mixing SS with biomass was found to be more efficient in upgrading the bio-oil and syngas than introducing SS in the reformer. The presence of SS in the feedstock might have a double

catalytic effect in the pyrolysis reactor and in the reforming unit further improving the fuel properties of the products. On the other hand, the implementation of SS in the reformer only upgrades the organic vapours in this stage of the experiment and not since the beginning as mentioned before. The use of SS in the TCR process originated better results for the bio-oil and syngas than some runs at higher pyrolysis temperatures (450 and 500 °C) and higher reforming temperatures (600 and 700 °C). SS proved its potential as a catalyst to improve the TCR products properties. Moreover, SS is a promising option to save energy by avoiding higher pyrolysis and reforming temperatures during the TCR experiments.

After HDO treatment, the TCR bio-oil showed better properties than the biodiesel. In fact, the results obtained were very close to diesel showing the potential of this pyrolysis oil for fuel applications in engines.

Despite the present project not producing a bio-oil rich in furans it is extremely important to highlight the findings of this research. SS could significantly improve the quality and the properties of the TCR bio-oil and syngas revealing an innovate pathway and perspective for biofuel production via catalytic conversion of biomass. SS is a solid and effective catalyst which is a waste from the steel industry making it a very economical option.

TCR technology presented a high efficiency in terms of mass balance and energy yield. In all trials, the biomass conversion into valuable products was higher than 92 wt%. For the energy yield, it was possible to observe some runs converting 98.3 and 99.7% of the total energy from the feedstocks into the chemical energy of the products. The energy losses were not higher than 12% except in the experiments with SS. The existence of SS

in the feedstock means less organic matter to be converted during pyrolysis, resulting in less bio-oil and syngas and consequently higher energy losses. Other mass and energy losses can be explained by errors during the weight measurements, escaping gases not detected by the gas totalizer and the bio-oil left in the condensing unit after each run which may not be detectable during cleaning. Additionally, during the separation of the organic and aqueous phase of the pyrolysis liquid some organic oil is left in the aqueous phase to avoid the contamination of the bio-oil submitted to characterisation. Adding these technical issues, it is normal to waste some mass and energy content affecting the mass and energy yield of the process. The mass and energy wastes can be also reduced with better and efficient isolation and by increasing the scale of the reactor.

TCR oil from SB and OH indicated some positive aspects to be applied as fuel for engines when compared to other pyrolysis technologies found in the literature review. However, some of the physical and chemical properties may affect the performance and the lifetime of the engine contrasting with the utilisation of the biodiesel and diesel as a transportation fuel. This only changed when the pyrolysis liquid was submitted to a HDO upgrading treatment. Nevertheless, TCR oil demonstrated sufficient quality to be burned in CHP engines, boilers, combustors or similar applications.

The pyrolytic gas produced in the TCR assays contains a reasonable amount of combustible gases (H_2, CO, CH_4 and other hydrocarbon gases) and HHV to be used as an energy vector. One of the applications could be the generation of heat and power through CHP units or burnt as a fuel onsite to meet the energy demands of the industrial plant.

TCR biochar contains a reasonable HHV which can be used for combustion in furnaces, gasifiers and boilers to generate heat and power. The same char has other

promising applications such as soil amendment, carbon sequestration, fertiliser and activated carbon. Another application of the char is the catalytic conversion, which is related to its surface properties and inorganic composition.

For future work it would be interesting to pre-treat the biomass to extract the lignin and inorganic content which are responsible for reducing the organic yields. This would improve the quality and quantity of the pyrolysis oil avoiding the production of high molecular weight polyphenols.

An increase in the number of repetitions for the analytical work and the TCR experiments is also recommended. More data improves the accuracy of the results making them more representative for statistical analysis. This would minimise the experimental error obtaining more realistic data to be used in scale-up for industrial plants.

The conversion of mixed biomasses (co-pyrolysis) should be tested to benefit the chemical properties of the feedstock increasing the quality of the products.

To apply the same conditions in larger reactors to understand how the scale-up can influence the results and how the process can be optimised in an industrial scenario.

Expanding the research borders to explore the value and the applicability of the TCR products (bio-oil, syngas and biochar) as an energy vector (for instance, CHP units).

The pyrolysis oil is composed of high molecular weight compounds which is hard to be detected through GC-MS analysis. To solve for this limitation, HPLC could be used to determine the presence of these heavy chemical elements.

Different TCR configurations could also be investigated such as solid residence times, heating rates, screw speeds and duration of the runs. The properties of the gas and

bio-oil could be improved applying higher pyrolysis and reforming temperatures than 400 and 500 °C, influencing the catalytic effect of SS.

The characterization of the HDO catalysts and a longer time in the HDO runs are also suggested to understand better how the properties of these materials could improve the quality of the TCR oil.

A techno-economic study for furans production would be interesting to understand the applicability and viability of this chemical compound in the current context.

REFERENCES

ABEDI, A. & DALAI, A. K. 2017. Study on the quality of oat hull fuel pellets using bio-additives. *Biomass & Bioenergy,* 106**,** 166-175.

ABU EL-RUB, Z., BRAMER, E. A. & BREM, G. 2004. Review of Catalysts for Tar Elimination in Biomass Gasification Processes. *Industrial & Engineering Chemistry Research,* 43**,** 6911-6919.

ADAM, J., ANTONAKOU, E., LAPPAS, A., STÖCKER, M., NILSEN, M. H., BOUZGA, A., HUSTAD, J. E. & ØYE, G. 2006. In situ catalytic upgrading of biomass derived fast pyrolysis vapours in a fixed bed reactor using mesoporous materials. *Microporous and Mesoporous Materials,* 96**,** 93-101.

AHMAD, E., JAGER, N., APFELBACHER, A., DASCHNER, R., HORNUNG, A. & PANT, K. K. 2018. Integrated thermo-catalytic reforming of residual sugarcane bagasse in a laboratory scale reactor. *Fuel Processing Technology,* 171**,** 277-286.

AHMAD, M., RAJAPAKSHA, A. U., LIM, J. E., ZHANG, M., BOLAN, N., MOHAN, D., VITHANAGE, M., LEE, S. S. & OK, Y. S. 2014. Biochar as a sorbent for contaminant management in soil and water: A review. *Chemosphere,* 99**,** 19-33.

AKHTAR, J. & SAIDINA AMIN, N. 2012. A review on operating parameters for optimum liquid oil yield in biomass pyrolysis. *Renewable and Sustainable Energy Reviews,* 16**,** 5101-5109.

AL ARNI, S. 2018. Comparison of slow and fast pyrolysis for converting biomass into fuel. *Renewable Energy,* 124**,** 197-201.

ANTAL, M. J. & GRONLI, M. 2003. The art, science, and technology of charcoal production. *Industrial & Engineering Chemistry Research,* 42**,** 1619-1640.

AQSHA, A., TIJANI, M. M., MOGHTADERI, B. & MAHINPEY, N. 2017. Catalytic pyrolysis of straw biomasses (wheat, flax, oat and barley) and the comparison of their product yields. *Journal of Analytical and Applied Pyrolysis,* 125**,** 201-208.

AZIZ, A. A. & DERAMAN, M. 2013. Pore Structure of Carbon Granules Prepared from Slow Pyrolysis of Oil Palm Empty Fruit Bunch Fibres. *Journal of Oil Palm Research,* 25**,** 216-227.

BALAT, M. 2011. An Overview of the Properties and Applications of Biomass Pyrolysis Oils. *Energy Sources, Part A: Recovery, Utilization, and Environmental Effects,* 33**,** 674-689.

BATIDZIRAI, B., MIGNOT, A. P. R., SCHAKEL, W. B., JUNGINGER, H. M. & FAAIJ, A. P. C. 2013. Biomass torrefaction technology: Techno-economic status and future prospects. *Energy,* 62**,** 196-214.

BLANCO, A. & CHEJNE, F. 2016. Modeling and simulation of biomass fast pyrolysis in a fluidized bed reactor. *Journal of Analytical and Applied Pyrolysis,* 118**,** 105-114.

BÖRJESSON, P. 2009. Good or bad bioethanol from a greenhouse gas perspective – What determines this? *Applied Energy,* 86**,** 589-594.

BOUSSARSAR, H., ROGE, B. & MATHLOUTHI, M. 2009. Optimization of sugarcane bagasse conversion by hydrothermal treatment for the recovery of xylose. *Bioresource Technology,* 100**,** 6537-6542.

BRIDGWATER, A. V. 2012. Review of fast pyrolysis of biomass and product upgrading. *Biomass and Bioenergy,* 38**,** 68-94.

CARLSON, T. R., JAE, J., LIN, Y.-C., TOMPSETT, G. A. & HUBER, G. W. 2010. Catalytic fast pyrolysis of glucose with HZSM-5: The combined homogeneous and heterogeneous reactions. *Journal of Catalysis,* 270**,** 110-124.

CARRIER, M., HUGO, T., GORGENS, J. & KNOETZE, H. 2011. Comparison of slow and vacuum pyrolysis of sugar cane bagasse. *Journal of Analytical and Applied Pyrolysis,* 90**,** 18-26.

CHANDEL, A. K., ANTUNES, F. A. F., FREITAS, W. L. C. & DA SILVA, S. S. 2013. Sequential Acid-Base Pretreatment of Sugarcane Bagasse: A Facile Method for the Sugars Recovery After Enzymatic Hydrolysis. *Journal of Bioprocess Engineering and Biorefinery,* 2**,** 11-19.

CHAREONLIMKUN, A., CHAMPREDA, V., SHOTIPRUK, A. & LAOSIRIPOJANA, N. 2010. Catalytic conversion of sugarcane bagasse, rice husk and corncob in the presence of TiO2, ZrO2 and mixed-oxide TiO2–ZrO2 under hot compressed water (HCW) condition. *Bioresource Technology,* 101**,** 4179-4186.

CHARUSIRI, W. & NUMCHAROENPINIJ, N. 2017. Characterization of the optimal catalytic pyrolysis conditions for bio-oil production from brown salwood (Acacia mangium Willd) residues. *Biomass and Bioenergy,* 106**,** 127-136.

CHAUHAN, M. K., VARUN, CHAUDHARY, S., KUMAR, S. & SAMAR 2011. Life cycle assessment of sugar industry: A review. *Renewable and Sustainable Energy Reviews,* 15**,** 3445-3453.

CHEN, W., YANG, H., CHEN, Y., CHEN, X., FANG, Y. & CHEN, H. 2016. Biomass pyrolysis for nitrogen-containing liquid chemicals and nitrogen-doped carbon materials. *Journal of Analytical and Applied Pyrolysis,* 120**,** 186-193.

CHENG, S. Y., WEI, L., JULSON, J. & RABNAWAZ, M. 2017. Upgrading pyrolysis bio-oil through hydrodeoxygenation (HDO) using non-sulfided Fe-Co/SiO2 catalyst. *Energy Conversion and Management,* 150**,** 331-342.

CHIA, M. & DUMESIC, J. A. 2011. Liquid-phase catalytic transfer hydrogenation and cyclization of levulinic acid and its esters to gamma-valerolactone over metal oxide catalysts. *Chemical Communications,* 47**,** 12233-12235.

CHIARAMONTI, D., BONINI, M., FRATINI, E., TONDI, G., GARTNER, K., BRIDGWATER, A. V., GRIMM, H. P., SOLDAINI, I., WEBSTER, A. & BAGLIONI, P. 2003. Development of emulsions from biomass pyrolysis liquid and diesel and their use in engines—Part 2: tests in diesel engines. *Biomass and Bioenergy,* 25**,** 101-111.

COLLARD, F.-X. & BLIN, J. 2014. A review on pyrolysis of biomass constituents: Mechanisms and composition of the products obtained from the conversion of cellulose, hemicelluloses and lignin. *Renewable and Sustainable Energy Reviews,* 38**,** 594-608.

CONG, H., MAŠEK, O., ZHAO, L., YAO, Z., MENG, H., HU, E. & MA, T. 2018. Slow Pyrolysis Performance and Energy Balance of Corn Stover in Continuous Pyrolysis-Based Poly-Generation Systems. *Energy & Fuels,* 32**,** 3743-3750.

CONTI, R., JÄGER, N., NEUMANN, J., APFELBACHER, A., DASCHNER, R. & HORNUNG, A.

CROMBIE, K. & MAŠEK, O. 2014. Investigating the potential for a self-sustaining slow pyrolysis system under varying operating conditions. *Bioresource Technology*, 162**,** 148-156.

CZERNIK, S. & BRIDGWATER, A. V. 2004. Overview of Applications of Biomass Fast Pyrolysis Oil. *Energy & Fuels,* 18**,** 590-598.

DANON, B., MARCOTULLIO, G. & DE JONG, W. 2014. Mechanistic and kinetic aspects of pentose dehydration towards furfural in aqueous media employing homogeneous catalysis. *Green Chemistry,* 16**,** 39-54.

DASAPPA, S., PAUL, P. J., MUKUNDA, H. S., RAJAN, N. K. S., SRIDHAR, G. & SRIDHAR, H. V. 2004. Biomass gasification technology - a route to meet energy needs. *Current Science,* 87**,** 908-916.

DE LA HOZ, A., DIAZ-ORTIZ, A. & MORENO, A. 2005. Microwaves in organic synthesis. Thermal and non-thermal microwave effects. *Chemical Society Reviews,* 34**,** 164-178.

DE, S., SAHA, B. & LUQUE, R. 2015. Hydrodeoxygenation processes: Advances on catalytic transformations of biomass-derived platform chemicals into hydrocarbon fuels. *Bioresource Technology,* 178**,** 108-118.

DHYANI, V. & BHASKAR, T. 2018. A comprehensive review on the pyrolysis of lignocellulosic biomass. *Renewable Energy,* 129**,** 695-716.

DIAS, A. S., PILLINGER, M. & VALENTE, A. A. 2005. Dehydration of xylose into furfural over micro-mesoporous sulfonic acid catalysts. *Journal of Catalysis,* 229**,** 414-423.

DICKERSON, T. & SORIA, J. 2013. Catalytic Fast Pyrolysis: A Review. *Energies,* 6**,** 514-538.

DILCIO ROCHA, J., LUENGO, C. A. & SNAPE, C. E. 1999. The scope for generating bio-oils with relatively low oxygen contents via hydropyrolysis. *Organic Geochemistry,* 30**,** 1527-1534.

DONG, F., ZHU, Y. L., ZHENG, H. Y., ZHU, Y. F., LI, X. Q. & LI, Y. W. 2015. Cr-free Cu-catalysts for the selective hydrogenation of biomass-derived furfural to 2-methylfuran: The synergistic effect of metal and acid sites. *Journal of Molecular Catalysis a-Chemical,* 398**,** 140-148.

DOUMER, M. E., ARÍZAGA, G. G. C., SILVA, D. A. D., YAMAMOTO, C. I., NOVOTNY, E. H., SANTOS, J. M., SANTOS, L. O. D., WISNIEWSKI, A., ANDRADE, J. B. D. & MANGRICH, A. S. 2015. Slow pyrolysis of different Brazilian waste biomasses as sources of soil conditioners and energy, and for environmental protection. *Journal of Analytical and Applied Pyrolysis,* 113**,** 434-443.

DUAN, P. & SAVAGE, P. E. 2011. Catalytic hydrotreatment of crude algal bio-oil in supercritical water. *Applied Catalysis B: Environmental,* 104**,** 136-143.

DUMAN, G., PALA, M., UCAR, S. & YANIK, J. 2013. Two-step pyrolysis of safflower oil cake. *Journal of Analytical and Applied Pyrolysis,* 103**,** 352-361.

ENGTRAKUL, C., MUKARAKATE, C., STARACE, A. K., MAGRINI, K. A., ROGERS, A. K. & YUNG, M. M. 2016. Effect of ZSM-5 acidity on aromatic product selectivity during upgrading of pine pyrolysis vapors. *Catalysis Today,* 269**,** 175-181.

FAHMI, R., BRIDGWATER, A. V., DONNISON, I., YATES, N. & JONES, J. M. 2008. The effect of lignin and inorganic species in biomass on pyrolysis oil yields, quality and stability. *Fuel,* 87**,** 1230-1240.

FAN, L. L., ZHANG, Y. N., LIU, S. Y., ZHOU, N., CHEN, P., CHENG, Y. L., ADDY, M., LU, Q., OMAR, M. M., LIU, Y. H., WANG, Y. P., DAI, L. L., ANDERSON, E., PENG, P., LEI, H. W. & RUAN, R. 2017. Bio-oil from fast pyrolysis of lignin:

Effects of process and upgrading parameters. *Bioresource Technology,* 241**,** 1118-1126.

FOSTER, A. J., JAE, J., CHENG, Y.-T., HUBER, G. W. & LOBO, R. F. 2012. Optimizing the aromatic yield and distribution from catalytic fast pyrolysis of biomass over ZSM-5. *Applied Catalysis A: General,* 423-424**,** 154-161.

FRENCH, R. & CZERNIK, S. 2010. Catalytic pyrolysis of biomass for biofuels production. *Fuel Processing Technology,* 91**,** 25-32.

GANDARIAS, I., REQUIES, J., ARIAS, P. L., ARMBRUSTER, U. & MARTIN, A. 2012. Liquid-phase glycerol hydrogenolysis by formic acid over Ni-Cu/Al2O3 catalysts. *Journal of Catalysis,* 290**,** 79-89.

GARCÌA-PÉREZ, M., CHAALA, A., PAKDEL, H., KRETSCHMER, D., RODRIGUE, D. & ROY, C. 2006. Multiphase Structure of Bio-oils. *Energy & Fuels,* 20**,** 364-375.

GHOLIZADEH, M., GUNAWAN, R., HU, X., DE MIGUEL MERCADER, F., WESTERHOF, R., CHAITWAT, W., HASAN, M. M., MOURANT, D. & LI, C.-Z. 2016. Effects of temperature on the hydrotreatment behaviour of pyrolysis bio-oil and coke formation in a continuous hydrotreatment reactor. *Fuel Processing Technology,* 148**,** 175-183.

GOYAL, H. B., SEAL, D. & SAXENA, R. C. 2008. Bio-fuels from thermochemical conversion of renewable resources: A review. *Renewable & Sustainable Energy Reviews,* 12**,** 504-517.

GREENHALF, C. E., NOWAKOWSKI, D. J., HARMS, A. B., TITILOYE, J. O. & BRIDGWATER, A. V. 2012. Sequential pyrolysis of willow SRC at low and high heating rates - Implications for selective pyrolysis. *Fuel,* 93**,** 692-702.

GREENHALF, C. E., NOWAKOWSKI, D. J., HARMS, A. B., TITILOYE, J. O. & BRIDGWATER, A. V. 2013. A comparative study of straw, perennial grasses and hardwoods in terms of fast pyrolysis products. *Fuel,* 108**,** 216-230.

GUOXIN, H., HAO, H. & YANHONG, L. 2009. Hydrogen-Rich Gas Production from Pyrolysis of Biomass in an Autogenerated Steam Atmosphere. *Energy & Fuels,* 23**,** 1748-1753.

GUST, S. 1997. Combustion Experiences of Flash Pyrolysis Fuel in Intermediate Size Boilers. *In:* BRIDGWATER, A. V. & BOOCOCK, D. G. B. (eds.) *Developments in Thermochemical Biomass Conversion: Volume 1 / Volume 2.* Dordrecht: Springer Netherlands.

HAGNER, M., TIILIKKALA, K., LINDQVIST, I., NIEMELÄ, K., WIKBERG, H., KÄLLI, A., RASA, K. J. W. & VALORIZATION, B. 2018. Performance of Liquids from Slow Pyrolysis and Hydrothermal Carbonization in Plant Protection.

HASAN, M. D. M., WANG, X. S., MOURANT, D., GUNAWAN, R., YU, C., HU, X., KADARWATI, S., GHOLIZADEH, M., WU, H., LI, B., ZHANG, L. & LI, C.-Z. 2017. Grinding pyrolysis of Mallee wood: Effects of pyrolysis conditions on the yields of bio-oil and biochar. *Fuel Processing Technology,* 167**,** 215-220.

HE, M., XIAO, B., LIU, S., HU, Z., GUO, X., LUO, S. & YANG, F. 2010. Syngas production from pyrolysis of municipal solid waste (MSW) with dolomite as downstream catalysts. *Journal of Analytical and Applied Pyrolysis,* 87**,** 181-187.

HE, R., YE, X. P., ENGLISH, B. C. & SATRIO, J. A. 2009. Influence of pyrolysis condition on switchgrass bio-oil yield and physicochemical properties. *Bioresource Technology,* 100**,** 5305-5311.

HENKEL, C., MULEY, P. D., ABDOLLAHI, K. K., MARCULESCU, C. & BOLDOR, D. 2016. Pyrolysis of energy cane bagasse and invasive Chinese tallow tree (Triadica sebifera L.) biomass in an inductively heated reactor. *Energy Conversion and Management,* 109**,** 175-183.

HOOD-NOWOTNY, R., WATZINGER, A., WAWRA, A. & SOJA, G. 2018. The Impact of Biochar Incorporation on Inorganic Nitrogen Fertilizer Plant Uptake; An Opportunity for Carbon Sequestration in Temperate Agriculture. *Geosciences*, 8.

HORNUNG, A. 2013. Intermediate pyrolysis of biomass. *Biomass Combustion Science, Technology and Engineering***,** 172-186.

HORNUNG, A. 2014. Transformation of Biomass Theory to Practice Preface. *Transformation of Biomass: Theory to Practice***,** Xvii-Xviii.

HORNUNG, A., APFELBACHER, A. & SAGI, S. 2011. Intermediate pyrolysis: A sustainable biomass-to-energy concept - Biothermal valorisation of biomass (BtVB) process. *Journal of Scientific & Industrial Research,* 70**,** 664-667.

HOSSAIN, A. K., OUADI, M., SIDDIQUI, S. U., YANG, Y., BRAMMER, J., HORNUNG, A., KAY, M. & DAVIES, P. A. 2013. Experimental investigation of performance, emission and combustion characteristics of an indirect injection multi-cylinder CI engine fuelled by blends of de-inking sludge pyrolysis oil with biodiesel. *Fuel,* 105**,** 135-142.

HU, X. & GHOLIZADEH, M. 2019. Biomass pyrolysis: A review of the process development and challenges from initial researches up to the commercialisation stage. *Journal of Energy Chemistry,* 39**,** 109-143.

HUANG, B.-S., CHEN, H.-Y., CHUANG, K.-H., YANG, R.-X. & WEY, M.-Y. 2012. Hydrogen production by biomass gasification in a fluidized-bed reactor promoted by an Fe/CaO catalyst. *International Journal of Hydrogen Energy,* 37**,** 6511-6518.

HUBER, G. W., IBORRA, S. & CORMA, A. 2006. Synthesis of transportation fuels from biomass: Chemistry, catalysts, and engineering. *Chemical Reviews,* 106**,** 4044-4098.

IKURA, M., STANCIULESCU, M. & HOGAN, E. 2003. Emulsification of pyrolysis derived bio-oil in diesel fuel. *Biomass and Bioenergy,* 24**,** 221-232.

ILIOPOULOU, E. F., ANTONAKOU, E. V., KARAKOULIA, S. A., VASALOS, I. A., LAPPAS, A. A. & TRIANTAFYLLIDIS, K. S. 2007. Catalytic conversion of biomass pyrolysis products by mesoporous materials: Effect of steam stability and acidity of Al-MCM-41 catalysts. *Chemical Engineering Journal,* 134**,** 51-57.

ISAHAK, W. N. R. W., HISHAM, M. W. M., YARMO, M. A. & YUN HIN, T.-Y. 2012. A review on bio-oil production from biomass by using pyrolysis method. *Renewable and Sustainable Energy Reviews,* 16**,** 5910-5923.

ISLAM, M. R., PARVEEN, M. & HANIU, H. 2010. Properties of sugarcane waste-derived bio-oils obtained by fixed-bed fire-tube heating pyrolysis. *Bioresource Technology,* 101**,** 4162-4168.

JAE, J., TOMPSETT, G. A., FOSTER, A. J., HAMMOND, K. D., AUERBACH, S. M., LOBO, R. F. & HUBER, G. W. 2011. Investigation into the shape selectivity of zeolite catalysts for biomass conversion. *Journal of Catalysis,* 279**,** 257-268.

JAE, J., ZHENG, W. Q., LOBO, R. F. & VLACHOS, D. G. 2013. Production of Dimethylfuran from Hydroxymethylfurfural through Catalytic Transfer

Hydrogenation with Ruthenium Supported on Carbon. *Chemsuschem,* 6**,** 1158-1162.

JAGER, N., CONTI, R., NEUMANN, J., APFELBACHER, A., DASCHNER, R., BINDER, S. & HORNUNG, A. 2016. Thermo-Catalytic Reforming of Woody Biomass. *Energy & Fuels,* 30**,** 7923-7929.

JAIN, A., WEI, Y. Z. & TIETJE, A. 2016. Biochemical conversion of sugarcane bagasse into bioproducts. *Biomass & Bioenergy,* 93**,** 227-242.

KABE, T., ISHIHARA, A., QIAN, E. W., SUTRISNA, I. P. & KABE, Y. 2004. Coal and coal-related compounds - Structures, reactivity and catalytic reactions. *Coal and Coal-Related Compounds: Structures, Reactivity and Catalytic Reactions,* 150**,** Ix-+.

KALLIOINEN, A., VAARI, A., RÄTTÖ, M., KONN, J., SIIKA-AHO, M. & VIIKARI, L. 2003. Effects of bacterial treatments on wood extractives. *Journal of Biotechnology,* 103**,** 67-76.

KAN, T., STREZOV, V. & EVANS, T. J. 2016. Lignocellulosic biomass pyrolysis: A review of product properties and effects of pyrolysis parameters. *Renewable & Sustainable Energy Reviews,* 57**,** 1126-1140.

KARNJANAKOM, S., BAYU, A., XIAOKETI, P., HAO, X. G., KONGPARAKUL, S., SAMART, C., ABUDULA, A. & GUAN, G. Q. 2016. Selective production of aromatic hydrocarbons from catalytic pyrolysis of biomass over Cu or Fe loaded mesoporous rod-like alumina. *Rsc Advances,* 6**,** 50618-50629.

KEBELMANN, K., HORNUNG, A., KARSTEN, U. & GRIFFITHS, G. 2013. Thermo-chemical behaviour and chemical product formation from Polar seaweeds during

intermediate pyrolysis. *Journal of Analytical and Applied Pyrolysis,* 104**,** 131-138.

KIRBY, M. E., HORNUNG, A., OUADI, M. & THEODOROU, M. K. 2017. The role of thermo-catalytic reforming for energy recovery from food and drink supply chain wastes. *Energy Procedia,* 123**,** 15-21.

LAIRD, D. A. 2008. The charcoal vision: A win-win-win scenario for simultaneously producing bioenergy, permanently sequestering carbon, while improving soil and water quality. *Agronomy Journal,* 100**,** 178-181.

LANGE, J. P., VAN DER HEIDE, E., VAN BUIJTENEN, J. & PRICE, R. 2012. FurfuralυA Promising Platform for Lignocellulosic Biofuels. *Chemsuschem,* 5**,** 150-166.

LAPPAS, A. A., KALOGIANNIS, K. G., ILIOPOULOU, E. F., TRIANTAFYLLIDIS, K. S. & STEFANIDIS, S. D. 2016. Catalytic Pyrolysis of Biomass for Transportation Fuels. *Advances in Bioenergy: The Sustainability Challenge***,** 45-56.

LAWFORD, H. G., ROUSSEAU, J. D. & TOLAN, J. S. 2001. Comparative ethanol productivities of different Zymomonas recombinants fermenting oat hull hydrolysate. *Applied Biochemistry and Biotechnology,* 91-3**,** 133-146.

LEDE, J., DIEBOLD, J. P., PEACOCKE, G. V. C. & PISKORZ, J. 1997. The Nature and Properties of Intermediate and Unvaporized Biomass Pyrolysis Materials. *In:* BRIDGWATER, A. V. & BOOCOCK, D. G. B. (eds.) *Developments in Thermochemical Biomass Conversion: Volume 1 / Volume 2*. Dordrecht: Springer Netherlands.

LEE, J., KIM, Y. T. & HUBER, G. W. 2014. Aqueous-phase hydrogenation and hydrodeoxygenation of biomass-derived oxygenates with bimetallic catalysts. *Green Chemistry*, 16**,** 708-718.

LEE, Y., PARK, J., RYU, C., GANG, K. S., YANG, W., PARK, Y.-K., JUNG, J. & HYUN, S. 2013. Comparison of biochar properties from biomass residues produced by slow pyrolysis at 500°C. *Bioresource Technology,* 148**,** 196-201.

LEHMANN, J., GAUNT, J. & RONDON, M. 2006. Bio-char Sequestration in Terrestrial Ecosystems – A Review. *Mitigation and Adaptation Strategies for Global Change,* 11**,** 403-427.

LEHTO, J., OASMAA, A., SOLANTAUSTA, Y., KYTÖ, M. & CHIARAMONTI, D. 2014. Review of fuel oil quality and combustion of fast pyrolysis bio-oils from lignocellulosic biomass. *Applied Energy,* 116**,** 178-190.

LI, H., XU, Q., XUE, H. & YAN, Y. 2009. Catalytic reforming of the aqueous phase derived from fast-pyrolysis of biomass. *Renewable Energy*, 34**,** 2872-2877.

LI, J., LI, X., ZHOU, G., WANG, W., WANG, C., KOMARNENI, S. & WANG, Y. 2014. Catalytic fast pyrolysis of biomass with mesoporous ZSM-5 zeolites prepared by desilication with NaOH solutions. *Applied Catalysis A: General,* 470**,** 115-122.

LICHTENTHALER, F. W. & PETERS, S. 2004. Carbohydrates as green raw materials for the chemical industry. *Comptes Rendus Chimie,* 7**,** 65-90.

LUO, S. Y. & FENG, Y. 2016. The production of hydrogen-rich gas by wet sludge pyrolysis using waste heat from blast-furnace slag. *Energy*, 113**,** 845-851.

LUO, S. Y. & FENG, Y. 2017. The production of fuel oil and combustible gas by catalytic pyrolysis of waste tire using waste heat of blast-furnace slag. *Energy Conversion and Management,* 136**,** 27-35.

MAHMOOD, A. S. N., BRAMMER, J. G., HORNUNG, A., STEELE, A. & POULSTON, S. 2013. The intermediate pyrolysis and catalytic steam reforming of Brewers spent grain. *Journal of Analytical and Applied Pyrolysis,* 103**,** 328-342.

MAISANO, S., URBANI, F., MONDELLO, N. & CHIODO, V. 2017. Catalytic pyrolysis of Mediterranean sea plant for bio-oil production. *International Journal of Hydrogen Energy,* 42**,** 28082-28092.

MANTE, O. D., DAYTON, D. C., CARPENTER, J. R., WANG, K. & PETERS, J. E. 2018. Pilot-scale catalytic fast pyrolysis of loblolly pine over γ-Al2O3 catalyst. *Fuel,* 214**,** 569-579.

MANTE, O. D., RODRIGUEZ, J. A., SENANAYAKE, S. D. & BABU, S. P. 2015. Catalytic conversion of biomass pyrolysis vapors into hydrocarbon fuel precursors. *Green Chemistry,* 17**,** 2362-2368.

MARYANA, R., OKTAVIANI, K., TANIFUJI, K. & OHI, H. 2014. Comparison between acid sulfite and soda-AQ delignification methods for effective bio-ethanol production from sugarcane bagasse and oil palm empty fruit bunch. *2014 Pan Pac. Conf. TAPPI; May 28; Taiwan***,** E46-E52.

MATTHAIOU, V., OULEGO, P., FRONTISTIS, Z., COLLADO, S., HELA, D., KONSTANTINOU, I. K., DIAZ, M. & MANTZAVINOS, D. 2019. Valorization of steel slag towards a Fenton-like catalyst for the degradation of paraben by activated persulfate. *Chemical Engineering Journal,* 360**,** 728-739.

MAYER, Z. A., APFELBACHER, A. & HORNUNG, A. 2012. A comparative study on the pyrolysis of metal- and ash-enriched wood and the combustion properties of the gained char. *Journal of Analytical and Applied Pyrolysis,* 96**,** 196-202.

MCDONNELL, K., WARD, S., LEAHY, J. J. & MCNULTY, P. 1999. Properties of rapeseed oil for use as a diesel fuel extender. *Journal of the American Oil Chemists Society,* 76**,** 539-543.

MCKENDRY, P. 2002. Energy production from biomass (part 1): overview of biomass. *Bioresource Technology,* 83**,** 37-46.

MENDES, F. L., XIMENES, V. L., DE ALMEIDA, M. B. B., AZEVEDO, D. A., TESSAROLO, N. S. & DE REZENDE PINHO, A. 2016. Catalytic pyrolysis of sugarcane bagasse and pinewood in a pilot scale unit. *Journal of Analytical and Applied Pyrolysis,* 122**,** 395-404.

MESA-PÉREZ, J. M., ROCHA, J. D., BARBOSA-CORTEZ, L. A., PENEDO-MEDINA, M., LUENGO, C. A. & CASCAROSA, E. 2013. Fast oxidative pyrolysis of sugar cane straw in a fluidized bed reactor. *Applied Thermal Engineering,* 56**,** 167-175.

MILNE, T., AGBLEVOR, F., DAVIS, M., DEUTCH, S. & JOHNSON, D. 1997. A Review of the Chemical Composition of Fast-Pyrolysis Oils from Biomass. *In:* BRIDGWATER, A. V. & BOOCOCK, D. G. B. (eds.) *Developments in Thermochemical Biomass Conversion: Volume 1 / Volume 2*. Dordrecht: Springer Netherlands.

MOHAN, D., SARSWAT, A., OK, Y. S. & PITTMAN, C. U. 2014. Organic and inorganic contaminants removal from water with biochar, a renewable, low cost

and sustainable adsorbent - A critical review. *Bioresource Technology,* 160**,** 191-202.

MOLLINEDO, J., SCHUMACHER, T. E. & CHINTALA, R. 2015. Influence of feedstocks and pyrolysis on biochar's capacity to modify soil water retention characteristics. *Journal of Analytical and Applied Pyrolysis,* 114**,** 100-108.

MONTANE, D., SALVADO, J., TORRAS, C. & FARRIOL, X. 2002. High-temperature dilute-acid hydrolysis of olive stones for furfural production. *Biomass & Bioenergy,* 22**,** 295-304.

MOREIRA, R., ORSINI, R. D., VAZ, J. M., PENTEADO, J. C. & SPINACE, E. V. 2017. Production of Biochar, Bio-Oil and Synthesis Gas from Cashew Nut Shell by Slow Pyrolysis. *Waste and Biomass Valorization,* 8**,** 217-224.

MORF, P., HASLER, P. & NUSSBAUMER, T. 2002. Mechanisms and kinetics of homogeneous secondary reactions of tar from continuous pyrolysis of wood chips. *Fuel,* 81**,** 843-853.

MOUD, P. H., KANTARELIS, E., ANDERSSON, K. J. & ENGVALL, K. 2018. Biomass pyrolysis gas conditioning over an iron-based catalyst for mild deoxygenation and hydrogen production. *Fuel,* 211**,** 149-158.

MULLEN, C. A., BOATENG, A. A., GOLDBERG, N. M., LIMA, I. M., LAIRD, D. A. & HICKS, K. B. 2010. Bio-oil and bio-char production from corn cobs and stover by fast pyrolysis. *Biomass & Bioenergy,* 34**,** 67-74.

MURADOV, N. 2017. Low to near-zero CO2 production of hydrogen from fossil fuels: Status and perspectives. *International Journal of Hydrogen Energy,* 42**,** 14058-14088.

NAKAGAWA, Y., TAMURA, M. & TOMISHIGE, K. 2013. Catalytic Reduction of Biomass-Derived Furanic Compounds with Hydrogen. *ACS Catalysis,* 3**,** 2655-2668.

NAQVI, S. R., UEMURA, Y., YUSUP, S., SUGIURA, Y. & NISHIYAMA, N. 2015. In situ catalytic fast pyrolysis of paddy husk pyrolysis vapors over MCM-22 and ITQ-2 zeolites. *Journal of Analytical and Applied Pyrolysis,* 114**,** 32-39.

NEUMANN, J., BINDER, S., APFELBACHER, A., GASSON, J. R., RAMÍREZ GARCÍA, P. & HORNUNG, A. 2015. Production and characterization of a new quality pyrolysis oil, char and syngas from digestate – Introducing the thermo-catalytic reforming process. *Journal of Analytical and Applied Pyrolysis,* 113**,** 137-142.

NEUMANN, J., JAGER, N., APFELBACHER, A., DASCHNER, R., BINDER, S. & HORNUNG, A. 2016a. Upgraded biofuel from residue biomass by Thermo-Catalytic Reforming and hydrodeoxygenation. *Biomass & Bioenergy,* 89**,** 91-97.

NEUMANN, J., MEYER, J., OUADI, M., APFELBACHER, A., BINDER, S. & HORNUNG, A. 2016b. The conversion of anaerobic digestion waste into biofuels via a novel Thermo-Catalytic Reforming process. *Waste Management,* 47**,** 141-148.

NGUYEN, T. S., ZABETI, M., LEFFERTS, L., BREM, G. & SESHAN, K. 2013. Catalytic upgrading of biomass pyrolysis vapours using faujasite zeolite catalysts. *Biomass and Bioenergy,* 48**,** 100-110.

NOKKOSMÄKI, M. I., KUOPPALA, E. T., LEPPÄMÄKI, E. A. & KRAUSE, A. O. I. 2000. Catalytic conversion of biomass pyrolysis vapours with zinc oxide. *Journal of Analytical and Applied Pyrolysis,* 55**,** 119-131.

OASMAA, A., KUOPPALA, E. & SOLANTAUSTA, Y. 2003. Fast pyrolysis of forestry residue. 2. Physicochemical composition of product liquid. *Energy & Fuels,* 17**,** 433-443.

ORDOMSKY, V. V., SCHOUTEN, J. C., VAN DER SCHAAF, J. & NIJHUIS, T. A. 2013. Biphasic single-reactor process for dehydration of xylose and hydrogenation of produced furfural. *Applied Catalysis a-General,* 451**,** 6-13.

OUADI, M., BRAMMER, J. G., YANG, Y., HORNUNG, A. & KAY, M. 2013. The intermediate pyrolysis of de-inking sludge to produce a sustainable liquid fuel. *Journal of Analytical and Applied Pyrolysis,* 102**,** 24-32.

OUADI, M., GREENHALF, C., JAEGER, N., SPERANZA, L. G. & HORNUNG, A. 2018. Thermo-catalytic reforming of co-form (R) rejects (waste cleansing wipes). *Journal of Analytical and Applied Pyrolysis,* 132**,** 33-39.

OUADI, M., JAEGER, N., GREENHALF, C., SANTOS, J., CONTI, R. & HORNUNG, A. 2017. Thermo-Catalytic Reforming of municipal solid waste. *Waste Management,* 68**,** 198-206.

OUADI, M., KAY, M., BRAMMER, J. & HORNUNG, A. 2012. Waste to power. *Tappi Journal,* 11**,** 55-64.

PAN, P., HU, C., YANG, W., LI, Y., DONG, L., ZHU, L., TONG, D., QING, R. & FAN, Y. 2010. The direct pyrolysis and catalytic pyrolysis of Nannochloropsis sp. residue for renewable bio-oils. *Bioresource Technology,* 101**,** 4593-4599.

PANAGIOTOPOULOU, P. & VLACHOS, D. G. 2014. Liquid phase catalytic transfer hydrogenation of furfural over a Ru/C catalyst. *Applied Catalysis a-General,* 480**,** 17-24.

PARK, J., LEE, Y., RYU, C. & PARK, Y. K. 2014. Slow pyrolysis of rice straw: Analysis of products properties, carbon and energy yields. *Bioresource Technology,* 155**,** 63-70.

PARK, Y. K., YOO, M. L., HEO, H. S., LEE, H. W., PARK, S. H., JUNG, S. C., PARK, S. S. & SEO, S. G. 2012. Wild reed of Suncheon Bay: Potential bio-energy source. *Renewable Energy,* 42**,** 168-172.

PASCHOAL, G. B., MULLER, C. M. O., CARVALHO, G. M., TISCHER, C. A. & MALI, S. 2015. ISOLATION AND CHARACTERIZATION OF NANOFIBRILLATED CELLULOSE FROM OAT HULLS. *Química Nova,* 38**,** 478-482.

PATEL, M. A., BALDANZA, M. A. S., TEIXEIRA DA SILVA, V. & BRIDGWATER, A. V. 2013. In situ catalytic upgrading of bio-oil using supported molybdenum carbide. *Applied Catalysis A: General,* 458**,** 48-54.

PATTIYA, A. 2018. 1 - Fast pyrolysis. *In:* ROSENDAHL, L. (ed.) *Direct Thermochemical Liquefaction for Energy Applications.* Woodhead Publishing.

PATTIYA, A., SUKKASI, S. & GOODWIN, V. 2012. Fast pyrolysis of sugarcane and cassava residues in a free-fall reactor. *Energy,* 44**,** 1067-1077.

PATTIYA, A. & SUTTIBAK, S. 2017. Fast pyrolysis of sugarcane residues in a fluidised bed reactor with a hot vapour filter. *Journal of the Energy Institute,* 90**,** 110-119.

POURZOLFAGHAR, H., ABNISA, F., DAUD, W. M. A. W. & AROUA, M. K. 2018. Atmospheric hydrodeoxygenation of bio-oil oxygenated model compounds: A review. *Journal of Analytical and Applied Pyrolysis,* 133**,** 117-127.

PRINS, M. J., PTASINSKI, K. J. & JANSSEN, F. J. J. G. 2006. Torrefaction of wood: Part 1. Weight loss kinetics. *Journal of Analytical and Applied Pyrolysis,* 77**,** 28-34.

QAZANFARZADEH, Z. & KADIVAR, M. 2016. Properties of whey protein isolate nanocomposite films reinforced with nanocellulose isolated from oat husk. *International Journal of Biological Macromolecules,* 91**,** 1134-1140.

QI, X. H., WATANABE, M., AIDA, T. M. & SMITH, R. L. 2008. Catalytic dehydration of fructose into 5-hydroxymethylfurfural by ion-exchange resin in mixed-aqueous system by microwave heating. *Green Chemistry,* 10**,** 799-805.

RAMOS, L. P., DA SILVA, L., BALLEM, A. C., PITARELO, A. P., CHIARELLO, L. M. & SILVEIRA, M. H. L. 2015. Enzymatic hydrolysis of steam-exploded sugarcane bagasse using high total solids and low enzyme loadings. *Bioresource Technology,* 175**,** 195-202.

RATHMANN, R., SZKLO, A. & SCHAEFFER, R. 2010. Land use competition for production of food and liquid biofuels: An analysis of the arguments in the current debate. *Renewable Energy,* 35**,** 14-22.

REN, H., YU, W. T., SALCICCIOLI, M., CHEN, Y., HUANG, Y. L., XIONG, K., VLACHOS, D. G. & CHEN, J. G. G. 2013. Selective Hydrodeoxygenation of Biomass-Derived Oxygenates to Unsaturated Hydrocarbons using Molybdenum Carbide Catalysts. *Chemsuschem,* 6**,** 798-801.

ROCHA, G. J. D., NASCIMENTO, V. M., GONCALVES, A. R., SILVA, V. F. N. & MARTIN, C. 2015. Influence of mixed sugarcane bagasse samples evaluated by elemental and physical-chemical composition. *Industrial Crops and Products,* 64**,** 52-58.

ROMAN-LESHKOV, Y., BARRETT, C. J., LIU, Z. Y. & DUMESIC, J. A. 2007. Production of dimethylfuran for liquid fuels from biomass-derived carbohydrates. *Nature,* 447**,** 982-U5.

ROUT, T., PRADHAN, D., SINGH, R. K. & KUMARI, N. 2016. Exhaustive study of products obtained from coconut shell pyrolysis. *Journal of Environmental Chemical Engineering,* 4**,** 3696-3705.

ROY, C., PAKDEL, H. & BROUILLARD, D. 1990. The Role of Extractives during Vacuum Pyrolysis of Wood. *Journal of Applied Polymer Science,* 41**,** 337-348.

SAKO, T., SUGETA, T., NAKAZAWA, N., OTAKE, K., SATO, M., ISHIHARA, K. & KATO, M. 1995. High-Pressure Vapor-Liquid and Vapor-Liquid-Liquid Equilibria for Systems Containing Supercritical Carbon-Dioxide, Water and Furfural. *Fluid Phase Equilibria,* 108**,** 293-303.

SANTOS, J., OUADI, M., JAHANGIRI, H. & HORNUNG, A. 2019. Integrated intermediate catalytic pyrolysis of wheat husk. *Food and Bioproducts Processing,* 114**,** 23-30.

SCHLEICHER, T., WERKMEISTER, R., RUSS, W. & MEYER-PITTROFF, R. 2009. Microbiological stability of biodiesel–diesel-mixtures. *Bioresource Technology,* 100**,** 724-730.

SCOTT, D. S., PATERSON, L., PISKORZ, J. & RADLEIN, D. 2001. Pretreatment of poplar wood for fast pyrolysis: rate of cation removal. *Journal of Analytical and Applied Pyrolysis,* 57**,** 169-176.

SHAFIZADEH, F. & LAI, Y. Z. 1972. Thermal-Degradation of 1,6-Anhydro-Beta-D-Glucopyranose. *Journal of Organic Chemistry,* 37**,** 278-+.

SHEN, J., WANG, X.-S., GARCIA-PEREZ, M., MOURANT, D., RHODES, M. J. & LI, C.-Z. 2009. Effects of particle size on the fast pyrolysis of oil mallee woody biomass. *Fuel,* 88**,** 1810-1817.

SITTHISA, S. & RESASCO, D. E. 2011. Hydrodeoxygenation of Furfural Over Supported Metal Catalysts: A Comparative Study of Cu, Pd and Ni. *Catalysis Letters,* 141**,** 784-791.

SKIBA, E. A., BUDAEVA, V. V., BAIBAKOVA, O. V., ZOLOTUKHIN, V. N. & SAKOVICH, G. V. 2017. Dilute nitric-acid pretreatment of oat hulls for ethanol production. *Biochemical Engineering Journal,* 126**,** 118-125.

SPOKAS, K. A., CANTRELL, K. B., NOVAK, J. M., ARCHER, D. W., IPPOLITO, J. A., COLLINS, H. P., BOATENG, A. A., LIMA, I. M., LAMB, M. C., MCALOON, A. J., LENTZ, R. D. & NICHOLS, K. A. 2012. Biochar: A Synthesis of Its Agronomic Impact beyond Carbon Sequestration. *Journal of Environmental Quality,* 41**,** 973-989.

SRIVASTAVA, S., JADEJA, G. C. & PARIKH, J. 2016. A versatile bi-metallic copper-cobalt catalyst for liquid phase hydrogenation of furfural to 2-methylfuran. *RSC Advances,* 6**,** 1649-1658.

STAMATOV, V., HONNERY, D. & SORIA, J. 2006. Combustion properties of slow pyrolysis bio-oil produced from indigenous Australian species. *Renewable Energy,* 31**,** 2108-2121.

STEFANIDIS, S. D., KALOGIANNIS, K. G., ILIOPOULOU, E. F., MICHAILOF, C. M., PILAVACHI, P. A. & LAPPAS, A. A. 2014. A study of lignocellulosic biomass pyrolysis via the pyrolysis of cellulose, hemicellulose and lignin. *Journal of Analytical and Applied Pyrolysis,* 105**,** 143-150.

STEPHANIDIS, S., NITSOS, C., KALOGIANNIS, K., ILIOPOULOU, E. F., LAPPAS, A. A. & TRIANTAFYLLIDIS, K. S. 2011. Catalytic upgrading of lignocellulosic biomass pyrolysis vapours: Effect of hydrothermal pre-treatment of biomass. *Catalysis Today,* 167**,** 37-45.

SUN, Y. Q., SEETHARAMAN, S. & ZHANG, Z. T. 2018. Integrating biomass pyrolysis with waste heat recovery from hot slags via extending the C-loops: Product yields and roles of slags. *Energy,* 149**,** 792-803.

TAN, S., ZHANG, Z., SUN, J. & WANG, Q. 2013. Recent progress of catalytic pyrolysis of biomass by HZSM-5. *Chinese Journal of Catalysis,* 34**,** 641-650.

TEIXEIRA CARDOSO, A. R., CONRADO, N. M., KRAUSE, M. C., BJERK, T. R., KRAUSE, L. C. & CARAMÃO, E. B. 2019. Chemical characterization of the bio-oil obtained by catalytic pyrolysis of sugarcane bagasse (industrial waste) from the species Erianthus Arundinaceus. *Journal of Environmental Chemical Engineering,* 7**,** 102970.

THANGALAZHY-GOPAKUMAR, S., WEI LEE, C., GAN, S., KIAT NG, H. & YEE LEE, L. 2018. Comparison of Bio-Oil Properties from Non-Catalytic and In-Situ Catalytic Fast Pyrolysis of Palm Empty Fruit Bunch. *Materials Today: Proceedings,* 5**,** 23456-23465.

TREEDET, W., TAECHAJEDCADARUNGSRI, S. & SUNTIVARAKORN, R. 2017. Fast Pyrolysis of Sugarcane Bagasse in Circulating Fluidized Bed Reactor - Part B: Modelling of Bio-Oil Production. *Energy Procedia,* 138**,** 806-810.

UDDIN, M. N., DAUD, W. M. A. W. & ABBAS, H. F. 2014. Effects of pyrolysis parameters on hydrogen formations from biomass: a review. *Rsc Advances,* 4**,** 10467-10490.

VALDEBENITO, F., PEREIRA, M., CIUDAD, G., AZOCAR, L., BRIONES, R. & CHINGA-CARRASCO, G. 2017. On the nanofibrillation of corn husks and oat hulls fibres. *Industrial Crops and Products,* 95**,** 528-534.

VAMVUKA, D. 2011. Bio-oil, solid and gaseous biofuels from biomass pyrolysis processes-An overview. *International Journal of Energy Research,* 35**,** 835-862.

VAN DE VELDEN, M., BAEYENS, J., BREMS, A., JANSSENS, B. & DEWIL, R. 2010. Fundamentals, kinetics and endothermicity of the biomass pyrolysis reaction. *Renewable Energy,* 35**,** 232-242.

VAN DER STELT, M. J. C., GERHAUSER, H., KIEL, J. H. A. & PTASINSKI, K. J. 2011. Biomass upgrading by torrefaction for the production of biofuels: A review. *Biomass and Bioenergy,* 35**,** 3748-3762.

VARMA, A. K. & MONDAL, P. 2017. Pyrolysis of sugarcane bagasse in semi batch reactor: Effects of process parameters on product yields and characterization of products. *Industrial Crops and Products,* 95**,** 704-717.

VECINO MANTILLA, S., GAUTHIER-MARADEI, P., ÁLVAREZ GIL, P. & TARAZONA CÁRDENAS, S. 2014. Comparative study of bio-oil production from sugarcane bagasse and palm empty fruit bunch: Yield optimization and bio-oil characterization. *Journal of Analytical and Applied Pyrolysis,* 108**,** 284-294.

VITOLO, S., BRESCI, B., SEGGIANI, M. & GALLO, M. G. 2001. Catalytic upgrading of pyrolytic oils over HZSM-5 zeolite: behaviour of the catalyst when used in repeated upgrading-regenerating cycles. *Fuel,* 80**,** 17-26.

VLACHOS, D. G. & CARATZOULAS, S. 2010. The roles of catalysis and reaction engineering in overcoming the energy and the environment crisis. *Chemical Engineering Science,* 65**,** 18-29.

WANG, H., WANG, X., CUI, Y., XUE, Z. & BA, Y. 2018. Slow pyrolysis polygeneration of bamboo (Phyllostachys pubescens): Product yield prediction and biochar formation mechanism. *Bioresource Technology,* 263**,** 444-449.

WANG, K., JOHNSTON, P. A. & BROWN, R. C. 2014. Comparison of in-situ and ex-situ catalytic pyrolysis in a micro-reactor system. *Bioresource Technology,* 173**,** 124-131.

WANG, S. R., DAI, G. X., YANG, H. P. & LUO, Z. Y. 2017. Lignocellulosic biomass pyrolysis mechanism: A state-of-the-art review. *Progress in Energy and Combustion Science,* 62**,** 33-86.

WEI, Y., LEI, H., ZHU, L., ZHANG, X., LIU, Y., YADAVALLI, G., ZHU, X., QIAN, M. & YAN, D. 2016. Hydrocarbon produced from upgrading rich phenolic compound bio-oil with low catalyst coking. *Fuel,* 178**,** 77-84.

WEINGARTEN, R., CHO, J., CONNER, W. C. & HUBER, G. W. 2010. Kinetics of furfural production by dehydration of xylose in a biphasic reactor with microwave heating. *Green Chemistry,* 12**,** 1423-1429.

WEINSTETN, M. & BROIDO, A. 1970. Pyrolysis-Crystallinity Relationships in Cellulose. *Combustion Science and Technology,* 1**,** 287-292.

WILLIAMS, P. T. & BESLER, S. 1996. The influence of temperature and heating rate on the slow pyrolysis of biomass. *Renewable Energy,* 7**,** 233-250.

WILLIAMS, P. T. & NUGRANAD, N. 2000. Comparison of products from the pyrolysis and catalytic pyrolysis of rice husks. *Energy,* 25**,** 493-513.

XIONG, K., WAN, W. M. & CHEN, J. G. G. 2016. Reaction pathways of furfural, furfuryl alcohol and 2-methylfuran on Cu(111) and NiCu bimetallic surfaces. *Surface Science,* 652**,** 91-97.

XIU, S. N. & SHAHBAZI, A. 2012. Bio-oil production and upgrading research: A review. *Renewable & Sustainable Energy Reviews,* 16**,** 4406-4414.

YAMANE, K., UETA, A. & SHIMAMOTO, Y. 2001. Influence of physical and chemical properties of biodiesel fuels on injection, combustin and exhaust emission characteristics in a direct injection compression ignition engine. 2**,** 249-261.

YAN, K., WU, G. S., LAFLEUR, T. & JARVIS, C. 2014. Production, properties and catalytic hydrogenation of furfural to fuel additives and value-added chemicals. *Renewable & Sustainable Energy Reviews,* 38**,** 663-676.

YANG, H. P., YAN, R., CHEN, H. P., LEE, D. H. & ZHENG, C. G. 2007. Characteristics of hemicellulose, cellulose and lignin pyrolysis. *Fuel,* 86**,** 1781-1788.

YANG, J., LI, S., ZHANG, L., LIU, X., WANG, J., PAN, X., LI, N., WANG, A., CONG, Y., WANG, X. & ZHANG, T. 2017. Hydrodeoxygenation of furans over Pd-FeOx/SiO2 catalyst under atmospheric pressure. *Applied Catalysis B: Environmental,* 201**,** 266-277.

YANG, J., ZHENG, H.-Y., ZHU, Y.-L., ZHAO, G.-W., ZHANG, C.-H., TENG, B.-T., XIANG, H.-W. & LI, Y. 2004. Effects of calcination temperature on performance of Cu–Zn–Al catalyst for synthesizing γ-butyrolactone and 2-methylfuran through the coupling of dehydrogenation and hydrogenation. *Catalysis Communications,* 5**,** 505-510.

YANG, T., SHI, L., LI, R., LI, B. & KAI, X. 2019. Hydrodeoxygenation of crude bio-oil in situ in the bio-oil aqueous phase with addition of zero-valent aluminum. *Fuel Processing Technology,* 184**,** 65-72.

YANG, Y., BRAMMER, J. G., MAHMOOD, A. S. N. & HORNUNG, A. 2014. Intermediate pyrolysis of biomass energy pellets for producing sustainable liquid, gaseous and solid fuels. *Bioresource Technology*, 169**,** 794-799.

YANG, Y., BRAMMER, J. G., OUADI, M., SAMANYA, J., HORNUNG, A., XU, H. M. & LI, Y. 2013. Characterisation of waste derived intermediate pyrolysis oils for use as diesel engine fuels. *Fuel,* 103**,** 247-257.

YAO, X., YU, Q. B., HAN, Z. R., XIE, H. Q., DUAN, W. J. & QIN, Q. 2018. Kinetic and experimental characterizations of biomass pyrolysis in granulated blast furnace slag. *International Journal of Hydrogen Energy,* 43**,** 9246-9253.

YILDIRIM, I. & PREZZI, M. 2015. Geotechnical Properties of Fresh and Aged Basic Oxygen Furnace Steel Slag. *Journal of Materials in Civil Engineering,* 27**,** 04015046.

YILDIZ, G., PRONK, M., DJOKIC, M., VAN GEEM, K. M., RONSSE, F., VAN DUREN, R. & PRINS, W. 2013. Validation of a new set-up for continuous catalytic fast pyrolysis of biomass coupled with vapour phase upgrading. *Journal of Analytical and Applied Pyrolysis,* 103**,** 343-351.

YIN, R., LIU, R., MEI, Y., FEI, W. & SUN, X. 2013. Characterization of bio-oil and bio-char obtained from sweet sorghum bagasse fast pyrolysis with fractional condensers. *Fuel,* 112**,** 96-104.

ZEITSCH, K. J. 2000. Furfural production needs chemical innovation. *Chemical Innovation,* 30**,** 29-32.

ZHANG, C., HU, X., GUO, H., WEI, T., DONG, D., HU, G., HU, S., XIANG, J., LIU, Q. & WANG, Y. 2018a. Pyrolysis of poplar, cellulose and lignin: Effects of

acidity and alkalinity of the metal oxide catalysts. *Journal of Analytical and Applied Pyrolysis,* 134**,** 590-605.

ZHANG, H., XIAO, R., HUANG, H. & XIAO, G. 2009. Comparison of non-catalytic and catalytic fast pyrolysis of corncob in a fluidized bed reactor. *Bioresource Technology,* 100**,** 1428-1434.

ZHANG, L., HU, X., HU, K., HU, C., ZHANG, Z., LIU, Q., HU, S., XIANG, J., WANG, Y. & ZHANG, S. 2018b. Progress in the reforming of bio-oil derived carboxylic acids for hydrogen generation. *Journal of Power Sources,* 403**,** 137-156.

ZHANG, Q., CHANG, J., WANG, T. J. & XU, Y. 2007. Review of biomass pyrolysis oil properties and upgrading research. *Energy Conversion and Management,* 48**,** 87-92.

ZHANG, Q. C., CHEN, G. S., ZHENG, Z. Q., LIU, H. F., XU, J. & YAO, M. F. 2013a. Combustion and emissions of 2,5-dimethylfuran addition on a diesel engine with low temperature combustion. *Fuel,* 103**,** 730-735.

ZHANG, S., YAN, Y., LI, T. & REN, Z. 2005. Upgrading of liquid fuel from the pyrolysis of biomass. *Bioresource Technology,* 96**,** 545-550.

ZHANG, X. H., GHAMARI, M. & RATNER, A. 2013b. Numerical modeling of co-firing a light density biomass, oat (Auena sativa) hulls, and chunk coal in fluidized bed boiler. *Biomass & Bioenergy,* 56**,** 239-246.

ZHAO, H. B., HOLLADAY, J. E., BROWN, H. & ZHANG, Z. C. 2007. Metal chlorides in ionic liquid solvents convert sugars to 5-hydroxymethylfurfural. *Science,* 316**,** 1597-1600.

ZHENG, H.-Y., ZHU, Y.-L., HUANG, L., ZENG, Z.-Y., WAN, H.-J. & LI, Y.-W. 2008. Study on Cu–Mn–Si catalysts for synthesis of cyclohexanone and 2-methylfuran through the coupling process. *Catalysis Communications,* 9**,** 342-348.

ZHOU, Y. X., BERRUTI, F., GREENHALF, C., TIAN, X. H. & HENRY, H. A. L. 2017. Increased retention of soil nitrogen over winter by biochar application: Implications of biochar pyrolysis temperature for plant nitrogen availability. *Agriculture Ecosystems & Environment,* 236**,** 61-68.

APPENDIX A

Detailed temperature program for moisture determination

1. Heat from 20.0 to 105.0 °C at 10 °C/min
2. Keep at 105.0 °C for 3 h
3. Cool down from 105.0 to 20 °C at 10 °C/min

Detailed temperature program for ash determination

1. Heat from 20.0 to 575.0 °C at 10 °C/min
2. Keep at 575.0 °C for 5 h
3. Cool down from 575.0 to 20 °C at 10 °C/min

Detailed temperature program for volatiles a fixed carbon determination

1. Heat from 20.0 to 900.0 °C at 10 °C/min
2. Keep at 900.0 °C for 15 min
3. Cool down from 900.0 to 20 °C at 10 °C/min

APPENDIX B

Mass Balance calculations

Table 34 - Mass balance calculations (1)

Feedstock	**3500.0 g**
Remaining Feedstock	
Hopper	10.0 g
Pyrolysis reactor	40.0 g
Total	**50.0 g**
Feedstock converted	**3450.0 g**
Condensate	
Washing bottle	
Initial weight	1200.0 g
Final weight	1250.0 g
=	**50.0 g**
Activated carbon bottle	
Initial weight	700.0 g
Final weight	720.0 g
=	**20.0 g**
Cooler	
Organic phase	200.0 g
Aqueous phase	600.0 g
Bio-oil produced	**800.0 g**
Total Condensate	**870.0 g**
Biochar	
Candle Filter	
Initial weight	500.0 g
Final weight	520.0 g
=	**20.0 g**

Glass wool filter	
Initial weight	600.0 g
Final weight	605.0 g
=	**5.0 g**
Reformer	
Initial biochar	500.0 g
Final biochar	1200.0 g
Biochar produced	**700.0 g**
Total Biochar	**725.0 g**
Syngas	
Initial gas meter reading	5.0 m^3
Final gas meter reading	7.3 m^3
Syngas produced	2.3 m^3
Syngas density	0.70 kg/m^3
Total Syngas	**1610.0 g**
Total Losses	**245.0 g**

Total syngas = Syngas produced * Syngas density * 1000

Losses = Feedstock converted – (Total Condensate + Total Biochar + Total Syngas)

Table 35 - Mass balance calculations (2)

Condensate	25.2 wt%	Oil	6.3 wt%
		Water	18.9 wt%
Biochar	21.0 wt%		
Syngas	46.7 wt%		
Losses	7.1 wt%		

Condensate (wt%) = (Total Condensate / Feedstock Converted) * 100

Oil (wt%) = (Organic phase / Bio-oil produced) * Condensate

Water (wt%) = (Aqueous phase / Bio-oil produced) * Condensate

Biochar (wt%) = (Total Biochar / Feedstock Converted) * 100

Syngas (wt%) = (Total Syngas / Feedstock Converted) * 100

Losses (wt%) = (Total Losses / Feedstock Converted) * 100

Energy Yield calculations

Table 36 - Energy yield calculations

Organic phase (kg)	Organic phase (MJ)	Organic phase (%)
0.22	7.2	12.8

Organic phase (kg) = (Oil * Feedstock converted) / 1000

Organic phase (MJ) = Organic phase HHV (33.2 MJ/kg) * Organic phase (kg)

Organic phase (%) = (Organic phase (MJ) / Feedstock energy (56.2 MJ)) * 100

The same methodology was applied to determine the energy yield of the biochar, syngas and losses.

APPENDIX C

Table 37 - SB characterisation (average, standard deviation and coefficient of variation)

	C (wt%)	H (wt%)	N (wt%)	S (wt%)	O (wt%)	Moisture (wt%)	Ash (wt%)	Fixed Carbon (wt%)	Volatiles (wt%)	HHV (MJ/kg)
Average	43.7	5.1	0.10	0.62	46.5	6.0	4.0	17.2	72.8	16.4
Standard deviation	0.24	0.08	0.00	0.09	0.84	0.42	0.58	0.76	2.1	0.09
Coefficient of variation (%)	0.55	1.5	0.00	14.9	1.8	6.9	14.6	4.4	2.9	0.54

Table 38 - OH characterisation (average, standard deviation and coefficient of variation)

	C (wt%)	H (wt%)	N (wt%)	S (wt%)	O (wt%)	Moisture (wt%)	Ash (wt%)	Fixed Carbon (wt%)	Volatiles (wt%)	HHV (MJ/kg)
Average	40.6	6.0	1.1	<0.1	49.9	14.8	2.4	26.4	56.4	16.0
Standard deviation	0.14	0.36	0.05	-	1.1	0.46	0.07	0.81	1.2	0.54
Coefficient of variation (%)	0.33	5.9	4.2	-	2.2	3.1	2.9	3.1	2.1	3.4

Table 39 - SB bio-oil characterisation at different reforming temperatures (Pyrolysis temperature = 450 °C) (average, standard deviation and coefficient of variation)

500 °C	**C (wt%)**	**H (wt%)**	**N (wt%)**	**S (wt%)**	**O (wt%)**	**HHV (MJ/kg)**	**Ash (wt%)**	**Water (wt%)**	**TAN (mg KOH/g)**	**Viscosity (mm^2/s)**	**Density (kg/m^3)**
Average	71.3	7.1	0.69	0.10	20.8	31.1	<0.001	4.7	27.7	24.9	1062
Standard deviation	0.66	0.13	0.08	0.00	1.2	0.24	-	0.22	3.8	2.9	12.3
Coefficient of variation (%)	0.93	1.8	11.6	0.00	5.8	0.77	-	4.7	13.7	11.6	1.2
600 °C											
Average	74.6	7.4	0.56	0.10	17.4	33.0	<0.001	2.2	17.3	13.7	1060
Standard deviation	0.84	0.17	0.08	0.00	1.1	0.69	-	0.28	3.1	1.6	9.4
Coefficient of variation (%)	1.1	2.3	14.3	0.00	6.3	2.1	-	12.7	17.9	11.7	0.89
700 °C											
Average	77.2	8.0	0.54	0.18	14.1	34.9	<0.001	1.9	15.6	12.1	1059
Standard deviation	1.8	0.45	0.04	0.01	1.4	0.92	-	0.13	2.9	1.0	7.7
Coefficient of variation (%)	2.3	5.6	7.4	5.6	9.9	2.6	-	6.8	18.6	8.3	0.73

Table 40 - OH bio-oil characterisation at different reforming temperatures (Pyrolysis temperature = 450 °C) (average, standard deviation and coefficient of variation)

500 °C	**C (wt%)**	**H (wt%)**	**N (wt%)**	**S (wt%)**	**O (wt%)**	**HHV (MJ/kg)**	**Ash (wt%)**	**Water (wt%)**	**TAN (mg KOH/g)**	**Viscosity (mm^2/s)**	**Density (kg/m^3)**
Average	72.2	8.2	1.9	0.68	17.0	33.2	<0.001	4.8	30.5	36.5	1074
Standard deviation	0.92	0.42	0.07	0.06	1.4	0.52	-	0.27	5.7	4.1	9.4
Coefficient of variation (%)	1.3	5.2	3.7	8.8	8.2	1.6	-	5.6	18.7	11.2	0.88
600 °C											
Average	77.4	7.5	2.7	0.76	11.7	34.6	<0.001	3.9	21.4	35.4	1082
Standard deviation	0.51	0.11	0.10	0.06	0.55	0.11	-	0.35	4.0	2.8	1.6
Coefficient of variation (%)	0.65	1.4	3.6	7.5	4.7	0.33	-	9.2	18.5	7.8	0.15
700 °C											
Average	78.8	7.2	2.5	0.77	10.7	35.0	<0.001	2.3	17.7	17.8	1072
Standard deviation	1.5	0.30	0.09	0.07	1.2	0.31	-	0.00	3.8	3.6	8.2
Coefficient of variation (%)	1.9	4.2	3.7	8.8	11.3	0.90	-	0.00	21.5	20.2	0.76

Table 41 - SB gas compositon at different reforming temperatures (Pyrolysis temperature = 450 °C) (average, standard deviation and coefficient of variation)

500 °C	**H_2 (vol%)**	**CH_4 (vol%)**	**CO (vol%)**	**CO_2 (vol%)**	**C_xH_y (vol%)**	**Non-detectable (vol%)**	**HHV (MJ/kg)**	**Density (kg/m^3)**
Average	25.7	13.5	20.2	28.8	2.3	9.5	15.9	0.89
Standard deviation	0.61	0.98	1.7	0.66	0.09	1.1	0.82	0.04
Coefficient of variation (%)	2.4	7.3	8.4	2.3	3.9	11.6	5.2	4.5
600 °C								
Average	30.4	9.6	18.5	25.6	2.0	13.9	17.0	0.78
Standard deviation	1.0	0.92	1.9	0.00	0.07	1.9	1.1	0.02
Coefficient of variation (%)	3.3	9.6	10.3	0.00	3.5	13.7	6.5	2.6
700 °C								
Average	30.9	10.2	23.6	21.8	1.4	12.1	18.4	0.73
Standard deviation	0.63	0.28	0.92	0.42	0.00	0.14	2.4	0.01
Coefficient of variation (%)	2.03	2.7	3.9	1.9	0.00	1.2	13.0	1.4

Table 42 - OH gas compositon at different reforming temperatures (Pyrolysis temperature = 450 °C) (average, standard deviation and coefficient of variation)

500 °C	**H_2 (vol%)**	**CH_4 (vol%)**	**CO (vol%)**	**CO_2 (vol%)**	**C_xH_y (vol%)**	**Non-detectable (vol%)**	**HHV (MJ/kg)**	**Density (kg/m^3)**
Average	15.8	7.0	25.5	25.6	2.7	23.4	15.3	1.2
Standard deviation	1.7	0.62	1.8	0.94	0.41	1.3	0.39	0.02
Coefficient of variation (%)	10.8	8.9	7.1	3.7	15.2	5.6	2.6	1.7
600 °C								
Average	30.1	5.8	21.2	20.9	2.4	19.7	18.0	1.0
Standard deviation	3.0	0.57	1.4	0.42	0.49	2.0	0.21	0.04
Coefficient of variation (%)	9.9	9.8	6.7	2.0	21.1	10.4	1.2	4.1
700 °C								
Average	31.6	6.9	25.2	18.5	1.5	16.5	18.8	0.96
Standard deviation	1.5	0.35	1.8	0.78	0.21	0.14	0.15	0.02
Coefficient of variation (%)	4.7	5.2	7.3	4.2	14.6	0.86	0.79	1.8

Table 43 - SB biochar characterisation at different reforming temperatures (Pyrolysis temperature = 450 °C) (average, standard deviation and coefficient of variation)

500 °C	**C (wt%)**	**H (wt%)**	**N (wt%)**	**S (wt%)**	**O (wt%)**	**Ash (wt%)**	**HHV (MJ/kg)**
Average	70.3	1.6	0.39	<0.10	11.6	16.1	24.9
Standard deviation	1.1	0.19	0.02	-	0.33	0.99	0.47
Coefficient of variation (%)	1.6	11.9	5.1	-	2.8	6.1	1.9
600 °C							
Average	77.0	1.5	0.34	<0.10	2.1	19.0	28.0
Standard deviation	0.80	0.13	0.01	-	0.18	0.73	0.62
Coefficient of variation (%)	1.0	8.7	2.9	-	8.6	3.8	2.2
700 °C							
Average	78.2	1.3	0.43	<0.10	1.1	18.8	28.4
Standard deviation	1.7	0.09	0.02	-	0.06	1.0	0.31
Coefficient of variation (%)	2.2	6.9	4.6	-	5.4	5.3	1.1

Table 44 - OH biochar characterisation at different reforming temperatures (Pyrolysis temperature = 450 °C) (average, standard deviation and coefficient of variation)

500 °C	**C (wt%)**	**H (wt%)**	**N (wt%)**	**S (wt%)**	**O (wt%)**	**Ash (wt%)**	**HHV (MJ/kg)**
Average	79.3	2.0	1.1	<0.10	5.7	11.8	29.2
Standard deviation	0.70	0.21	0.04	-	0.34	0.35	0.19
Coefficient of variation (%)	0.88	10.5	3.6	-	6.0	3.0	0.65
600 °C							
Average	81.0	1.9	1.0	<0.10	5.1	10.8	29.7
Standard deviation	0.26	0.05	0.04	-	0.93	0.58	0.23
Coefficient of variation (%)	0.33	2.6	3.4	-	18.2	5.3	0.79
700 °C							
Average	78.6	1.8	1.0	<0.10	5.3	13.2	28.7
Standard deviation	1.8	0.32	0.05	-	0.23	1.7	0.28
Coefficient of variation (%)	2.3	17.9	4.4	-	4.5	12.9	0.97

Table 45- Mass balance of SB trials at different reforming temperatures (Pyrolysis temperature = 450 °C) (average, standard deviation and coefficient of variation)

500 °C	**Bio-oil (wt%)**	**A. phase (wt%)**	**Char (wt%)**	**Gas (wt%)**	**Losses (wt%)**
Average	7.2	25.4	26.6	36.3	4.5
Standard deviation	0.76	1.4	0.37	1.3	0.20
Coefficient of variation (%)	10.6	5.5	1.4	3.6	4.4
600 °C					
Average	4.8	23.0	22.9	43.8	5.5
Standard deviation	0.61	2.7	0.77	2.8	0.34
Coefficient of variation (%)	12.8	11.7	3.4	6.4	6.2
700 °C					
Average	2.7	19.5	20.9	50.4	6.6
Standard deviation	0.19	1.6	0.39	4.3	0.27
Coefficient of variation (%)	7.0	8.2	1.9	8.5	4.1

Table 46 - Mass balance of OH trials at different reforming temperatures (Pyrolysis temperature = 450 °C) (average, standard deviation and coefficient of variation)

500 °C	**Bio-oil (wt%)**	**A. phase (wt%)**	**Char (wt%)**	**Gas (wt%)**	**Losses (wt%)**
Average	7.6	33.2	22.9	33.1	3.2
Standard deviation	0.81	0.95	0.37	1.0	0.18
Coefficient of variation (%)	10.7	2.9	1.6	3.0	5.6
600 °C					
Average	4.2	25.5	20.1	45.7	4.5
Standard deviation	1.3	0.97	0.06	1.8	0.39
Coefficient of variation (%)	31.2	3.8	0.28	3.9	8.7
700 °C					
Average	3.2	22.0	17.0	53.2	4.6
Standard deviation	0.53	0.60	0.51	1.1	0.44
Coefficient of variation (%)	16.6	2.7	3.0	2.0	9.5

Table 47 - Energy yield of SB trials at different reforming temperatures (Pyrolysis temperature = 450 °C) (average, standard deviation and coefficient of variation)

500 °C	**Bio-oil (%)**	**Char (%)**	**Gas (%)**	**Losses (%)**
Average	13.6	40.4	35.1	10.9
Standard deviation	1.3	0.87	0.99	1.7
Coefficient of variation (%)	9.6	2.2	2.8	15.6
600 °C				
Average	9.7	39.1	45.4	5.8
Standard deviation	2.0	1.0	1.1	0.83
Coefficient of variation (%)	20.6	2.6	2.4	14.3
700 °C				
Average	5.7	36.1	56.5	1.7
Standard deviation	0.8	0.91	1.5	0.66
Coefficient of variation (%)	14.0	2.5	2.7	38.8

Table 48 - Energy yield of OH trials at different reforming temperatures (Pyrolysis temperature = 450 °C) (average, standard deviation and coefficient of variation)

500 °C	**Bio-oil (%)**	**Char (%)**	**Gas (%)**	**Losses (%)**
Average	15.7	41.7	31.6	11.1
Standard deviation	1.8	0.76	0.62	1.4
Coefficient of variation (%)	11.5	1.8	2.0	12.6
600 °C				
Average	9.0	37.2	51.1	2.7
Standard deviation	1.6	0.40	1.4	0.38
Coefficient of variation (%)	17.8	1.1	2.7	14.1
700 °C				
Average	7.0	30.5	62.3	0.28
Standard deviation	1.1	0.62	0.76	0.17
Coefficient of variation (%)	15.7	2.0	1.2	60.7

Table 49 - SB bio-oil characterisation at different pyrolysis temperatures (Reforming temperature = 500 °C) (average, standard deviation and coefficient of variation)

400 °C	**C (wt%)**	**H (wt%)**	**N (wt%)**	**S (wt%)**	**O (wt%)**	**HHV (MJ/kg)**	**Ash (wt%)**	**Water (wt%)**	**TAN (mg KOH/g)**	**Viscosity (mm^2/s)**	**Density (kg/m^3)**
Average	63.4	8.3	0.41	0.39	27.5	29.1	<0.001	9.9	32.2	47.8	1077
Standard deviation	0.53	0.24	0.04	0.06	2.2	0.18	-	0.69	4.1	7.8	4.9
Coefficient of variation (%)	0.84	2.9	9.8	15.3	8.0	0.62	-	6.9	12.7	16.3	0.45
450 °C											
Average	71.3	7.1	0.69	0.10	20.8	31.1	<0.001	4.7	27.7	24.9	1062
Standard deviation	0.66	0.13	0.08	0.00	1.2	0.24	-	0.22	3.8	2.9	12.3
Coefficient of variation (%)	0.93	1.8	11.6	0.00	5.8	0.77	-	4.7	13.7	11.6	1.2
500 °C											
Average	72.2	8.6	0.76	0.29	18.2	33.4	<0.001	4.2	25.8	23.7	1061
Standard deviation	0.61	0.30	0.05	0.02	1.4	0.37	-	0.31	1.6	1.4	3.5
Coefficient of variation (%)	0.85	3.5	6.6	6.9	7.7	1.1	-	7.4	6.2	5.9	0.33

Table 50 - OH bio-oil characterisation at different pyrolysis temperatures (Reforming temperature = 500 °C) (average, standard deviation and coefficient of variation)

400 °C	**C (wt%)**	**H (wt%)**	**N (wt%)**	**S (wt%)**	**O (wt%)**	**HHV (MJ/kg)**	**Ash (wt%)**	**Water (wt%)**	**TAN (mg KOH/g)**	**Viscosity (mm^2/s)**	**Density (kg/m^3)**
Average	70.7	8.6	1.8	1.3	17.6	33.1	<0.001	7.8	33.5	38.1	1078
Standard deviation	0.86	0.53	0.03	0.11	1.3	0.27	-	1.1	3.9	3.3	6.5
Coefficient of variation (%)	1.2	6.2	1,7	8.5	7.4	0.82	-	14.1	11.6	8.7	0.60
450 °C											
Average	72.2	8.2	1.9	0.68	17.0	33.2	<0.001	4.8	30.5	36.5	1074
Standard deviation	0.92	0.42	0.07	0.06	1.4	0.52	-	0.27	5.7	4.1	9.4
Coefficient of variation (%)	1.3	5.2	3.7	8.8	8.2	1.6	-	5.6	18.7	11.2	0.88
500 °C											
Average	72.8	8.3	1.8	0.68	16.4	33.5	<0.001	4.4	24.2	35.3	1072
Standard deviation	0.61	0.59	0.04	0.08	1.3	0.44	-	0.18	4.2	1.9	3.7
Coefficient of variation (%)	0.84	7.1	2.2	11.8	7.9	1.3	-	4.1	17.4	5.4	0.35

Table 51 - SB gas compositon at different pyrolysis temperatures (Reforming temperature = 500 °C) (average, standard deviation and coefficient of variation)

400 °C	**H_2 (vol%)**	**CH_4 (vol%)**	**CO (vol%)**	**CO_2 (vol%)**	**C_xH_y (vol%)**	**Non-detectable (vol%)**	**HHV (MJ/kg)**	**Density (kg/m^3)**
Average	21.5	15.6	21.2	30.5	2.5	8.7	13.8	0.90
Standard deviation	0.42	0.83	2.0	0.98	0.07	0,60	0.60	0.05
Coefficient of variation (%)	1.9	5.3	9.4	3.2	2.8	6.9	4.3	5.6
450 °C								
Average	25.7	13.5	20.2	28.8	2.3	9.5	15.9	0.89
Standard deviation	0.61	0.98	1.7	0.66	0.09	1.1	0.82	0.04
Coefficient of variation (%)	2.4	7.3	8.4	2.3	3.9	11.6	5.2	4.5
500 °C								
Average	19.9	10.9	32.6	23.6	2.7	10.3	13.4	0.98
Standard deviation	0.33	0.35	3.7	0.36	0.09	0,80	0.71	0.07
Coefficient of variation (%)	1.7	3.2	11.3	1.5	3.3	7.8	5.3	7.1

Table 52 - OH gas compositon at different pyrolysis temperatures (Reforming temperature = 500 °C) (average, standard deviation and coefficient of variation)

400 °C	**H_2 (vol%)**	**CH_4 (vol%)**	**CO (vol%)**	**CO_2 (vol%)**	**C_xH_y (vol%)**	**Non-detectable (vol%)**	**HHV (MJ/kg)**	**Density (kg/m^3)**
Average	16.5	11.6	26.5	30.1	3.0	12.3	16.2	0.91
Standard deviation	1.3	0.49	1.1	0.99	0.22	0.74	0.36	0.05
Coefficient of variation (%)	7.9	4.2	4.2	3.3	7.3	6.0	2.2	5.5
450 °C								
Average	15.8	7.0	25.5	25.6	2.7	23.4	15.3	1.2
Standard deviation	1.7	0.62	1.8	0.94	0.41	1.3	0.39	0.02
Coefficient of variation (%)	10.8	8.9	7.1	3.7	15.2	5.6	2.6	1.7
500 °C								
Average	23.1	6.4	29.5	21.2	3.4	16.4	17.3	0.85
Standard deviation	1.9	0.55	1.4	0.76	0.25	1.0	0.44	0.03
Coefficient of variation (%)	8.2	8.6	4.7	3.6	7.4	6.1	2.5	3.5

Table 53 - SB biochar characterisation at different pyrolysis temperatures (Reforming temperature = 500 °C) (average, standard deviation and coefficient of variation)

400 °C	**C (wt%)**	**H (wt%)**	**N (wt%)**	**S (wt%)**	**O (wt%)**	**Ash (wt%)**	**HHV (MJ/kg)**
Average	79.6	2.2	0.44	<0.10	2.7	15.0	29.7
Standard deviation	2.2	0.17	0.02	-	0.11	0.74	0.68
Coefficient of variation (%)	2.8	7.7	4.5	-	4.1	4.9	2.3
450 °C							
Average	70.3	1.6	0.39	<0.10	11.6	16.1	24.9
Standard deviation	1.1	0.19	0.02	-	0.33	0.99	0.47
Coefficient of variation (%)	1.6	11.9	5.1	-	2.8	6.1	1.9
500 °C							
Average	77.1	1.5	0.47	<0.10	2.6	18.2	28.1
Standard deviation	1.5	0.08	0.03	-	0.13	1.3	0.44
Coefficient of variation (%)	1.9	5.3	6.4	-	5.0	7.1	1.6

Table 54 - OH biochar characterisation at different pyrolysis temperatures (Reforming temperature = 500 °C) (average, standard deviation and coefficient of variation)

400 °C	**C (wt%)**	**H (wt%)**	**N (wt%)**	**S (wt%)**	**O (wt%)**	**Ash (wt%)**	**HHV (MJ/kg)**
Average	78.2	2.7	1.4	<0.10	2.2	15.5	29.3
Standard deviation	0.81	0.16	0.06	-	0.18	0.51	0.19
Coefficient of variation (%)	1.0	5.9	4.3	-	8.2	3.3	0.65
450 °C							
Average	79.3	2.0	1.1	<0.10	5.7	11.8	29.2
Standard deviation	0.70	0.21	0.04	-	0.34	0.35	0.19
Coefficient of variation (%)	0.88	10.5	3.6	-	6.0	3.0	0.65
500 °C							
Average	79.0	2.3	1.3	<0.10	1.2	16.1	29.3
Standard deviation	0.88	0.14	0.03	-	0.07	0.80	0.21
Coefficient of variation (%)	1.1	6.1	2.3	-	5.8	4.9	0.72

Table 55 - Mass balance of SB trials at different pyrolysis temperatures (Reforming temperature = 500 °C) (average, standard deviation and coefficient of variation)

400 °C	**Bio-oil (wt%)**	**A. phase (wt%)**	**Char (wt%)**	**Gas (wt%)**	**Losses (wt%)**
Average	7.8	26.6	27.2	31.6	6.8
Standard deviation	0.38	1.1	0.33	2.5	0.52
Coefficient of variation (%)	4.9	4.1	1.2	7.9	7.6
450 °C					
Average	7.2	25.4	26.6	36.3	4.5
Standard deviation	0.76	1.4	0.37	1.3	0.20
Coefficient of variation (%)	10.6	5.5	1.4	3.6	4.4
500 °C					
Average	6.8	23.2	26.1	36.8	7.2
Standard deviation	0.29	0.93	0.17	1.1	0.59
Coefficient of variation (%)	4.3	4.0	0.65	3.0	8.2

Table 56 - Mass balance of OH trials at different pyrolysis temperatures (Reforming temperature = 500 °C) (average, standard deviation and coefficient of variation)

400 °C	**Bio-oil (wt%)**	**A. phase (wt%)**	**Char (wt%)**	**Gas (wt%)**	**Losses (wt%)**
Average	9.3	34.4	24.8	26.7	4.8
Standard deviation	0.76	0.97	0.60	1.5	0.29
Coefficient of variation (%)	8.2	2.8	2.4	5.6	6.0
450 °C					
Average	7.6	33.2	22.9	33.1	3.2
Standard deviation	0.81	0.95	0.37	1.0	0.18
Coefficient of variation (%)	10.7	2.9	1.6	3.0	5.6
500 °C					
Average	7.5	30.9	22.2	33.7	5.9
Standard deviation	0.69	0.88	0.57	0.89	0.22
Coefficient of variation (%)	9.2	2.8	2.6	2.6	3.7

Table 57 - Energy yield of SB trials at different pyrolysis temperatures (Reforming temperature = 500 °C) (average, standard deviation and coefficient of variation)

400 °C	**Bio-oil (%)**	**Char (%)**	**Gas (%)**	**Losses (%)**
Average	13.8	49.4	26.7	10.2
Standard deviation	1.1	0.92	0.66	1.3
Coefficient of variation (%)	8.0	1.9	2.5	12.7
450 °C				
Average	13.6	40.4	35.1	10.9
Standard deviation	1.3	0.87	0.99	1.7
Coefficient of variation (%)	9.6	2.2	2.8	15.6
500 °C				
Average	13.8	44.7	30.0	11.4
Standard deviation	1.3	0.95	0.82	1.6
Coefficient of variation (%)	9.4	2.1	2.7	14.0

Table 58 - Energy yield of OH trials at different pyrolysis temperatures (Reforming temperature = 500 °C) (average, standard deviation and coefficient of variation)

400 °C	**Bio-oil (%)**	**Char (%)**	**Gas (%)**	**Losses (%)**
Average	19.3	45.3	27.0	8.4
Standard deviation	1.9	0.88	0.47	1.0
Coefficient of variation (%)	9.8	1.9	1.7	11.9
450 °C				
Average	15.7	41.7	31.6	11.1
Standard deviation	1.8	0.76	0.62	1.4
Coefficient of variation (%)	11.5	1.8	2.0	12.6
500 °C				
Average	15.6	40.4	36.3	7.7
Standard deviation	1.3	0.59	0.75	0.86
Coefficient of variation (%)	8.3	1.5	2.1	11.2

Table 59 - SB bio-oil characterisation at different SS ratios (Pyrolysis and Reforming temperatures = 400 and 500 °C) (average, standard deviation and coefficient of variation)

30 wt% (Reformer)	**C (wt%)**	**H (wt%)**	**N (wt%)**	**S (wt%)**	**O (wt%)**	**HHV (MJ/kg)**	**Ash (wt%)**	**Water (wt%)**	**TAN (mg KOH/g)**	**Viscosity (mm^2/s)**	**Density (kg/m^3)**
Average	68.2	7.2	1.9	1.7	21.0	30.2	<0.001	8.4	29.1	45.8	1073
Standard deviation	1.1	0.49	0.12	0.05	1.2	0.78	-	0.27	3.1	6.2	9.4
Coefficient of variation (%)	1.6	6.8	6.3	2.9	5.7	2.6	-	3.2	10.6	13.5	0.88
70 wt% (Reformer)											
Average	71.7	8.3	1.4	1.2	17.5	33.0	<0.001	6.5	22.6	30.9	1067
Standard deviation	0.90	0.16	0.04	0.03	1.5	0.41	-	0.19	3.3	2.8	16.1
Coefficient of variation (%)	1.2	1.9	2.9	2.5	8.6	1.2	-	2.9	14.6	9.1	1.5
100 wt% (Reformer)											
Average	74.9	9.0	1.1	1.6	13.5	33.5	<0.001	5.7	16.7	25.5	1060
Standard deviation	1.7	0.38	0.09	0.03	2.0	0.39	-	0.20	1.6	3.3	18.5
Coefficient of variation (%)	2.3	4.2	8.2	1.9	14.8	1.2	-	3.5	9.6	12.9	1.7

Table 60 - OH bio-oil characterisation at different SS ratios (Pyrolysis and Reforming temperatures = 400 and 500 °C) (average, standard deviation and coefficient of variation)

30 wt% (Reformer)	**C (wt%)**	**H (wt%)**	**N (wt%)**	**S (wt%)**	**O (wt%)**	**HHV (MJ/kg)**	**Ash (wt%)**	**Water (wt%)**	**TAN (mg KOH/g)**	**Viscosity (mm^2/s)**	**Density (kg/m^3)**
Average	64.2	7.9	2.8	1.3	23.8	29.3	<0.001	6.7	29.2	35.7	1069
Standard deviation	2.6	0.39	0.34	0.07	1.9	1.2	-	0.34	2.8	1.9	12.9
Coefficient of variation (%)	4.1	4.9	12.1	5.4	8.0	4.1	-	5.7	9.6	5.3	1.2
70 wt% (Reformer)											
Average	69.8	8.8	1.7	1.0	18.7	32.9	<0.001	6.2	27.4	32.3	1055
Standard deviation	0.94	0.62	0.05	0.08	1.6	0.79	-	0.38	1.7	2.3	9.1
Coefficient of variation (%)	1.3	7.0	2.9	8.0	8.6	2.4	-	6.1	6.2	7.1	0.86
100 wt% (Reformer)											
Average	74.4	8.9	1.9	0.91	13.9	35.1	<0.001	5.4	14.3	30.8	1051
Standard deviation	1.8	0.27	0.05	0.05	1.1	0.93	-	0.41	4.0	1.8	7.6
Coefficient of variation (%)	2.4	3.0	2.6	5.5	7.9	2.6	-	7.6	28.0	5.8	0.72
10 wt% (Feed)											
Average	65.9	9.6	1.8	0.95	21.8	32.1	<0.001	6.6	21.1	28.2	1040
Standard deviation	0.77	0.56	0.07	0.07	1.0	0.37	-	0.88	2.3	2.0	12.8
Coefficient of variation (%)	1.2	5.8	3.9	7.4	4.6	1.2	-	13.3	10.9	7.1	1.2
20 wt% (Feed)											
Average	67.9	9.3	2.0	1.0	19.8	32.6	<0.001	5.1	17.3	26.9	1038
Standard deviation	1.9	0.39	0.09	0.08	0.94	0.29	-	0.55	1.4	4.4	7.5
Coefficient of variation (%)	2.8	4.2	4.5	8.0	4.7	0.89	-	10.8	8.1	16.3	0.72
30 wt% (Feed)											
Average	73.5	9.4	2.5	1.3	13.3	35.4	<0.001	3.5	11.5	21.0	1026
Standard deviation	1.2	0.17	0.13	0.08	0.62	0.40	-	0.29	1.5	3.1	9.8
Coefficient of variation (%)	1.6	1.8	5.2	6.2	4.7	1.1	-	8.3	13.0	14.8	0.95

Table 61 - SB gas compositon at different SS ratios (Pyrolysis and Reforming temperatures = 400 and 500 °C) (average, standard deviation and coefficient of variation)

30 wt% (Reformer)	**H_2 (vol%)**	**CH_4 (vol%)**	**CO (vol%)**	**CO_2 (vol%)**	**C_xH_y (vol%)**	**Non-detectable (vol%)**	**HHV (MJ/kg)**	**Density (kg/m^3)**
Average	20.4	15.1	24.9	30.4	2.0	7.2	13.6	0.91
Standard deviation	0.53	0.69	1.2	0.70	0.05	0.48	0.56	0.03
Coefficient of variation (%)	2.6	4.6	4.8	2.3	2.5	6.7	4.1	3.3
70 wt% (Reformer)								
Average	19.5	14.7	25.8	29.2	2.1	8.7	13.5	0.92
Standard deviation	0.28	0.31	1.4	0.30	0.08	0.52	0.69	0.04
Coefficient of variation (%)	1.4	2.1	5.4	1.0	3.8	6.0	5.1	4.3
100 wt% (Reformer)								
Average	18.9	13.1	28.6	28.3	2.8	8.3	13.3	0.95
Standard deviation	0.22	0.29	1.5	0.43	0.07	0.36	0.64	0.03
Coefficient of variation (%)	1.2	2.2	5.2	1.5	2.5	4.3	4.8	3.2

Table 62 - OH gas compositon at different SS ratios (Pyrolysis and Reforming temperatures = 400 and 500 °C) (average, standard deviation and coefficient of variation)

30 wt% (Reformer)	**H_2 (vol%)**	**CH_4 (vol%)**	**CO (vol%)**	**CO_2 (vol%)**	**C_xH_y (vol%)**	**Non-detectable (vol%)**	**HHV (MJ/kg)**	**Density (kg/m^3)**
Average	15.7	10.7	28.9	29.6	3.7	11.4	13.7	0.92
Standard deviation	1.2	0.58	2,0	0.89	0.29	0.76	0.41	0.06
Coefficient of variation (%)	7.6	5.4	6.9	3.0	7.8	6.7	3.0	6.5
70 wt% (Reformer)								
Average	15.4	10.1	29.2	29.3	3.1	12.9	13.3	0.99
Standard deviation	0.4	0.77	2.3	1.6	0.18	0.81	0.25	0.03
Coefficient of variation (%)	2.6	7.6	7.9	5.5	5.8	6.3	1.9	3.0
100 wt% (Reformer)								
Average	14.5	8.8	31.5	27.0	3.0	15.2	12.8	1.0
Standard deviation	0.88	0.54	1.7	1.0	0.22	0.69	0.36	0.02
Coefficient of variation (%)	6.1	6.1	5.4	3.7	7.3	4.5	2.8	2.0
10 wt% (Feed)								
Average	23.2	7.3	22.6	35.8	2.7	8.4	17.4	0.91
Standard deviation	1.4	0.46	1.1	0.85	0.17	0.64	0.3	0.02
Coefficient of variation (%)	6.0	6.3	4.9	2.4	6.3	7.6	1.7	2.2
20 wt% (Feed)								
Average	24.4	8.4	21.5	34.2	2.7	8.8	17.7	0.91
Standard deviation	1.3	0.38	1.3	0.94	0.19	0.5	0.27	0.04
Coefficient of variation (%)	5.3	4.5	6.0	2.7	7.0	5.7	1.5	4.4
30 wt% (Feed)								
Average	29.7	8.7	17.4	32.2	2.5	9.5	18.2	0.89
Standard deviation	2.0	0.31	0.97	1.5	0.18	0.78	0.61	0.02
Coefficient of variation (%)	6.7	3.6	5.6	4.7	7.2	8.2	3.4	2.2

Table 63 - SB biochar characterisation at different SS ratios (Pyrolysis and Reforming temperatures = 400 and 500 °C) (average, standard deviation and coefficient of variation)

30 wt% (Reformer)	**C (wt%)**	**H (wt%)**	**N (wt%)**	**S (wt%)**	**O (wt%)**	**Ash (wt%)**	**HHV (MJ/kg)**
Average	75.3	1.8	1.0	<0.10	5.1	16.7	27.5
Standard deviation	1.3	0.15	0.04	-	0.26	0.70	0.81
Coefficient of variation (%)	1.7	8.3	4.0	-	5.1	4.2	2.9
70 wt% (Reformer)							
Average	74.6	1.9	0.52	<0.10	6.5	16.3	27.3
Standard deviation	1.5	0.11	0.03	-	0.49	0.66	0.90
Coefficient of variation (%)	2.0	5.8	5.8	-	7.5	4.0	3.3
100 wt% (Reformer)							
Average	73.9	2.2	0.52	<0.10	8.2	15.1	27.2
Standard deviation	1.2	0.14	0.03	-	0.29	0.55	0.98
Coefficient of variation (%)	1.6	6.4	5.8	-	3.5	3.6	3.6

Table 64 - OH biochar characterisation at different SS ratios (Pyrolysis and Reforming temperatures = 400 and 500 °C) (average, standard deviation and coefficient of variation)

30 wt% (Reformer)	C (wt%)	H (wt%)	N (wt%)	S (wt%)	O (wt%)	Ash (wt%)	HHV (MJ/kg)
Average	79.3	1.9	1.2	<0.10	5.6	12.0	29.1
Standard deviation	0.91	0.13	0.05	-	0.28	0.41	0.56
Coefficient of variation (%)	1.1	6.8	4.2	-	5.0	3.4	1.9
70 wt% (Reformer)							
Average	75.3	2.5	1.6	<0.10	3.2	17.3	28.5
Standard deviation	1.6	0.17	0.05	-	0.11	0.88	0.23
Coefficient of variation (%)	2.1	6.8	3.1	-	3.4	5.1	0.81
100 wt% (Reformer)				-			
Average	75.2	2.6	1.3	<0.10	6.2	14.6	28.4
Standard deviation	1.3	0.09	0.02	-	0.34	0.66	0.48
Coefficient of variation (%)	1.7	3.5	1.5	-	5.5	4.5	1.7
10 wt% (Feed)							
Average	56.9	1.7	0.87	<0.10	1.8	38.7	20.8
Standard deviation	0.75	0.08	0.03	-	0.06	2.9	0.58
Coefficient of variation (%)	1.3	4.7	3.4	-	3.3	7.5	2.8
20 wt% (Feed)							
Average	47.6	1.6	0.7	<0.10	1.8	48.1	17.3
Standard deviation	0.87	0.05	0.05	-	0.09	3.6	0.48
Coefficient of variation (%)	1.8	3.1	7.1	-	5.0	7.5	2.8
30 wt% (Feed)							
Average	43.1	1.3	0.52	<0.10	2.6	52.4	15.2
Standard deviation	1.0	0.03	0.06	-	0.14	2.2	0.39
Coefficient of variation (%)	2.3	2.3	11.5	-	5.4	4.2	2.6

Table 65 - Mass balance of SB trials at different SS ratios (Pyrolysis and Reforming temperatures = 400 and 500 °C) (average, standard deviation and coefficient of variation)

30 wt% (Reformer)	**Bio-oil (wt%)**	**A. phase (wt%)**	**Char (wt%)**	**Gas (wt%)**	**Losses (wt%)**
Average	5.7	25.7	29.8	31.5	7.3
Standard deviation	0.27	1.4	0.65	1.6	0.38
Coefficient of variation (%)	4.7	5.4	2.2	5.1	5.2
70 wt% (Reformer)					
Average	7.4	27.6	25.9	32.4	6.7
Standard deviation	0.73	1.0	1.4	1.0	0.42
Coefficient of variation (%)	9.9	3.6	5.4	3.1	6.3
100 wt% (Reformer)					
Average	9.3	29.2	22.0	33.9	5.6
Standard deviation	0.49	0.97	1.3	0.76	0.55
Coefficient of variation (%)	5.3	3.3	5.9	2.2	9.8

Table 66 - Mass balance of OH trials at different SS ratios (Pyrolysis and Reforming temperatures = 400 and 500 °C) (average, standard deviation and coefficient of variation)

30 wt% (Reformer)	Bio-oil (wt%)	A. phase (wt%)	Char (wt%)	Gas (wt%)	Losses (wt%)
Average	8.4	31.6	27.2	26.5	6.3
Standard deviation	0.59	0.72	0.85	1.3	0.44
Coefficient of variation (%)	7.0	2.3	3.1	4.9	7.0
70 wt% (Reformer)					
Average	9.1	32.5	24.5	28.8	5.1
Standard deviation	0.33	0.67	0.78	2.1	0.16
Coefficient of variation (%)	3.6	2.1	3.2	7.3	3.1
100 wt% (Reformer)					
Average	9.8	33.3	20.2	31.3	5.4
Standard deviation	0.46	0.5	0.67	1.3	0.22
Coefficient of variation (%)	4.7	1.5	3.3	4.2	4.1
10 wt% (Feed)					
Average	7.4	26.7	29.2	31.1	5.6
Standard deviation	0.28	1.7	0.99	2.0	0.43
Coefficient of variation (%)	3.8	6.4	3.4	6.4	7.7
20 wt% (Feed)					
Average	7.1	23.3	39.0	26.2	4.4
Standard deviation	0.16	1.2	1.5	0.88	0.56
Coefficient of variation (%)	2.3	5.2	3.8	3.4	12.7
30 wt% (Feed)					
Average	6.7	20.1	43.5	25.1	4.6
Standard deviation	0.17	1.4	1.1	0.69	0.35
Coefficient of variation (%)	2.5	7.0	2.5	2.7	7.6

Table 67 - Energy yield of SB trials at different SS ratios (Pyrolysis and Reforming temperatures = 400 and 500 °C) (average, standard deviation and coefficient of variation)

30 wt% (Reformer)	**Bio-oil (%)**	**Char (%)**	**Gas (%)**	**Losses (%)**
Average	10.5	50.0	26.1	13.4
Standard deviation	0.77	1.4	0.30	0.86
Coefficient of variation (%)	7.3	2.8	1.1	6.4
70 wt% (Reformer)				
Average	15.0	43.1	26.7	15.3
Standard deviation	1.1	0.68	0.43	0.58
Coefficient of variation (%)	7.3	1.6	1.6	3.8
100 wt% (Reformer)				
Average	20.1	36.5	27.5	15.9
Standard deviation	1.3	0.37	0.64	1.2
Coefficient of variation (%)	6.5	1.0	2.3	7.5

Table 68 - Energy yield of OH trials at different SS ratios (Pyrolysis and Reforming temperatures = 400 and 500 °C) (average, standard deviation and coefficient of variation)

30 wt% (Reformer)	**Bio-oil (%)**	**Char (%)**	**Gas (%)**	**Losses (%)**
Average	15.3	49.3	22.6	12.8
Standard deviation	1.6	1.0	0.47	1.0
Coefficient of variation (%)	10.5	2.0	2.1	7.8
70 wt% (Reformer)				
Average	18.6	43.5	23.9	14.0
Standard deviation	1.2	1.3	0.39	0.77
Coefficient of variation (%)	6.5	3.0	1.6	5.5
100 wt% (Reformer)				
Average	21.4	35.7	25.0	17.9
Standard deviation	1.7	0.85	0.64	1.1
Coefficient of variation (%)	7.9	2.4	2.6	6.1
10 wt% (Feed)				
Average	14.8	37.9	33.7	13.5
Standard deviation	0.92	0.48	0.81	0.75
Coefficient of variation (%)	6.2	1.3	2.4	5.6
20 wt% (Feed)				
Average	14.5	42.1	28.9	14.5
Standard deviation	0.67	1.2	0.34	1.2
Coefficient of variation (%)	4.6	2.9	1.2	8.3
30 wt% (Feed)				
Average	14.7	41.2	28.5	15.6
Standard deviation	1.0	1.7	0.22	1.3
Coefficient of variation (%)	6.8	4.1	0.77	8.3

Table 69 - TCR bio-oil characterization after HDO treatment (average, standard deviation and coefficient of variation)

30 wt% (Reformer)	**C (wt%)**	**H (wt%)**	**N (wt%)**	**S (wt%)**	**O (wt%)**	**HHV (MJ/kg)**	**Ash (wt%)**	**Water (wt%)**	**TAN (mg KOH/g)**	**Viscosity (mm^2/s)**	**Density (kg/m^3)**
Average	83.4	10.7	2.2	0.87	3.0	41.4	<0.001	1.7	1.2	6.3	999
Standard deviation	1.4	0.38	0.10	0.02	0.09	0.67	-	0.08	0.03	0.55	7.7
Coefficient of variation (%)	1.7	3.6	4.5	2.3	3.0	1.6	-	4.7	2.5	8.7	0.77

LIST OF PUBLICATIONS

Journals:

OUADI, M., JAEGER, N., GREENHALF, C., **SANTOS, J.**, CONTI, R. & HORNUNG, A. 2017. Thermo-Catalytic Reforming of municipal solid waste. *Waste Management,* 68, 198-206.

SANTOS, J., OUADI, M., JAHANGIRI, H. & HORNUNG, A. 2019. Integrated intermediate catalytic pyrolysis of wheat husk. *Food and Bioproducts Processing*, 114, 23-30.

SANTOS, J., OUADI, M., JAHANGIRI, H. & HORNUNG, A. 2020. Thermochemical conversion of agricultural wastes applying different reforming temperatures. *Fuel Processing Tecnhology*, 203, 106402.

SANTOS, J., OUADI, M., JAHANGIRI, H. & HORNUNG, A. 2020. Valorisation of lignocellulosic biomass investigating different pyrolysis temperatures. *Journal of the Energy Institute*, [Article in Press Accepted].

SANTOS, J., OUADI, M., JAHANGIRI, H. & HORNUNG, A. 2020. The upgradation of bio-oil and syngas using steel slag as catalyst by intermediate pyrolysis. *Waste Management*, [Article in Press Review].

JAHANGIRI, H., **SANTOS, J**., HORNUNG, A. & OUADI, M.. 2020. Thermochemical conversion of Biomass and upgrading of bio-products to produce fuels and chemicals. *Springer Nature Switzerland AG*, [Article in Press Review].

Conferences:

SANTOS, J., OUADI, M., GREENHALF, C. & HORNUNG, A. 2017. The conversion of biomass to methyl-furans using green hydrogen. *Fuel Cell and Hydrogen Conference*, Birmingham, UK, May 2017.

SANTOS, J., OUADI, M. & HORNUNG, A. 2018. The conversion of biomass to methyl-furans through Thermo-Catalytic Reforming. *22nd International Symposium on Analytical and Applied Pyrolysis*, Kyoto, Japan, June 2018.

SANTOS, J., OUADI, M. & HORNUNG, A. 2018. Thermo-Catalytic Reforming of lignocellulosic biomass using steel slag as catalyst. *6th International Conference on Renewable & Non-Renewable Energy*, Miami, USA, May 2019.

SANTOS, J., OUADI, M. & HORNUNG, A. 2018. Thermo-Catalytic Reforming of lignocellulosic biomass using steel slag as catalyst. *7th International Conference on Sustainable Solid Waste Management*, Crete, Greece, June 2019.